REMOVAL OF NITROGENOUS HETEROCYCLIC COMPOUNDS FROM AQUEOUS SOLUTION

Ph.D. THESIS

by

HIWARKAR AJAY DEVIDAS

DEPARTMENT OF CHEMICAL ENGINEERING
INDIAN INSTITUTE OF TECHNOLOGY ROORKEE
ROORKEE - 247 667 (INDIA)

July, 2015

REMOVAL OF NITROGENOUS HETEROCYCLIC COMPOUNDS FROM AQUEOUS SOLUTION

A THESIS

Submitted in partial fulfilment of the requirements for the award of the degree

of

DOCTOR OF PHILOSOPHY

in

CHEMICAL ENGINEERING

by

HIWARKAR AJAY DEVIDAS

DEPARTMENT OF CHEMICAL ENGINEERING
INDIAN INSTITUTE OF TECHNOLOGY ROORKEE
ROORKEE - 247 667 (INDIA)

July, 2015

INDIAN INSTITUTE OF TECHNOLOGY ROORKEE

ROORKEE

CANDIDATE'S DECLARATION

I hereby certify that the work which is being presented in this thesis entitled **"REMOVAL OF NITROGENOUS HETEROCYCLIC COMPOUNDS FROM AQUEOUS SOLUTION**" in partial fulfilment of the requirement for the award of the Degree of Doctor of Philosophy and submitted in the Department of Chemical Engineering of the Indian Institute of Technology Roorkee is an authentic record of my own work carried out during a period from July, 2011 to July, 2015 under the supervision of Dr. Indra Deo Mall, Retired Professor and Dr. V. C. Srivastava, Associate Professor, Department of Chemical Engineering, Indian Institute of Technology Roorkee, Roorkee.

The matter presented in this thesis has not been submitted by me for the award of any other degree of this or any other Institute.

(HIWARKAR AJAY DEVIDAS)

This is to certify that the above statement made by the candidate is correct to the best of our knowledge.

(I. D. Mall)
Supervisor

(V. C. Srivastava)
Supervisor

The Ph.D. Viva-Voce Examination of Hiwarkar Ajay Devidas, Research Scholar, has been held on **Sept. 24, 2015**.

Chairman, SRC

(I. D. Mall)
Supervisor

(V. C. Srivastava)
Supervisor

(P. K. Bhattacharya)
External Examiner

This is to certify that the student has made all the corrections in the thesis.

Dated : Sept. 24, 2015

(I. D. Mall)
Supervisor

(V. C. Srivastava)
Supervisor

Head of the Department

ABSTRACT

Nitrogenous heterocyclic compounds are one of the most important classes of chemicals. Nitrogenous compounds containing wastewater are generated in industries like petroleum, pharmaceutical, textile, chemicals, etc. Nitrogen containing hetero-aromatic compounds like pyridine, quinoline, indole, pyrrole, etc. has received immense attention recently because of their presence in the environment and their toxic and carcinogenic potential. Heterocycles are also produced in large quantities as a result of industrial activity. Gas oil fractions derived from sand and coals liquid have higher nitrogen concentration than those of petroleum fractions. Crude oil spills contaminate ground water with polycyclic aromatic hydrocarbons and heterocyclic compounds. Their heterocyclic structure makes them more soluble than their homocyclic analogues, and therefore they can get easily transported through the soil and contaminate ground water. Due to their toxicity, mutagenicity and carcinogenicity, they constitute a danger for environment and odour potential. Because of their properties, pyrrole and indole are considered as non-basic nitrogenous compounds whereas pyridine and quinoline are considered as basic nitrogenous compounds.

The different physico-chemical methods available for treatment of wastewaters containing nitrogenous heterocyclic compounds include methods like thermal catalytic incineration, deep well injection, soil percolation, ultra filtration, chemical coagulation and adsorption on various materials. In this context, researchers are exploring the feasibility of using various alternative processes such as ultrafiltration, advanced oxidation process, membrane separation, pervaporation, etc.

Physicochemical methods such as adsorption utilizing activated carbon and other adsorbents including low cost adsorbents have generated much interest among researchers and practitioners of environmental engineering and science. Adsorption has been proven to be one of the most efficient, promising and widely used technique in removal of wide variety of compounds from wastewater. Low cost adsorbents such as bagasse fly ash (BFA) have also been by a number of investigators. Conventional biological methods are believed to be the most economical treatment options for these heterocyclic compounds. However, anaerobic degradation of organic compounds are found to be slow, and therefore, less attractive for full scale application. Major areas in electrochemical treatment are electro-coagulation, electro-flotation and electro-oxidation. In electrochemical treatment, organic pollutants present in the wastewater are oxidized to give carbon dioxide, water and other oxides. In this process, adsorbed hydroxyl radical or chemisorbed active oxygen is responsible for oxidation of organic pollutants.

The Taguchi's method was developed by Genichi Taguchi to optimize the experimental variables as it minimizes time as well as cost of experiment. Optimization of parameters is generally carried out so as to obtain one factor at time. Taguchi method is

popular and powerful approach used in optimization of process. This methodology has been extensively used in chemical and environmental engineering field. Analysis of variance (ANOVA) utilizes the experimental information providing information regarding statistically significant variables for particular operation. Taguchi's methodology was applied previously for separation of copper ions by electrodialysis, for the removal of metal from ternary system.

A review of the literature shows that only few studies are reported on adsorption of pyrrole and indole from aqueous media. In these studies, most important aspects of adsorption studies such as adsorption process control mechanism, adsorption kinetic and thermodynamic aspects were not discussed. Studies on simultaneous adsorption of heterocyclic nitrogenous compounds like pyrrole, indole, etc. from aqueous solutions are scarcely reported. Study on simultaneous adsorption of pyrrole and indole from aqueous solution is very necessary for understanding the effect of adsorption of one compound on other. However, no study is reported on simultaneous adsorptive removal of pyrrole and indole from binary aqueous mixture. Electrochemical treatment including electro-oxidation of pyrrole and indole from aqueous solution by platinum coated titanium plate electrode (Pt/Ti) has been very scarcely reported.

In the present study, individual and simultaneous adsorptive removal of pyrrole and indole was studied by granular activated carbon (GAC) and BFA separately. Physico-chemical characterization including textural analysis, X-ray diffraction (XRD), scanning electron microscopy (SEM), and Fourier transform infrared spectroscopy (FTIR) analyses of the GAC and BFA before and after adsorption were carried out to understand the adsorption mechanism. Effect of various parameters such as pH, adsorbent dose (m), contact time (t), initial concentration (C_o) and temperature (T) on the adsorption of pyrrole and indole by GAC and BFA were studied. Maximum removal of pyrrole and indole was observed at their natural pH without any pH adjustment for both GAC and BFA. Equilibrium contact time for adsorption of both pyrrole and indole onto GAC and BFA was same i.e. 8 h. Optimum value (m_{opt}) for pyrrole and indole removal by GAC was same i.e. 20 $g.l^{-1}$. However, with BFA, m_{opt} value pyrrole and indole removal was found to be 15 and 7 $g.l^{-1}$, respectively. For C_o=500 $mg.l^{-1}$, T=303 K and t=8 h, maximum 84% pyrrole removal and 95% indole removal was obtained with GAC at m_{opt}=20 $g.l^{-1}$. Maximum pyrrole and indole removal of 93% and 95%, respectively, was observed with BFA using m_{opt} values for C_o=500 $mg.l^{-1}$, T=303 K and t=8 h.

Adsorption equilibrium, kinetic and thermodynamic study for individual adsorption were carried out with both the adsorbents. The pseudo-second-order kinetics best represented the adsorptive removal of pyrrole and indole by GAC and BFA individually. Intra-particle diffusion study showed that the pore diffusion was the rate limiting step. Redlich–Peterson isotherm model was found to best-represent the individual adsorption equilibrium data for both the adsorbates onto GAC and BFA. Values for entropy change and heat of adsorption

for indole adsorption onto GAC were found as 101 $kJ.mol^{-1}.K^{-1}$ and 12.4 $kJ.mol^{-1}$ whereas for BFA respective values were 198.88 $kJ.mol^{-1}.K^{-1}$ and 32.22 $kJ.mol^{-1}$. Similarly, values for entropy change and heat of adsorption for pyrrole adsorption onto BFA were found as 47.6 $kJ.mol^{-1}.K^{-1}$ and -3.9 $kJ.mol^{-1}$ whereas for BFA respective values were 74.3 $kJ.mol^{-1}.K^{-1}$ and 2.1 $kJ.mol^{-1}$. The negative value of change in Gibbs free energy (ΔG^o) indicated the feasibility and spontaneity of adsorption on by GAC. Reusability and adsorptive capacity of adsorbents, desorption study was carried out where adsorption capacity of pyrrole for GAC was found much less as compared to that of indole after successive thermal desorption. BFA showed very less desorption efficiency and that removal efficiencies using regenerated BFA was comparatively lower than that of GAC.

Simultaneous adsorption of pyrrole and indole from aqueous solution was carried out with GAC and BFA separately. First, Taguchi's method (L_{27} orthogonal array) was applied to optimize various parameters like C_o, m, T and t for their simultaneous adsorption onto both the adsorbents. Thereafter, binary adsorption equilibrium data were generated and modelled by various multi-component isotherm models. During initial optimization of parameters by Taguchi's methodology, 27 sets of experiments were conducted for the binary adsorption. Amount of adsorbate adsorbed per unit mass of adsorbent (q) was taken as the response. m and the interaction between initial concentrations C_o's were found to be the most significant factor. The values of $q_{tot,}$ q_{Py} and q_{Ind} are found to be highly dependent on various parameters (C_{oi} T, m and t). The adsorption of pyrrole and indole from the binary solutions onto GAC or BFA was found to be antagonistic in nature. Indole adsorption onto GAC was found to be higher than that of pyrrole. The predicted maximum value of q_{tot}, q_{Py} and q_{Ind} for GAC were 0.35, 0.15 and 0.20 $mmol.g^{-1}$, respectively. For BFA, respective values were found to be 0.78, 0.32 and 0.46 $mmol.g^{-1}$, respectively. Three confirmation experiments were conducted at selected optimal levels for the simultaneous removal of pyrrole and indole from binary solution by GAC. The calculated value of q_{tot}, q_{Py} and q_{Ind} are within 95% confidence interval. After optimization of operating parameters, binary adsorption equilibrium data were generated and modeled by various multi-component isotherm models such as non-modified Langmuir, modified Langmuir, extended-Langmuir, extended-Freundlich and Sheindorf–Rebuhn–Sheintuch (SRS) models. Extended-Langmuir or extended-Freundlich isotherm best-represented the isotherm data at 30 ^oC for simultaneous adsorption of pyrrole and indole from aqueous solution onto BFA and GAC.

Electrochemical treatment of pyrrole and indole in aqueous solution was carried by Pt/ Ti electrode individually. Experiments were performed in circular glass batch reactor having 1 litre volume. Experiments were performed under controlled current condition using a direct current (D.C.) power supply. Pt/Ti electrodes were used having actual anodic dip area of 0.012 m^2 in the aqueous solution containing pyrrole and indole individually with 1cm electrode gap. For binary system both solutions were mixed in varying concentration.

Solutions were mixed with constant stirring speed of 600 rpm by magnetic stirrer. Conductivity of the solution was adjusted by adding NaCl. All experiments were conducted with controlled temperature of 30±2 ^{o}C. After desired treatment time, the treated solution was centrifuged and used for determining residual concentration in terms of chemical oxygen demand (COD). Full factorial central composite (CCD) design was used to study the effect of four key process parameters on the COD reduction. The parameters used in this study were: initial pH (pH_o): 2.8 – 8.8; current density (j): 83.34–416.66 A.m^{-2}; conductivity (k): 2.91–6.7 mS.cm^{-1} and electrolysis time (t): 30–150 min. Quadratic models were developed and further used for determining parametric condition for maximum COD and minimum specific energy consumption. An increase in j and t was found to increase the concentration of ions generated (as per Faraday's law) causing adsorption of pollutants and formation of polymeric species in the solution which increased the treatment efficiencies. The optimum operational parameters during electrochemical treatment of pyrrole were found to be pH=8.76, j=175.19 A.m^{-2}, k=2.94 mS.cm^{-1} and t=150 min. Under this optimized conditions predicted values of percent COD removal and specific energy consumption were found to be 69.30% , 99.25 kWh/kg of COD removed, respectively. The value of overall desirability (D) was found to be equal to 0.975. Similarly, optimum operational parameters during electrochemical treatment of indole were found to be pH=8.61, j=161.02 A.m^{-2}, k=6.69 mS.cm^{-1} and t=150 min. The predicted values of percent COD removal and specific energy consumption were found to be 82.92%, 37.75 kWh/kg of COD removed, respectively. Parameters for electrochemical treatment of binary mixture of pyrrole and indole by Pt/Ti were optimized using Taguchi's design of experiments (L_{16} orthogonal array). Optimum values for removal efficiency of pyrrole, indole and COD were found to be 46.1%, 62.4% and 61.4%, respectively.

Scum generated has also been characterized by FTIR, SEM, energy dispersive X-ray (EDX) analysis and thermo-gravimetric analysis (TGA) so as to evaluate its disposal aspect. Mechanism of EC treatment was studied by carrying out UV-visible, UPLC, FTIR and cyclic voltammetric analysis of solution before and after treatment. It was found that the electrochemical treatment of pyrrole and indole occurred by a combination of electro-oxidation and electro-floatation process. Overall, adsorptive removal of pyrrole and indole was most economic process among the treatment methods studied. Though, considering the mineralization of pyrrole and indole, electrochemical treatment by Pt/Ti is a good option of treatment.

ACKNOWLEDGEMENT

I would like to express my sincere gratitude to my both the thesis supervisors Dr. Indra Deo Mall, Professor and Dr. Vimal Chandra Srivastava, Associate Professor, Department of Chemical Engineering, Indian Institute of Technology Roorkee, for their guidance, enthusiasm and insight in supervising the thesis. They provided a motivating, enthusiastic and critical atmosphere during discussions. I thank them for their immense support, outstanding guidance and encouragement. It was a great pleasure for me to conduct this thesis under their supervision. I owe them lots of gratitude for giving the freedom of thought, amiable environment and motivation which provided in me a confidence in analysing my research problems. The enormous knowledge that I gained during their inspiring guidance would be enormously valuable to me for all my future endeavors.

I wish to express my sincere thanks to Prof. I. M. Mishra, Prof. Basheshwar Parsad and Dr. Vimal Kumar, Department of Chemical Engineering, IIT Roorkee, and their invaluable and unconditional support. Their inspiration provided me the strength to carry out this research. I wish to express my sincere gratitude to the members of advisory committee namely Prof. Pradeep Kumar, Prof. Sri Chand for their encouragement and critical input to work hard during the course of my Ph.D. degree.

I would like to take this opportunity to put on record my gratitude to Head, Prof. C. B. Majumder, Department of Chemical Engineering, IIT Roorkee for providing the various basic facilities for carrying out the present research work. My sincere thanks are also for Prof. V. K. Agarwal, Prof. Bikash Mohanty, Prof. Shishir Sinha and all other faculty members of the Department of Chemical Engineering, IIT Roorkee for their kind assistance and encouragement. I am also thankful to Prof. Ramesh Chandra, Head, Institute Instrumentation Centre, IIT Roorkee for his generous assistance and facilitation in the analysis of the samples.

I owe my grateful thanks to my friends, especially, Dr. V. Subbaramaiah, Dr. Chandrakant Thakur, Dr. Seema Singh, Abrham Bayeh Wassie, T. Sandeep Kumar, Kartikeya Shukla and many others who generously helped and encouraged me during my research work. I am also greatly indebted to Praveen Kumar, Ravikant Gupta, Vijay Verma, Anil Verma, Satyanarayana Murthy, Nitin Pandhare, Ranvir Singh, Jyoti Sharma, Parth Kundu, Nilamber , Amit Rai, Lokendra Thakur, Vineet Kumar Thakur, Nandkishore Kinhekar, Leeladhar Malviya, T. P. Singh, Ram Pravesh and Kaushal Kishor for their moral encouragement

I would like to thank all employees and former employees of the Department: Dr. Rajendra Bhatnagar, Shri Satyapal Singh, Shri Arvind Kumar, Shri Vipin Ikka, Shri Tara

Chand, Shri Ayodhya Prasad, Shri Suresh Sani, Shri S. K. Shisodia, etc., who helped me during the course of my experimental work and analysis of the samples. Finally my warm thanks to Shri Arun Kumar, Shri Shadab Ali and Shri Sudesh.

I am also very thankful to Mrs. Indira Mall and Mrs. Kanchan Lata Srivastava with beloved Bhavishya for their cooperation and warm-hearted nature, whenever I went to their residence.

I sincerely thank the Indian Institute of Technology, Roorkee and the Ministry of Human Resource and Development, Government of India, for providing financial support to undertake the work. The Institute is great and the environment is supportive to the research activities. I am also thankful to Co-ordinator, Quality Improvement Program (QIP), IIT Roorkee and their staff members Mr. Rajeev, Mr. Anil Kumar and other staff members for their unconditional support during my research under this QIP program. I am also thankful to Director, Bundelkhand Institute of Engineering and Technology, Jhansi and Government of Utter Pradesh for sponsoring me for this research program under Quality Improvement Program scheme.

I would like to express my sincere love and affection to my father Shri Devidas, mother Shrimati Satyafula, my sisters Mamta, Maya and Sangita, my brother Dr. Vijay Hiwarkar and all my family members for their persistent love, support and encouragement in my life. I have no any suitable word for my mother and father, for their everlasting love and blessing to me. I am extremely conscious of the crucial role played by my wife Mrs. Rajshree Hiwarkar, my both kids Arnav and Atharv during my research work. Without their support it is simply impossible for me to complete my doctoral research work. I thank them from the bottom of my heart for their patience and support at each step of this journey.

I fully understand that the research experience and knowledge which I have gathered during the course of my Ph.D. program would be highly useful for my academic profession. This work was possible only due to contribution of many people. I would like to thank all of them and extremely sorry if anyone is left out in the acknowledgement. I thank God for helping me in one way or the other and providing strength to me and to my family members to bear the pains of remaining away from them for long duration.

HIWARKAR AJAY DEVIDAS

CONTENT

LIST OF FIGURES

LIST OF TABLES

NOMENCLATURE

ABBRIVATIONS

AES	Auger electron spectroscopy
AOP	Advanced oxidation processes
AMSA	Aminomethanesulfonic acid
ANOVA	Analysis of variance
BET	Brunauer-Emmett-Teller
BFA	Bagasse fly ash
BJH	Barrett-Joyner-Halenda
BOD	Biological oxygen demand
CC	Central composite
COD	Chemical oxygen demand, $mg.l^{-1}$
CDAE	Carboxylated diaminoethane
CV	Cyclic voltammetry
D	Overall desirability
DOF or f	Degree of freedom
DFT	Density functional theory
DO	Dissolved oxygen
DTG	Differential thermal analysis
DTA	Differential thermal analysis
ED	Ethylenediamine
EIS	Electrochemical impedance spectroscopy
EDX	Energy-dispersive X-ray spectroscopy
FE-SEM	Field emission scanning electron microscope
FTIR	Fourier transform infrared
GAC	Granular Activated carbon commercial
GO	Graphite Oxide
GC-MS	Gas chromatography mass spectrometry

HPLC	High performance liquid chromatography
HREELS	High resolution electron energy loss spectroscopy
HMS	Hexagonal molecular sieve
Ind	Indole
MA	Molecular area
MCM	Mobil Composition of Matter
MOF	Metal organic frame works
MP	Melting point
MPSD	Marquardt's percent standard deviation
MV	Molecular Volume
MW	Molecular weight
NEXAFS	Near edge X-ray absorption fine structure
OA	Orthogonal array
PRESS	Predicted residual sum of square
PES	photoemission spectroscopy
RHA	Rice husk ash
RP	Redlich-Peterson isotherm
RSM	Response surface methodology
SERS	Surface enhanced Raman Scattering
SEM	Scanning electron microscopic
SEM-EDX	Scanning electron microscope-energy dispersive atomic spectra
SSE	Sum of square of errors
SWV	Square wave voltammetry
TGA	Thermo gravimetric analysis
TPD	Temperature programmed desorption
TEAp-TS	Tetraethylammonium p-toluene sulfonate
Ti/Pt	Platinum coated titanium electrode
UPS	Ultra-violet photoelectron spectroscopy
UPLC	Ultra performance liquid chromatography

XPS	X-ray photoelectron spectroscopy
XRD	X-ray diffraction
2FI	two factor interaction

NOTATIONS

1/n	Freundlich heterogeneity factor
A, B, C, D, E	Interaction parameters
$\overline{A_3}$, $\overline{B_3}$, $\overline{C_3}$, $\overline{D_1}$,	Average values of the response at different levels
Ad_i	Individual adsorption yield
Ad_{Tot}	Total adsorption yield
A	Filtration area (m^2)
C	Solid concentration in slurry ($kg.m^{-3}$)
a_R	Constant of Redlich- Peterson isotherm ($l.mmol^{-1}$)
q_m	Adsorption capacity of adsorbent
°C	Degree centigrade
C_o	Initial concentration of adsorbate in solution
C_e	Concentration of the single-component at equilibrium
$C_{0,i}$	Initial concentration of each component in solution ($mmol.l^{-1}$)
$C_{0,Py}$	Initial concentration of pyrrole ($mmol.l^{-1}$)
$C_{0,Ind}$	Initial concentration of indole ($mmol.l^{-1}$)
$C_{e,i}$	Equilibrium concentration of adsorbate ($mmol.l^{-1}$)
d_i	One sided desirability
ΔG^0	Gibbs free energy change ($KJ.mol^{-1}$)
h	Initial sorption rate ($mmol.g^{-1}.min^{-1}$)
ΔH^0	Enthalpy change ($KJ.mol^{-1}$)
I	Boundary layer thickness
J	Current density, $A.m^{-2}$

k	Number of responses
k_f	Pseudo-first order rate constant
k_s	Pseudo-second order rate constant
K	Conductivity ($mS.cm^{-1}$)
K_D	Equilibrium adsorption constant
$K_{EL,i}$	Individual extended Langmuir isotherm constant of each component ($l.mmol^{-1}$)
K_F	Mono component (non-competitive) constant of Freundlich isotherm of single component $((mmol.g^{-1})/(l.mmol^{-1})^{1/n})$
$K_{F,i}$	Individual Freundlich isotherm constant of each component $((mmol\ g^{-1})/(l.mmol^{-1})^{1/n})$
K_F	Mono component (non-competitive) constant of Freundlich isotherm of single component $((mmol.g^{-1})/(l.mmol^{-1})^{1/n})$
$K_{F,i}$	Individual Freundlich isotherm constant of each component $((mmol\ g^{-1})/(l.mmol^{-1})^{1/n})$
K_L	Langmuir isotherm constant of each component ($l.\ mmol^{-1}$)
$K_{L,i}$	Individual Langmuir isotherm constant of each component ($l.\ mmol^{-1}$)
K_R	Constant of Redlich- Peterson isotherm ($l.\ g^{-1}$)
m	Adsorbent dosage ($g.l^{-1}$)
n_i	Individual Freundlich heterogeneity factor of each component
$\eta_{L,i}$	Multicomponent (competitive) Langmuir adsorption constant of each component, dimensionless
P	Percent Contribution
Py	Pyrrole
pH_{pzc}	Point of zero charge
pH_o	Initial pH
pH_f	Final pH

$q_{e,cal}$	Calculated value of solid phase concentration of adsorbate at equilibrium (mmol.g^{-1})
$q_{e,\exp}$	Experimental value of solid phase concentration of adsorbate at equilibrium (mmol.g^{-1})
$q_{e,Ind}$	Amount of indole adsorbed per unit mass of adsorbent at equilibrium (mmol.g^{-1})
$q_{e,Py}$	Amount of pyrrole adsorbed per unit mass of adsorbent at equilibrium (mmol.g^{-1})
$q_{\max}$	Constant in extended Langmuir isotherm
q_{tot}	Total amount of solute adsorbed per unit mass of adsorbent (mmol.g^{-1})
$q_{tot,predicted}$	Predicted total amount of solute adsorbed per unit mass of adsorbent (mmol.g^{-1})
R	Universal gas constant
R_m	resistance of filter medium in (m^{-1})
R^2	Cofficient of determination
S	Total Variance of Each Factor
S`	Pure sum of square
ΔS^0	Entropy change (KJ.mol^{-1}K^{-1})
t	Time
T	Temperature
$\overline{T}$	Overall mean of response
V	Variance
Ve	Error variance
Y_1	COD removal efficiency
Y_2	Specific energy consumed (kWh per kg of COD removed)
Y_{opt}	Optimal values of the response
Δt	interval of filtration
ΔV	filtrate volume (m^3)

Subscripts

o or 0	Initial
e	Equilibrium concentration
i,j	Component

Greek Letters

α_i	Constant in SRS model for each component, dimensionless
α	specific cake resistance to filtration
β	Constant of Redlich-Peterson isotherm ($0< \beta <1$)
β_i	Constant in SRS model for each component, dimensionless
μ	Viscosity of liquid filtrate (Pa.s)

Chapter-1

INTRODUCTION

1.1 GENERAL

Nature has been gracious and kind in providing enough water all over the world. However fast industrialization, deforestation, unplanned urbanization and population has resulted in large scale of water pollution. Organic chemical industries have higher pollution load discharging toxic effluents into water. This practice results in serious health hazard and threat to human being. According to World health organization more than 1.2 million people in the world shall have no access to drink water [Mall, 2007]. Primary control methods such as raw material substitution, reduction or recycling methods, etc. help in the reducing the pollution load at the source, however, it is not always possible to have primary control which sometimes decreases the quality of the product. Treatment of wastewater generally involves secondary control for particular industry [Padoley et al., 2008]. Nitrogenous heterocyclic compounds are one of the most important classes of chemicals. These are present naturally in the environment and are generated due to anthropogenic activities as well. Contamination of ground water and subsoil due to percolation of many hetero-aromatic pollutants has been reported [Fetzner, 1998]. A number of industries discharge wastewater containing refractory nitrogenous heterocyclic compounds such as pyrrole, indole, etc. Mineralization and removal of these nitrogenous heterocyclic compounds from aqueous streams is necessary from environmental and health point of view.

1.2 NITROGENOUS HETEROCYCLIC COMPOUNDS

Nitrogenous heterocyclic compounds generally contain five or six atom ring. The compounds containing five-atom ring compounds are indole, pyrrole and carbazole considered as non-basic compounds and six-atom ring such as pyridine, quinoline and acridine are considered as basic compounds.

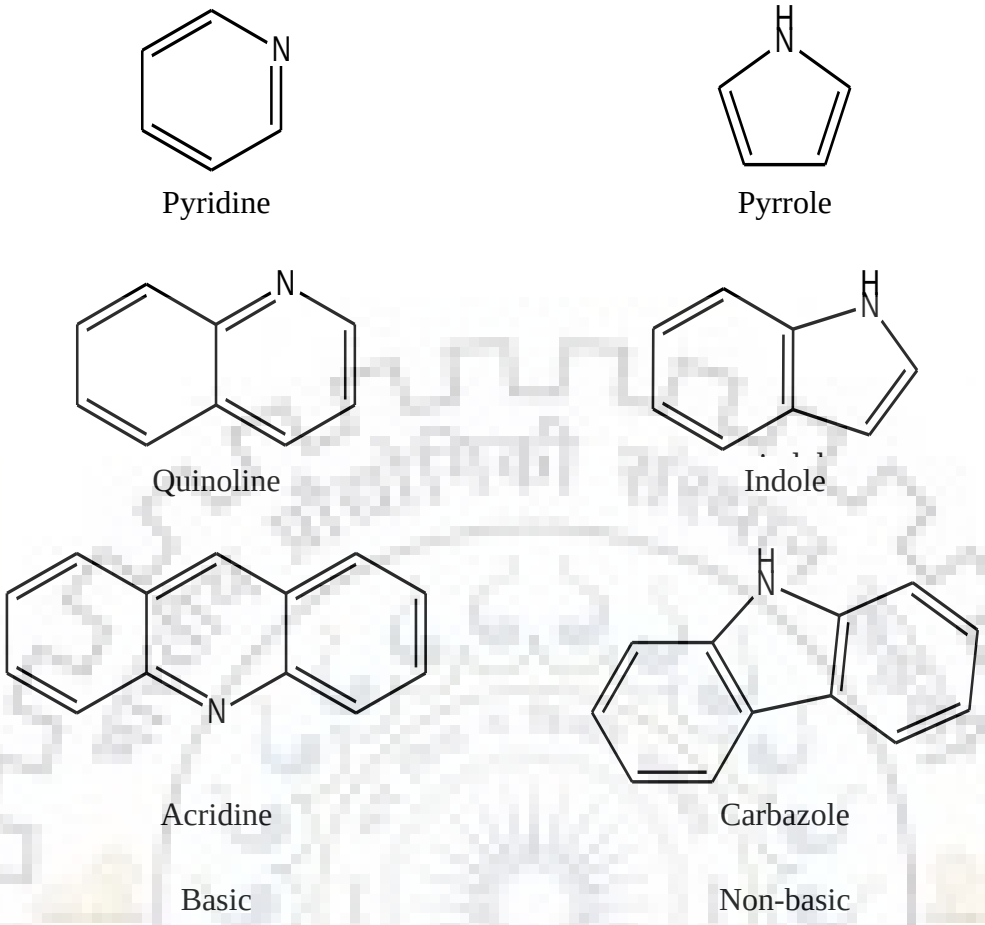

Figure 1.2.1: Basic and non-basic nitrogenous heterocyclic compounds.

Nitrogenous compounds containing wastewater are generated in industries like petroleum, pharmaceutical, textile, chemicals, etc. (Tables 1.2.1 and 1.2.2) [Padoley et al., 2008]. Nitrogen containing hetero-aromatic compounds are highly toxic and carcinogenic. Many researchers have recently given immense attention in removal of compounds such as pyridine, picoline, quinoline, indole, pyrrole, etc. from the environment [Sims and Loughlin, 1989; Padoley et al., 2008].

During coal processing such as carbonization, gasification and liquification, indole along with pyridine derivatives are produced. These nitrogenous heterocyclic compounds are also produced in large quantities during various industrial activities [Fetzner, 1998; Padoley

et al., 2008]. Shale oil production generates almost equal quantity of wastewater containing pyridine and quinoline derivatives [Dobson et al., 1985]. Creosote wood preservation and fossil fuel processing generate wastewater having large amount of iso-quinoline and its derivatives [Pereira et al., 1983]. Gas oil fractions derived from sand and coal-liquid have higher nitrogen concentration than those of petroleum fractions.

Ground water contamination may occur due to polycyclic aromatic hydrocarbons and heterocyclic compounds during crude oil spills [Gundlach et al., 1983]. Compounds having heterocyclic structure are more soluble than homocyclic analogues of nitrogenous compounds. Therefore, they can get easily transported through the soil and contaminate ground water [Kuhn and Suflita, 1989; Padoley et al., 2008]. The odor of heterocyclic compounds reduces the portability of groundwater undesirable taste [Maya, 1981].

Pyridine and its derivatives constitute an important class of compounds with wide applications in pharmaceuticals, pesticide manufacture, chemical manufacture, agricultural chemicals, drugs, dyestuffs and paints, rubber products, polycarbonate resins, and textile water-repellents as industrial solvent, etc. [Fetzner, 1998]. Pyridine and its derivatives concentration in India is generally in the range of 20–300 $mg.l^{-1}$. During emergency spills, the concentration can be as high as 600–1000 $mg.l^{-1}$ [Lataye et al., 2008]. Quinoline is found in shale oil, petroleum refining and coal processing effluents. Petroleum refining is known to be major contributor of the quinoline production [Collin and Hoke, 1993; Rameshraja et al., 2012].

The approximate contents of nitrogen containing hetero-aromatic compounds in high-temperature coal tar is 0.9% carbazole, 0.2%-0.3% quinoline, 0.2% indole, 0.1%-0.2% isoquinoline, 0.1%-0.2% 2-methylquinoline, 0.1% acridine, 0.03% pyridine and 0.02% 2-methylpyridine [Collin and Hoke, 1989, 1995].

1.2.1 Toxicity of Nitrogenous Heterocyclic Compounds

Nitrogenous heterocyclic compounds have high odor and due to their toxicity, mutagenicity and carcinogenicity, they constitute a danger for environment [Kaiser et al., 1996]. These are carcinogen and causes severe health hazards because of their toxic nature [Mudliar et al., 2008]. Many of the pyridine derivatives are known to be poor substrates to indigenous microorganisms, and are hazardous as they persist for a long time in the environment [Rogers et al., 1985]. Exposure to pyridine derivatives causes harmful effects on liver, kidneys, immune systems and reproductive function [Niu and Conway, 2002]. Pyridine exposure is harmful for liver, kidneys, immune systems and reproductive functions [Lataye et al., 2006; Kumar et al., 1995]. Indole is one of the many toxic and recalcitrant nitrogenous heterocyclic compounds, which is considered as an environmental pollutant [Ochiai et al., 1986; Samah et al., 2011]. The role of nitrogen in indole revealed increased mutagenic nature due to substitution at C-2, C-3, C-5 and C-6 position [Kamath and Vaidyanathan, 1991]. Chlorine disinfection of indole containing wastewater leads to the formation of carcinogenic chlorinated aromatic products [Lin and Carlson, 1984]. Considering various toxicity aspects, most of the nitrogenous heterocyclic compounds are considered as priority pollutants by United States environmental protection agency (USEPA) [Thomsen and Kilen, 1998; Meyer et al., 1999; Huang and Wang, 2007].

1.2.2 Properties of Nitrogenous Heterocyclic Compounds

Various properties of nitrogenous heterocyclic compounds are compiled in Table 1.2.3. Heterocyclic compounds are generally more polar than their homocyclic compounds which possess lower octanol/water partition coefficients (K_{ow}) [Sims and Loughlin, 1989]. log (K_{ow}) for pyrrole, indole and quinoline are 0.75, 2.0 and 2.03, respectively [Broholm. et al., 1999]. Nitrogen atom in the five- or six-atom ring is more electronegative than the carbon [Kirk and Othmer, 1996]. The N*H* proton in pyrrole is moderately acidic with pK_a value of 16.5. Because of its properties, pyrrole and indole are considered as non-basic nitrogenous compounds whereas pyridine and quinoline are considered as basic nitrogenous compounds.

Table 1.2.1: Industries generating wastewaters containing heterocyclic nitrogenous pollutants [Padoley et al., 2008].

Industries	Source of heterocyclic nitrogenous pollutants	Pollutants in effluents
Pharmaceutical industry	• Cetyl pyridine (anticeptic) • Isoanizide (anti-tuberculosis) • Coramine (nicotinic acid, • N, N-dimethyl amide)	• Pyridine and picoline • Picoline and quinoline
Coal processing	• Coal carbonization • Coal gasification • Coal liquification	• Pyridine and derivatives quinoline, isoquinoline
Shale oil processing	• Retorting of oil shale to • release product oil	• 2, 6-dimethylpyridine, N-N-dimethylpyridine, 2, 4, 6-imethylpyridine, quinoline, isoquinoline
Pesticide	• Picloram, diquat, paraquat, fluridone, nitrapyridinerin	• Pyridine, picoline and pyridine derivatives
Dyes	• Fabric, cyamoalphyes of • clinical use	• Pyridine, quinoline
Food additive	• Vitamin-B6 (pyridineridoxin) • Nicotinic acid	• Picoline
Chemical manufacturing industries	• Nitrogenous compounds • Water repellent • Detergent • Corrosion inhibitor	• Pyridine, quinoline

Table 1.2.2: Industrial processes generating wastewaters containing heterocyclic nitrogenous pollutants [Padoley et al., 2008].

Process	Conditions	Source	Contaminants
Coal Processing • Coal carbonization	LTC 600–700 ^{0}C HTC 900–1200 ^{0}C	Coke oven wastewater	Pyridine, quinoline and isoquinoline
• Coal gasification	Gasification of fossil raw material biomass	High temperature coal tar	Pyridine, quinoline, indole
• Coal liquification	Distillation	Distillation unit outlet	Quinoline, isoquinoline
Shale oil retorting	Water vapor at high temperature and pressure is held in contact with oil and solid matrix	Retort water	Hydroxy pyridines Pyridine carboxylic acids
Creosote Wood preservation	Wood preservation is carried out by applying creosote as a primary chemical	Process wastewater	Isoquinoline, quinoline, 4-methylquinoline, pyridinerrole, pyridinerrolidine, acridine
Crude oil processing	Oil processing	Oil spills, volatilization	Pyridine, quinoline

Table 1.2.3. Characteristics properties of few nitrogenous heterocyclic compounds.

Properties of compounds	Pyridine	Quinolene	Indole	Pyrrole
Molecular formula	C_5H_5N	C_9H_7N	C_8H_7N	C_4H_5N
Molecular properties[d]	Basic	Basic	Neutral	Neutral
MW[b] ($g.mol^{-1}$)	79.1	129.16	117.15	67.09
BP[a] (^oC)	115.2	238	254	129
MP[b] (^oC)	-41.6	−15.6	52.5	−23.4
Critical diameter[e] (Å)		7.1	7.2	
Appearance	Colorless liquid	Liquid	White solid	Liquid
Density[b] ($g.ml^{-1}$)	0.98	1.092	1.22	0.969
Solubility in water[a] ($\mu mol.l^{-1}$)		49000	16000	
pK_a	5.25	4.9[c]	16.2	16.5[f]
log (K_{ow})[c]	0.65	2.03	2.0	0.75
log (K_{oc})[c]		1.82	1.79	0.54
MA($Å^2$)[a]		150.7	140.6	
MV ($Å^3$)[a]		122.0	110.0	
ESP charge (on N atom)		−0.699	−0.449	
Dipole moment[d] (D)	2.2	2.103	1.844	

MW: molecular weight, MP: melting point, MA: molecular area, MV: Molecular Volume, log (K_{ow}): log partition n-octanol/water

[a]Pearlman [1984]; [b]Lide [1992]; [c]Broholm et al. [1999]; [d]Liu et al. [2008]; [e] Almarri et al. [2009]; [f]Larrubia et al. [2002].

1.2.3 Pyrrole and Indole

Pyrrole (C_4H_5N) is widely found in natural crude oil, coal tar and bone oil. It is also obtained by zinc-acetic acid reduction of succinimide [Higasio and Shoji, 2001]. It is a non-basic organo-nitrogen heterocyclic compound possessing lone electron pair of nitrogen delocalized over the Π system of the ring. This reacts readily with electrophiles and is not susceptible to nucleophilic attack as it is an electron rich molecule [Jorgebsen and Salem, 1973; Jones and Bean, 1977; Abdallah and Nelson, 2005]. The N*H* proton in pyrrole is moderately acidic with a pK_a of 16.5 [Larrubia et al., 2002]. The lone-pair electrons of the nitrogen atom and two C=C bonds form a six-electron conjugated Π electron system. [DuBois et al., 2000].

Indole is a popular component of fragrances and the precursor to many pharmaceuticals. It is a common product generated by industries for various applications including pharmaceuticals, cosmetics, pesticides, disinfectants, agrochemicals, and dyestuffs [Novotny et al., 1981; Paudler and Cheplen, 1979]. It also contributes to the unpleasant odor [Ochiai et al., 1986; Bethea and Narayan, 1972]. Indole present in dilute aqueous solution of chlorine, chlorine dioxide, or chloramines results in the formation of chlorinated aromatic products [Lin and Carlson, 1984], which are known to be toxic and carcinogenic. Indole and associated compounds are also formed during fermentation of tryptophan generated in the meat industry [Erciyes et al., 2004].

1.3 TREATMENT OF NITROGENOUS HETEROCYCLIC COMPOUNDS

Different physico-chemical and biological methods have been reported for the treatment of wastewaters containing nitrogenous heterocyclic compounds. These methods include chemical coagulation, adsorption onto various materials, thermal catalytic incineration, etc. [Khandegar and Saroha, 2012, 2013, 2014]. In this context, several researchers have also explored feasibility of using various other alternative processes such as ultrafiltration [De and Bhattacharya, 1997; Desai and Murthy, 2014], advanced oxidation process [Sharma et al., 2010a, 2013; Hasan et al., 2012], membrane separation [Agrahari et al., 2012], pervaporation [Nemmani et al., 2009], etc.

Physico-chemical methods such as adsorption utilizing activated carbon and other adsorbents including low cost adsorbents have generated much interest among researchers and practitioners of environmental engineering and science. Adsorption has been proven to be one of the most efficient, promising and widely used technique in removal of wide variety of compounds from wastewater [Lataye et al., 2006; Rameshraja et al., 2012].

Conventional biological methods are believed to be the most economical treatment options for these heterocyclic compounds. However, anaerobic degradation of organic nitrogenous compounds is found to be slow, and therefore, less attractive for full scale

application. Nitrogenous compounds are non-biodegradable and get hardly biodegraded in activated sludge process because of presence of refractory and biologically inhibitory organic compounds [Li et al., 2003]. It is also difficult to reduce NH_3 by conventional processes. Moreover, biological methods require long residence time to treat refractory pollutants. With these considerations, it is very important to look for technologies that are capable of oxidizing the nitrogenous heterocyclic compounds from wastewater.

Electrochemical treatment of wastewater has gained a lot of attention in recent years. Major mechanisms of electrochemical treatment are electro-coagulation, electro-flotation and electro-oxidation. In electro-flotation, buoyant gases bubbles generated during electrolysis take pollutant to the surface of liquid body. A layer of foam containing gas bubbles and floated particles is formed at the surface of water body [Kushwaha et al., 2010, 2011]. The rate of floation depends upon surface tension, size distribution of particle, residence time of solution, bubble size distribution and its density, zeta potential, temperature and pH of the solution [Singh et al., 2013]. Electro-oxidation of pollutants is achieved in two ways i.e. by direct anodic oxidation or by indirect oxidation. In anodic oxidation, organic compounds are adsorbed and oxidized at the surface of the electrode whereas in indirect oxidation oxidizing agents are generated electrochemically [Kushwaha et al., 2010]. In this operation, organic pollutants present in the wastewater oxidized to give carbon dioxide, water and other oxides. In this process, adsorbed hydroxyl radical or chemisorbed active oxygen is responsible for oxidation of organic pollutants. Mechanistic outline for oxidation of organic matter on an electrode surface composed of metal oxide [MO_x] is as follows [Panizza and Cerisola, 2009]:

$$H_2O + MO_X \longrightarrow MO_X[OH] + H^+ + e^- \quad (1.3.1)$$

The adsorbed hydroxyl radicals may form chemisorbed active oxygen.

$$MO_X[OH] \longrightarrow MO_{X+1} + H^+ + e^- \quad (1.3.2)$$

The liberated chemisorbed active oxygen is helpful for oxidation of organic material. In this toxic and non-biocompatible pollutants are converted into bio-degradable organic for further treatment. Few investigators have reported degradation of nitrogenous compounds such as

aniline, nitrophenol, etc. by electrochemical methods [Kumar et al., 2015; Zaggout et al., 2008; Liu et al. 2012; Chen and Huang, 2015; Hu et al., 2015; Ferreira et al., 2015]. Many researchers were applied graphitic carbon nitride electrode for aniline removal from aqueous solution [Hu et al., 2015; Ferreira et al., 2015]. Similarly, ruthenium oxide coated titanium, lead oxide/titanium modified electrode, etc. were applied for the removal of nitrophenol from aqueous solution [Kumar et al., 2015; Zaggout and Ghalwa, 2008]. Liu et al. [2012] carried out electrochemical oxidation of nitrophenol. Chen and Huang [2015] studied oxidative degradation of aniline in aqueous solution by coupling electrolysis with persulfate oxidation. These studies were found to be promising for the treatment of nitrogenous compounds in wastewater.

1.4 GRANULAR ACTIVATED CARBON (GAC), BAGASSE FLY ASH (BFA) AND PLATINUM COATED TITANIUM ELECTRODE (Pt/Ti)

Granular activated carbon (GAC) has been used extensively in adsorption studies and in field-scale treatment of wastewaters. The adsorption capacity of GAC depends on characteristics: texture (surface area, pore size distributions), surface chemistry (surface functional groups), and ash content. It also depends on adsorbate characteristics: molecular weight, polarity, pK_a, molecular size, and functional groups. Bagasse fly ash (BFA) is low cost adsorbent which is collected from the particulate collection equipments placed in industries which use bagasse as fuel. It is mainly used for land filling, and partly used as filler in building materials, paper and wood boards. This low cost adsorbent has sufficient amount of carbon and silica in it. BFA has shown good adsorption capacity for treatment of dairy wastewater [Kushwaha et al., 2010] and paper mill effluents [Srivastava et al., 2005]. Various investigators utilized it for the removal of phenolic compounds [Srivastava et al., 2006, 2008a], dyes [Mane et al., 2007] and metals [Srivastava et al., 2007a,b, 2008b,c]. Aim of present work is to explore the possibility of BFA being utilized as an adsorbent for the removal of nitrogenous heterocyclic compounds.

Individual adsorption of indole from diesel fuels, light cycle oils and aqueous solution onto activated carbons has been reported in few studies [Almarri et al., 2009; Wen et al., 2010; Friedrich et al., 1988; Reschke et al., 1986; Kim et al., 2006; Han et al., 2014]. A few studies are also reported in literature on simultaneous adsorption of simple aromatic nitrogenous compounds such as aniline, nitrophenol, nitrobenzene, etc. Suresh et al. [2011a] reported adsorptive removal of phenol, aniline and nitrophenol from aqueous solution using GAC. They applied Taguchi's method of design to study the effect of each parameter at three levels. Lataye et al. [2008] reported pyridine and 2,4 picoline removal by adsorption from aqueous solution using BFA. However, in both these studies, multicomponent isotherm modelling was not done and only optimization of parameters was studied. Jadhav and Srivastava [2013] studied the simultaneous adsorption of nitrobenzene, aniline and phenol onto activated carbon where isotherm modeling of the adsorption data was done by ideal adsorbed solution theory (IAST) and real adsorption solution theory (RAST). However, optimization of parameters was not reported in this study.

Several types of dimensionally stable anode (DSA) such as instant boron doped diamond, titanium coated with metal oxides (e.g. RuO_2, PbO_2, TiO_2 and SnO_2), etc. have been researched in the literature for the treatment of wastewaters [Vaghela et al., 2005; Li et al., 2006a,b]. Transition metals such as ruthenium, tantalum, iridium, tin, antimony, etc. can be used for fabrication of DSA type of electrodes [Comninellis and Vercesi, 1991; Hu et al., 1996]. Compared to other metal oxides, RuO_2 is highly stable and has high mechanical and chemical resistance even under strong acid conditions. Platinum based materials find extensive applications as aviation components, electrode materials in electrochemical treatment as it has high corrosion resistance and conductivity property [Hosseini et al., 2007]. Platinum coated titanium (Pt/Ti) electrodes have been used for the mineralization of a number of aromatic compounds by electrochemical treatment. Volume of solid waste generated after mineralization using Pt/Ti electrodes is very less as compared to iron and aluminum electrode [Kamachi-Mudali et al., 1992, 2000; Mallika et al., 2007]. These are

used in many electrochemical industries particularly in reprocessing plants [Kamachi-Mudali et al., 1992]. During the development of this electrode, chloride salts of platinum are painted on the pretreated titanium substrate. This operation is followed by high temperature annealing under high vacuum. Fabrication of uniform coating on titanium electrode with platinum loading gives better results [Jena and Raj, 2008].

1.5 TAGUCHI'S EXPERIMENTAL DESIGN

Generally optimization of parameters is carried out to obtain one factor at time. Interaction among the various factors can't be studied using this approach. Taguchi's orthogonal array is a fractional factorial based design which can be used to investigate the effects of multiple factors as well as their potential interactions in lesser time and cost effective manner.

The Taguchi's method was developed by Genichi Taguchi to optimize the experimental variables as it minimizes time as well as cost of experiment [Chiang, 2005; Zolfaghari et al., 2011]. Analysis of variance (ANOVA) utilizes the experimental information providing information regarding statistically significant variables for particular operation.

This methodology has been extensively used in chemical and environmental engineering field. Taguchi's methodology was applied for separation of copper ions by electrodialysis [Mohammadi et al., 2004], for wastewater treatment with spiral wound osmosis element [Madaeni and Koocheki, 2006], for the removal of metals from ternary system [Srivastava et al., 2007b; 2008c], for multicomponent adsorption of pyridine [Lataye et al., 2008]. Plessis and Villiers [2007] evaluated mechanical flotation during waste activated sludge thickening by Taguchi optimization technique. In the present study L_{27} OA Taguchi's methodology was adopted for optimization of parameters in adsorptive removal of nitrogenous compounds from binary mixture and L_{16} for electro-oxidation.

1.6 OBJECTIVES OF THE PRESENT STUDY

Based on the critical review of the literature and research gaps identified, it is found that only a few studies have been reported for the removal of pyrrole and indole from aqueous solution. Considering various possibilities, the following objectives were set for the present study:

- Adsorptive removal of pyrrole and indole by GAC and BFA
    - Characterization of GAC and BFA.
    - Optimization of parameters for individual removal of pyrrole and indole by GAC and BFA.
    - Optimization of parameters for simultaneous removal of pyrrole and indole by GAC and BFA using Taguchi's design of experiments.
    - Multi component isotherm study for simultaneous removal of pyrrole and indole by GAC and BFA.
- Treatment of pyrrole and indole electrochemical method using platinum coated titanium electrode (Pt/Ti)
    - Study of the effect of various parameters such as pH, current density, conductivity and electrolysis time on individual removal of pyrrole and indole was studied in terms of chemical oxygen demand (COD) and specific energy consumed (kWh/kg of COD removed) using response surface methodology (RSM). Use of desirability approach to simultaneously maximize COD removal and minimize specific energy consumption.
    - Optimization of parameters using Taguchi's method for simultaneous removal of pyrrole and indole by electrochemical method.
    - Study of the treatment mechanism by characterizing solution (during the treatment), electrode and residue (before and after treatment) and performing sludge disposal study.

Chapter-2

LITERATURE REVIEW

2.1 GENERAL

This chapter presents an overview of the research work available in the open literature for the treatment of nitrogenous heterocyclic compounds by various methods such as adsorption, biological methods and electro-chemical treatment. Various sections in this chapter focus on the treatment of nitrogenous heterocyclic compounds such as pyrrole, indole, pyridine, picoline, quinoline, etc. Areas where further research and attention are required have been identified in the last section of this chapter.

2.2 PHYSICO-CHEMICAL METHODS OF NITROGENOUS HETEROCYCLIC COMOUNDS

The traditional and existing treatment technologies for the treatment of nitrogenous heterocyclic compounds bearing wastewater include physico-chemical, biological and electrochemical treatment; thermal incineration and advanced oxidation processes. Different physico-chemical methods such as thermal catalytic incineration, ultrafiltration, chemical coagulation and adsorption on various materials, UV/ozone gas scrubbing, advanced oxidation processes (AOPs), etc. are available for the treatment of wastewater containing nitrogenous heterocyclic compounds.

Among various techniques, adsorption is known to be highly efficient technique for recalcitrant pollutants. The adsorbents used in the adsorption process must be cheap, easily available, and if possible, regenerable having large surface area and high sorption capacity. Adsorption of indole from diesel fuels, light cycle oils and aqueous solution has been investigated by various researchers using activated carbon, metal organic framework and other adsorbents. Studies on simultaneous adsorption of heterocyclic nitrogenous compounds

like pyrrole, indole, etc. from aqueous solutions are rarely reported. However, few studies are reported on adsorption from liquid fuels of these compounds as given in Table 2.2.1**.**

2.2.1 Theoretical Adsorption Studies

Pan and Stair [1986] investigated adsorption of pyridine and pyrrole on a model iron oxide surfaces by X-ray photoelectron spectroscopy (XPS). Both molecules adsorbed at room temperature with intact molecular identity. Upon heating above 320 K, pyridine decomposed on the surface whereas pyrrole desorbed at 345 K with intact molecular identity. It was found that the pyridine bonded via electron donation from the non-bonding nitrogen lone pair to the surface while pyrrole formed bonds via electron donation from a n-bonding orbital to the surface.

Tourillon and Raaen [1987] studied adsorption of pyrrole and N-methylpyrrole onto Pt(111) using near edge X-ray absorption fine structure (NEXAFS). It was observed that pyrrole oriented itself with molecular plane normal to the surface whereas N-methylpyrrole remained orientationally disordered. Kim et al. [2005] performed the chemical and geometrical characteristics of pyrrole on Si(100)-2 x1. In this study, photoemission spectroscopy (PES) and NEXAFS were used. PES results at 300 K gave the confirmation of pyrrole bonding with surface because of breaking of N-H and C-H groups.

Becerik and Kadirgan [1997] investigated adsorption characteristic and orientations model of pyrrole onto platinum electrode. Experiments were performed at natural pH so as to study its effect during adsorption kinetics as function of initial concentration, time and applied potential. Temkin isotherm was found to well-represent the experimental data.

Qiao et al. [2003] also studied adsorption and thermal reactions of pyrrole on Si(100)-2x1. In this study, X-ray and ultra-violet photoelectron spectroscopy (XPS and UPS) techniques and high resolution electron energy loss spectroscopy (HREELS) were used. It was observed that at 120 K, pyrrole chemisorbed molecularly via π interaction with its ring parallel to the surface. Pyrrole assembly was found to be highly thermally stable which is obtained at 350 K after conversion of π bonded species. At increased coverage, chemisorbed

molecules tilted towards the surface normal because of the adsorbate–adsorbate interactions. The N–H bond scission of the p-bonded species occurred at ~350 K, resulting in Si–H and vertically N-bonded pyrrole on the surface. Pyrrole species were found to be thermally stable up to 700 K.

Abdallah and Nelson [2005] studied temperature programmed desorption (TPD) of pyrrole from Mo(110) and C/N-Mo(110) surfaces. Here desorption of pyrrole occurred at 351 K with first order activation energy of 21.9±0.6 kcal.mol^{-1}.

Sun et al. [2005] investigated adsorption and first step hydrogenation of pyridine and pyrrole onto Ni-promoted (1010) edge of MoS_2 using density functional theory (DFT). Most stable configuration for adsorbed pyridine on the Ni-edge surface was found with the molecular plane perpendicular to the surface through N–Ni bonding. Bonding of an α-carbon of the pyrrole to a nickel site was observed with the molecular plane flat on the surface.

Ren et al. [2007] carried out density functional theory (DFT) computations on the adsorption of NO, NO_2, pyridine and pyrrole on the α-Mo_2C (0001). π-face was found to be the most stable adsorption mode for pyridine and pyrrole.

Marandi et al. [2010] carried out pyrrole (Py) adsorption and electro polymerization processes onto Au(111) surfaces from aqueous solution of 0.1 M Py plus 0.1 M $LiClO_4$. In this study, the layers were examined using atomic force microscopy under both dried condition in air atmosphere as well as in the pyrrole solution. AFM images clearly show that in all the cases, surface of the Au (111) electrode was covered with polymolecular adsorbed layer of pyrrole.

2.2.2 Experimental Adsorption Studies

Reschke et al. [1986] carried out experiments with four activated carbons for the removal of phenol and indole from aqueous solution to obtain breakthrough curves. These experiments were carried out in the activated carbon packed column. Redlich-Peterson parameters were calculated for given range of experimental conditions. Here two-zone

diffusion model was applied and it was observed that fourfold increase in initial concentration resulted in two fold increase in surface diffusivity.

Friedrich et al. [1988] investigated kinetics of adsorption of phenol and indole from aqueous solutions on activated carbons. Various diffusion models with its applicability in intraparticle diffusion during adsorption of phenol and indole were studied. Ellis and Korth, [1994] investigated removal of nitrogen compounds from hydro treated shale oil by adsorption on zeolite. In this investigation, the total N concentration of the hexane solution of eight bases was 275 ppmw with optimum dose of 50 $mg.ml^{-1}$. It was found that the total mass of N compounds exceeded the maximum adsorption capacity of the zeolite at the lowest zeolite dose. Pyridine adsorbed more strongly than indole in the simultaneous adsorption. Reutilization of zeolite was done by hydrotreatment and thermal treatment methods so as to remove these heterocyclic compounds. Erciyes et al. [2004] studied adsorption of indole and 2-methyl indole on ligand exchange matrix. This adsorption carried out onto cobalt (II) carboxylated diaminoethane sporopollenin (CDAE-sporopollenin) at 25^{o} C using fixed bed column. Experimental results showed that both Langmuir and Freundlich isotherm tests gave satisfactory fit to Freundlich isotherm within the concentration range studied. Though, indole and 2-methyl indole have same number of donor nitrogen atom but adsorption capacity of 2-methyl indole was found to be higher than indole due to the presence of methyl group.

Kim et al. [2006] studied ultra-deep desulfurization and denitrogenation of diesel fuel by selective adsorption. Three different adsorbents namely activated carbon, activated alumina and nickel-based adsorbents were used in fixed-bed adsorption system. Adsorptive capacity and selectivity studies on various compounds of diesel fuel were determined and comparison was done through breakthrough curves. The molar concentration of each compound in the model fuel was taken 10.7 $\mu mol.g^{-1}$ for appropriate dose. For removing total sulfur, the breakthrough capacity of the activated carbon was about 3.3 times higher than that of Ni/SiO_2-Al_2O_3 and about 4.6 times higher than that of the activated alumina. For removing nitrogen, breakthrough capacity of the activated carbon was about 4.4 times higher than that

of the Ni/SiO_2-Al_2O_3 and about 2.5 times higher than that of the activated alumina. It was found that the activated carbon has higher adsorption capacity and selectivity for both sulfur and nitrogen containing compounds. Almarri et al. [2009] evaluated the performance of seven representative activated carbon samples and three activated alumina samples in a batch adsorption system. The main objective is to perform adsorptive de-nitrogenation of liquid hydrocarbon streams for producing ultraclean fuels and a fixed-bed flow adsorption system for removing quinoline and indole. Activated carbons generally showed higher capacity than activated alumina samples in removing the nitrogen compounds. They correlated the adsorption capacity and selectivity of the activated carbons for nitrogen compounds with their textural properties and oxygen content. The results showed that the spent activated carbons can be regenerated to completely recover the adsorption capacity. It was concluded that the activated carbons may be promising adsorbents for deep denitrogenation of liquid hydrocarbon streams as they have high capacity and selectivity for the nitrogen compounds, along with their good regenerability.

Wen et al. [2010] studied adsorption of heterocyclic sulfur and nitrogen compounds by the use of activated carbon. Quinoline showed a greater removal rate than indole and carbazole in batch adsorption test. The experimental data obtained in this work followed pseudo second-order kinetics. Activated carbon was found to posses highly heterogeneous surface for DBT, quinoline and indole adsorption as concluded by isotherm. Negative value of free energy suggested that the adsorption process was spontaneous and favorable for all S/N compounds. Nuzhdin et al. [2010] studied removal of nitrogen compounds from liquid hydrocarbon streams by selective sorption onto metal-organic framework (MIL-101). This adsorbent selectivity and sorption capacity towards N-containing compounds were found high for this framework. For this purpose, hydro desulfurization (HDS) method was applied and found convenient for the sorption of these compounds.

Zhang et al. [2010] and Zhang and Song [2012] studied adsorption of pyrrole and indole along with other nitrogenous compounds from diesel fuel by molecular sieve Ti-HMS

and MCM-41. It was observed that MCM-41 is found to be most suitable for maximum uptake of indole and Ti-HMS for pyrrole adsorption. Ahmed et al. [2013a,b,c] investigated adsorptive denitrogenation of model fuel by metal organic frame works (MOFs). Langmuir, Freundlich and Temkin isotherms were applied to interpret the adsorption data for the removal of compounds like indole and quinoline. Voorde et al. [2013] studied the influence of metal ions in MOFs on adsorptive removal of these heterocyclic compounds by combining isotherms with microcalorimetric and IR spectroscopic characterizations. Han et al. [2014] carried out regeneration studies to restore carbon adsorptive capacity for dibenzothiophene and neutral nitrogen heteroaromatic compounds removal. Regeneration of activated carbon was done by using thermal, ultrasound and solvent approaches. The obtained result showed that micropore played the significant factor after carbon regeneration than mesopores due to adsorption of S and N. Here thermal regeneration resulted in loss of pores and decomposition of functional group.

Pahari and Sharma [1991] investigated the adsorption of heterocyclic amines, such as morpholine, pyridine, picolines, quinoline, and isoquinoline from dilute aqueous streams, with or without electrolytes and at different pH on activated carbons and polymeric adsorbent using fixed bed systems. A mathematical model, based on external mass transfer and pore diffusion, was used for forecasting theoretical breakthrough profiles. Kumar et al. [1995] investigated adsorption of pyridine on to activated carbon in batch and continuous column. Removal efficiency of pyridine was found to be 94% at an initial concentration of 200 $mg.l^{-1}$. The final adsorption step was very rapid and the overall rate of adsorption was controlled either by film diffusion or by internal diffusion. Density theory was used to investigate the interaction of pyridine, 2-vinylpyridine, and 4-vinylpyridine with silica surfaces. Interaction was highly dominated by hydrogen bond formed between the nitrogen atom and hydroxyl group [Diez and Amalvy, 2003].

Mohan et al. [2005] studied removal of pyridine derivatives from aqueous solution by activated carbons developed from agricultural waste materials. Here adsorption of pyridine

on different AC derived from different sources (FAC: activated carbon derived from coconut fibres, SAC: coconut shells), ATFAC-acid treated coconut fibres and ATSAC-acid treated coconut shells).The experimental data was well described by Langmuir adsorption isotherm model and kinetic study followed the pseudo-first order. Lataye et al. [2006, 2008a,b] carried out removal of pyridine onto BFA and rice husk ash (RHA) from wastewater. The adsorption data was well-fitted to Langmuir isotherm. It was concluded that total sorption uptake was significantly influenced by interaction between initial concentration of pyridine.

Zhu et al. [1995] adsorbed quinoline from aqueous solutions onto combusted rundle spent shale and found that the Langmuir adsorption isotherm best represented the experimental data. Mechanism of proton transfer to the quinoline molecule was found to be important for the adsorption of quinoline in ammonium solutions. Moon et al. [1989] studied adsorption isotherms for m-cresol, quinoline, and 1-naphthol onto silica gel in n-hexane at 30°C. The concentration was kept between 1-30 $mol.m^{-3}$. Experimental results for m-cresol and quinoline were well-represented by the generalized Toth isotherm. Relative affinity of quinoline with respect to silica surface was larger than those of the other two components. Burgos et al. [2002] measured adsorption of quinoline and background electrolyte ($CaCl_2$) onto specimen kaolinite and montmorillonite. Maximum sorption of quinoline occurred at pH 3.5-4.0 for kaolinite, and pH 3.0-5.0 for montmorillonite. Gupta et al. [2005] employed bottom plant and de-oiled soya, an agricultural waste material, for the removal and recovery of quinoline. On the basis of kinetic studies, specific rate constants involved in the processes were calculated and first-order adsorption kinetics was observed in both the cases. Langmuir and Freundlich adsorption models were used for isotherm modeling. Rameshraja et al. [2012] studied adsorption of quinoline onto granular activated carbon (GAC) and bagasse fly ash (BFA) in a batch system. The adsorbent dose for GAC and BFA was found to be of 5 $g.l^{-1}$ and 10 $g.l^{-1}$, respectively. Pseudo-second-order kinetic model was found to fit the adsorption kinetic data. Redlich and Peterson isotherm generally fitted the experimental data for quinoline adsorption onto GAC and BFA.

Table 2.2.1: Literature on adsorption of pyrrole, indole, pyridine and quinoline by various adsorbents.

Components	Model oil/ Solvent	Adsorbent	Techniques used / processes	Process Conditions	Percent Removal/ adsorption capacity	References
Pyrrole and pyridine		Iron oxide	XPS	T=300 K		Pan and Stair,1986
Pyrrole (C_4H_5N) and N-methylpyrrole (C_5H_7N)		Pt(III)	(NEXAFS)	Initial deposition at T=84 K up to 1000 K, P=1×10^{-10} Torr		Tourillon and Raaen,1987
Pyrrole	Ultrapure water	Platinum electrode	electroadsorption	Scan rate 0.05 to 2 V s^{-1} At pH=6.8, C_o=5×10^{-6} M		Becerik. and Kadlrgan,1997
Pyrrole		Si(100)-2×1	XPS	P=2×10^{-10} Torr, T=120K, 350 K and 900K during annealing		Qiao et al., 2003
Pyrrole		Mo(110) and C/N-Mo(110)	TPD and AES	T=351 K, activation energy=21.9±0.6 kcal.mol^{-1}, Exposures range=0.5-5 L, P=5×10^{-10} Torr		Abdallah and Nelson, 2005
Pyrrole		Si(100)-2×1	PES and NEXAFS	Pyrrole exposure=20 L (1×10^{-6} Torr) P=5×10^{-10} Torr		Kim et al., 2005
Pyrrole and Pyridine		NiMoS	DFT study			Sun et al., 2005
Pyrrole, NO, NO_2 and pyridine		α-Mo_2C(0001)	DFT study			Ren et al., 2007
Pyrrole	Millipore water	Au(111)	AFM	C_o=0.1 M Pyrrole plus 0.1 M $LiClO_4$, potential sweep 0 to 0.75 V Scan rate=50 $mV.s^{-1}$		Marandi et al., 2010
Indole and phenol	Distilled water	Activated Carbon	Continuous process	C_o=0.35 $mmol.l^{-1}$		Reschke et al., 1986
Indole and phenol	Distilled water	Activated carbon	Batch Process	C_o=2 $mmol.l^{-1}$		Friedrich et al., 1988
Indole, pyridine, quinoline, carbazole, etc.	Hexane	Zeolite	Batch Process	T=293 K C_o=0.68 $mmol.l^{-1}$ each compounds	20 wt%	Ellis and Korth, 1994
Indole and 2-methylindole	Distilled water	Cobalt II carboxylated diamino ethane sporopollenin	Fixed-bed column	T=298 K, C_o=0.0125 to 0.200 $mmol.l^{-1}$	q_{Ind}=0.17 $mmol.g^{-1}$	Erciyes et al., 2004
Indole, naphthalene, dibenzothiophene, etc.	Diesel fuel	Activated carbon, activated alumina and nickel-based adsorbent	Fixed-bed adsorption	C_o=10.7 $\mu mol.g^{-1}$	AC, q_{Ind}=0.705 $mmol.g^{-1}$ activated alumina, q_{Ind}=0.195 $mmol.g^{-1}$ Ni/SiO_2-Al_2O_3, q_{Ind}=0.167 $mmol.g^{-1}$	Kim et al., 2006

Components	Model oil/ Solvent	Adsorbent	Techniques used / processes	Process Conditions	Percent Removal/ adsorption capacity	References
Indole and quinoline	Model Oil, decane	Activated carbon(AC1, AC3, AC4, AC6)	Batch Process	C_o=20 µmol.g^{-1} m=0.2 g each	q_{Ind} for AC1=15.9, AC3=23.2, AC4=19.3, AC6=9.4 mg (N).g^{-1}	Almarri et al., 2009
Indole, carbazole dibenzothiophene etc.	Diesel fuels, light cycle oils	Activated carbon	Batch Process	T=298 K, 313 K and 328 K C_o=23.8 µmol.g^{-1}	q_{Ind}=1.32 mmol.g^{-1} q_{Qui}=1.17 mmol.g^{-1}	Wen et al., 2010
Indole, carbazole etc.	Model fuel, isooctane	(Materials of Institute Lavoisier)MIL-101	Batch Process	m=10 mg C_o=78 ppmw	q_{Ind}=18 mg (N).g^{-1}	Nuzhdin et al., 2010
Indole, pyridine, quinoline and pyrrole.	Model fuel, n-octane	Ti-HMS	Batch Process	C_{oInd}=10.93 mmol.l^{-1} C_{oPy}=10.71 mmol.l^{-1} T=293-333 K, M=0.1 g V=10 ml	q_{Ind}=0.132 mol g^{-1} q_{Py}=0.145 mmol.g^{-1}	Zhang et al., 2010
Indole, pyridine, quinoline and pyrrole.	Model fuel, n-octane	Hexagonal molecular sieve(HMS),(Mobil Composition of Matter No. 41) MCM-41	Batch Process	C_{oInd}=10.93 mmol.l^{-1} C_{opy}=10.71 mmol.l^{-1}	HMS, q_{Ind}=0.128 mmol.g^{-1} q_{Py}=0.143 mmol.g^{-1} and MCM-41q_{Ind}=0.137 mmol.g^{-1} q_{Py}=0.14 mmol.g^{-1}	Zhang and Song, 2012
Indole, quinoline and benzothiophene	Model fuel n-octane and p-xylene.	MIL-101 and MIL-101 (1.0% PWA) phosphotungstic acid	Batch Process	V=5 ml m=5 mg C_o=2.5-10.3 mmol.l^{-1}	For MIL-101 q_{Ind}=1.38 mmol.g^{-1} MIL-101 (1.0% PWA) q_{Ind}=1.30 mmol.g^{-1}	Ahmed et al., 2013a
Indole, quinoline and benzothiophene	Model fuel n-octane and p-xylene	MIL-100(Cr), Ethylenediamine(ED)-MIL-100(Cr), amino-methane sulfonic acid (AMSA)-MIL-100(Cr)	Batch Process	V=10 ml m=10 mg C_o=1.3-10.3 mmol.l^{-1}	MIL-100 (Cr), q_{Ind}=0.88 mmol g^{-1} ED-MIL-100 (Cr), q_{Ind}=0.80 mmol.g^{-1} AMSA-MIL-100(Cr), q_{Ind}=0.83 mmol.g^{-1}	Ahmed et al., 2013b
Indole, quinoline and benzothiophene	Model fuel n-octane and p-xylene	MIL-101 and 0.25% Graphite Oxide (GO)/ MIL-101	Batch Process	V=5 ml m=5 mg C_o=2.5-10.3 mmol.l^{-1}	MIL-101, q_{Ind}=2.08 mmol.g^{-1} 0.25% GO/ MIL-101 q_{Ind}=2.72 mmol.g^{-1}	Ahmed et al., 2013c

Components	Model oil/ Solvent	Adsorbent	Techniques used / processes	Process Conditions	Percent Removal/ adsorption capacity	References
Indole, thiophene, 1,2dimethylindole	Model fuel, heptane	MIL-100 (Fe, Cr, Al, V)	Batch Process	V=1.8ml m=0.025 g C_o=0.004 M Temp.=298 K	MIL-100(Al) q_{Ind}=670 MIL-100(Cr) q_{Ind}=560 MIL-100(Fe) q_{Ind}=670 MIL-100(V) q_{Ind}=370 mol per unit cell	Voorde et al., 2013
Indole, carbazole, diabenzothiophene, etc	Model fuel, Ethyl acetate	Activated carbon	Batch Process	m=1 g C_o=23.8 µmol. g^{-1} each	q_{Ind}=0.31 mmol.g^{-1}	Han et al., 2014
Pyridine, Quinoline etc.	Water	Activated Carbon, Polymeric Adsorbent (XAD-4)		pH=8.5		Pahari and Sharma et al., 1991
Pyridine		Activated carbon (AC)	Batch type	Batch and Column study C_o=50-250 mg.l^{-1}	94% (q_e=1.203mg.g-1).	Kumar et al., 1995
Pyridine		Silica		DFT study		Diez and Amalvy., 2003
Pyridine		AC		C_o=1-100 mg.l^{-1} t=48h T=283-313 K		Mohan et al., 2005
Pyridine	Water	BFA	Batch type	pH=2-12 m=2-30 g.l^{-1} t=3 h C_o=50-600 mg.l^{-1} T=283-323K	95% at C_o=600 mg.l^{-1} and dose 25 g.l^{-1}	Lataye et al., 2006
Pyridine	Water	RHA, GAC	Batch type	rpm=150 pH=2-12 C_o=50-600 mg.l^{-1} T=283-323 M=5-60 g.l^{-1}	79.5% and 84% at (600 mg.l^{-1} l) at 50 and 30 g.l^{-1} of RHA, GAC	Lataye et al., 2008a
Pyridine, 2-Picoline, and 4-Picoline	Water	BFA	Batch type	C_o=0-100 mg. l^{-1}, T=293-313 K, pH=4-8, m=4-12 g.l^{-1} t=30-90 min	Removal efficiency50%	Lataye et al., 2008b
Pyridine and quinoline Quinoline	Water	Rundle Spent Shale	Batch Process	pH=8		Zhu et al., 1988
Quinoline, m-cresol and 1-naphtholl	n-Hexane	Silica Gel		T=30°C C=1-30 mol.m^{-3}		Moon et al., 1989
Quinoline	Water	Kaolinite and Montmorillonite		pH=3.5-4 for kaolinite pH=3.5-5 for Montmorillonite		Burgos et al., 2002
Quinoline	Water	De-oiled soya	Batch type			Gupta et al., 2005
Quinoline	Water	GAC and BFA	Batch type	pH=5.5 time=8hrs, GAC and BFA were found to be of 5 and 10 g.l^{-1}		Rameshraja et al., 2012

2.3 BIOLOGICAL TREATMENT OF NITROGENOUS HETEROCYCLIC COMPOUNDS

Nitrogenous compounds are refractory and generally non-biodegradable in nature. They are difficult to biodegrade in aerobic and anaerobic processes [Mensah and Forster, 2003]. Some nitrogenous organic compounds which don't biodegrade, accumulate in the biomass and thus increasing the pollution problem on its disposal [Hongwei et al., 2006]. However, many authors have reported biodegradation of nitrogenous heterocyclic compounds in aerobic and anaerobic conditions [Bai et al., 2010a,b; Padoley et al., 2011].

Few authors considered the biological treatment as one the techno-economical feasible options for heterocyclic compounds removal [Padoley et al., 2011; Deng et al., 2011]. Hydroxylation is a cardinal step in mineralization where microorganisms metabolize nitrogenous compounds by hydroxylating them. Bacteria utilize them as carbon source and hence degrade them [Kamath and Vaidyanathan, 1991]. In comparison to similar non-heteroaromatic compounds, indole has low octanol/water partition coefficient and high water solubility. Therefore, it is necessary to calculate exposure risk to understand potential environmental fate. Few reports on aerobic biotransformation of these compounds by soil bacteria are available [Fukuoka et al., 2015]. Jensen et al. [1988] carried out biodegradation of nitrogenous compounds from an oil contaminated aquifer. He reported that pyrrole gets degraded in the groundwater after a lag time of 480 hour in the single substrate experiment. Kamath and Vaidyanathan [1991] carried out studies on toxicity and mutageninty of indole. Studies on biological treatment of nitrogenous heterocyclic compounds are given in Table 2.3.1.

Various innovative processes have been developed to improve biological treatment efficiency of these heterocyclic compounds. Bai et al. [2010b] studied biodegradation of pyridine and quinoline by sequential batch reactor (SBR) with four different bacterial strains. Rotating rope bioreactor (RRB) was developed by Mudliar et al. [2008] for degradation of organic compounds at high concentration. Hu et al. [2011] investigated possibility of

electricity production with nitrogenous heterocyclic compounds under anaerobic condition. Researchers are now-a-days focusing on developing novel biological treatment technologies associated with high energy recovery and low operational cost [Zhang et al., 2009].

Many authors have focused on biodegradation of nitrogenous heterocyclic compounds using isolated strain. Yin et al. [2005] investigated microbial degradation of indole by enrichment culture and *Pseudomonas aeruginosa* Gs from mangrove sediment. Katapodis et al. [2007] carried out biodegradation of indole by thermophlilic fungus. Fukuoka et al. [2015] studied the biotransformation of nitrogen-containing heterocyclic environmental pollutants by isolated soil bacterium. Many authors investigated the biodegradation of pyridine using isolated bacteria limited to low concentration because of its toxicity [Uma and sandhya 1997]. Bai et al. [2010a] studied biodegradation of pyridine and quinoline by bio-zeolite composed mixed bacteria. Quinoline biodegradation was carried out by various researchers using different strains [Jianlong et al., 2001; Zhu et al., 2008; Sun et al., 2009; Li et al., 2010; Lin and Jianlong, 2010; Tuo et al., 2012; Zhao et al., 2014; Zhuang et al., 2015]. Different strains are capable of utilizing quinoline as sole source of carbon, nitrogen and energy. Some of these have been isolated from activated sludge [Zhu et al., 2008]. Transformation of quinoline, isoquinoline and 2-methylquinoline under nitrate-reducing conditions was studied by Li et al. [2010]. Table 2.3.1 compiles biodegradation of pyrrole, indole, pyridine and quinoline using various strains.

Table 2.3.1: Biodegradation of pyrrole, indole, pyridine and quinoline.

Organic compounds	Bacteria /Fungus	Reactor/ Reaction conditions	Process parameters and brief description	References
Pyrrole		Aspirator bottle of 5 L in fixed film reactor, Aqueous, T=150 °C to 240 °C, pH=6.1	• Pyrrole showed more resistant nature than other compounds. • High biodegradation potential for indole, quinoline, flournone and o-cresol results in degradation of these compounds within 5-15 days with initial concentration of 0.5 $mg.l^{-1}$ using both the mixed and single substrate experiments. • Biodegradability of the compounds was also tested in a laboratory by adapting fixed film culture under aerobic conditions.	Jensen et al., 1988
Indole	*Aspergillus niger*	160 rpm, 50 ml of 50 mM, Sodium Phosphate buffer, pH=7 having 0.1% catechol	• Studies on toxicity and mutageninty of indole. • Pathways for biodegradation of indole by micro-organism, plants and animals are discussed. • Hydroxylation and detoxification reactions of indole by organisms presented.	Kamath and Vaidyanathan, 1991
Indole	*Pseudomonas aeruginosa*	Autoclave, 3mM, pH=7.0, salinity 5%, with 1N NaOH, T=120 °C	• Studies on microbial degradation of indole by enrichment culture and *Pseudomonas aeruginosa* Gs from mangrove sediment. • Degradation mechanism reported confirming zero order kinetic model depending on initial concentration of indole.	Yin et al., 2005
Indole	*Sporotrichum* Thermophile	Orbital shaker at 200 rpm, C_o=1 $g.l^{-1}$, pH=5.0, 1 N NaOH	• Studies on biodegradation of indole by thermoplilic fungus. • *Sporotrichum* thermophiles were grown up in a persolvent fermentation system. • The medium used 20% by volume soybean oil containing up to 2 $g.l^{-1}$ indole concentration. • Indole consumed entirely in 6 days when organism grown up having indole concentration 1 $g.l^{-1}$.	Katapodis et al., 2007
Indole	*Cupriavidussp* strain (Strain KK10)	Shaking Incubator at 150 rpm, 50 $mg.l^{-1,}$ 20 m M glycerol, Phosphate buffer=50m M, pH=7.0, One day	• Studies on biotransformation of nitrogen-containing heterocyclic environmental pollutants by isolated soil bacterium. • A soil bacterium was isolated, recognized as a member of the genus *Cupriavidu*s and was found to grow on indole. • Biodegradation of indole by this organism through both N-heterocyclic and carbocyclic aromatic ring fission. • The culture was done at 28°C in rotary shaking incubator at 150 rpm in dark and was extracted at neutral and acidic pH with ethyl acetate.	Fukuoka et al., 2015
Pyridine	Bacillus coagulants	Packed bed reactor	• Examined the biodegradation of pyridine by Bacillus coagulans strain immobilised on AC. • Pyridine was used as a source of nitrogen for bacteria. • Packed bed reactor filled with AC and immobilized bacteria were utilized. • Ammonia was generated rapidly as by-product that was controlled by AC. • 82% TOC (total organic carbon) removal for feed flow rate of 64 mg. $dm^{-3,}$ h^{-1}.	Uma and Sandhya, 1997

Organic compounds	Bacteria /Fungus	Reactor/ Reaction conditions	Process parameters and brief description	References
Pyridine	*Pseudomonas* (P12)	Activated sludge process	• P12 bacteria were utilized for the biodegradation of pyridine bearing wastewater in activated sludge process. • Pyridine degradation and growth parameters of isolated strain were evaluated under aerobic condition.	Mohan et al., 2003
Pyridine	*Pseudoaligenes*-KPN	Activated sludge process, MLSS=1200 $mg.l^{-1}$ C_o=25-200 $mg.l^{-1}$ feedflow rate=20-123 $ml.min^{-1}$	• 97% pyridine degradation was achieved at optimum pyridine to mixed liquor suspended solids (MLSS) of 0.251 kg pyridine/(kg MLSS × day) and HRT of 24 h. • During pyridine metabolism ammonia-nitrogen (NH_3-N) was formed and degraded the pyridine efficiently in the concentration range of 50-300 $mg.l^{-1}$.	Padoley et al., 2006
Pyridine	*Pseudoaligenes*-KPN	Biofilter: thickens 6 mm L=1 m dia.=20 cm airflowrate 1-5 $l.min^{-1}$	• Feasibility of biofilter was examined for the biodegradation of pyridine in the form of gas. • *Pseudomonas pseudoalcaligenes* KPN enriched bacteria was immobilized on the surface of wood chips and as compost in a packed biofilter. • Treated pyridine gas was observed free from odor and more than 99% pyridine removal efficiency was attained at optimum bed retention time 28 sec, 68% moisture content and organic loading of 434 g $pyridine.m^{-2}h^{-1}$.	Pandey et al., 2007
Pyridine	Rotating rope bioreactor (RRB)	C_o=< 1000 $mg.l^{-1}$ HRT=9-18 h Loading=< 400 $mg.m^{-2}.h^{-1}$.	• RRB offers high mass transfer rate of oxygen with a minimal turbulence, greater stability of microbial culture and more interfacial area. • Novel RRB degraded the pyridine bearing wastewater up to 1000 $mg.l^{-1}$ with the degradation efficiency of > 85%. • RRB operated for 15 months without any loss in the activity of bio-film.	Mudliar et al., 2008
Pyridine	*Paracoccus sp.* BW001	Batch reactor C_o=400-3000 $mg.l^{-1}$	• Isolated bacterial strain *Paracoccus sp.* BW001 was used for the degradation of pyridine bearing wastewater obtained from coking industry under aerobic condition. • *Paracoccus sp.* strain could degrade pyridine completely within 49.5 h with initial concentration of pyridine being 2614 $mg.l^{-1}$. • During pyridine degradation, ammonia was produced. • Addition of glucose into medium as extra carbon source expedited the biodegradation of pyridine and transformation of the nitrogen. • BW001 was found to have high potential ability to reduce NO_2 to NO or N_2O than N_2.	Bai et al., 2008
Pyridine and 2-Picoline	*Pseudomonas* and *Nocardiasp*	C_o=50-200 $mg.l^{-1}$ of pyridine and picoline, pH=5.5-8.0 T=293-313 K.	• With addition of phosphorous only, pyridine and picoline biodegradation enhanced without presence of nitrogen source in the microbial medium. • Ammonia was produced as by-product during degradation process and utilized for growth of bacterium.	Padoley et al., 2009
Pyridine	MFC	C_o=0-1000	• Two types of graphite packed and graphite fiber	Zhang et

Organic compounds	Bacteria /Fungus	Reactor/ Reaction conditions	Process parameters and brief description	References
		$mg.l^{-1}$ C_o=100-500 $mg.l^{-1}$ glucose t=20-90 day	brush microbial fuel cell were used for the degradation of pyridine (500 $mg.l^{-1}$). • With and without presence of glucose (500 $mg.l^{-1}$), maximum voltage of 623 mV and 116 mV volts of power was generated, respectively. • After 24 h reaction 95% pyridine removal was achieved. • Ammonium as by-product identified in the anode solution.	al.,2009
Pyridine, picoline, Phenol and Formaldehyde	ITRCEM1 and ITRCEM2	T=305 K rpm=120 picoline C_o=2200 $mg.l^{-1}$ Phenol C_o=500 $mg.l^{-1}$ Formaldehyde C_o=100 $mg.l^{-1}$ t=24 h.	• Mixed bacterial culture was more effective when compare with CEM1 and ITCEM2 bacterium for pyridine degradation. • Presence of mineral salt medium (1% glucose and 0.2% peptone) along with phenol and formaldehyde medium showed inhibitory effect on degradation of pyridine. • Picoline medium favored the pyridine degradation and bacterial growth	Chandra et al., 2009
Pyridine and Quinoline	*Paracoccus sp.* BW001, *Shinella zoogloeoides* BC026, *Pseudomonas sp.* BW003 & BC001	SBR design: L=500 mm W=200 mm H=500 mm C_o=60-70 $mg.l^{-1}$ (pyridine and quinoline) t=71.5 h.	• Bioaugmented SBR process was explored for the biodegradation of nitrogenous organic wastewater from coking industry. • Suspended growth process was employed in coking wastewater. • Two isolated strains of pyridine and quinoline were utilized were utilized for the degradation of pyridine and quinoline bearing wastewater. • SBR showed better treatment efficiency with high shock load. • As time progress, the diversity of bacteria community was reduced in the SBR.	Bai et al., 2010b
Pyridine and Quinoline	BW001 and BW003 strains, Bioaugmented Zeolites	Batch Study rpm=110 T=303 K	• Biodegradation of pyridine and quinoline by bio-zeolite composed mixed bacteria was investigated. • During the biotransformation, ammonium was frequently generated as by-product which was successfully removed by Zeolite.	Bai at al., 2010a
Pyridine	*Achromobactersp.* (DN-06)	C_o=500 $mg.l^{-1}$ pH=5-10 T=293-313K rpm=100-190	• Feasibility of pyridine bearing wastewater by isolated bacterium (*Achromobactersp.* DN-06) under aerobic condition was examined. • More than 95% degradation was achieved. • Five growth kinetic model were fitted, among that Haldane and Yano kinetic models were well described.	Deng et al., 2011
Pyridine and Cyanopyridine	*Pseudomonas pseudoalcaligenes*	Optical density=0.2 pH=7 T=303 K	• Treatment option for pyridine and cyanopyridine manufacturing plants wastewater, investigated with extremely high COD (65000 $mg.l^{-1}$ for pyridine plant, 25624 $mg.l^{-1}$ for cyanopyridine plant). • Pretreated pyridine and cyanopyridine wastewater BOD/COD ratio was improved and biological treatment was carried out by isolated *Pseudomonas pseudoalcaligenes*-KPN in batch culture. • Duing biological treatment, pyridine and	Padoley et al., 2011

Organic compounds	Bacteria /Fungus	Reactor/ Reaction conditions	Process parameters and brief description	References
			cyanopyridine removal efficiency was observed to be 84% and > 99%, respectively.	
Pyridine, Indole and Quinoline	MFC	T=303 K pH=7.0	• Possibility of electricity production with nitrogenous hetrocyclic compounds (pyridine, indole and quinoline) by MFC under anaerobic condition was examined. • Anaerobic sludge was acclimated for several months to increase number of electricity generating bacteria in anode chamber and reduce the anaerobic fermentation process of other microorganisms. • Maximum removal of organic compound up to 90% and maximum COD removal 88% was achieved. • MFC anode solutions analyzed by GC-MS (Gas chromatography mass spectrometry) and metabolic intermediate products were identified.	Hu et al., 2011
m-Cresol and Pyridine	*Lysiniba cillus, cresolivo rans*	T=308 K rpm=170 C_o=0-1200 mg.l^{-1} of m-cresol C_o=30-150 mg.l^{-1} of pyridine t=24 h.	• *Lysinibacillus cresolivorans* bacterium capability for the degradation of phenol and pyridine substrates as individual and binary substrates was studied. • Haldane kinetic model was well described by single substrate degradation, the simulated kinetic data was good agreement with the experimental data.	Yao et al., 2011
Pyridine	*Paracoc cus sp.* BW001, *Pseudom onas sp.* BW003	Column Study 40 mm dia, h=400 mm t=0-91 days,C_o=60-130 mg.l^{-1} pyridine and quinoline	• The treatment option for coking wastewater containing pyridine and quinoline by bio-augmentation and adsorption was investigated. • High efficiency degrading bacterial were used as the inocula to develop bio-film on the surface of zeolites, and zeolites act as ammonium changers. • The investigation was carried in column study i.e. adding isolated degrading bacteria into biological aerated filled with zeolites as adsorbent for the removal of quinoline, pyridine, ammonium and TOC. • During the process, ammonium was produced which may cause eutrophication and disruption of biological treatment.	Bai et al., 2011
Pyridine and Quinoline	*Paracoc cus sp.* BW001, *Pseudom ons sp.* BW003	pH=8.75-8.95 DO=5-8 mg.l^{-1} Pyridine=59-130 mg.l^{-1} quinoline=53-134 mg.l^{-1}	• Comparison of zeolite-biological aerated filters with bioaugmented and non-bioaugmented filters for denitrifier communities was studied. • Bioaugmented and non-bioaugmented filters of denitrifiers belonged to α-, β-and γ-proteobacteria. • Nitrate and nitrite removal by bioaugmented filters showed stable performance compare with non-bioaugmented zeolite-biological aerated filters	Bai et al., 2012
Quinoline	*Bulkhod eria sp.*	Sodium alginate=20 g.l^{-1}, biomass/20 ml gel, Calcium ion=0.2M $CaCl_2$, t=1 h, bead size=3 mm	• Calcium alginate gel used as carrier for immobilization of microbial cells • Degradation of quinoline was done rapidly by microorganism immobilized calcium alginate gel • Effectiveness of immobilization method was observed without significant bio-activity loss.	Jianlong et al., 2001

Organic compounds	Bacteria /Fungus	Reactor/ Reaction conditions	Process parameters and brief description	References
Quinoline	*Rhodoc-occus sp.*	T=35-40ºC and pH=8.0	• Quinoline utilized as sole source of carbon, nitrogen and energy was isolated from activated sludge. • Optimum temperature and the pH was found to be 35-40 and 8.0, respectively. • Haldane's model used to study degradation kinetics.	Zhu et al., 2008
Quinoline	*Pseudomonas sp.* BW003	T=30ºC and pH=8	• Degradation occurred for solutions having initial concentration of quinoline as 192-911 $mg.l^{-1}$ and removal efficiency ranging from 96% to 98%. • Optimum conditions for degradation of quinoline were found to be T=30ºC and pH=8. • The study showed the process of elimination of quinoline by controlling the C/N ratio using BW003.	Sun et al., 2009
Quinoline, isoquinoline and 2-methylquinoline		Optimum ratio (COD/NO_3-N)=7)	• The transformation of quinoline, isoquinoline and 2-methylquinoline under nitrate-reducing conditions was studied. • Accumulation of nitrite was transiently observed using quinoline • No accumulation of nitrite were observed using isoquinoline or 2-methylquinoline. • 2-methylquinoline was degraded under anaerobic conditions.	Li et al., 2010
Quinoline	*Pseudomanas putida*	pH=7.2, C_o=500 $mg.l^{-1}$	• Removal of quinoline with 500 $mg.l^{-1}$ conc. in 3 h was observed. • During quinoline degradation N-atom was released as NH_3. • Biodegradation occurred by hydroxylation reaction.	Lin and Jianlong, 2010
Quinoline	*Bacillus sp.*	T=30ºC, pH=8-10	• Biodegradation characteristics and bioaugmentation potential for a novel strain were studied. • Remarkable enhanced quinoline biodegradation ability achieved. • Quinoline-N was released as ammonia.	Tuo et al., 2012
Quinoline and m-cresol	*Lysinibacillus sp.* SC03 and *Achromobacter sp.* DN-06	T=35ºC. pH=7-8 C_o=100 $mg.l^{-1}$	• Effect of extra substrates, phenolic and N-heterocyclic compounds, on the performance of pure culture and mixed strains under single and dual substrates conditions was studied. • Complete degradation of 100 $mg.l^{-1}$ m-cresol and little degradation of quinoline was observed due to *Lysibacillus sp*. SC03. • The complete degradation of quinoline in 32 h was due to achromobacter sp DN-06 but it could not remove m-cresol	Zhao et al., 2014
Quinoline	*Streptomyces sp.* N01	T.=20-45ºC. pH=5-10 C_o=100-400 $mg.l^{-}$	• Biodegration of quinoline by Streptomyces sp. N01 immobilized on bamboo carbon supported Fe_3O_4 nanoparticles was studied. • Against the change of temperature and pH, Fe_3O_4/BC immobilized cells performed better at higher quinoline concentration and protected the bacteria efficiently.	Zhuang et al., 2015

2.4 ELECTRO-CHEMICAL (EC) METHODS FOR THE TREATMENT OF NITROGENOUS HETEROCYCLIC COMPOUNDS

Electrochemical treatment methods are simple and cost effective for treatment of nitrogenous heterocyclic compounds thereby reducing secondary pollutants. Electrochemical mechanisms include charge neutralization, double layer compression, flocculation, adsorption, electro-flotation, electrochemical oxidation, etc. [Kushwaha et al., 2010]. Destabilization of colloidal suspension by this method due to metal cation generation reduces the negative charge of colloids [Mahesh et al., 2006a,b; Canizares et al., 2008a,b] The main species responsible for electrochemical oxidation of nitrogenous heterocyclic compounds is the electron along with metallic ions generated from the electrodes used. Several authors quoted the possibility to obtain the degradation of different model compounds by electrolysis [Sakalis et al., 2005; Wang et al., 2009]. The main advantage of this technique is having close control of reaction. Direct electrochemical treatment of nitrogenous heterocyclic compounds hasn't been reported, however, studies have been carried out for electro-polymerization and electro-conversion of nitrogenous heterocyclic compounds. Comparative analysis of these studies is presented in Table 2.4.1.

Yamamoto et al. [1991] investigated electro-polymerization of pyrrole using tantalum as electrode. Tantalum electrode retards polymerization at lower pyrrole concentrations because of the development of insulating Ta_2O_5. Polymerization rate of pyrrole was faster than that of acrylamide during electrochemical polymerization of pyrrole in acrylamide solution [Sarac et al., 1999]. Scienza and Thompson [2001] reported the electro-polymerization of pyrrole at aluminum electrode in aqueous medium. Polypyrrole film generated duing electrochemical oxidation in aqueous dodecylbenzene sulfonic acid medium during treatment on copper electrode [Prissanaroon et al., 2004]. Copolymer formed is strong as compared to two homo-polymers with better flexibility. Electrical conductivity of copolymers increased with the amount of polypyrrole [Li et al., 2006b]. Molina et al. [2008] studied chemical and electrochemical polymerization of pyrrole on polyester textiles in presence of phosphotungstic acid. Polymerization of pyrrole in presence of $FeCl_3$ for preparation of conductive cotton fabric was carried out by Wiener et al. [2013]. Wu et al.

[2013] investigated electrochemical performance of Li electrode and effect of $AlCl_3$ and pyrrole on SEI formation. Behavior of indole and its substituent group at the C_3 position was studied by Enache and Brett [2011]. Indole undertakes irreversible pH dependent oxidation whereas oxidations of indole derivatives are complex. It was observed that oxidation occurred at C_2 position of pyrrole ring followed by hydroxylation at the C_7 position. Investigations during electrochemical fluorination on the product distribution pattern of pyridine and 2-fluoropyridine was carried out by Sartori et al. [1998]. Devillers et al. [2013] carried electrochemical characterization of pyridine by crystallization.

Voltammetric and impedance studies of electrochemical oxidation of pyrrole in aqueous medium were carried out by Shiu et al. [1995]. Polypyrrole film reduced reactivity by sulfide medium during electrochemical oxidation of pyrrole on zinc surface [Zaid et al., 1998; Aeiyach et al., 1999]. Reversible voltammograms obtained at moderate to high scan rate showed chemical evolutions of cationic radicals observed. Andrieux et al. [1997] also investigated substituent effects on the electrochemical properties of pyrrole and oligo-pyrroles by cyclic voltammetry. Cyclic voltammetry studies on quinoline have been reported by various researchers [An et al., 1989; Zhu et al., 2011; Zhao et al., 2011; Gao et al., 2014].

2.5 LITERATURE SURVEY OVERVIEW

Literature review illustrates the existing treatment methods for the treatment of nitrogenous heterocyclic compounds. Science citation index (SCI) database was used through Scopus for treatment methods of pyrrole and indole with keywords search as pyrrole removal, indole removal, adsorption, biodegradation, electrochemical treatment (Figure 2.5.1). In this search conference papers were excluded. Research papers on use of adsorption and biological methods for removal of pyrrole and indole are growing in numbers in recent years. Analysis of number of publications and citation data show great interest of scientist, chemical and environmental engineers in treatment of nitrogenous heterocyclic compounds. It may be mentioned that not many papers are available on direct electrochemical treatment of nitrogenous heterocyclic compounds in aqueous solutions, however, studies are reported for electro-polymerization and electro-conversion of pyrrole and indole.

Table 2.4.1: Electrochemical studies using pyrrole, indole, pyridine and quinoline.

Pollutant	Experimental setup	Experimental/ Optimized Conditions	Remarks	Reference
Pyrrole	**Reactor** Acetonitrile solution **Electrode** Material: Platinum Electrode	C_o=0.1M Water+Ethanol:3:1 T=100ºC Potential range=0-1.5V	• Electropolymerization of pyrrole carried tantalum as electrode. • Polypyrrole film yield at high concentrations of pyrrole. • Electropolymerization characteristics on tantalum and platinum behave similarly.	Yamamoto et al., 1991
Pyrrole	**Reactor** Aqueous solution **Electrode** Material: Platinum Electrode Dimension: D=1.0mm	C_{oi}=0.1M pH=2 t=20s Amplitude=5 mV Frequency=250 Hz	• Electropolymerization of pyrrole at platinum electrode was carried out. • Cyclic voltammetry, impedance techniques are applied. • The impedance responses were affected by the applied potential.	Shiu et al., 1995
Pyrrole	**Reactor** Aqueous solution acetonitrile with tetraethylammonium **Electrode** Counter and working electrode : Platinum electrode, Reference calomel electrode	Scan rate=0.05-5 Vs^{-1}	• Electrochemical oxidation of sterically hindered pyrrole and thiopene in acetonitrile solution. • At low scan rate reverse cyclic voltammogram for pyrroles were obtained indicating large stability.	Audebert et al.,1996
Pyrrole	**Reactor** Aqueous sodium oxalate **Electrode** Material: Zinc electrode Dimension:15mm×40 mm	T=3min 0.35mA.cm^{-2} Na_2S=0.2M C_o=0.9M $Na_2C_2O_4$=0.1M	• Electrochemical oxidation of pyrrole by zinc electrode. • Cyclic voltammetry, impedancemetry accompanied by XPS studies.	Zaid et al., 1997
Pyrrole	**Reactor :** Acetonitrile with traethylammonium tetrafluo-roborate electrolyte **Electrode** Counter Platinum electrode, Reference calomel electrode used	E=0.405 V, Scan rate=0.05-5 Vs^{-1}	• Study on effects of the electrochemical properties of pyrrole and oligopyrroles by cyclic voltammetry. • Reversible voltammograms obtained at moderate to high scan rate. • Lifetime and stability of cation radicals examined and estimated as function of chain lengthand its nature.	Andrieux et al., 1997
Pyrrole	**Reactor** Aqueous solution **Electrode** Material: Zinc electrode Dimension: 15 mm×40 mm	C_o=0.7M j=4-20 mA.cm^{-2} pH=5 $Na_2C_2O_4$=0.1M Efficiency=90%	• Electropolymerization starts at lower pyrrole concentration. • Polypyrrole films achieved on zinc remain very adherent. • Coulombic efficiency (γ=90%) was achieved during electropolymerization.	Aeiyach et al., 1999
Pyrrole	**Reactor** Aqueous solution acetonitrile **Electrode** Counter and working electrode : Platinum electrode	V=1.5 V C_o=3.22×10^{-3}M	• Study of electrochemical polymerization of pyrrole in acrylamide solution. • Polymerization rate of pyrrole was faster than that of acrylamide.	Sarac et al.,1999

Pollutant	Experimental setup	Experimental/ Optimized Conditions	Remarks	Reference
Pyrrole	**Reactor** Aqueous electrolytes **Electrode** Material: Aluminum Dimension: 4cm×1.5cm×0.1cm.	C_o=0.1M t=20 min *j*=2 mA.cm^{-2}	• Aluminum is used as substrate to support conducting polymers. • Polypyrrole film found on high purity aluminum substrates under anodic polarization. • SEM, XRD, XPS etc done for analysis.	Scienza and Thompson, 2001
Pyrrole	**Reactor** Aqueous dodecylbenzene sulfonic acid **Electrode** Material: Copper Dimension: 1.5mm thick	C_o=0.05M T=15 min V=1.0-3.5V Scan rate=50 mVs^{-1}	• Cyclic voltammetry accompanied by X-ray photoelectron spectroscopy has been used. • electropolished copper electrode surface was partially passivated by Cu_2O. • polypyrrole coatings on copper electrodes suggest possible use in electronic and sensing applications.	Prissanaroon et al.,2004
Pyrrole	**Reactor** Nitromethane with Bu_4NBF_4 electrolyte **Electrode** Working electrode **Indium-tin oxide (ITO)**: Counter Platinum electrode, Reference electrode Ag/AgCl	C_o=0.1 M with THF V=1.6 V K=1.69 S.cm^{-1} and 0.71 S.cm^{-1}	• Study on electrochemical copolymerization of pyrrole and tetrahydrofuran in various monomer ratio. • Nitromethane solution was applied to this potentiostatic method. • Characterization like. FTIR, SEM, EDX, cyclic voltametry (CV) • Copolymer formed has better flexibility than to homopolymer.	Li et al., 2006b
Pyrrole	**Reactor** Ultrasonic bath with voltammetry **Electrode** Counter electrode Stainless Steel, Conducting textile electrode. Reference electrode Ag/AgCl	C_o=0.2 M in N_2 atmosphere Synthesis v=1.5 V. pH=1-13 T=Room Temp.	• Polymerization of pyrrole done on polyester textiles in presence of phosphotungstic acid. • Polymirezation occurs giving the rise of voltammogram. • Characterization like. FTIR, SEM, EDX, electrochemical impedance spectroscopy (EIS), cyclic voltametry (CV).	Molina et al., 2008
Pyrrole	**Bath tub** **Oxidant**=$FeCl_3$	$FeCl_3$=0.25 ML$^{-1,}$ TEAp-TS=0.125 ML^{-1}, C_o=0.3 m.l^{-1}, T=25˚C and t=4 h	• polymerization of pyrrole in presence of $FeCl_3$ for preparation of conductive cotton fabric. • Tetraethylammonium p-toluene sulfonate (TEAp-TS) was used as doping agent whereas $FeCl_3$ as oxidizing agent.	Wiener et al., 2013
Pyrrole	**Reactor** Ultrasonic bath with cyclic voltammetry **Electrode** Li electrode	C_o=0.1M, $AlCl_3$ C_o=0.1M, Electrolyte applied $LiPF_6$/EC+DMC	• Study of electrochemical performance of Li electrode and effect of $AlCl_3$ and pyrrole on SEI formation. • Non-aqueous $LiPF_6$/EC+DMC electrolyte used • AC impedance, cathodic polarization and galvanostatic charge/discharge cyclic test were performed.	Wu et al., 2013
Indole	**Reactor** Differential pulse voltammetry in solution **Electrode** Material: Glassy carbon Dimension: D=1.5mm	C_o=25 µM pH=7.0 *t*=30s phosphate buffer electrolyte=0.1 Mconductivity ≤ 0.1µscm^{-}1	• Indole substituent at the C_3 position. • In indole derivatives substitution at C_2 position of pyrrole ring followed by hydroxylation at the C_7 position.	Enache and Brett et al., 2011

Pollutant	Experimental setup	Experimental/ Optimized Conditions	Remarks	Reference
Pyridine	**Electrode** The working electrode is silver plate	C_o=0.05M Incident angle=45^o V_{SCE}=+O.l v to-0.6 v t=10 s λ=5145Å	• In the first stage of the adatomic adsorption of pyridine at the silver atoms reduced from AgCl. • In the second stage formation of ellipsoidal silver particle clusters takes place.	Kim and Shin., 1985
Pyridine	**Reactor** Stainless steel **Electrode** Nickel anodes and cathode used as a electrode (effective anode area, 3.8 dm^2).	J=0.53 Adm^{-3} I=2.0 A V=4.6-5.0 T=0°C T=30 h	• 19% conversion yield of perfluoropiperidine was obtained during the electrochemical process • All the ECF experiments were carried out at 0°C	Sartori et. al., 1998
Pyridine	**Reactor** Acetonitrile material **Electrode** The working electrode was a platinum disk electrode and reference electrode was a saturated calomel electrode	T=20±3°C	• In spectro electrochemical experiments, a UV-vis immersion probe was connected through a fibre optic to the same spectrophotometer.	Devillers et. al., 2013
Quinoline	**Reactor** one-compartment cell **Electrode** glass as working electrode and a Pt plate as a counter electrode	T=25°C Voltage=2-3 V J=0.1-4 $mA.cm^{-2}$ K=10^{-3}-10^{-5} $S.cm^{-1}$	• Cyclic voltammograms were performed in acetonitrile containing $LiClO_4$ using a Pt c ounter electrode and Ag/AgC1 reference electrode. • Electrochemical measurement were carried out using a potentiostat a function generator and an X-Y recorder.	An et al., 1989
Quinoline	**Reactor** Material: Acetonitrile **Electrode** 3.0 mm diameter glassy carbon disk working electrode, an Ag quasi reference electrode	C_o=0.1M V=-0.5V t=30 min	• Electrochemical measurement were performed in a electrochemical analyzer. • Pt wire counter electrode that was separated from the working electrode with a glass capillary to avoid the background emission, which had been described before.	Zhu et al., 2011
Quinoline	**Reactor** Multi-wall carbon nanotube (MWCN). **Electrode** working electrode MWNT, reference electrode is a saturated calomel electrode, counter electrode is a platinum wire	t=2 min V=0.3-0.9 V pH=8 Scan rate=40 $mV.s^{-1}$	• Electrochemical measurement was conducted on an electrochemical workstation with a conventional three electrode system. • Comparing with the unmodified electrode oxidation peak current of quinoline yellow showed notable enhancement effect. • The effects of pH value, MWNT, accumulation potential and time were significant factor for the oxidation peak observed.	Zhao et al., 2011
Quinoline	**Reactor** Single-walled carbon nanotubes. **Electrode** glassy carbon electrode, saturated calomel electrode (SCE) as the reference electrode, and a platinum wire as the counter electrode.	t=2 min V=0.75 V pH=10 Scan rate=100 $mV.s^{-1}$	• Cyclic voltametry (CV) and square wave voltammetry (SWV) were applied for successful completion of analysis • Fabricated electrode performance found to be good for oxidation of quinoline yellow. • Oxidation peak current at 0.75 V was measured as the analytical signal of quinoline yellow.	Gao et al., 2014

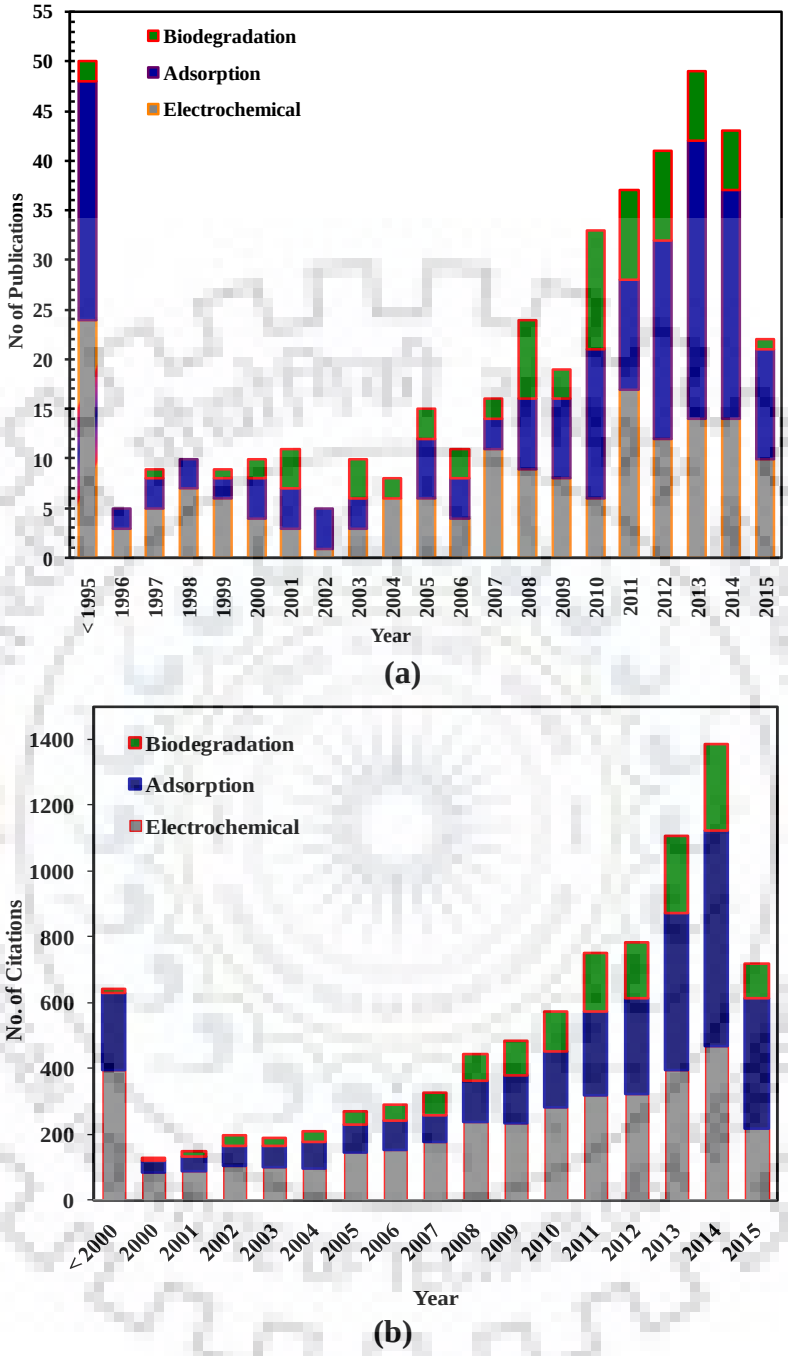

Figure 2.5.1: (a) Treatment of nitrogenous heterocyclic compounds, number of research article published in biodegradation, adsorption and electrochemical treatment since 1995 (Scopus database searched July 07, 2015), (b) Number of citations of papers (Scopus database searched July 07, 2015).

2.6 PATENT DETAILS

Few patents are available for removal of nitrogenous heterocyclic compounds by adsorption and electrochemical treatment. These are listed in Table 2.6.1. To the best of author's knowledge, no patent has been filed against removal of pyrrole and indole by BFA using adsorption method or by electrochemical method using platinum coated titanium (Pt/Ti) electrode. Patent search in open literature showed that no patent has been filed for simultaneous removal of pyrrole and indole from aqueous solution using adsorption and electrochemical method.

2.7 RESEARCH GAP

Biotreatment is an effective method for treatment of pollutants as it mineralizes the pollutants naturally. However, nitrogenous heterocyclic compounds are refractory and generally non-biodegradable in nature and are difficult to biodegrade in aerobic and anaerobic processes [Mensah and Forster, 2003]. Some nitrogenous organic compounds which don't biodegrade, accumulate in the biomass and thus increasing the pollution problem on its disposal [Hongwei et al., 2006]. However, many authors have reported biodegradation of nitrogenous heterocyclic compounds in aerobic and anaerobic conditions [Bai et al., 2010a,b; Padoley et al., 2011]. Only one study is reported on pyrrole biodegradation [Jensen et al., 1988]. In this study, 15 days were required for biodegradation of pyrrole with initial concentration of 0.5 $mg.l^{-1}$ using both the mixed and single substrates. Similarly, only few studies [Kamath and Vaidyanathan, 1991; Yin et al., 2005; Katapodis et al., 2007; Fukuoka et al., 2015] are reported on indole degradation. In these studies also, approximately 5-7 days were required for biodegradation. Overall, considering the toxicity and highly stable structure of pyrrole and indole, biological processes take more time for their biodegradation as compared to biodegradation of simple organic compounds.

The adsorption of indole with other components from diesel fuels, light cycle oils and aqueous solution on activated carbons [Reschke et al., 1986; Friedrich et al., 1988; Kim et al., 2006; Almarri et al., 2009; Wen et al., 2010; Han et al., 2014] and other adsorbents with few metal organic frame work [Ellis and Korth, 1994; Erciyes et al., 2004; Nuzhdin et al., 2010; Zhang et al., 2010; Zhang and Song, 2012; Ahmed et al., 2013a,b,c; Voorde et al.,2013;] have been investigated by various researchers (Table 2.2.1). Few studies have been reported on adsorption of pyrrole along with other components onto metal and other surfaces [Sexton,

1985; Pan and Stair, 1986; Becerik and Kadirgan, 1997; Qiao et al., 2003; Sun and Nelson, 2005; Kim et al., 2005; Abdallah and Nelson, 2005; Ren et al., 2007; Marandi et al., 2010]. In these studies, most important aspects of adsorption studies such as adsorption process control mechanism, adsorption kinetic and thermodynamic aspects were not discussed.

A few studies are reported in literature on simultaneous adsorption of simple aromatic nitrogenous compounds such as aniline, nitrophenol, nitrobenzene, etc. [Suresh et al., 2011a; Lataye et al., 2008b; Jadhav et al., 2013]. Literature review shows that studies on simultaneous adsorption of heterocyclic nitrogenous compounds like pyrrole, indole, etc. from aqueous solutions are scarcely reported. However, few studies are reported on their adsorption from liquid fuels. Ahmed et al. [2013] investigated adsorptive denitrogenation of model fuel by metal organic frame works (MOFs). Langmuir, Freundlich and Temkin isotherms were applied to interpret the adsorption data for the removal of compounds like indole and quinoline. Voorde et al. [2013] studied the influence of metal ions in MOFs on adsorptive removal of these heterocyclic compounds by combining isotherms with micro-calorimetric and IR spectroscopic characterizations. Zhang et al. [2010, 2013] studied adsorption of pyrrole and indole along with other nitrogenous compounds from diesel fuel by molecular sieve Ti-HMS and MCM-41. It was observed that MCM-41 found to be most suitable for maximum uptake of indole and Ti-HMS for pyrrole adsorption.

Study on simultaneous adsorption of pyrrole and indole from aqueous solution is very necessary for understanding the effect of adsorption of one compound on other. However, no study is reported on simultaneous adsorptive removal of pyrrole and indole from binary aqueous mixture.

In the literature, studies are reported on electro-polymerization of pyrrole by various electrodes such as tantalum, platinum, zinc, aluminum, Li, etc. giving polypyrrole. Electrochemical oxidation of indole has been reported on glassy carbon electrode in one study [Enache and Brett, 2011]. However, no work has been reported on electrochemical treatment of pyrrole and indole with respect to their mineralization in aqueous solution.

The main aim and detail objectives of this present study (as given in sections 1.6) have been formulated based upon the research gaps identified in the literature (as discussed above).

Table 2.6.1: List of patents on adsorptive removal and electrochemical treatment of nitrogenous heterocyclic compounds.

Title	Patent No	Organization	Authors and Year
Removal of nitrogen compounds from FCC distillate	US8673134 B2	ExxonMobil Research and Engineering Company (Annandale, NJ, US)	Siporin et al., 2014
Denitrification of a hydrocarbon feed	US8540871	Chevron U.S.A. Inc. (San Ramon, CA, US)	Zhan et al., 2013
Selective removal of aromatics	EP2338955 A1	BP Oil International Limited (Chertsey Road, Sunbury on Thames Middlesex TW16 7BP, GB)	Anonymous, 2011
Methods of denitrogenating diesel fuel	US7749377 B2	UOP LLC, Des Plaines, IL (US)	Serban and Kocal, 2010
Denitrogenation of liquid fuels	US20050150 837 A1	Yang Ralph T., Hernandez-Maldonado Arturo J.	Yang et al., 2005
Process for removal of nitrogen containing contaminants from gas oil feedstreams	20040118748 A1	Lesemann Markus Friedrich Manfred Setzer Constanze	Lesemann et al., 2004
Removal of nitrogen compounds	WO/2004/03 5712 A1	Johnson Matthey PLC (2-4 Cockspur Street, Trafalgar Square, London SW1Y 5BQ, GB)	Carnell et al., 2004
Process for the denitrogenation of nitrogen-containing hydrocarbon compounds	EP0210709 A3	Exxon Research and Engineering Company	Hudson, 1988
Process for the denitrogenation of nitrogen-containing hydrocarbon compounds	EP0210709A 2	Exxon Research and Engineering Company	Hudson, 1987
Denitrification of nitrogen-containing hydrocarbon compound	JPS6232183	Exxon Research and Engineering Company	Hudson, 1987
Process for the denitrogenation of nitrogen-containing hydrocarbon compounds	4591430	Exxon Research and Engineering Company (Florham Park, NJ)	Hudson, 1986
Removal of basic nitrogen compounds from hydrocarbon liquids	4521299	International Coal Refining Company, Allentown, Pa	Edwin et al., 1985
Removal of metals and nitrogen from hydrocarbon feed stocks	US3036968	Universal Oil Prod Co.	Gatsis,1962
Purification of heterocyclic organic nitrogen compounds	US2982771 A	Houdry Process Corp	Bond and George, 1961

Chapter-3

EXPERIMENTAL

This chapter provides description of materials and methods used during adsorption and electrochemical treatment studies performed for the removal of pyrrole and indole from aqueous solution.

3.1 MATERIALS AND METHODS

3.1.1 Adsorbent and Adsorbates

GAC was procured from NICE Chemicals private limited, Kochi, India. BFA collected from the Triveni sugar mill, Deoband, Uttar Pradesh, India was used directly after sieving. Platinum coated titanium (Pt/Ti) electrode was procured from Titanium Tantalum products limited, Chennai, India. Indole was obtained from Himedia Laboratories private limited, Mumbai, India. Pyrrole was procured from Sigma-Aldrich, Bangalore, India. All analytical reagent (AR) grade chemicals were used in this study. The working solutions were prepared by appropriate dilutions of stock solution in distilled water. Millipore water was used for the preparation of analytical standards, eluent preparation and sample dilution in chromatography. All other solvents used in the chromatography were of high performance liquid chromatography (HPLC) grade.

3.2 ANALYTICAL METHODS

3.2.1 Ultra Performance Liquid Chromatography (UPLC)

The separation module was Waters Acquity ultra performance liquid chromatograph (UPLC) H Class. The system consisted of a sample manager, solvent manager, and column manager. UPLC separation was performed by injecting two microliter of specimen on a Waters Acquity UPLC BEH C18 column (2.1 x 50 mm, 1.7 m particle size). Chromatographic separation was achieved by gradient elution at flow rate of 0.5 $ml.min^{-1}$ while maintaining the column and sample temperatures at 35°C and 20°C, respectively. Mobile phases used during analysis were 60% millipore water and 40% acetonitrile.

Separations on the column are achieved by partitioning of solute between mobile phase and stationary phase. Samples and mobile phase were filtered through 0.2 µm pore size membrane before using these samples on UPLC. Wavelength in UV detector was kept at 205 nm for measurement of indole and pyrrole. To quantify the pyrrole and indole concentration in aqueous solution, calibration curves (prepared with known pyrrole and indole concentration solutions) were used.

3.3 CHARACTERIZATION

Characterization plays an important role in understanding the physico-chemical and thermal properties of the adsorbents, electrodes and the treated solutions. Various characterization techniques used in this study are described in this section.

3.3.1 Proximate Analysis

The proximate analysis of GAC and BFA were performed according to code IS-1350 (Part-I)-1984. The parameters determined during proximate analysis include moisture content, volatile matter, ash content and fixed carbon.

Moisture content was calculated by determining loss of mass after keeping known mass of GAC and BFA in oven at 105±2°C. For determining the volatile matter, pre-weighed quantity of air dried sample of these samples were taken in cylindrical silica crucible with well fitted lid and then it was heated at 900±10°C in muffle furnace for 7 min. The difference in weight before and after heating gave volatile matter present in the samples. For determining the ash content, known weight of GAC and BFA were taken in silica crucible and heated at 500°C for 30 min in muffle furnace. This temperature was raised to 815±10°C in further 30 min and maintained at this temperature up to run-up period.

$$\text{Ash content } (\%) = \left[\frac{W_3 - W_4}{W_2 - W_1}\right] 100 \qquad (3.3.1)$$

where, W_1 is the weight of empty crucible, W_2 is the weight of crucible along with sample, W_3 is the weight of crucible along with ash, and W_4 is the weight of crucible along with

sample after brushing out and reweighing. Fixed carbon was calculated by deducting the sum of moisture content, volatile matter and ash content (%) from the value 100:

Fixed Carbon (%) = 100-(Moisture content + Volatile matter + Ash content)

(3.3.2)

3.3.2 Point of Zero Charge (pH_{PZC})

For determining the point of zero charge (pH_{PZC}) of adsorbents, 45 ml of KNO_3 solution of known strength was transferred to the series of 100 ml conical flask. The pH_o in the range 2 to 12 was adjusted by the addition of 0.1 N NaOH or HNO_3 solutions. The total volume of the solution was made to 50 ml by adding KNO_3 solution of same strength. One gram of adsorbent was added to each flask and capped immediately. The suspension were manually shaken for 48 h and allowed to equilibrate with intermittent shaking. The pH values of supernatant liquid were recorded. The difference between initial and final pH gave ΔpH which were plotted against pH_o. The point of intersection of curve with the x-axis gives the value of pH_{PZC}. Same procedure was repeated with another concentration of KNO_3 solution [Srivastava et al., 2008b].

3.3.3 Surface Area and Pore Size Distribution Analysis

Textural properties of the samples were analyzed by adsorption of N_2 at 77 K using Micromeritics ASAP 2020 apparatus. Brunauer-Emmett-Teller (BET) model was applied for calculating surface area of porous materials by physical adsorption of gases at boiling temperature.

$$\frac{P}{V_{N_2}(P_o - P)} = \frac{1}{V_{N_2,m}C} + \frac{(C-1)P}{V_{N_2,m}CP_o} \qquad (3.3.3)$$

where, V_{N_2} is adsorbed liquid nitrogen volume, $V_{N_2,m}$ is the volume necessary for the formation of one monolayer, P and P_o are the equilibrium and saturation pressures, C is constant depending upon heat of adsorption and heat of liquefaction of nitrogen gas. Fractal dimension was determined by Frenkel-Halsey-Hill (FHH) equation to the N_2 adsorption isotherm:

$$\frac{V_{N_2}}{V_{N_2,m}} = K\left[\ln\left(\frac{P_o}{P}\right)\right]^{D_f-3} \qquad (3.3.4)$$

where, K is constant and D_f is the fractal dimension. It is known that for smooth surface, D_f has a value of 2 whereas for rough irregular surface its value is about 3.

Barrett-Joyner-Halenda (BJH) analysis was carried out using the desorption branch of isotherm to compute pore size distribution using following equation:

$$\ln\left(\frac{P}{P_o}\right) = -2\sigma V_{N_2}\cos\left(\frac{\theta}{r_k R}\right) \qquad (3.3.5)$$

where, σ is surface tension, θ is the wetting angle and R is the gas constant, r_k is the Kelvin's radius. Before analysis, the samples were degassed at 200°C for 3 h [Han et al., 2014].

3.3.4 Scanning Electron Microscopic Analysis

Scanning electron microscope (SEM) is a basic tool of microscopic analysis which shows morphologies of samples with elemental analysis**.** Field emission scanning electron microscope (FE-SEM)/energy dispersed X-ray spectra (EDX) QUANTA, Model 200 FEG, USA was used for this analysis. Here conductivity of samples provided using gold coated sputtering coater (Edwards S150). FE-SEMs were taken at an acceleration voltage of 20 kV under low vacuum and then EDX were taken to find out the metal content of sample. In this method, error in the results obtained is upto±10%.

3.3.5 Fourier Transform Infra Red (FTIR) Spectral Analysis

Fourier transform infra red (FTIR) spectroscopy is a very powerful technique to identify the existence of functional groups present in the samples. Principle of FTIR is based on characteristic frequencies of vibration of bonds and groups of bonds. Infrared source emits the infra red radiation of different wavelengths. These infrared rays pass through interferometer which modulates the infrared radiation. Thereafter it passed through sample which absorbs infrared energy at a particular frequency. This frequency is detected by detector of FTIR spectrometer and record the background spectrum. Nicolet Avatar 370 CsI

spectrometer (Thermo Electron Corporation, USA) was used to obtain FTIR spectra over a range of 4000-400 cm^{-1} using KBr pellet.

3.3.6 Thermo Gravimetric Analysis (TGA)

Thermo gravimetric analysis (TGA) is powerful technique which permits monitoring of continuous weight loss of the sample as a function of temperature or time under oxidative or inert atmosphere. TGA studies were performed under air atmosphere having flow rate 200 $ml.min^{-1}$ and temperature range from room temperature to 1000°C with heating rate 10°C.min^{-1}. Aluminium was used as reference material with 8 mg sample taken in ceramic crucible.

3.3.7 Cyclic Voltammetry

Cyclic voltammetric analysis of pyrrole and indole containing aqueous solution before and after electrochemical treatment were done by voltammetric analyzer (Autolab potentiostat/galvanostat, model PGSTAT101). The assembly consisted of glassy carbon electrode as working electrode. Other platinum and Ag/AgCl electrodes were known to be counter and reference electrodes, respectively. Here voltammograms were recorded using working electrode between -2.0 and +2.0V with scan rate 100 $mV.s^{-1}$. Potentiometric data were collected at 25±3°C by getting cyclic voltammograms with reference to Ag/AgCl electrode.

3.3.8 Filterability

In this study, ceramic Buchner funnel of 90 mm internal diameter and filter area of 6.363×10^{-3} m^2 was used. A filter paper having pore size 11 µm (grade 1) was supported on this funnel for filtration purpose. Slurry of pyrrole and indole treated aqueous solution was filled upto 60% volume of funnel and filtration characteristics was studied at ambient temperature. Here filtrate was collected in 10.5 mm internal diameter and 1.12 m long vertical cylinder at regular interval of time by neglecting filtrate volume in first two minutes [Gale, 1967]. The filtration end obtained when $\Delta t/\Delta V$ versus V plot deviated from straight line [Zingler, 1969]. Filtered cake was carefully removed and dried at 105°C in the oven so as to attain constant weight.

3.4 ADSORPTION

3.4.1 Single-component Batch Adsorption Study

Batch adsorption experiments were carried out to optimize the adsorption process parameters like initial pH (pH_o), contact time (t), adsorbent dose (m) and temperature (T) for individual removal of pyrrole and indole from aqueous solution. For single component adsorption, 100 ml of known pyrrole or indole solution was taken in 250 ml stoppered conical flask with known amount of adsorbents. 0.1 M HCl and NaOH solutions were used to adjust the initial pH of the solution. Mixture was agitated at constant speed of 150 rpm in a temperature controlled orbital shaker maintaining specific temperatures such as 15°C, 30°C and 45°C. The residual concentration of pyrrole or indole was determined in the supernatant obtained after centrifuging the experimental sample.

3.4.2 Binary Mixture Adsorption Study using Taguchi (L_{27}) Methodology

Parameters for adsorption of the compounds from binary mixture of pyrrole and indole by using GAC and BFA were optimized by using Taguchi's design of experiments. Taguchi statistical design has been employed to carry out less number of experiments by screening important factors from multiple factors. This screening improves the quality characteristic of process parameters and reduces time and cost of experimental investigation. Taguchi's optimization process involves four main phases:

I. Planning the experiments

II. Performing the experiments

III. Analysis of experimental data

IV. Validation of the optimized conditions

Step involved in phase I for adsorptive removal of pyrrole and indole from binary mixture of aqueous solution using GAC and BFA was to design the matrix experiment and to define data analysis procedure. First step is the identification of performance characteristics and selection of process parameters. Second step is to decide the number of process parameters and their interaction. Based on the previous study for individual compound

adsorption, factors that affected the simultaneous removal of pyrrole and indole from waste water onto GAC and BFA were identified. In the present study, five process parameters were selected for experimental design. The process parameters and their level are given in Table 3.4.1. In simultaneous adsorption, two parameter interactions between initial concentrations of adsorbates ($C_{o,Py} \times C_{o,Ind}$) are very important as removal efficiency is sometimes highly dependent on the characteristic interactive properties of the compounds.

Third step is to select orthogonal array (OA) and assign parameters to it. The selected OA must satisfy the inequality that the total degree of freedom required for the experiment should be less than or equal to total degree of freedom (DOF) of the OA. The total required degree of freedom for the experiment is 14 ($5 \times (3-1) + 1 \times 4 = 14$). This is due to the fact that three level parameter has DOF=2 (number of levels-1) and for each two parameter interaction DOF value is 4 (2x2). Based upon the number of parameters and their levels, L_{27} OA (Table 3.4.2) was used for carrying out experiments for simultaneous pyrrole and indole adsorption onto GAC and BFA.

Table 3.4.1: Multi-component adsorption study parameters for the adsorption of pyrrole and indole onto GAC and BFA using Taguchi's OA.

	Parameters		Units	Levels GAC			Levels BFA		
				0	1	2	0	1	2
A:	Initial concentration of pyrrole	$C_{o,Py}$	(mmol.l^{-1})	0	3.73	7.45	0	3.73	7.45
B:	Initial concentration of indole	$C_{o,Ind}$	(mmol.l^{-1})	0	2.13	4.27	0	2.13	4.27
C:	Temperature	T	(°C)	15	30	45	15	30	45
D:	Adsorbent dose	m	(g.l^{-1})	4	12	20	4	9	14
E:	Contact time	t	(min)	60	360	660	60	300	540

In phase II, batch adsorption experiments were conducted for simultaneous removal of binary compounds. Synthetic stock solution of pyrrole and indole were prepared with double distilled water to 500 mg.l^{-1} and 1000 mg.l^{-1}. Mixing were done in equal proportion to get binary mixture each having concentrations 250 mg.l^{-1} or 500 mg.l^{-1}. Similarly, binary mixtures of different concentrations of each solute were prepared. In each experimental run, 100 ml of a solution containing desired concentration of indole and pyrrole with desired adsorbent dose of GAC and BFA were taken in a 250 ml conical flask with glass stopper. This flask was kept in an orbital shaker under controlled temperature at shaking rate of 150 rpm. Most of the experiments were performed at three temperatures (i.e. at 15, 30 and 45°C) while isotherm study was done at 30°C only. After the desired contact time, samples were withdrawn, centrifuged at 10,000 rpm for 5 min using research centrifuge (Remi Instruments, Mumbai) and analyzed for residual pyrrole and indole concentration with the help of UPLC.

The equilibrium adsorption uptake ($q_{e,i}$), individual adsorption yield ($Ad_i\%$) and total adsorption yields ($Ad_{Tot}\%$) were calculated using the following expressions:

$$q_{e,i} = (C_{o,i} - C_{e,i})V/w, \text{ (mmol of adsorbate.g}^{-1}\text{ of adsorbent)} \qquad (3.4.1)$$

$$Ad_i\% = 100\,(C_{o,i} - C_{e,i})/C_{0,i} \qquad (3.4.2)$$

$$Ad_{Tot}\% = 100\sum(C_{o,i} - C_{e,i})\Big/\sum C_{0,i} \qquad (3.4.3)$$

where, C_o and C_e are initial and equilibrium adsorbate concentration (mmol.l^{-1}), V is the volume of the adsorbate containing solution (l) and w is the mass of the adsorbent (g).

In phase III, the experimental data was analyzed (i) to obtain the optimum conditions for adsorption, (ii) to identify the effect of individual parameters on adsorption, and (iii) to estimate q_{tot} at optimum conditions. Taguchi has suggested many methods for analyzing the data and in this present study, plot of average response curves and analysis of variance (ANOVA) of data have been used.

Table 3.4.2 : Taguchi's L_{27} (3^{13}) orthogonal array for multi-component adsorption of pyrrole and indole system onto GAC and BFA.

Exp. No.	GAC					BFA				
	A	B	C	D	E	A	B	C	D	E
1	0	0	15	4	1	0	0	15	4	1
2	0	0	30	12	6	0	0	30	9	5
3	0	0	45	20	11	0	0	45	14	9
4	0	2.13	15	4	1	0	2.13	15	4	1
5	0	2.13	30	12	6	0	2.13	30	9	5
6	0	2.13	45	20	11	0	2.13	45	14	9
7	0	4.27	15	4	1	0	4.27	15	4	1
8	0	4.27	30	12	6	0	4.27	30	9	5
9	0	4.27	45	20	11	0	4.27	45	14	9
10	3.73	0	15	12	11	3.73	0	15	9	9
11	3.73	0	30	20	1	3.73	0	30	14	1
12	3.73	0	45	4	6	3.73	0	45	4	5
13	3.73	2.13	15	12	11	3.73	2.13	15	9	9
14	3.73	2.13	30	20	1	3.73	2.13	30	14	1
15	3.73	2.13	45	4	6	3.73	2.13	45	4	5
16	3.73	4.27	15	12	11	3.73	4.27	15	9	9
17	3.73	4.27	30	20	1	3.73	4.27	30	14	1
18	3.73	4.27	45	4	6	3.73	4.27	45	4	5
19	7.45	0	15	20	6	7.45	0	15	14	5
20	7.45	0	30	4	11	7.45	0	30	4	9
21	7.45	0	45	12	1	7.45	0	45	9	1
22	7.45	2.13	15	20	6	7.45	2.13	15	14	5
23	7.45	2.13	30	4	11	7.45	2.13	30	4	9
24	7.45	2.13	45	12	1	7.45	2.13	45	9	1
25	7.45	4.27	15	20	6	7.45	4.27	15	14	5
26	7.45	4.27	30	4	11	7.45	4.27	30	4	9
27	7.45	4.27	45	12	1	7.45	4.27	45	9	1

In phase IV, confirmation of experiments is decisive step in which conclusion was drawn from previous step of experiments. The optimum experimental conditions are set for the significant factors and preferred numbers of experiments are performed under constant specified conditions. Average confirmation experimental results are compared with the predicted average based on parameters and levels tested. To avoid any kind of personal or subjective bias the experiments were carried out in randomized sequence.

3.4.3 Multi-Component Isotherm Study

For binary isotherm study, binary mixture of pyrrole and indole were taken and simultaneous adsorption was studied at 30°C. For each initial concentration of indole: 50, 100, 250, 500 and 750 $mg.l^{-1}$, initial concentration of pyrrole was varied from 50 to 750 $mg.l^{-1}$. Experiments were performed in orbital shaker with 20 $g.l^{-1}$ GAC and 7 $g.l^{-1}$ BFA. Samples were withdrawn and analyzed for residual concentration of pyrrole and indole using UPLC.

Various multi-component isotherms (Table 3.4.3) like non-modified, modified and extended-Langmuir, R-P models, extended-Freundlich, etc. were used to fit the data obtained from simultaneous adsorption of pyrrole and indole onto GAC and BFA using sum of square of error (SSE) as the error function. SSE for multi-component adsorption of pyrrole and indole by GAC and BFA is given as under:

$$SSE = \sum_{i=1}^{n} ((q_{e,meas} - q_{e,calc})_{Ind} + (q_{e,meas} - q_{e,calc})_{Py})_i^2 \qquad (3.4.4)$$

Table 3.4.3: Multicomponent isotherm models.

Name of the model	Model equation	Reference
Non-modified Langmuir model	$q_{e,i} = \frac{q_{m,i} K_{L,i} C_{e,i}}{1 + \sum_{j=1}^{N} K_{L,j} C_{e,j}}$	
Modified Langmuir model	$q_{e,i} = \frac{q_{m,i} K_{L,i} \left(\frac{C_{e,i}}{\eta_{L,i}} \right)}{1 + \sum_{j=1}^{N} K_{L,j} \left(\frac{C_{e,j}}{\eta_{L,j}} \right)}$	[Bellot and Condoret, 1993]
Extended Langmuir	$q_{e,i} = \frac{q_{\max} K_{EL,i} C_{e,i}}{1 + \sum_{j=1}^{N} K_{EL,j} C_{e,j}}$	[Yang, 1987]
Extended Freundlich	$q_{e,1} = \frac{K_{F,1} C_{e,1}^{n_1 + x_1}}{C_{e,1}^{x_1} + y_1 C_{e,2}^{z_1}}$, $q_{e,2} = \frac{K_{F,2} C_{e,2}^{n_2 + x_2}}{C_{e,2}^{x_2} + y_2 C_{e,1}^{z_2}}$	[Fritz and Schluender, 1974]
Non-modified Redlich-Peterson	$q_{e,i} = \frac{K_{R,i} C_{e,i}}{1 + \sum_{j=1}^{N} a_{R,j} C_{e,j}^{\beta_j}}$	
Modified Redlich-Peterson	$q_{e,i} = \frac{K_{R,i} \left(\frac{C_{e,i}}{\eta_{R,i}} \right)}{1 + \sum_{j=1}^{N} a_{R,j} \left(\frac{C_{e,j}}{\eta_{R,j}} \right)^{\beta_j}}$	[Srivastava et al., 2006]
Sheindorf-Rebuhn-Sheintuch (SRS) Model	$q_{e,i} = K_{F,i} C_{e,i} \left(\sum_{j=1}^{N} a_{ij} C_{e,j} \right)^{(1/n_i)-1}$	[Sheindorf et al., 1981]

3.5 ELECTROCHEMICAL TREATMENT

3.5.1 Experimental Program for Electrochemical Treatment

Electrochemical treatment experiments were performed in circular glass batch reactor having 1 litre volume. Dimensional characteristics of electrochemical cell used in this study are given in Table 3.5.1. Experiments were performed under controlled current condition which was monitored by a direct current (D.C.) power supply.

Pt/Ti electrodes were used having actual dipped anodic area of 0.012 m^2 in the aqueous solution containing pyrrole and indole individually with 1 cm electrode gap (Figure 3.5.1). For binary system, both solutions were mixed in varying concentration. Conductivity of the solution was adjusted by adding NaCl [Sengil and Ozdemir, 2012]. All experiments were conducted with controlled temperature of 30±2°C. After desired treatment time, the treated solution was centrifuged and residual concentration in terms of chemical oxygen demand (COD) was determined.

Table 3.5.1: Dimensional characteristics of electrochemical cell.

Reactor Characteristics	
Material	Glass
Reactor type	Batch
Working volume	1litre
Stirring mechanism	Magnetic bar
Electrode Characteristics	
Material (Anode and Cathode)	Platinum coated with Titanium plate
Shape	Rectangular plate
Size of each plate (cm)	10×8.5
Thickness (mm)	1.5
Plate arrangement	Parallel
Submergence(deeped anodic area)	0.012 m^2

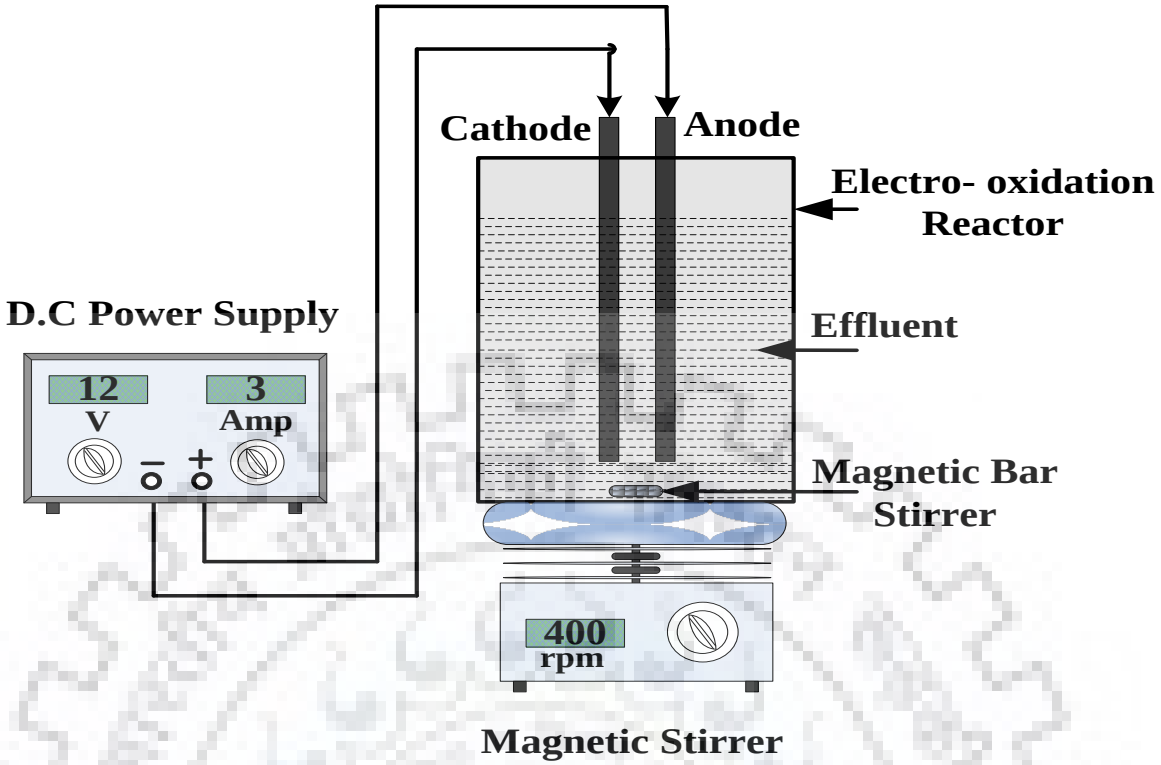

Figure 3.5.1: Schematic diagram of experimental setup.

3.5.2 Response Surface Methodology (RSM) for Experimental Design

Response surface methodology (RSM) is the statistical technique used for optimizing responses. The main advantage of this technique is to reduce the number of experiments for getting responses. In the present study, four factor and five levels central composite (CC) design was used (Table 3.5.2). Experimental data obtained were analyzed by Design expert software version 6.0.8 (STAT-EASE Inc., Minneapolis, USA).

Levels of four factors were coded as x_i for statical calculation of parameters X_i (X_1 (pH_0)), X_2 (J), X_3 (K), X_4 (t) based on levels designated as −2, −1, 0, +1, and +2 [Thakur et al., 2009].

$$x_i = \frac{(X_i - X_0)}{\delta X} \qquad (3.5.1)$$

where, x_i is coded value of factor X_i, X_o and δX *denotes* step change. Percent COD removal (Y_1) and specific energy consumption (Y_2) in (kWh/kg COD removed) have been taken as responses for this design given in Table 3.5.3.

Following second-order polynomial equation was used to fit the experimental data obtained:

$$Y = c_o + \sum_{i=1}^{4} c_i X_i + \sum_{i=1}^{4} c_{ii} X_i^2 + \sum_{i=j}^{3} \sum_{i=j+1}^{4} c_{ij} X_{ij} \qquad (3.5.2)$$

where, Y is response; c_o, c_i, c_{ii}, c_{ij} are constant coefficients and X_i are the independent variables.

Since in this study, there were two responses, therefore, multi-response processes optimization by desirability function approach used to optimize the electrochemical treatment. Simultaneous optimization combines all the different response requirements into one composite requirement. Among the multi-response optimization techniques, desirability function approach is one of the most frequently used in practice (Derringer et al., 1980). One-sided desirability d_i is given by:

$$d_i = \begin{cases} 0 & if \quad Y_i \le Y_{i-\min} \\ \left[\dfrac{Y_i - Y_{i-\min}}{Y_{i-\max} - Y_{i-\min}}\right]^r & If \ Y_{i-\min} < Y_i < Y_{i-\max} \\ 1 & if \ Y_i \ge Y_{i-\max} \end{cases} \qquad (3.5.3)$$

where, Y_i is known to be response value, $Y_{i\text{-}min}$ and $Y_{i\text{-}max}$ are known as minimum and maximum values of response *i*, respectively. *r* is known as positive constant [Kushwaha et al., 2010].

Table 3.5.2: Parameters and their level used to design model.

Factor	Variable	Range of actual and coded variables				
		-2	-1	0	1	2
A	Initial pH, pH_0	2.8	4.3	5.8	7.3	8.8
B	Current density, j ($A.m^{-2}$)	83.34	166.67	250	333.33	416.66
C	Conductivity, *k* ($ms.cm^{-1}$)	2.91	3.86	4.80	5.75	6.7
D	Time of electrolysis, *t* (min)	30	60	90	120	150

Table 3.5.3: Full factorial design for prediction of COD removal (Y_1) and Energy consumption (Y_2) in (kWh per kg COD removed).

Std order	pH_0	Current density, j ($A.m^{-2}$)	Conductivity, k ($mS.cm^{-1}$)	Time (min)
1	4.3	166.67	3.86	60
2	7.3	166.67	3.86	60
3	4.3	333.33	3.86	60
4	7.3	333.33	3.86	60
5	4.3	166.67	5.75	60
6	7.3	166.67	5.75	60
7	4.3	333.33	5.75	60
8	7.3	333.33	5.75	60
9	4.3	166.67	3.86	120
10	7.3	166.67	3.86	120
11	4.3	333.33	3.86	120
12	7.3	333.33	3.86	120
13	4.3	166.67	5.75	120
14	7.3	166.67	5.75	120
15	4.3	333.33	5.75	120
16	7.3	333.33	5.75	120
17	2.8	250	4.80	90
18	8.8	250	4.80	90
19	5.8	83.34	4.80	90
20	5.8	416.66	4.80	90
21	5.8	250	2.91	90
22	5.8	250	6.69	90
23	5.8	250	4.80	30
24	5.8	250	4.80	150
25	5.8	250	4.80	90
26	5.8	250	4.80	90
27	5.8	250	4.80	90
28	5.8	250	4.80	90
29	5.8	250	4.80	90
30	5.8	250	4.80	90

If a response falls within the unacceptable intervals, the desirability is 0, and if a response reaches its ideal value, the desirability is 1. Meanwhile, when a response fails to reach its ideal value, the desirability lies between 0 and 1. The more closely the response approaches the ideal values, the closer the desirability is to 1. In the multi-response processes optimization, desirability function transforms each response to a corresponding desirability value between 0 and 1. All the desirability is combined to form a composite desirability function which converts a multi-response into a one single response. The individual desirability functions are combined in order to obtain the overall desirability D, as follows:

$$D = (d_1 \times d_2 \times d_3 .....)^{\frac{1}{i}} \qquad (3.5.4)$$

where, $0 \leq D \leq 1$ and i is known as number of responses. If all of the quality characteristics reach their ideal values, the desirability d_i is 1 for all i. Consequently, the total desirability is also 1. If any one of the responses does not reach its ideal value, the desirability d_i is below 1 for that response and the total desirability is below 1. If any one of the responses cannot meet the quality requirements, the desirability d_i is 0 for that response. Total desirability will then be 0.

3.5.3 Binary Mixture Electrochemical Treatment using Taguchi (L_{16}) Methodology

Parameters for electrochemical treatment of binary mixture of pyrrole and indole by platinum coated titanium (Pt/Ti) electrode were optimized by using Taguchi's design of experiments (L_{16}). Taguchi's optimization process involves phases as planning the experiments, performing the experiments, analysis of experimental data, validation of the optimized conditions. First step is the identification of performance characteristics and selection of process parameters. Second step is to decide the number of process parameters and their interaction. In the present study, five process parameters and four levels were selected for experimental design. The process parameters and their level are given in Table 3.5.4. Third step is to select orthogonal array (OA) and assigned parameters to it. Based upon the number of parameters and their levels, L_{16} OA (Table 3.5.5) was used for carrying out

experiments for simultaneous electrochemical treatment of pyrrole and indole by Pt/Ti electrode.

In phase II, batch experiments were conducted for simultaneous electrochemical treatment of binary compounds. Synthetic stock solution of pyrrole and indole were prepared with double distilled water having different concentrations. Mixing was done in equal proportion to get appropriate concentrations as per OA for $L_{16.}$ Experiments were performed under controlled current electrolysis which was monitored by D.C. power Supply. Pt/Ti electrodes were used having actual dip anodic area 0.012 m^2 and 1cm electrode gap. Same procedure was repeated as done for individual compound as per standard order. After the desired contact time, Samples were withdrawn at appropriate time, centrifuged at 10,000 rpm for 5 min using research centrifuge (Remi Instruments, Mumbai) and analyzed for residual pyrrole and indole concentration with the help of UPLC.

Table 3.5.4: Parameters and levels for simultaneous electrochemical treatment of pyrrole and indole by Pt/Ti electrode using Taguchi's (L_{16}) OA.

	Parameters		Units	Levels			
				1	2	3	4
A:	Initial concentration of pyrrole	$C_{o,Py}$	$mg.l^{-1}$	50	200	350	500
B:	Initial concentration of indole	$C_{o,Ind}$	$mg.l^{-1}$	50	200	350	500
C:	Current density	j	$A.m^{-2}$	83.33	166.7	250	333.3
D:	Conductivity	k	$mS.cm^{-1}$	2.44	3.86	5.28	6.7
E:	Time	t	min	30	70	110	150

Table 3.5.5: Taguchi's L_{16} orthogonal array for multi-component electrochemical treatment of pyrrole and indole by Pt/Ti electrode.

Exp. no.	std. order	$C_{o,Py}$ ($mg.l^{-1}$)	$C_{o,Ind}$ ($mg.l^{-1}$)	j ($A.m^{-2}$)	k ($mS.cm^{-1}$)	t (min)
1	1	50	50	83.33	2.44	30
2	2	50	200	166.7	3.86	70
3	3	50	350	250	5.28	110
4	4	50	500	333.3	6.7	150
5	5	200	50	166.7	5.28	150
6	6	200	200	83.33	6.7	110
7	7	200	350	333.3	2.44	70
8	8	200	500	250	3.86	30
9	9	350	50	250	6.7	70
10	10	350	200	333.3	5.28	30
11	11	350	350	83.33	3.86	150
12	12	350	500	166.7	2.44	110
13	13	500	50	333.3	3.86	110
14	14	500	200	250	2.44	150
15	15	500	350	166.7	6.7	30
16	16	500	500	83.33	5.28	70

Chapter -4

RESULTS AND DISCUSSION

This chapter presents the results and discussion pertaining to removal/degradation of pyrrole and indole from aqueous solution by adsorption onto granular activated carbon (GAC) and bagasse fly ash (BFA), and electrochemical treatment using platinum coated titanium (Pt/Ti) electrode. This chapter has been sub divided into the following section:

- Characterization of GAC and BFA
- Adsorptive removal of pyrrole and indole by GAC
  - Optimization of parameters for individual removal of pyrrole and indole by GAC
  - Optimization of parameters for simultaneous removal of pyrrole and indole by GAC using Taguchi's methodology
  - Multi-component isotherm study for simultaneous removal of pyrrole and indole by GAC
- Adsorptive removal of pyrrole and indole by BFA
  - Optimization of parameters for individual removal of pyrrole and indole by BFA
  - Optimization of parameters for simultaneous removal of pyrrole and indole by BFA using Taguchi's methodology
  - Multi-component isotherm study for simultaneous removal of pyrrole and indole by BFA
- Treatment of pyrrole and indole electrochemical method using Pt/Ti electrode.
  - Optimization of parameters for individual removal of pyrrole and indole using response surface methodology (RSM)
    - ✓ Study of effect of various parameters such as pH, current density, conductivity and electrolysis time on simultaneous optimization of responses (maximization of chemical oxygen demand (COD) and minimization of specific energy consumed (kWh/kg of COD removed) by using desirability approach

- Optimization of parameters for simultaneous electrochemical treatment of pyrrole and indole in aqueous solution by using Taguchi's methodology.
- Characterization of electrode, aqueous solution containing pyrrole and indole, and the residues.

4.1 CHARACTERIZATION OF GAC AND BFA

4.1.1 Physico-chemical Characterization

The adsorbents, GAC and BFA were characterized for various physico-chemical properties such as surface area, pore volume, morphology, thermal stability, etc. Proximate analysis showed the presence of 9.1% moisture, 27.3% volatile matter, 2.1% ash and 61.5% fixed carbon in the blank GAC. Moisture content, volatile matter, ash content and fixed carbon in blank BFA were found to be 10.9%, 33.8%, 22.8% and 32.5%, respectively. Bulk density for GAC and BFA were found to be 628 $kg.m^{-3}$ and 133 $kg.m^{-3}$, respectively. Physico-chemical characteristics of GAC and BFA are given in Table 4.1.1.

Pore size distribution of adsorbents helps in understanding the structural heterogeneity of porous materials. GAC and BFA have wide distribution of surface area and pore volume as shown in Figure 4.1.1 [Aroua et al., 2008]. Before adsorption, GAC (355 $m^2.g^{-1}$) was found to have greater Brunauer-Emmett-Teller (BET) surface area as compared to BFA (201 $m^2.g^{-1}$). Similarly, Barrett-Joyner-Halenda (BJH) adsorption/desorption surface area of pores for GAC and BFA were found to be 47.98/36.64 $m^2.g^{-1}$ and 42.22/32.74 $m^2.g^{-1}$, respectively. Single point total pore volume of pores for GAC and BFA were found to be 0.18 and 0.11 $cm^3.g^{-1}$, whereas BJH adsorption/desorption cumulative pore volume for GAC and BFA were 0.029/0.022 $cm^3.g^{-1}$ and 0.029/0.023 $cm^3.g^{-1}$, respectively. Overall micro-pores (pore diameter (d) < 20 Å) accounted for total pore area of 42.88% in GAC and 34.76% in BFA. Also, meso-pores (20 Å < d < 500 Å) accounted for total pore area of 57.11% in GAC and 65.24% in BFA.

Table 4.1.1: Physico-chemical characteristics of GAC and BFA.

Characteristics	**GAC-Blank**	**BFA-Blank**
Proximate analysis		
Moisture content	9.1	10.9
Volatile matter (%)	27.3	33.8
Ash content (%)	2.1	22.8
Fixed carbon (%)	61.5	32.5
Bulk density ($kg.m^{-3}$)	628	133
Textural characterization		
Surface area of pores ($m^2.g^{-1}$)		
(i) BET	355	201
(ii) BJH		
(b) Adsorption cumulative	47.98[b]	42.22[b]
(b) Desorption cumulative	36.64[b]	32.74[b]
BJH cumulative pore volume($cm^3.g^{-1}$)		
Single point total	0.188[a]	0.112[a]
BJH adsorption	0.029[b]	0.029[b]
BJH desorption	0.022 [b]	0.023[b]
Average pore diameter (Å)		
(i) BET	21.25	22.17
(ii) BJH adsorption	24.55	28.04
(iii) BJH desorption	23.96	27.61
Point of zero charge (pH_{pzc})	9.9	9.43

[a]Pores less than 207.69Å diameter; [b]Pores between 17 and 3000Å diameter

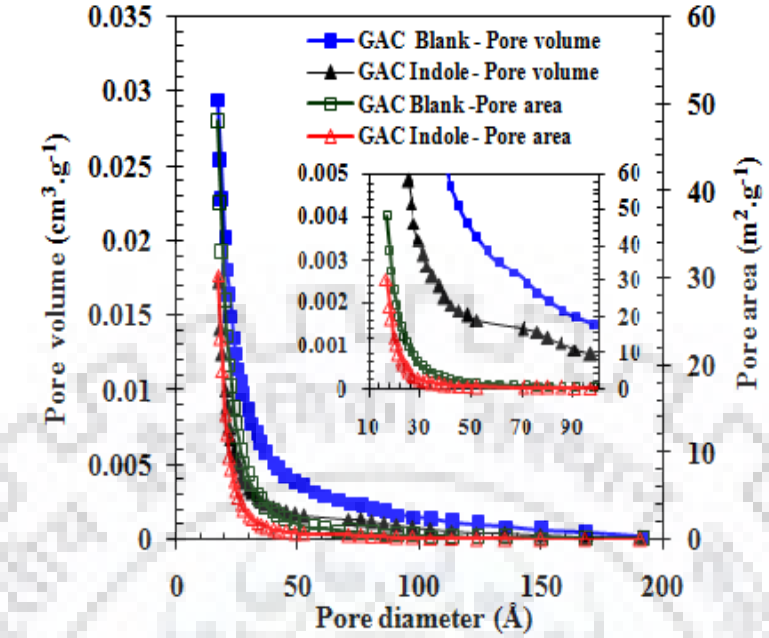

(a) GAC

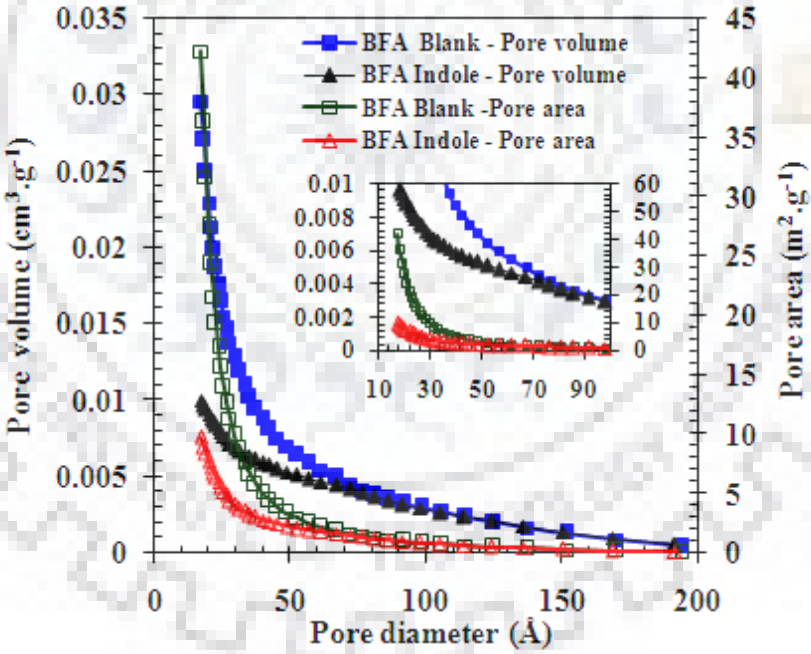

(b) BFA

Figure 4.1.1: Pore Size distribution of blank and loaded, GAC and BFA.

Frenkel-Halsey-Hill (FHH) equation (equation 3.3.4) was used for finding the value of fractal dimension (D_f) for both GAC and BFA. Values of D_f for GAC and BFA were found to be 2.978 and 2.957, respectively. It is known that for smooth surface, the D_f has a value of 2 whereas for rough irregular surface its value is about 3 [Srivastava et al., 2008b]. Thus, overall GAC is more porous in nature as compared to BFA, however, both GAC and BFA are mesoporous in nature and that both have similar heterogeneous surface.

4.1.2 Point of Zero Charge (pH_{PZC})

System pH affects the adsorptive process through dissociation of functional groups on the active sites of the adsorbent surface. This pH change affects the kinetics and equilibrium characteristics of the adsorption process. To understand the adsorption mechanism, it is necessary to determine the point of zero charge (pH_{PZC}) of the GAC and BFA. Lower value of pH_{PZC} results in adsorption of cations, whereas high value helps in specific adsorption of anions. Figure 4.1.2 shows that for all the concentrations of KNO_3, the zero value of ΔpH and hence, pH_{PZC} for GAC and BFA lies at the pH_0 value of ≈9.5. At low pH (e.g., pH < pH_{PZC}), adsorbents are positively charged. The adsorption of cations is favored at $pH > pH_{PZC}$, while the adsorption of anions is favored at $pH < pH_{PZC}$.

4.1.3 Scanning Electron Microscopy

Scanning electron micrographs (SEM), shown in Figure 4.1.3, were used to examine the morphologies of GAC and BFA. Both GAC and BFA are found to have similar heterogeneous surface. After adsorption of substrates (indole and pyrrole), surface of GAC and BFA seems to be more smooth as compared to that before adsorption. Energy-dispersive X-ray (EDX) spectroscopy analysis showed the presence of 95.5% C and 4.5% O in blank GAC while blank BFA was found to contain 85.57% C, 12.88% O, 0.23% K, 0.16% Mg, 0.22% Al, 0.75% Si, 0.09% Ca and 0.10% Fe. Thus, GAC contains more amount of carbon to BFA as shown by proximate analysis.

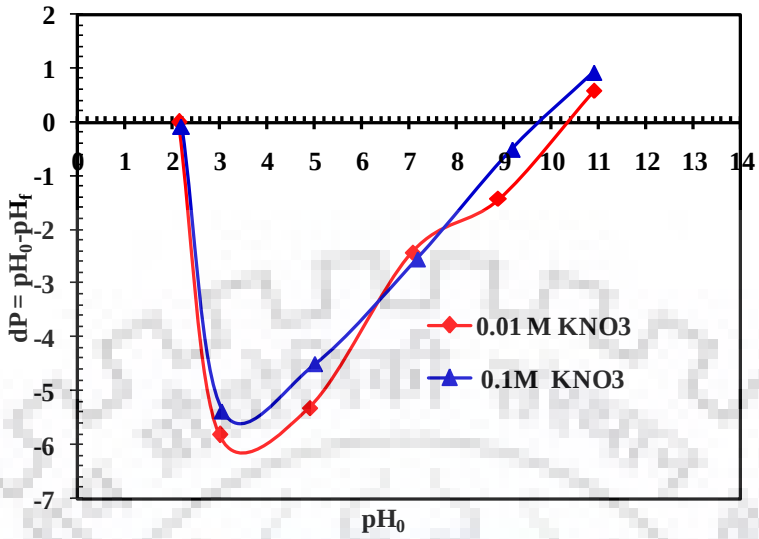

(a) GAC

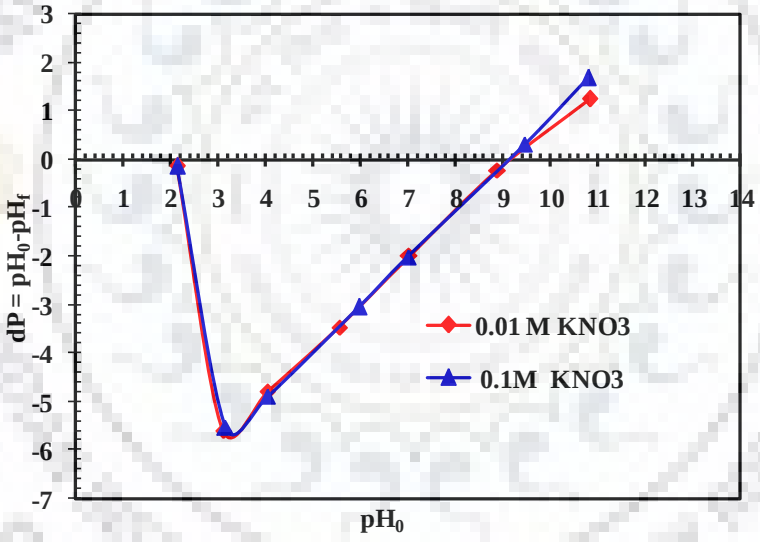

(b) BFA

Figure 4.1.2: Point of zero charge for GAC and BFA.

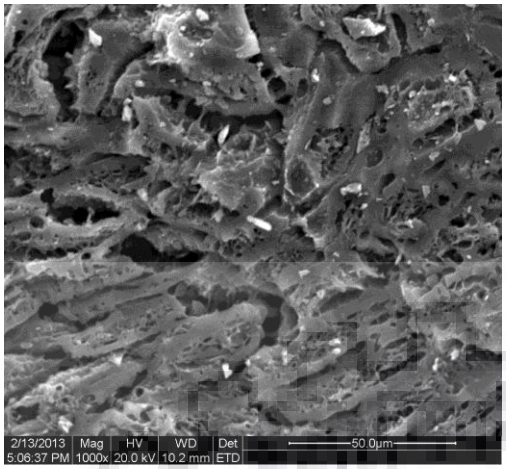

Blank GAC

Blank BFA

Pyrrole loaded GAC

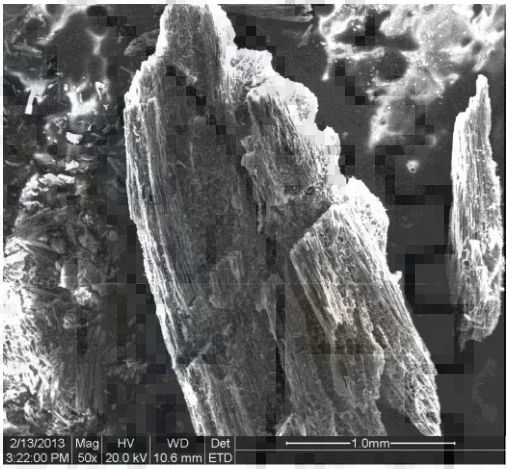

Pyrrole loaded BFA

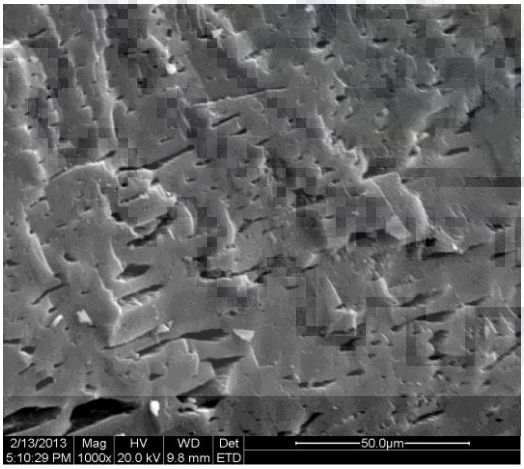

Indole loaded GAC

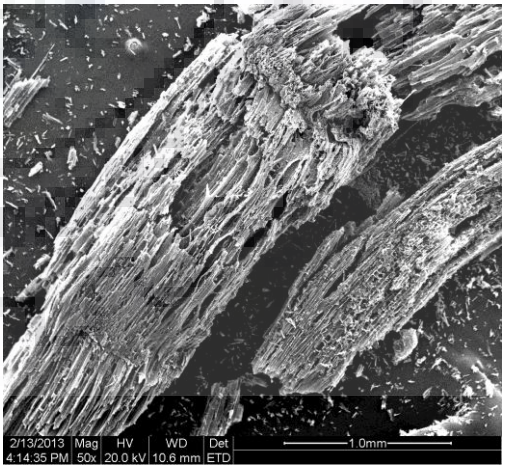

Indole loaded BFA

Figure 4.1.3: SEM of GAC and BFA before and after indole and pyrrole adsorption.

4.1.4 Fourier Transform Infrared (FTIR) Spectroscopy

FTIR spectrum (Figure 4.1.4) of GAC and BFA shows a broad band with peak at ≈3400 cm^{-1} indicating free and hydrogen-bonded OH groups. It also shows peaks at 1595 cm^{-1} and 1633 cm^{-1} indicating C=C stretch in the adsorbents. The band at 1352 and 1375 cm^{-1} is due to C-H bending in plane. The peak in the region of 1748 cm^{-1} indicates the presence of a CO group stretching from anhydride and esters. The sharp band at ≈3464 cm^{-1} is attributed to N-H stretching [Chen-Yang et al., 2004]. Bands at 2850 and 2917 cm^{-1} indicate C-H stretching on GAC and BFA. Band at 1590 cm^{-1} shows stretching and deformation of N-H bond and vibration modes of C2 and C3 aromatic bonds. The band at ≈1375 cm^{-1} is related to modes involving the C8-N-C2-C3 group. Band at ≈1235 cm^{-1} signifies the heterocyclic ring stretching modes. Also, the intensity of transmittance peaks (in blank GAC) decreases after adsorption indicating utilization of these peaks during the adsorption process. Since the adsorption of pyrrole and indole is less as compared to BFA, therefore, the shifts and increase in the intensity of peaks with respect to the functional groups of pyrrole or indole are not that visible as that for BFA. FTIR analysis shows presence of various functional groups on the surface of GAC and BFA. These groups may help in the adsorption of pyrrole and indole onto their surfaces. It is seen that alteration in transmittance observed after adsorption of substrates at various peaks suggests the breaking of bonds at particular wave number.

4.1.5 Thermogravimetric Analysis (TGA)

TGA and DTA analysis of blank GAC and BFA were done at 10 $K.min^{-1}$ heating rate (Figure. 4.1.5). It was found that weight loss due to loss of light volatile molecules and moisture for blank GAC and blank BFA were 28.6% at 381°C and 23.1% at 411°C, respectively. No endothermic transition was observed indicating no phase changes during the heating process up to these temperatures [Suresh et al., 2011b,c]. For blank BFA showed 54.9% weight loss was observed between 411°C and 503°C. For GAC, moisture and other volatile matter (~29%) gets removed up to 380 ^{o}C. After that GAC showed ~43% weight loss between 380-425°C due to degradation of hemicelluloses and cellulose. Also, a third weight loss zone occurs in the temperature range of 464-520°C with ~20% weight loss due to the degradation of lignin. This study shows that GAC is fully stable up to 381°C and that BFA is stable up to temperature of 411°C. Overall GAC and BFA can be oxidized in oxidative environment with sufficient recovery of energy.

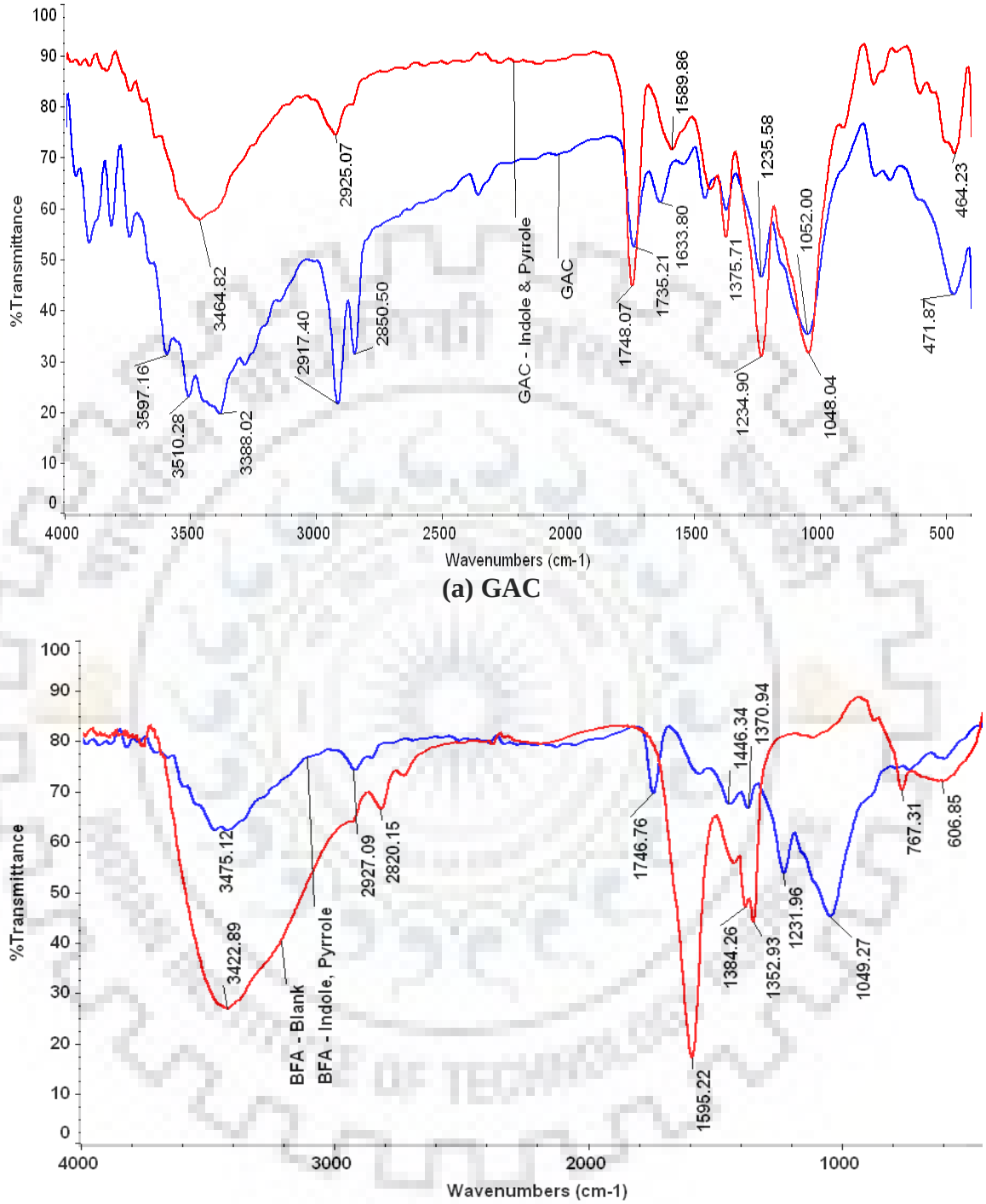

(a) GAC

(b) BFA

Figure 4.1.4: FTIR of GAC and BFA with and without indole-pyrrole adsorption.

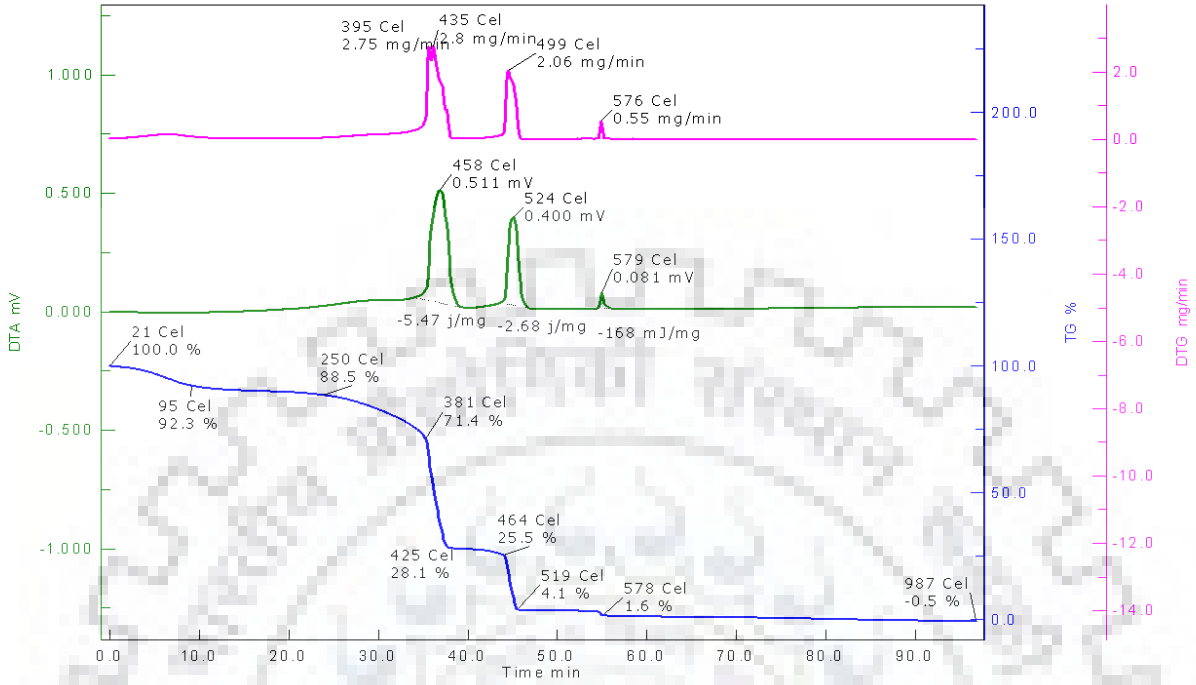

(a) GAC

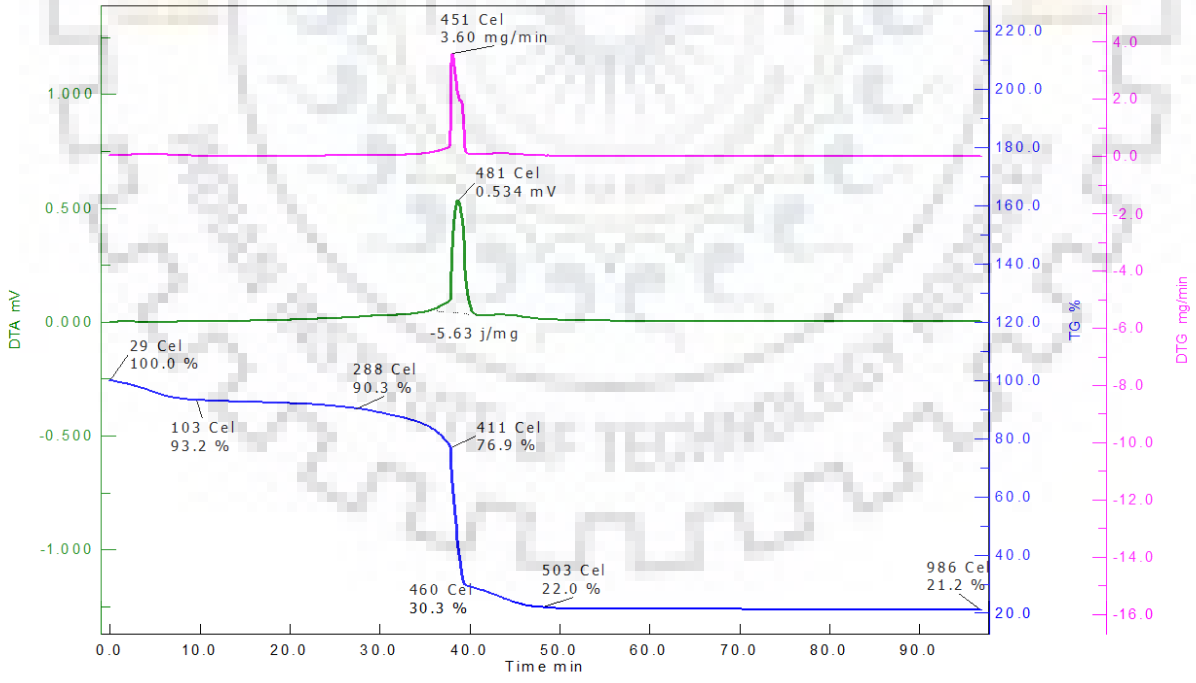

(b) BFA

Figure 4.1.5: Thermogravimetric analysis of GAC and BFA under air atmosphere.

4.2 ADSORPTIVE REMOVAL OF PYRROLE AND INDOLE BY GAC

4.2.1 Optimization of Parameters for Individual Removal of Pyrrole and Indole by GAC

In this section, various adsorption studies were carried out for adsorption of pyrrole and indole from aqueous solution onto GAC. Effect of initial pH (pH_o) ($2 \leq pH_o \leq 11$), initial indole concentration (C_o) ($100 \leq C_o \leq 1000$ mg.l^{-1}), adsorbent dose (m) ($1 \leq m \leq 20$ g.l^{-1}), contact time (t) ($0 \leq t \leq 8$ h) and temperature (T) ($288 \leq T \leq 318$ K) were investigated. Adsorption kinetics and isotherm modelling has been done by fitting the experimental data to various models. Thermodynamic parameters have been determined by classical approach.

4.2.1.1 Effect of initial pH (pH_o)

Solution pH is one of the most important parameter in adsorption operation. At lower pH concentration of H^+ is very high whereas it decreases at higher pH. The pH of the solution affects the surface charge of the adsorbents as well as degree of ionization. It is observed that surface adsorb anions at lower pH due to presence of H^+ ions whereas cations at higher pH due to deposition of OH^- ions.

Effect of initial pH (pH_o) on the adsorptive removal of pyrrole and indole was studied in the pH_o range of 2 to 11. Other parameters such as C_o (500 mg.l^{-1}), temperature (303 K), time (8 h), adsorbent dose (10 g.l^{-1} for pyrrole and 20 g.l^{-1} for indole) were kept constant. As pH_o was increased from 2.18 to 10.83, final pH (pH_f) increased from 2.53 to 10.7 for indole adsorption onto GAC. For $pH_o < 9$, adsorption of H^+ ions increased the pH_f of the solution in comparison to pH_o. However, for $pH_o \geq 9$, pH_f was $\approx pH_o$. Therefore, pH_f increased with increase in pH_o. It was observed that at all pH_o, removal efficiency of pyrrole was ≈65-67% (Figure 4.2.1) and that of indole onto GAC was ≈93-94% (Figure 4.2.2). Without adjusting the pH with HCl or NaOH, natural pH value of indole solution was found to be 5.7 approximately. At all pH_o values, the removal efficiency of pyrrole or indole from aqueous solution was found to be constant. Therefore, natural pH was selected for all further studies.

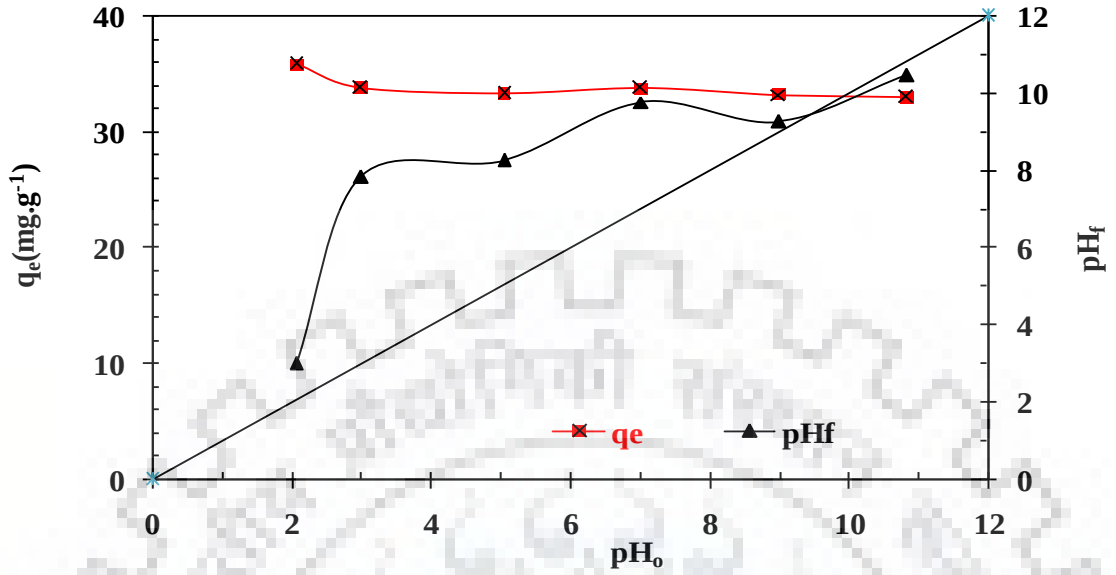

Figure 4.2.1: Effect of initial pH on the removal of pyrrole by GAC (C_o=500 mg.l^{-1}, m=10 g.l^{-1} for GAC, T=303 K, t=8 h).

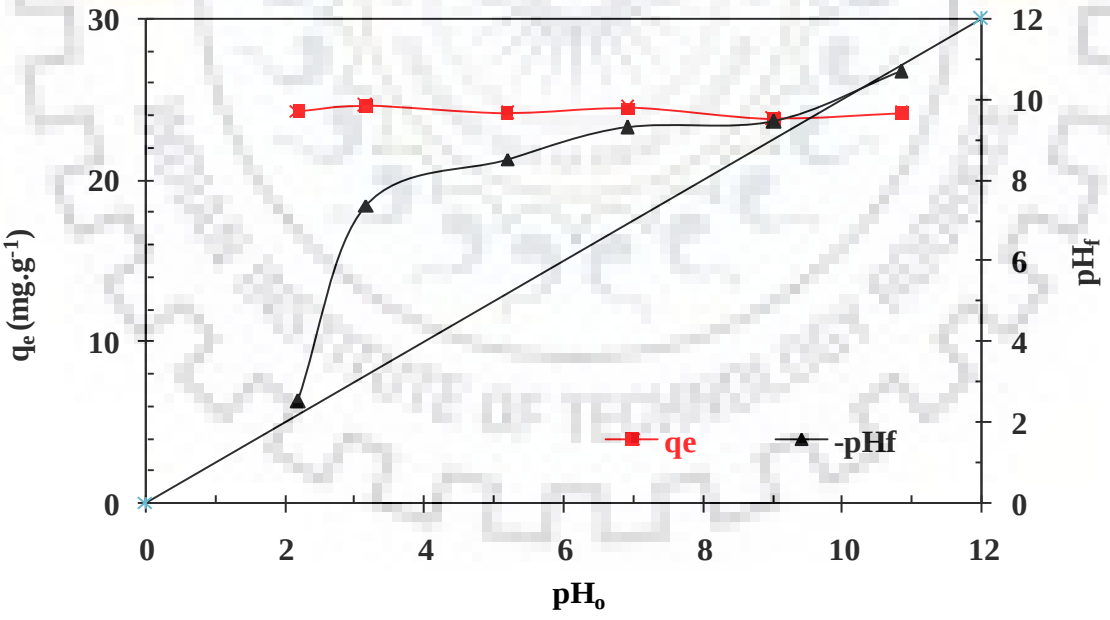

Figure 4.2.2: Effect of initial pH on the removal of indole by GAC (C_o=500 mg.l^{-1}, m=20 g.l^{-1} for GAC, T=303 K, t=8 h).

4.2.1.2 Effect of adsorbent dose

Adsorbent dose (m) is another significant factor in adsorption process. Optimization of m for pyrrole adsorption was carried out by varying GAC dose in the range 2-24 $g.l^{-1}$. Other parameter such as pH (natural), $C_{o,Py}$=500 $mg.l^{-1}$, shaking time=8 h and T=303 K were kept constant. It was observed (Figure 4.2.3) that as the m was increased, the availability of active sites for the adsorption of pyrrole increased. This increased removal efficiency of pyrrole from aqueous solution up to the GAC dose of 20 $g.l^{-1}$. Beyond this m (>20 $g.l^{-1}$), the adsorption of pyrrole was not significant and found to be constant giving 84% pyrrole removal with adsorption capacity 21.14 $mg.g^{-1}$ at specified conditions. Therefore, m=20 $g.l^{-1}$ for GAC was taken as the optimum for further studies on adsorption of pyrrole.

The effect of m value for indole adsorption onto GAC was also studied. In this study, m value was varied in the range of 1-30 $g.l^{-1}$, while C_o was 500 $mg.l^{-1}$, T=303 and t=8 h. It was observed that the increased in m value first increases uptake of indole onto GAC then it became constant (Figure 4.2.4). For indole adsorption onto GAC, removal efficiency remained constant for GAC dose ranging from 20-30 $g.l^{-1}$. For indole, optimum m (m_{opt}) was observed to be 20 $g.l^{-1}$ giving 94.9% indole removal efficiency. Therefore, m=20 $g.l^{-1}$ was taken as optimum for both pyrrole and indole adsorption onto GAC.

4.2.1.3 Effect of contact time and adsorption kinetics

Figure 4.2.5a gives the effect of time on pyrrole and indole adsorption onto GAC at different C_o (100 to1000 $mg.l^{-1}$) at natural pH. Rate of pyrrole and indole removal was found to be very rapid during first 15 min. For pyrrole adsorption onto GAC, equilibrium time was 2 h for solutions having low initial C_o and increased up to 6 h at higher C_o. This adsorptive removal of pyrrole decreased after 6 h with GAC. This may be because of large number of vacant surface sites were available for adsorption during initial stage and after lapse of time found difficulty in adsorption. This decrease in rate was due to repulsive forces between the solute present on the solid and bulk phases [Sharma et al., 2010b].

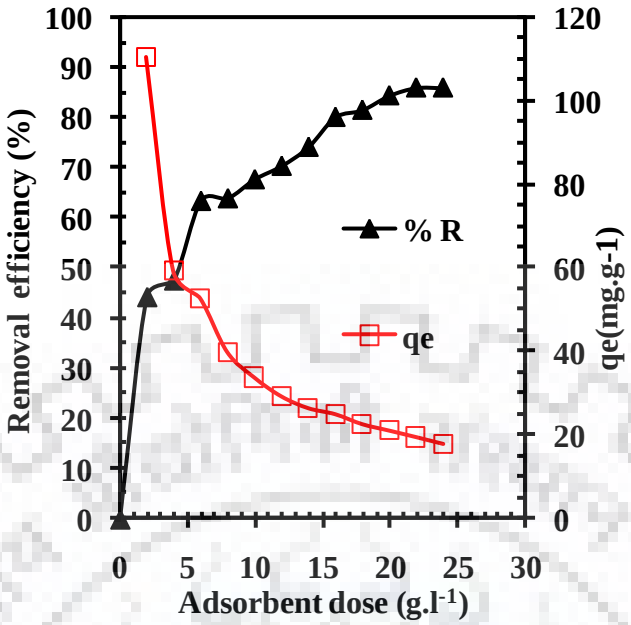

Figure 4.2.3: Effect of adsorbent dosage on the removal of pyrrole by GAC (C_o=500 mg.l^{-1}, pH_o=5.7, T=303 K, t=8 h).

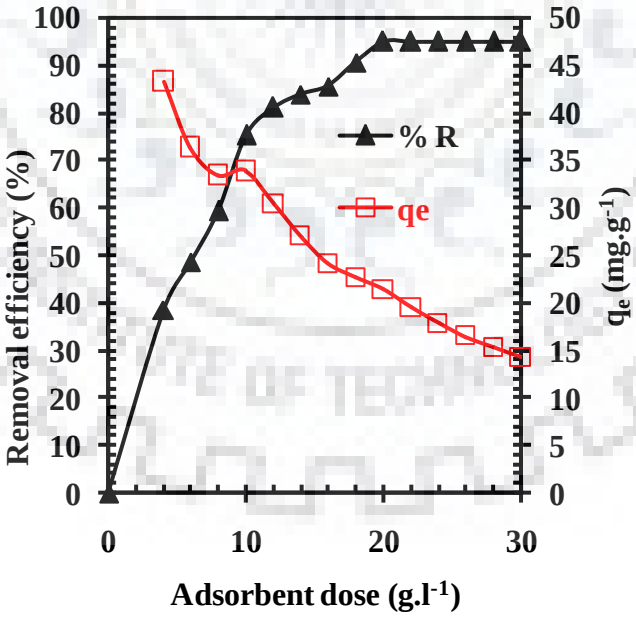

Figure 4.2.4: Effect of adsorbent dosage on the removal of indole by GAC (C_o=500 mg.l^{-1}, pH_o=5.7, T=303 K, t=8 h).

Similarly, adsorption of indole onto GAC was found to be dependent upon the indole concentration. It was very fast at the beginning of the adsorption process and slowed with decrease in residual indole concentration. Equilibrium time was found to increase with an increase in C_o. An increase in C_o increases the driving force and thus increasing the interaction between indole and the GAC. Indole adsorption onto GAC required higher equilibrium time i.e. 2 h for low concentration and 8 h for high concentration solutions. During the initial stages of adsorption, movement of indole through the film at the surface of the adsorbents is very fast, however, intraparticle diffusion in the inner pores of the adsorbents slowed down the adsorption in the second phase [Chen and Wang, 2004].

For 7.45 mmol.l^{-1} (500 mg,l^{-1}) of pyrrole, uptake of GAC after 15 min was 0.20 mmol.g^{-1} (13.32 mg.g^{-1}) and after 8 h, it was 0.33 mmol.g^{-1} (22.11 mg.g^{-1}). Similarly, for 4.27 mmol.l^{-1} (500 mg.l^{-1}) concentration of indole, uptake of GAC after 15 min was about 0.074 mmol.g^{-1} (8.61 mg.g^{-1}) and that after 8 h, it was 0.2 mmol.g^{-1} (23.33 mg.g^{-1}). Thus, the adsorption on pyrrole onto GAC was higher as compared to indole. This may be because of smaller size of pyrrole.

Pseudo-first-order kinetic model was first applied by Lagergren [1898]. It is given as under:

$$q_t = q_e \left[1 - \exp\left(-k_f t\right)\right] \qquad (4.2.1)$$

where, q_e (mg.g^{-1}) and q_t (mg.g^{-1}) show the amount of indole adsorbed on the adsorbent at equilibrium and at time t, respectively, and k_f is the pseudo first-order rate constant (min^{-1}). The pseudo second-order kinetic model is given as [Ho and McKay, 1998, 1999]:

$$q_t = \frac{t k_S q_e^2}{1 + t k_S q_e} \qquad (4.2.2)$$

The initial adsorption rate, h (mg.g^{-1}.min^{-1}), at $t \to 0$ is defined as

$$h = k_s q_e^2 \qquad (4.2.3)$$

where, k_s (g.mg^{-1}.min^{-1}) is the rate constant of the pseudo-second-order adsorption. Non-linear regression is used to check the validity of adsorption experimental data for these kinetic models. Marquardt's percent standard deviation (MPSD) error function [Marquardt, 1963] given by following equation was employed to decide the best kinetic model:

$$MPSD = 100\sqrt{\frac{1}{n-p}\sum_{i=1}^{n}\left(\frac{(q_{t,meas}-q_{t,calc})}{q_{t,meas}}\right)_i^2} \qquad (4.2.4)$$

Where, n is the number of measurements and p is the number of parameters, subscripts 'meas' and 'calc' refer to experimental and calculated values, respectively. For both pseudo-first order and pseudo-second order models, the best fit values of kinetic parameters such as k_f, h, q_e and k_s along with the coefficient of correlation (R^2) and MPSD values are shown in Tables 4.2.1 and 4.2.2, for pyrrole and indole adsorption onto GAC. Pseudo second-order kinetic model gives the best fitting to experimental data as shown low MPSD values and high R^2 values [Yaneva et al., 2013].

4.2.1.4 Intraparticle diffusion model

Intraparticle diffusion model is used to have better understanding of transport of adsorbate from the exterior surface to the pores of adsorbent [Arvindhan et al., 2007; Sharma and Das, 2013]. Intraparticle diffusion model was proposed by Weber and Morris [1963] and is represented as under:

$$q_t = k_{id}t^{1/2} + I \qquad (4.2.5)$$

where, k_{id} (mg.g^{-1}.min$^{-1/2}$) is intraparticle diffusion rate constant and I is constant representing thickness of boundary layer. Larger value of constant I shows higher thickness of boundary layer [Kavitha and Namasivayam, 2007]. If intraparticle diffusion is involved, plot of q_t versus $t^{1/2}$ should be linear in the adsorption processes. Intraparticle diffusion is said to be the rate-controlling step, if these lines pass through the origin [Gercel et al., 2007].

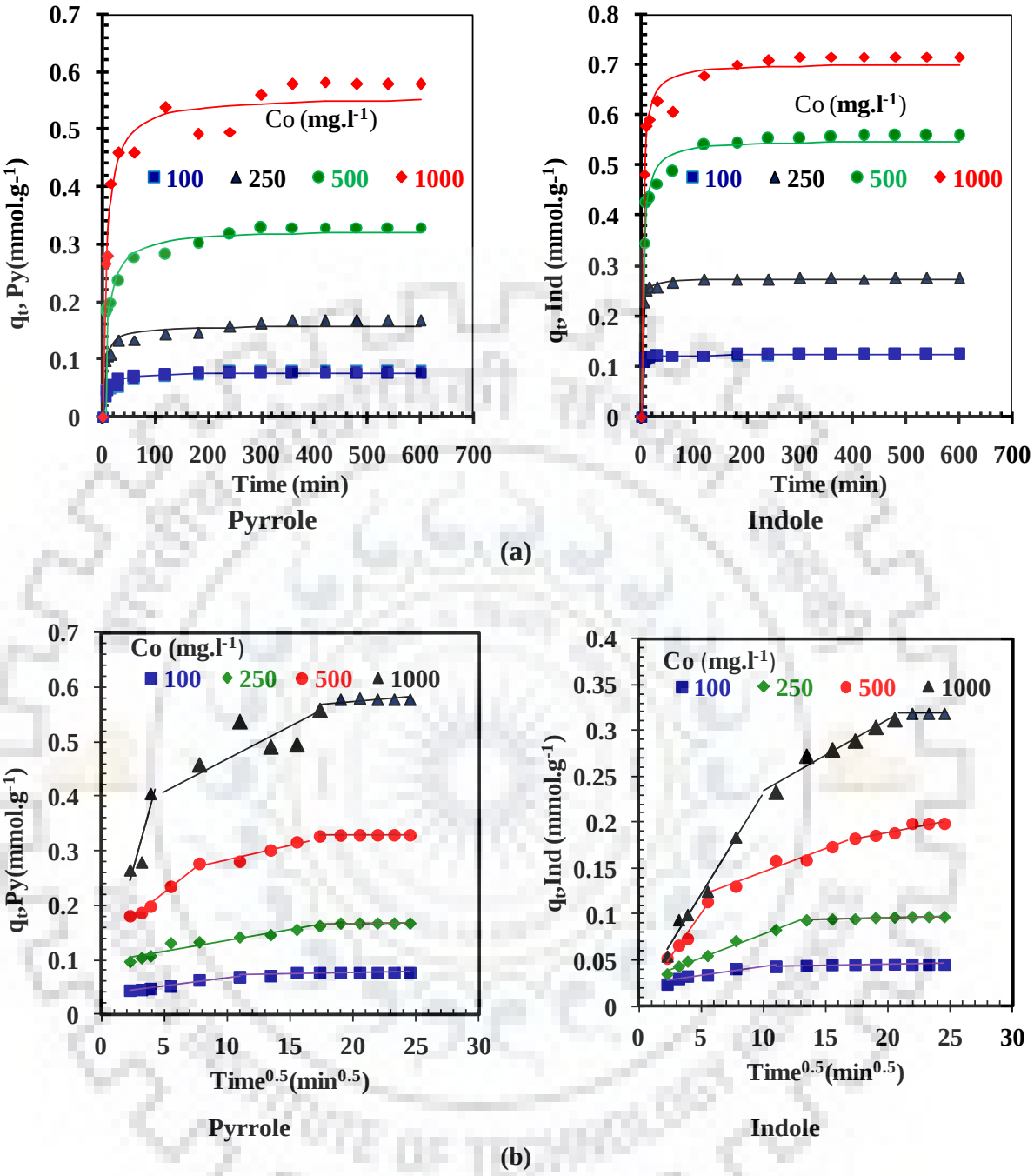

Figure 4.2.5: (a) Effect of contact time and initial concentration on the adsorption of pyrrole and indole by GAC. Experimental data points given by the symbols and the lines predicted by the pseudo-second-order model. (b) Weber-Morris plot for pyrrole and indole adsorption onto GAC C_o=100, 250, 500 and 1000 mg.l^{-1}, m_{opt}=20 g.l^{-1} for GAC , pH_o=5.7, T=303 K.

Table 4.2.1: Kinetic parameters for the removal of pyrrole by GAC (t=8 h, C_o=100-1000 mg.l^{-1}, m=20 g.l^{-1}, pH_o=5.7, T=303 K).

	C_o (mg.l^{-1})			
	100	**250**	**500**	**1000**
Pseudo 1st order				
k_f (min^{-1})	0.086	0.097	0.082	0.078
$q_{e,\exp}$ (mmol.g^{-1})	0.077	0.168	0.33	0.578
$q_{e,cal}$ (mmol.g^{-1})	0.077	0.17	0.33	0.58
R^2	0.88	0.891	0.90	0.93
MPSD	16.01	15.29	14.95	13.03
Pseudo 2nd order				
k_s (g.mmol^{-1}.min^{-1})	1.974	1.377	0.341	0.25
h (mmol.g^{-1}.min^{-1})	0.012	0.034	0.036	0.078
$q_{e,cal}$ (mmol.g^{-1})	0.076	0.157	0.322	0.551
R^2	0.947	0.949	0.83	0.962
MPSD	9.682	7.521	25.65	7.65
Weber Morris				
$k_{id,1}$ (mmol.g^{-1}.min$^{-1/2}$)	0.003	0.004	0.018	0.082
I_1	0.036	0.095	0.133	0.063
R^2	0.972	0.921	0.984	0.765
$k_{id,2}$ (mmol.g^{-1}.min$^{-1/2}$)	0.0005	0.0005	0.005	0.012
I_2	0.065	0.155	0.232	0.345
R^2	0.625	0.470	0.900	0.700
$k_{id,3}$ (mmol.g^{-1}.min$^{-1/2}$)	-	-	0.00	0.002
I_3	-	-	0.323	0.532
R^2	-	-	0.610	0.430

Table 4.2.2: Kinetic parameters for the removal of indole by GAC (t=8 h, C_o=100-1000 $mg.l^{-1}$, m=20 $g.l^{-1}$, pH_o=5.7, T=303 K).

	C_o ($mg.l^{-1}$)			
	100	**250**	**500**	**1000**
Pseudo 1st order				
k_f (min^{-1})	0.110	0.048	0.034	0.023
$q_{e,\exp}$ ($mmol.g^{-1}$)	0.046	0.098	0.199	0.319
$q_{e,cal}$ ($mmol.g^{-1}$)	0.046	0.098	0.199	0.319
R^2	0.942	0.927	0.943	0.956
MPSD	10.40	17.01	17.51	18.681
Pseudo 2nd order				
k_s ($g.mmol^{-1}.min^{-1}$)	4.370	0.857	0.281	0.104
h ($mmol.g^{-1}.min^{-1}$)	0.009	0.008	0.010	0.010
$q_{e,cal}$ ($mmol.g^{-1}$)	0.045	0.093	0.184	0.300
R^2	0.986	0.968	0.974	0.978
MPSD	4.223	9.404	8.921	10.677
Weber Morris				
$k_{id,1}$ ($mmol.g^{-1}.min^{-1/2}$)	0.002	0.005	0.019	0.022
I_1	0.022	0.027	0.007	0.014
R^2	0.902	0.986	0.968	0.972
$k_{id,2}$ ($mmol.g^{-1}.min^{-1/2}$)	0.0002	0.0004	0.005	0.008
I_2	0.042	0.089	0.094	0.588
R^2	0.734	0.933	0.904	0.941
$k_{id,3}$ ($mmol.g^{-1}.min^{-1/2}$)	-	-	0.002	0.0001
I_3	-	-	0.137	0.318
R^2	-	-	0.886	0.999

Figure 4.2.5b shows plot of q_t vs. $t^{1/2}$ for adsorption of pyrrole and indole onto GAC. This figure has two or three linear plots indicating more than one process controlling the adsorption process. Last linear portion indicate extremely low adsorbate concentrations left in the solution which slow down the intraparticle diffusion and final equilibrium reached. $k_{id,1}$ and $k_{id,2}$ are the slopes of the linear portions (Tables 4.2.1 and 4.2.2) and their values are increasing with C_o. This is due to increase in driving force with C_o and adsorption through meso- and micro-pores. Surface diffusion and intra-particle diffusion within the pores of GAC control the adsorption process as linear portion of all the plots did not pass through origin indicating adsorption mechanism was rather complex. As the value of the slope (k_{id}) of last section is higher, it represents that the pore diffusion is the rate limiting step. The intercept *I* indicates boundary layer thickness.

4.2.1.5 Adsorption equilibrium and thermodynamic study for individual adsorption

Figure 4.2.6 shows the plots of adsorption isotherms, q_e versus C_e, for pyrrole and indole onto GAC at 288, 303 and 318 K. Adsorption capacity of GAC for indole was also found to increase with an increase in T. Enhanced uptake of indole by GAC at higher temperature may be due to the increase in mobility of indole at higher T. However, pyrrole adsorption onto GAC wasn't affected much by the change in T.

The experimental equilibrium adsorption data of pyrrole and indole adsorption onto GAC have been tested by using the two-parameter Freundlich [Freundlich, 1906], Langmuir [Langmuir, 1918], Tempkin [Tempkin and Pyzhev, 1940] and the three parameter Redlich-Peterson (R-P) [Redlich and Peterson, 1959] equation. The following equations represent these isotherms:

Freundlich $$q_e = K_F C_e^{1/n} \quad (4.2.6)$$

Langmuir $$q_e = \frac{q_m K_L C_e}{1 + K_L C_e} \quad (4.2.7)$$

Tempkin $$q_e = B_T \ln K_T + B_T \ln C_e \quad (4.2.8)$$

Redlich-Peterson $$q_e = \frac{K_R C_e}{1 + a_R C_e^{\beta}} \quad (4.2.9)$$

where, K_F is the Freundlich constant (l.mg^{-1}), $1/n$ is the heterogeneity factor, K_L is the Langmuir adsorption constant (l.mg^{-1}) related to the energy of adsorption, q_m signifies the adsorption capacity (mg.g^{-1}), B_T is Tempkin constant related to the heat of adsorption, K_T is the equilibrium binding constant (l.mol^{-1}) corresponding to the maximum binding energy.K_R is R–P isotherm constant (l.g^{-1}), a_R is R–P isotherm constant (l.mg^{-1}) and β is the exponent which lies between 0 and 1.

Sum of square of error (SSE) was used to find out the best isotherm model for fitting experimental data [Glocheux, et al., 2013]. The isotherm parameters and the value of correlation coefficient R^2 are given in the Table 4.2.3. It can be seen that the R^2 value for R-P model are closer to unity as compared to other isotherm models. SSE value for R-P model is found to be minimum thereby giving the best fit for the experimental data obtained.

Following relationship between Gibbs free energy change (ΔG^0), enthalpy change (ΔH^0), entropy change (ΔS^0) and equilibrium adsorption constant (K_D) can be obtained from classical thermodynamics [Wen et al., 2010].

$$\ln K_D = -\frac{\Delta G^0}{RT} = \frac{\Delta S^0}{R} - \frac{\Delta H^0}{R}\frac{1}{T} \quad (4.2.10)$$

where, T is the absolute temperature (K), R the universal gas constant (8.314×10^{-3} kJ.mol^{-1} K^{-1}) and ($K_D = q_e/C_e$) the single point or linear sorption distribution coefficient. Value of K_D was obtained from the intercept of the ln q_e/C_e versus q_e plot [Srivastava et al., 2007a]. ΔH^0 and ΔS^0 values have been obtained from the van't Hoff plot of ln K_D versus 1/T. Values of ΔH^0, ΔS^0 and ΔG^0 are given in Table 4.2.4 ΔS^0 values are positive for both pyrrole and indole adsorption suggesting increased randomness on the interface and ΔG^0 values are found to be negative indicating the feasibility and spontaneity of adsorption of pyrrole and indole onto GAC. Positive values of ΔH^0 indicates the endothermic nature indole adsorption onto GAC. Figure 4.2.6a and very small ΔH^0 value indicates that temperature has no effect on pyrrole adsorption onto GAC.

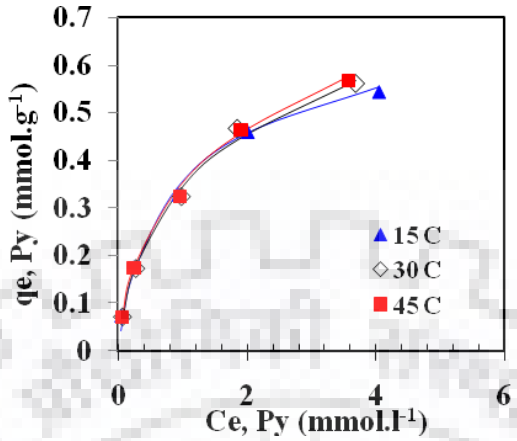

(a) Pyrrole

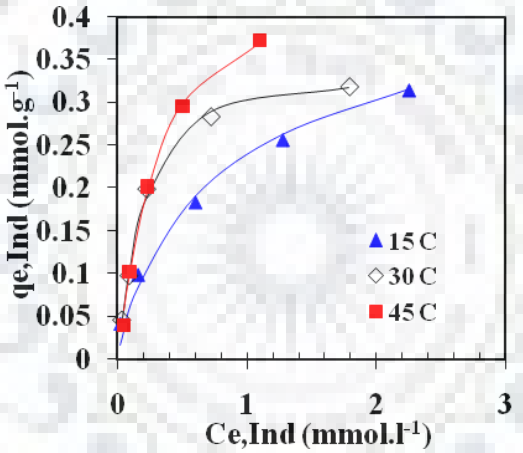

(b) Indole

Figure 4.2.6: Equilibrium adsorption isotherms at different temperature for the treatment of (a) pyrrole and (b) indole by GAC. Experimental data points given by symbols and the lines predicated by R-P isotherm model. t=8 h, C_o=100-1000 mg.l^{-1}, m=20 g.l^{-1} for GAC, pH_o=5.7.

Table 4.2.3: Isotherm parameters for individual adsorption of pyrrole and indole onto GAC (t=8 h, $C_{o,Py}$=1.49-14.91 mmol.l^{-1}, $C_{o,Ind}$=0.85-8.54 mmol.l^{-1}, m=20 g.l^{-1}).

Freundlich				
T(K)	K_F	1/n	R^2	SSE
Pyrrole				
288	0.324	0.397	0.987	0.002
303	0.332	0.426	0.994	0.004
318	0.330	0.447	0.993	0.001
Indole				
288	0.224	0.433	0.998	0.000
303	0.281	0.312	0.900	0.008
318	0.373	0.511	0.950	0.004
Langmuir				
T(K)	q_m	K_L	R^2	SSE
Pyrrole				
288	0.626	1.379	0.991	0.002
303	0.698	1.044	0.991	0.002
318	**0.690**	1.120	0.988	0.003
Indole				
288	0.359	1.794	0.987	0.001
303	0.364	4.573	0.994	0.0008
318	0.503	2.692	0.993	0.001
Redlich-Peterson				
T(K)	K_R	a_R	β	R^2	SSE
Pyrrole					
288	1.066	2.001	0.873	0.997	0.002
303	1.410	3.093	0.742	0.994	0.001
318	1.835	4.224	0.709	0.997	0.0006
Indole					
288	0.737	2.081	0.882	0.996	0.001
303	1.041	3.604	1.119	0.997	0.0002
318	1.146	2.140	1.215	0.995	0.0003

Table 4.2.4: Thermodynamic parameters for the adsorption of pyrrole and indole onto GAC (t=8 h, $C_{o,Py}$=1.49-14.91 mmol.l^{-1}, $C_{o,Ind}$=0.85-8.5 mmol.l^{-1}, m=20 g.l^{-1}).

Temp (K)	K_D x 10^3 (l.kg^{-1})	ΔG^0 (kJ.mol^{-1})	ΔH^0 (kJ.mol^{-1})	ΔS^0 (kJ.mol^{-1}K^{-1})
Pyrrole				
288	1.547	-17.60	-3.86	47.56
303	1.364	-18.19		
318	1.332	-19.03		
Indole				
288	1.139	-16.86	12.42	101.30
303	1.305	-18.08		
318	1.864	-19.92		

4.2.1.6 Reusability of adsorbent GAC

To determine reusability of adsorbents, desorption study was carried out. Desorption of pyrrole and indole in presence of acid, alcohol, acetone and water were found to be very low as compared to strong base. Pyrrole desorption efficiency for GAC was found to be 67% by NaOH whereas indole desorption efficiency was 6.6%. Rathula and Srivastava [2011] and Suresh et al. [2011c] tested desorption of adsorbate from spent adsorbents by thermal desorption method. Similar to that study, thermally desorbed adsorbents were again used for pyrrole and indole adsorption. After that, thermal desorption was again done on the pyrrole and indole loaded adsorbent individually. Decrease in active sites on adsorbents resulted in decrease in the adsorptive capacity of GAC during successive adsorption-desorption cycle (Figure 4.2.7). It can be seen that GAC can successfully be used for five cycles. The adsorption capacity of pyrrole for GAC was much less as compared to that of indole after successive thermal desorption.

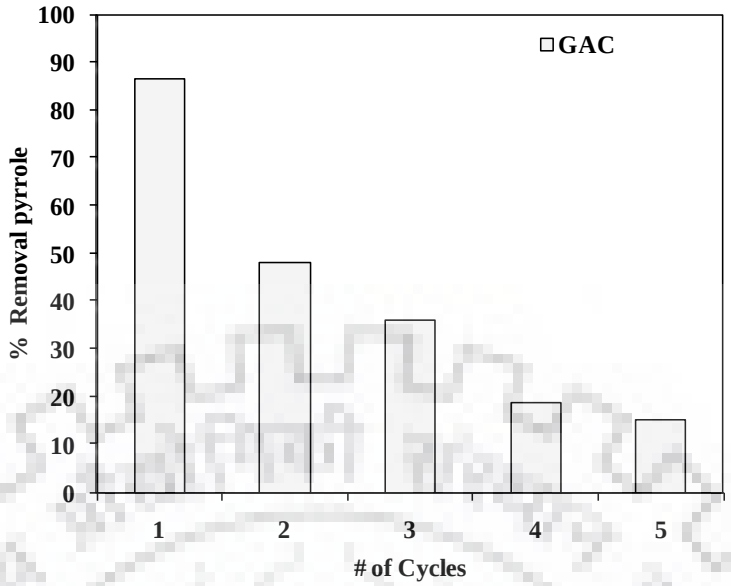

(a) Pyrrole desorption

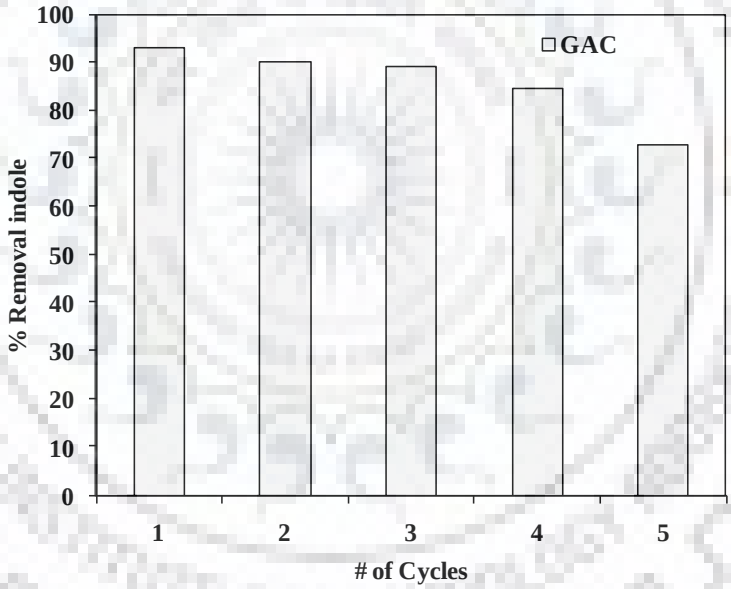

(b) Indole desorption

Figure 4.2.7: (a) Pyrrole and (b) indole removal efficiency of GAC after various thermal desorption-adsorption cycles.

4.2.2 Optimization of Parameters for Simultaneous Removal of Pyrrole and Indole by GAC using Taguchi's Design of Experiments

In this part of study, first the parameters for simultaneous adsorptive removal of pyrrole and indole from aqueous solution have been optimized by using Taguchi's methodology which is a statistical technique for optimization of multi-component adsorption. Thereafter, single and binary adsorption isotherm data at 30°C were obtained using the optimized condition obtained in the first step. These binary isotherm data have been further used for determination of binary isotherm parameters for pyrrole and indole.

4.2.2.1 Multi-component study using Taguchi's method: Taguchi's orthogonal array (OA) method was used to show the effects of parameters. In the optimization of a process by Taguchi's method, certain steps should be followed [Srivastava et al., 2007b]. First step is the identification of performance characteristics and selection of process parameters. Second step is to decide the number of process parameters and their interaction. Based on the previous study for individual compound adsorption, factors that affected the simultaneous removal of pyrrole and indole from waste water onto GAC were identified. In the present study, five process parameters were selected for experimental design. The process parameters and their level are given in Table 4.2.5.

Table 4.2.5: Multi-component adsorption study parameters for the adsorption of pyrrole and indole onto GAC using Taguchi's OA.

	Parameters		Units	Levels		
				0	1	2
A:	Initial concentration of pyrrole	$C_{o,Py}$	$mmol.l^{-1}$	0	3.73	7.45
B:	Initial concentration of indole	$C_{o,Ind}$	$mmol.l^{-1}$	0	2.13	4.27
C:	Temperature	T	(°C)	15	30	45
D:	Adsorbent dose	m	$(g.l^{-1})$	4	12	20
E:	Contact time	t	(min)	60	360	660

In simultaneous adsorption, two parameter interactions between initial concentrations of adsorbates ($C_{o,Py} \times C_{o,,Ind}$) is very important as removal efficiency is sometimes highly dependent on characteristics of each other. Third step is to select orthogonal array (OA) and assign parameters to it. The selected OA must satisfy the inequality that the total degree of freedom required for the experiment should be less than or equal to total degree of freedom (DOF) of the OA [Srivastava et al., 2007b, 2011]. The total required degree of freedom for the experiment is 14 (5 × (3-1) + 1 × 4=14). This is due to the fact that three level parameter has DOF=2 (number of levels-1) and for each two parameter interaction DOF value is 4 (2×2) [Suresh et al., 2011a]. Based upon the number of parameters and their levels, L_{27} OA (Table 4.2.6) was used for carrying out experiments for simultaneous pyrrole and indole adsorption onto GAC. The individual adsorption capacities of pyrrole and indole (q_{Py} and q_{Ind}) and the total adsorption capacity (q_{tot}) were estimated using following relationships:

$$q_{tot} = q_{Py} + q_{Ind} = [(C_{0,Py} - C_{e,Py}) + (C_{0,Ind} - C_{e,Ind})]/m \qquad (4.2.11)$$

It is seen that adsorption of both pyrrole and indole is highly dependent on the parametric conditions.

4.2.2.2 Process Parameters Effects

The effects of parameters on q_{tot}, q_{Py} and q_{Ind} for adsorption of pyrrole and indole onto GAC are given in the Figure 4.2.8. The values of $q_{tot,}$ q_{Py} and q_{Ind} are found to be highly dependent on various parameters (C_{oi} T, m and t). It can be seen from the graph that an increase in $C_{o,i,}$ and t from 1 to 2 and 2 to 3 resulted in an increase in q_{tot} value. Temperature (T) is found to affect the q_{Py} and q_{Ind} values differently. When T increases from 15°C to 45°C, q_{Py} decreases indicating exothermic nature of the adsorption process, however, q_{Ind} increases with an increase in T from 15°C to 30°C and decreases from 30°C to 45$^{°C}$. When adsorption of pyrrole decreases, q_{Ind} increases and when adsorption of indole decreases q_{Py} increases. This is because both pyrrole and indole compete for the same active sites.

Table 4.2.6: Taguchi's L_{27} (3^{13}) orthogonal array for multi-component adsorption of pyrrole and indole system onto GAC.

Exp. No.	A	B	A×B	A×B	C	D	E	q_{Py}	q_{Ind}	q_{tot}
1	0	0	0	0	15	4	1	0.00	0.00	0.00
2	0	0	0	0	30	12	6	0.00	0.00	0.00
3	0	0	0	0	45	20	11	0.00	0.00	0.00
4	0	2.13	1	1	15	4	1	0.00	0.09	0.09
5	0	2.13	1	1	30	12	6	0.00	0.16	0.16
6	0	2.13	1	1	45	20	11	0.00	0.11	0.11
7	0	4.27	2	2	15	4	1	0.00	0.14	0.14
8	0	4.27	2	2	30	12	6	0.00	0.22	0.22
9	0	4.27	2	2	45	20	11	0.00	0.20	0.20
10	3.73	0	1	2	15	12	11	0.18	0.00	0.18
11	3.73	0	1	2	30	20	1	0.09	0.00	0.09
12	3.73	0	1	2	45	4	6	0.19	0.00	0.19
13	3.73	2.13	2	0	15	12	11	0.09	0.15	0.24
14	3.73	2.13	2	0	30	20	1	0.05	0.09	0.14
15	3.73	2.13	2	0	45	4	6	0.07	0.14	0.21
16	3.73	4.27	0	1	15	12	11	0.05	0.14	0.19
17	3.73	4.27	0	1	30	20	1	0.03	0.11	0.14
18	3.73	4.27	0	1	45	4	6	0.03	0.16	0.19
19	7.45	0	2	1	15	20	6	0.25	0.00	0.25
20	7.45	0	2	1	30	4	11	0.39	0.00	0.39
21	7.45	0	2	1	45	12	1	0.18	0.00	0.18
22	7.45	2.13	0	2	15	20	6	0.12	0.10	0.22
23	7.45	2.13	0	2	30	4	11	0.03	0.13	0.16
24	7.45	2.13	0	2	45	12	1	0.05	0.06	0.11
25	7.45	4.27	1	0	15	20	6	0.08	0.16	0.24
26	7.45	4.27	1	0	30	4	11	0.09	0.26	0.35
27	7.45	4.27	1	0	45	12	1	0.03	0.06	0.09
Total								2.00	2.47	4.47

But effective q_{tot} increases with increase in all other parameters for particular designed adsorption process. Results may vary from those that were obtained for individual adsorption as there was a lot of interaction between pyrrole and indole for same adsorption sites.

It is seen that q_{tot} value increased with an increase in time from level 1 to 3 (i.e. from 1 h to 11 h). Adsorption of pyrrole and indole increases with an increase in contact time until equilibrium is achieved between the adsorbates and the adsorbent. It is observed that indole achieved equilibrium earlier as compared to pyrrole. During the initial stages numbers of vacant sites are available for adsorption but after sometime sites get occupied due to which repulsive forces come into play between the solute molecules. Adsorption slows down in the later stages because of pyrrole and indole molecule travel deeper into the pores of adsorbent creating resistance to transport molecules. q_{tot} decreases with increase in dose (m) from level 1 to 2 and then from 2 to 3 , however, percent removal (analysed separately) increased with an increase in adsorbent dose due to presence of more sites at higher adsorbent dose for adsorption.

Relative influence of various parameters can also be studied from Figure. 4.2.8. It can be seen that adsorbent dose has the greatest effect at level 1 on q_{tot} whereas temperature and time greatly affect at level 2 and $C_{o,Py}$ has highest effect at level 3. It can also be seen that overall $C_{o,i}$ and time have strongest influence on q_{tot} than other parameters. q_{Py} increased with $C_{o,i}$ because of the increase in mass transfer driving force which resulted in the decrease of resistance to the adsorbate uptake. $C_{o,Ind}$ has significant effect at level 1 on q_{Py} whereas $C_{o,Py}$ significantly affect at level 2 and 3. Highest difference between level 1 and level 2 for $C_{o,Py}$ indicates stronger influence on q_{Py} as compared to other parameters. Similarly, $C_{o,Py}$ and adsorbent dose significantly affect q_{Ind} at level 1. Again largest difference between level 1 and level 2 for $C_{o,Ind}$ indicates stronger influence on q_{Ind} as compared to other parameters.

The effect of concentration of one component with respect to other component i.e. the interaction between the components has a significant effect on q_{tot} values (Figure. 4.2.9). Parallel lines indicate no interaction whereas non-parallel lines indicate existence of an interaction between $C_{o,i}$ as seen in the interaction graph. Large difference in values of slopes of lines of $C_{o,Py}$ and $C_{o,Ind}$ results in significant interaction in the tested range [Kim et al., 2003; Singh et al., 2013]

ANOVA results for responses q_{tot}, q_{Py} and q_{Ind} during binary adsorption of pyrrole and indole onto GAC are given in Table 4.2.7. The level of factors can be controlled in a manner that higher or lower values produce the preferred results. Thus the level of factor which produces preferred result can easily be predicted.

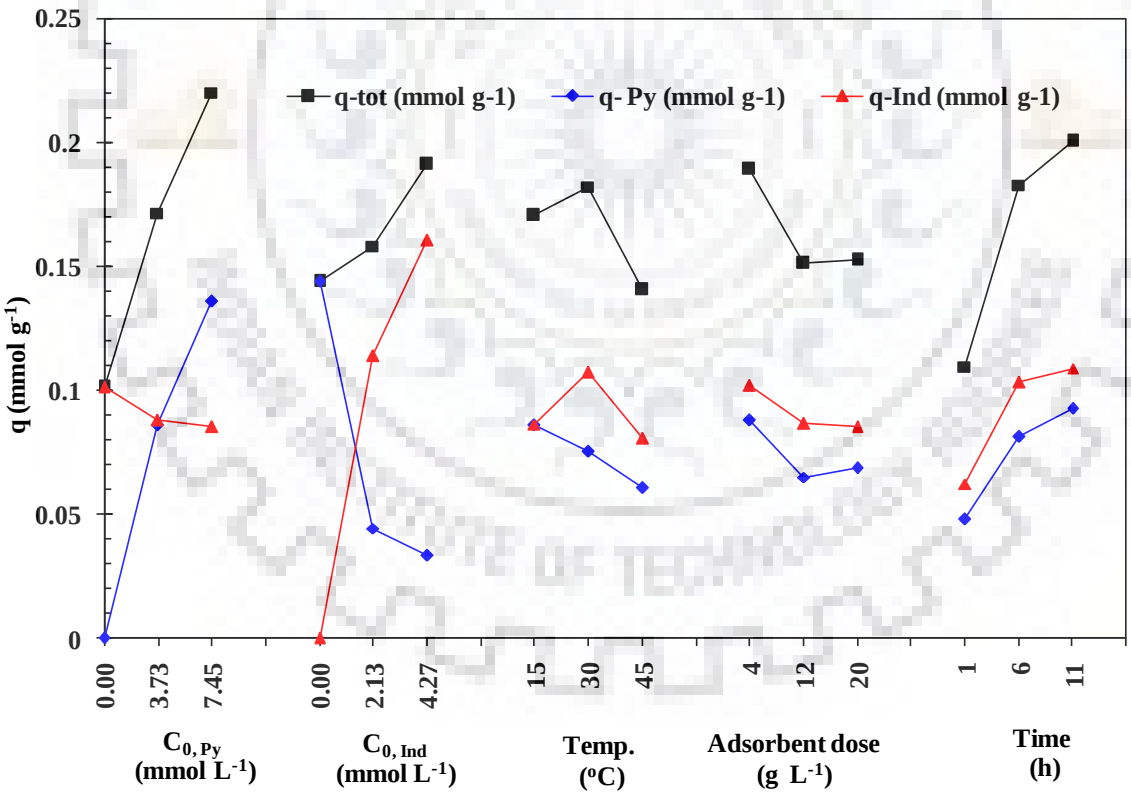

Figure 4.2.8: Effect of process parameters on q_{tot} for multicomponent adsorption of pyrrole and indole onto GAC.

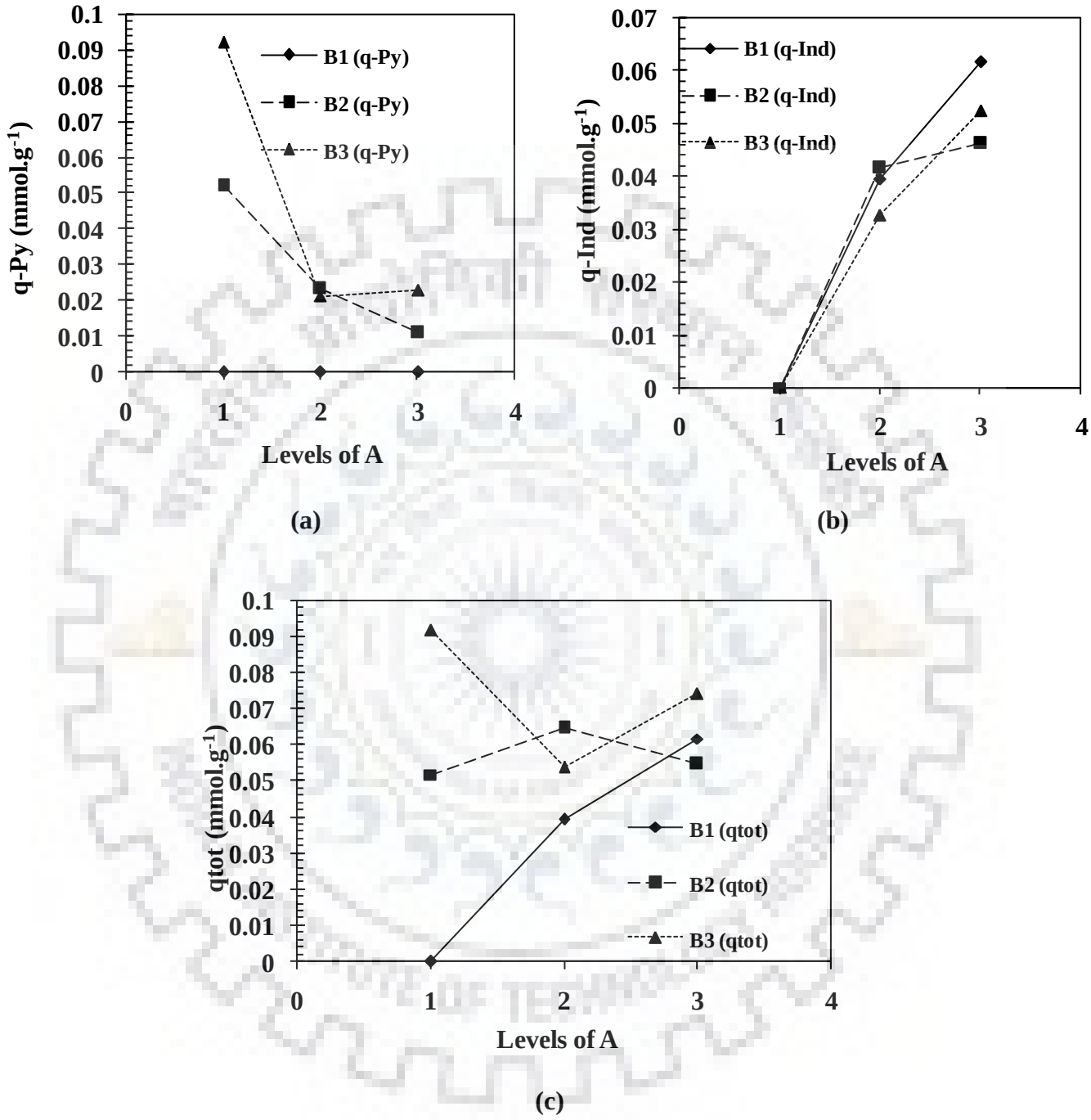

Figure 4.2.9: The effect of interaction between A and B at 3 levels on (a) q_{Py}, (b) q_{Ind} and (c) q_{tot} for multicomponent adsorption of pyrrole and indole onto GAC. B1, B2 and B3 are levels of B.

Table 4.2.7 : ANOVA of q_{tot} for multicomponent adsorption of pyrrole and indole onto GAC.

	Sum of squares	DOF	Mean square	% contribution	F-value
			q_{tot}		
A	0.06	2	0.03	29.44	18.85
B	0.01	2	0.01	4.81	3.08
C	0.01	2	0.00	3.82	2.45
D	0.01	2	0.00	3.88	2.48
E	0.04	2	0.02	19.20	12.30
$A\times B$	0.06	4	0.02	29.48	9.44
Residual	0.02	12	0.00	9.37	
Model	0.20	14	0.08	90.63	48.69
Cor. total	0.22	26	0.08	100.00	
			q_{Ind}		
A	0.00	2	0.00	0.86	0.61
B	0.12	2	0.06	78.06	55.38
C	0.00	2	0.00	2.27	1.61
D	0.00	2	0.00	3.88	0.70
E	0.01	2	0.01	7.39	5.24
$A\times B$	0.00	4	0.00	1.99	0.70
Residual	0.01	12	0.00	8.46	
Model	0.14	14	0.07	91.54	64.24
Cor. total	0.16	26	0.07	100.00	
			q_{Py}		
A	0.09	2	0.04	36.40	23.87
B	0.07	2	0.03	28.38	18.61
C	0.00	2	0.00	1.24	0.81
D	0.00	2	0.00	1.19	0.78
E	0.01	2	0.00	4.16	2.73
$A\times B$	0.05	4	0.01	19.48	6.39
Residual	0.02	12	0.00	9.15	
Model	0.21	14	0.09	90.85	53.18
Cor. total	0.23	26	0.10	100	

4.2.2.3 Optimum level selection and optimum response characteristics estimation

Optimum levels of parameters for maximum adsorption were obtained by examining the q_{tot} values. Higher value of q_{tot} were found to be at first level parameter for D (m), at second level parameter for C (temperature) and at third level parameter for A, B ($C_{o,i}$), and E (time). The optimal value of the response curve was measured by following relationship [Srivastava et al., 2007b; 2011]:

$$q_{tot,predicted} = \overline{T} + (\overline{A_3} - \overline{T}) + (\overline{B_3} - \overline{T}) + (\overline{C_2} - \overline{T}) + (\overline{D_1} - \overline{T}) + (\overline{E_3} - \overline{T}) \quad (4.2.12)$$

where, $\overline{C_2}$ and $\overline{D_1}$ is the average value of response at second level of parameter C and first level of parameter D, respectively. For parameters A and B, third level was chosen so as to check the adsorption efficiency for maximum concentration. The predicted maximum value of q_{tot}, q_{Py} and q_{Ind} for GAC were 0.35, 0.15 and 0.20 mmol.g^{-1}, respectively. Three confirmation experiments were conducted at selected optimal levels for the simultaneous removal of pyrrole and indole from binary solution by GAC. The calculated value of q_{tot}, q_{Py} and q_{Ind} for GAC were 0.34, 0.16 and 0.18 mmol.g^{-1}, respectively. These values are within 95% confidence interval.

4.2.3 Multi-Component Isotherm Study for Simultaneous Removal of Pyrrole and Indole by GAC

For binary isotherm study, binary mixture of pyrrole and indole were taken and simultaneous adsorption was studied at 30°C. For each C_o of indole: 50, 100, 250, 500 and 750 mg.l^{-1}, C_o of pyrrole was varied from 50 to 750 mg.l^{-1}. From Table 4.2.8, it is observed that equilibrium uptake of indole increased as its concentration was increased for fixed concentration of pyrrole. But individual percent removal decreased for the same component as pyrrole concentration increased. Similar trend was observed for pyrrole with increasing concentration of indole.

Binary isotherm study results show that for 4.27 mmol.l^{-1} (500 mg.l^{-1}) concentration of indole with presence of 7.45 mmol.l^{-1} (500 mg.l^{-1}) of pyrrole, q_{Ind} was 0.18 mmol.g^{-1}. Similarly for 6.402 mmol.l^{-1}(750 mg.l^{-1}) concentration of indole with presence of 11.17 mmol.l^{-1}(750 mg.l^{-1}) of pyrrole, q_{Ind} was 0.19 mmol.g^{-1}. Reduction in capacity for competitive adsorption is dependent on the molecular structure of the competing adsorbates, the C_o of the pollutants, and the surface structure of the adsorbent [Mirzaei et al., 2013]. Binary equilibrium adsorption data indicate that adsorption capacity of GAC is higher for indole than that of pyrrole. There are interactions between the species in the solution as well as on the surface. Solute-surface interactions complicate adsorptions in multicomponent systems. Multi-ion systems have received less attention than single-ion systems [Mohan et al., 2006]. Non-competitive Langmuir model is extension of the basic Langmuir model. Langmuir model assumed to be applicable for monolayer coverage and Freundlich model for multilayer adsorption. These isotherms are applied by various researchers for single component adsorption process. Adsorption of individual component constant may not define the exact behaviour in the multicomponent system. Therefore for better accuracy modified isotherms may be applied by using individual isotherm parameters obtained with correction factor.

Various multi-component isotherms like non-modified, modified and extended-Langmuir, R-P models, extended-Freundlich, etc. [Srivastava et al., 2008c] have been used to fit the data obtained from simultaneous adsorption of pyrrole and indole onto GAC using SSE. SSE for multi-component adsorption is given by [Choy et al., 2005; Wong et al., 2014]

$$SSE = \sum_{i=1}^{n} ((q_{e,meas} - q_{e,calc})_{Ind} + (q_{e,meas} - q_{e,calc})_{Py})_i^2 \qquad (4.2.13)$$

Table 4.2.9. shows SSE values between calculated and experimental q_e values for pyrrole and indole data with various parameters of multi-component isotherms. Non-modified models show poor fit for adsorption data for binary system as SSE values are very large for these models. For non-modified Langmuir model, SSE value is found to be 1.36

which is much higher than extended-Langmuir and modified-Langmuir model. It is also found that extended-Langmuir with SSE value 0.037 has better fit as compared to modified-Langmuir with SSE value 0.103. In extended-Langmuir model, K_i value reflects the affinity between adsorbate and adsorbent in a binary mixture which is 4.70 for indole and 0.66 for pyrrole while overall adsorbate uptake q_{max} is 0.32 mmol.g^{-1}. Extended-Langmuir model and Extended-Freundlich model gives SSE value 0.037 and 0.038, respectively. The parity plots (Figure 4.2.10) presents comparison between actual and theoretical q_e values of pyrrole and indole.

Non-modified Langmuir and non-modified Redlich-Peterson models use the parameters calculated from individual compound adsorption only for modeling binary adsorption isotherm and have large SSE values. Modified Langmuir model and modified Redlich-Peterson models use only one interaction parameter (η_i) for each compound for modeling binary adsorption isotherm in addition to individual compound isotherm parameters, and thus, show lower SSE values and better representation of experimental data as compared to non-modified models. However, still their predictions are not satisfactory. It is evident that the modification of the Freundlich equation as given by extended Freundlich model takes into accounts the interactive effects of individual adsorbates between and among themselves and the adsorbent reasonably well. Therefore, the binary adsorption of pyrrole and indole onto GAC can be represented satisfactorily and adequately by the extended Freundlich model (SSE=0.038). GAC has generally heterogeneous surface, although less heterogeneous as compared to other low cost adsorbents reported in the literature; and also the adsorption of the individual adsorbates have also been well represented by the Langmuir isotherm equation. Therefore, the lowest SSE value (SSE=0.037) was observed for the fitting of the extended-Langmuir model. Thus, any of extended-Langmuir or extended-Freundlich isotherm model can be used for representing the binary adsorption data.

Table 4.2.8: Comparison of individual and total adsorption uptakes and yields found at different pyrrole concentrations with increasing concentration of indole onto GAC.

$C_{e,Ind}$	$C_{e,Py}$	$q_{e,Ind}$	$q_{e,Py}$	Ad_{Ind}%	Ad_{Py}%	Ad_{tot}%
0.001	0.15	0.02	0.03	99.69	80.30	87.36
0.002	0.18	0.04	0.03	99.73	75.96	88.65
0.02	0.28	0.11	0.02	99.02	62.88	89.67
0.44	0.42	0.19	0.02	89.65	43.43	82.78
1.68	0.45	0.23	0.01	73.38	39.83	69.84
0.002	0.41	0.02	0.05	99.63	72.67	78.67
0.006	0.56	0.04	0.05	99.25	62.20	75.69
0.03	0.66	0.11	0.04	98.58	55.49	80.86
0.39	0.88	0.19	0.03	90.91	41.07	78.01
1.48	0.95	0.24	0.03	76.48	36.38	68.81
0.01	0.99	0.02	0.14	97.34	73.34	75.81
0.02	1.30	0.04	0.12	97.65	65.19	71.24
0.03	1.87	0.11	0.09	98.40	49.92	67.57
0.45	2.50	0.19	0.06	89.45	32.90	63.09
2.64	2.81	0.18	0.05	58.16	24.59	45.70
0.01	2.67	0.02	0.22	96.86	62.24	64.21
0.03	2.72	0.04	0.22	96.86	61.54	65.35
0.02	3.58	0.11	0.17	98.90	49.40	60.86
0.76	5.18	0.18	0.09	82.22	26.84	47.67
2.17	5.32	0.21	0.10	65.58	27.77	45.20
0.004	4.92	0.02	0.30	98.95	55.31	56.94
0.005	5.75	0.04	0.26	99.42	47.77	51.48
0.14	7.24	0.09	0.19	93.64	34.24	43.88
0.79	7.47	0.17	0.18	81.53	32.21	45.99
2.60	7.93	0.19	0.15	58.84	28.04	39.26

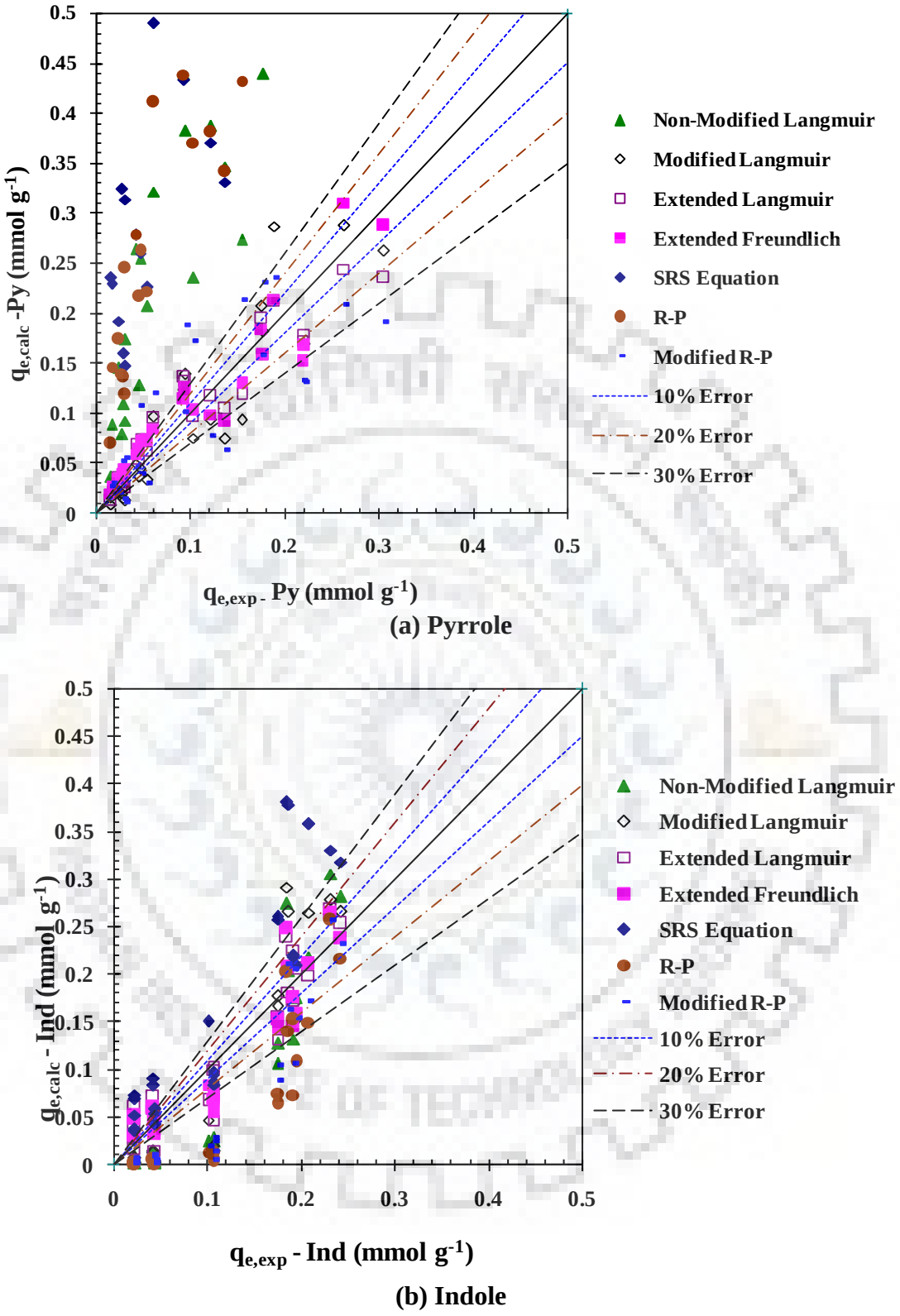

Figure 4.2.10: Comparison of actual and theoretical equilibrium adsorption values of pyrrole (Py) and indole (Ind) in a binary mixture.

Table 4.2.9: Individual and multi-component isotherm parameter values for the pyrrole and indole adsorption onto GAC at 30°C [Ng et al., 2002]

Individual isotherm models		**Parameter**	**Pyrrole**	**Indole**
Langmuir	$q_e = \frac{q_m k_L c_e}{1 + k_L c_e}$	q_m	0.698	0.364
		k_L	1.044	4.573
		SSE	0.002	0.0004
Freundlich	$q_e = k_F c_e^{1/n}$	k_F	0.332	0.281
		$1/n$	0.426	0.312
		SSE	0.004	0.008
Redlich-Peterson	$q_e = \frac{k_R c_e}{1 + a_R c_e^{\beta}}$	k_R	1.410	1.401
		a_R	3.093	3.604
		β	0.742	1.119
		SSE	0.001	0.0002
Multicomponent isotherm models				
Non-modified Langmuir model	$q_{e,i} = \frac{q_{m,i} K_{L,i} C_{e,i}}{1 + \sum_{j=1}^{N} K_{L,j} C_{e,j}}$	SSE	1.36	
Modified Langmuir model	$q_{e,i} = \frac{q_{m,i} K_{L,i} \left(\frac{C_{e,i}}{\eta_{L,i}}\right)}{1 + \sum_{j=1}^{N} K_{L,j} \left(\frac{C_{e,j}}{\eta_{L,j}}\right)}$	$\eta_{L,i}$	8.49	2.23
		SSE	0.10	
Extended Langmuir	$q_{e,i} = \frac{q_{\max} K_{EL,i} C_{e,i}}{1 + \sum_{j=1}^{N} K_{EL,j} C_{e,j}}$	K_i	0.66	4.70
		$q_{\max}$	0.32	
		SSE	0.037	
Extended Freundlich	$q_{e,1} = \frac{K_{F,1} C_{e,1}^{n_1 + x_1}}{C_{e,1}^{x_1} + y_1 C_{e,2}^{z_1}}$, $q_{e,2} = \frac{K_{F,2} C_{e,2}^{n_2 + x_2}}{C_{e,2}^{x_2} + y_2 C_{e,1}^{z_2}}$	X	0.30	0
		Y	7.67	0.35
		Z	0.24	0.42
		SSE	0.038	
Non-modified Redlich-Peterson	$q_{e,i} = \frac{K_{R,i} C_{e,i}}{1 + \sum_{j=1}^{N} a_{R,j} C_{e,j}^{\beta_j}}$	SSE	2.06	
Modified Redlich-Peterson	$q_{e,i} = \frac{K_{R,i} \left(\frac{C_{e,i}}{\eta_{R,i}}\right)}{1 + \sum_{j=1}^{N} a_{R,j} \left(\frac{C_{e,j}}{\eta_{R,j}}\right)^{\beta_j}}$	$\eta_{R,i}$	15.72	0.18
		SSE	0.14	

4.3 ADSORPTIVE REMOVAL OF PYRROLE AND INDOLE BY BFA

4.3.1 Optimization of Parameters for Individual Removal of Pyrrole and Indole

4.3.1.1 Effect of initial pH (pH_o)

The effect of pH_o on the adsorptive removal of pyrrole and indole onto BFA was studied by varying pH_o from 2 to 11. Other parameters such as pyrrole concentration (500 $mg.l^{-1}$), adsorbent dose (10 $g.l^{-1}$), temperature (303 K) and time (8 h) were kept constant. It was observed that at all pH removal efficiency of pyrrole onto BFA was found to be 83-85% approximately (Figure 4.3.1). In the range of pH_o from 2 to 11, the removal efficiency of indole (97-98%) did not affect much (Figure 4.3.2). Therefore, natural pH was selected for all further experiments. Compared to GAC, BFA showed better pyrrole and indole removal efficiencies as these adsorbates having greater affinity to BFA than GAC.

4.3.1.2 Effect of adsorbent dose

BFA dose (m) optimization were carried out by varying m in the range 2-24 $g.l^{-1}$ and 1-30 $g.l^{-1}$ for pyrrole and indole adsorption, respectively. Other parameters such as C_o was 500 $mg.l^{-1}$, T=303 K and t=8 h were maintained constant. The results are shown in Figures 4.3.3 and 4.3.4 where it is observed that as the BFA dose increased, the availability of active sites for the adsorption of pyrrole and indole increased. This increase in removal efficiency of pyrrole from aqueous solution was up to m_{opt}=15 $g.l^{-1}$. Beyond this m (>15 $g.l^{-1}$), the adsorption of pyrrole was not significant and found to be constant giving 93% pyrrole removal with adsorption capacity 31 $mg.g^{-1}$ at specified conditions. For indole, percent removal was found to be 95.61% at m=7 $g.l^{-1}$, beyond which it attained a steady removal of 97.10% was observed. By increasing the m value for BFA from 7-10 $g.l^{-1}$ indole removal increases by 1.49% only. Therefore, m_{opt} for indole adsorption onto BFA was taken to be 7 $g.l^{-1}$. Overall, m_{opt} was found to be 15 $g.l^{-1}$ and 7 $g.l^{-1}$ for pyrrole and indole adsorption onto BFA. Here it observed that for BFA (m=7 $g.l^{-1}$), adsorption capacity of BFA was found to be 65.46 $mg.g^{-1}$ and for GAC (m=20 $g.l^{-1}$), it was 23.33 $mg.g^{-1}$ in adsorptive removal of indole having C_o=500 $mg.l^{-1}$.

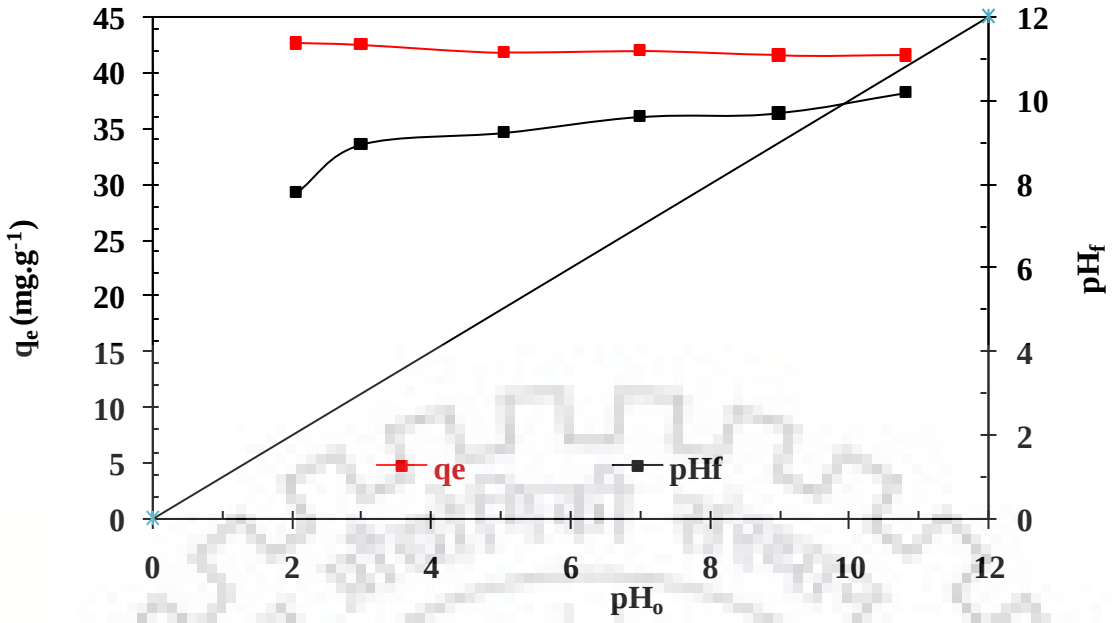

Figure 4.3.1: Effect of initial pH on the removal of pyrrole by BFA (C_o=500 mg.l^{-1}, m=10 g.l^{-1} for BFA , T=303 K, t=8 h).

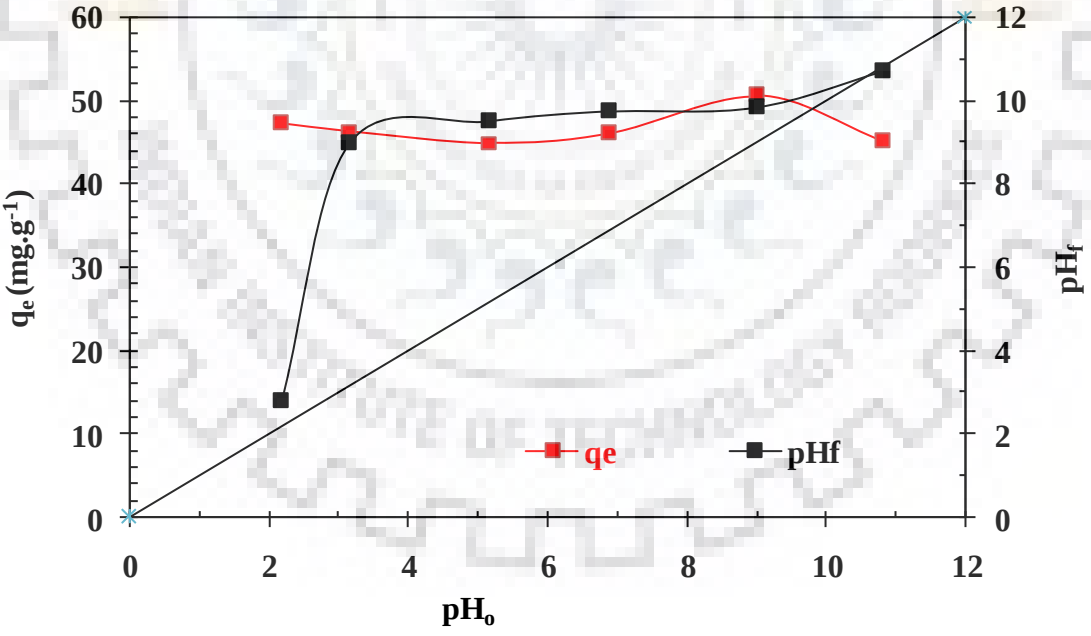

Figure 4.3.2: Effect of initial pH on the removal of indole by BFA (C_o=500 mg.l^{-1}, m=10 g.l^{-1} for BFA , T=303 K, t=8 h).

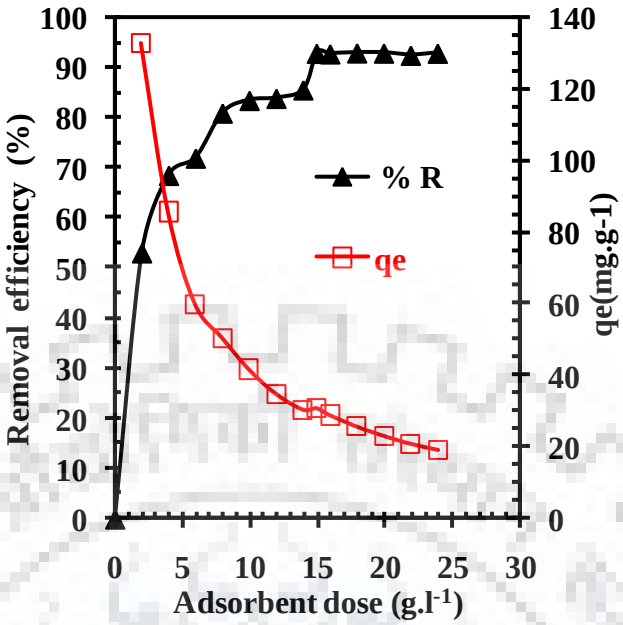

Figure 4.3.3: Effect of adsorbent dosage on the removal of pyrrole by BFA (Co=500 mg.l^{-1}, pH_o=5.7, T=303 K, t=8 h).

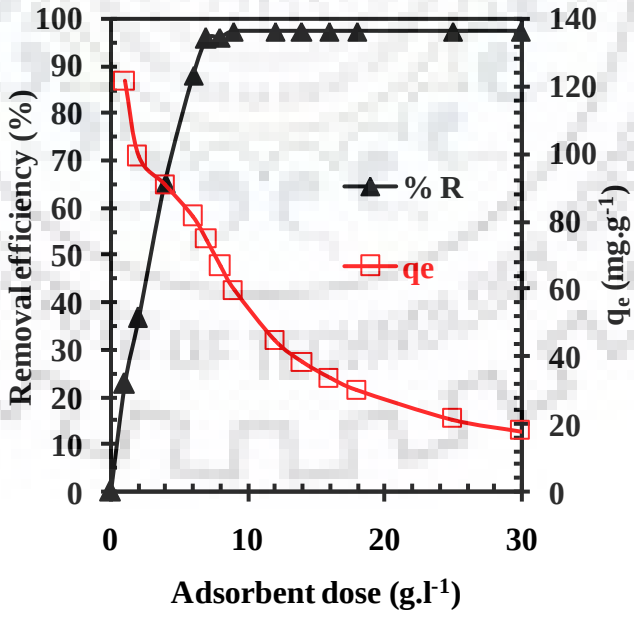

Figure 4.3.4: Effect of adsorbent dosage on the removal of indole by BFA (Co=500 mg.l^{-1}, pH_o=5.7, T=303 K, t=8 h).

4.3.1.3 Effect of contact time and adsorption kinetics

The effect of contact time (t) on the adsorption of pyrrole and indole onto BFA is shown in Figure 4.3.5a. It may be seen that pyrrole and indole adsorption onto BFA is very rapid in the first 15 min at all C_o (100 to1000 $mg.l^{-1}$). Pyrrole uptake by BFA at C_o=7.45 $mmol.l^{-1}$ (500 $mg.l^{-1}$) after 15 min was 0.40 $mmol.g^{-1}$ (27.05 $mg.g^{-1}$) and after 8 h it was 0.47 $mmol.g^{-1}$ (31.62 $mg.g^{-1}$). Similarly, at 4.27 $mmol.l^{-1}$ (500 $mg.l^{-1}$) concentration of indole, uptake of BFA after 15 min was about 0.43 $mmol.g^{-1}$ (50.80 $mg.g^{-1}$) and after 8 h it was 0.56 $mmol.g^{-1}$ (65.46 $mg.g^{-1}$). This decrease in pyrrole and indole adsorption rate was due to repulsive forces between the adsorbate present on the solid and bulk phases. For pyrrole, equilibrium time was 2 h for initial low concentration of pyrrole and which increased to 4 h at higher C_o. For indole, equilibrium time was 30 min for low C_o solutions ($\leq$ 500 $mg.l^{-1}$) whereas it was 3 h for high concentration solutions ($\geq$ 500 $mg.l^{-1}$). Equilibrium time was found to increase with an increase in C_o. An increase in C_o increased the driving force and thus increased the interaction between the adsorbates and the BFA.

Comparison of indole adsorption onto GAC and BFA shows that the indole adsorption rate for BFA was much faster than GAC. Lataye et al. [2008] have also reported almost instantaneous adsorption of 2-picoline onto BFA. In the present study, initial indole uptake onto BFA may be attributed to surface adsorption. After saturation of the exterior surface, indole adsorption takes place in the interior surface of BFA particles. Interior surface of BFA seems to be highly active and has high affinity toward indole. Hence a very high adsorption rate by BFA is observed. It is clear from figure that the rate of uptake is limited by the C_o. This uptake is limited by the diffusion coefficient of the adsorbates in the solid phase [Zogorski et al., 1976].

Kinetic parameters such as k_f, h, q_e and k_s along with the coefficient of correlation (R^2) and MPSD values for pyrrole and indole adsorption onto BFA are given in Tables 4.3.1 and 4.3.2, respectively.

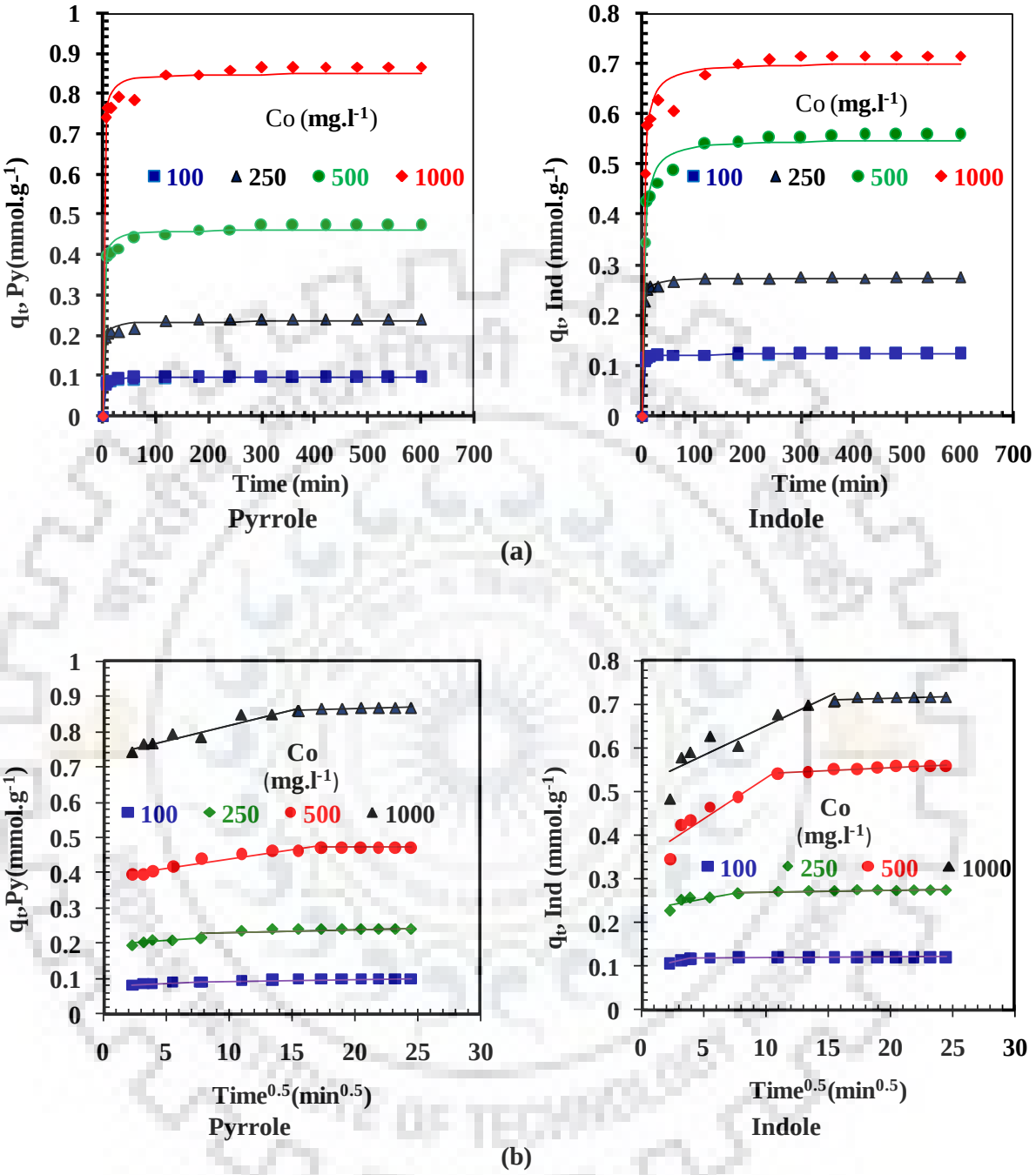

Figure 4.3.5: (a) Effect of contact time and initial concentration on the adsorption of pyrrole and indole by BFA. Experimental data points given by the symbols and the lines predicted by the pseudo-second-order model. (b) Weber-Morris plot for pyrrole and indole adsorption onto BFA C_o=100, 250, 500 and 1000 mg.l^{-1}, m=15 g.l-^{1}for pyrrole and m=7 g.l-^{1}for indole, pH_o=5.7, T=303 K.

Table 4.3.1: Kinetic parameters for the removal of pyrrole by BFA (t=8 h, C_o=100-1000 mg.l^{-1}, m=15 g.l^{-1}for pyrrole and m=7 g.l^{-1}for indole, pH_o=5.7, T=303 K).

	C_o (mg.l^{-1})			
	100	**250**	**500**	**1000**
Pseudo 1st order				
k_f (min^{-1})	0.304	0.280	0.288	0.331
$q_{e,\exp}$(mmol.g^{-1})	0.097	0.243	0.472	0.87
$q_{e,cal}$ (mmol.g^{-1})	0.097	0.24	0.47	0.87
R^2	0.969	0.958	0.955	0.969
MPSD	5.534	6.741	6.795	5.880
Pseudo 2nd order				
k_s(g.mmol^{-1}.min^{-1})	8.94	3.208	1.707	1.192
h (mmol.g^{-1}.min^{-1})	0.082	0.178	0.364	0.864
$q_{e,cal}$ (mmol.g^{-1})	0.096	0.235	0.461	0.850
R^2	0.990	0.984	0.985	0.988
MPSD	2.629	3.430	3.409	2.915
Weber Morris				
$k_{id,1}$(mmol.g^{-1}.min$^{-1/2)}$)	0.001	0.003	0.005	0.008
I_1	0.078	0.192	0.385	0.731
R^2	0.901	0.758	0.945	0.927
$k_{id,2}$ (mmol.g^{-1}.min$^{-1/2)}$	0.001	0.01	0.001	0.001
I_2	0.089	0.218	0.470	0.849
R^2	0.719	0.504	0.470	0.711

Table 4.3.2: Kinetic parameters for the removal of indole by BFA (t=8 h, C_o=100-1000 mg.l^{-1}, m=15 g.l^{-1} for pyrrole and m=7 g.l^{-1} for indole, pH_o=5.7, T=303 K).

	C_o (mg.l^{-1})			
	100	**250**	**500**	**1000**
Pseudo 1st order				
k_f (min^{-1})	0.396	0.327	0.154	0.190
$q_{e,\exp}$ (mmol.g^{-1})	0.122	0.275	0.559	0.716
$q_{e,cal}$ (mmol.g^{-1})	0.122	0.275	0.559	0.716
R^2	0.997	0.990	0.950	0.954
MPSD	1.49	3.106	8.38	7.627
Pseudo 2nd order				
k_s (g.mmol^{-1}.min^{-1})	11.489	3.502	0.558	0.588
h (mmol.g^{-1}.min^{-1})	0.172	0.263	0.169	0.290
$q_{e,cal}$ (mmol.g^{-1})	0.122	0.274	0.548	0.700
R^2	0.999	0.998	0.988	0.984
MPSD	0.351	1.042	3.309	3.671
Weber Morris				
$k_{id,1}$ (mmol.g^{-1}.min$^{-1/2}$)	0.006	0.005	0.018	0.013
I_1	0.091	0.226	0.344	0.515
R^2	0.948	0.680	0.871	0.817
$k_{id,2}$ (mmol.g^{-1}.min$^{-1/2}$)	0.001	0.001	0.001	0.001
I_2	0.119	0.265	0.526	0.071
R^2	0.578	0.67	0.884	0.426

The experimental and calculated values of equilibrium uptake from pseudo second-order kinetic model are very close to each other. The calculated R^2 are closer to unity for pseudo second-order kinetic model than the pseudo first-order kinetic model for adsorption of pyrrole and indole onto BFA which represents the best fit for experimental data.

4.3.1.4 Intraparticle diffusion model

Figure 4.3.5b shows the plot of q_t vs. $t^{1/2}$ at various C_o of pyrrole and indole adsorption onto BFA. This figure has non-linear plots over the whole time range and can be represented by multi-linear plots implying that more than one process is controlling the adsorption process. Values $k_{id,1}$ and $k_{id,2}$ increase with C_o increased driving force at higher C_o. Both surface and intra-particle diffusion within the pores of BFA control the adsorption process indicating rather complex adsorption mechanism [Wang and Jiang, 2007; Mohan, et al., 2008]. Overall, second linear portion indicates intra-particle diffusion and the rate-controlling step.

4.3.1.5 Adsorption equilibrium and thermodynamics study for individual adsorption

Adsorption isotherms (q_e versus C_e) plot for pyrrole and indole adsorption onto BFA at three different temperatures are shown in Figure 4.3.6. This study was carried out in the C_o range of 100-1000 $mg.l^{-1}$ of both pyrrole and indole and adsorbent doses of BFA for pyrrole and indole was taken as 15 $g.l^{-1}$ and 7 $g.l^{-1}$, respectively. Pyrrole removal by BFA was insignificantly affected by the change in temperature, however, indole adsorption increased with an increase in temperature. Physical adsorption as well chemical adsorption may involve cause variation in adsorption with an increase in temperature. Enhanced uptake of indole by BFA at higher temperature may be due to the increased mobility of indole from the bulk to the adsorbent surface at the increased temperature. All the isotherms of pyrrole and indole adsorption onto BFA were fitted to the Langmuir [Langmuir, 1918], Freundlich [Freundlich, 1906] and Redlich and Peterson (R-P) [Redlich and Peterson, 1959] isotherms using non-linear regression. SSE was used to find out the best isotherm model representing the experimental data. The isotherm parameters and the SSE values for these isotherm models are given in the Table 4.3.3.

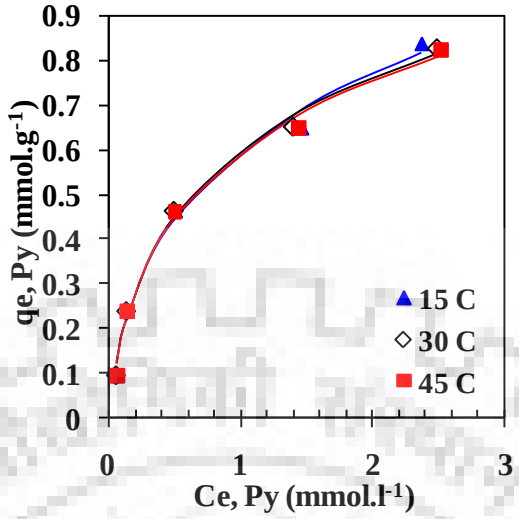

(a) Pyrrole

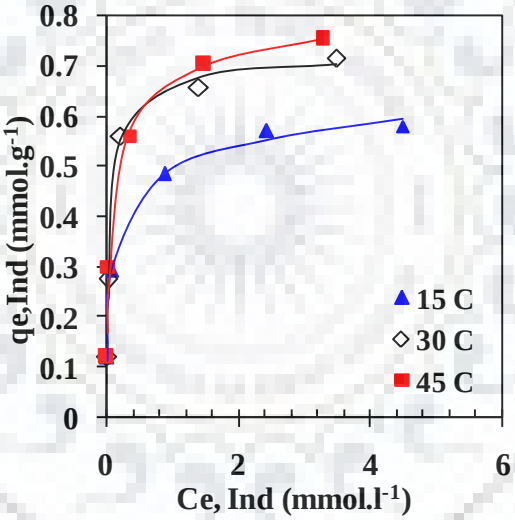

(b) Indole

Figure 4.3.6: Equilibrium adsorption isotherms at different temperature for the treatment of (a) pyrrole and (b) indole by BFA. Experimental data points given by symbols and the lines predicated by R-P isotherm model. T=8 h, C_o=100-1000 mg.l^{-1}, for BFA m=15 g.l^{-1}for pyrrole and m=7 g.l^{-1}for indole, pH_o=5.7.

It is observed that the R^2 value for R-P model is closer to unity and the SSE value is least for R-P model. Thus, R-P model best-represents the isotherm data at all temperatures for pyrrole and indole adsorption onto BFA. It may be seen in Figures 4.2.6a and 4.3.6a that temperature has no effect on pyrrole adsorption onto GAC and BFA. Therefore, for pyrrole adsorption, there is no specific trend and there is marginal difference in the values of Langmuir constants (q_m and K_L), Freundlich constants (K_F). Generally, adsorption is an exothermic process, however, for diffusion-controlled processes, adsorption becomes endothermic in nature. It seems that pyrrole adsorption onto GAC or BFA occurs by a combination of these processes; therefore, temperature has no effect on the adsorption of pyrrole onto these adsorbents. For indole adsorption, these values continuously increase with an increase in temperature, since adsorption of indole onto GAC and BFA is endothermic in nature.

Values of ΔH^0 and ΔS^0 values were obtained from the van't Hoff plot of ln K_D versus 1/T [Sharma et al., 2007, 2008; Wen et al, 2010]. Values of ΔH^0, ΔS^0 and ΔG^0 are given in Table 4.3.4. ΔS^0 values are positive for both pyrrole and indole adsorption onto BFA suggesting increased randomness on the interface. ΔG^0 values are found to be negative indicating the feasibility and spontaneity of adsorption of pyrrole and indole onto BFA. Positive values of ΔH^0 indicate the endothermic nature of the indole adsorption onto BFA.

4.3.1.6 Reusability of adsorbent BFA

Reusability of BFA was studied (as was that for GAC) by carrying out desorption study. Desorption of pyrrole and indole from loaded BFA in presence of acid, alcohol, acetone and water was found to be very low, however, pyrrole desorption efficiency using NaOH was 54% whereas indole desorption was 6.7%. Similar to earlier study for GAC, thermally desorbed BFA were again used for pyrrole and indole adsorption and the results are shown in Figure 4.3.7. It is seen that adsorption capacity of BFA decreased significantly after each desorption, though its adsorption capacity of indole was much higher as compared to that of pyrrole after successive thermal desorption. Decrease in active sites because of the change in structure resulted in decrease in the adsorptive capacity of BFA after successive adsorption-desorption cycles.

Table 4.3.3: Isotherm parameters for individual adsorption of pyrrole and indole onto BFA (t=8 h, $C_{o,Py}$=1.49-14.91 mmol.l^{-1}, $C_{o,Ind=}$0.85-8.54 mmol.l^{-1}, m=15 g.l^{-1} for pyrrole and m=7 g.l^{-1} for indole).

Freundlich				
T(K)	K_f	1/n	R^2	SSE
Pyrrole				
288	0.552	0.565	0.971	0.017
303	0.574	0.423	0.994	0.002
318	0.543	0.557	0.966	0.020
Indole				
288	0.454	0.201	0.950	0.008
303	0.611	0.160	0.953	0.012
318	0.610	0.235	0.920	0.025
Langmuir				
T(K)	q_m	K_l	R^2	SSE
Pyrrole				
288	0.927	2.093	0.978	0.008
303	0.930	2.095	0.986	0.005
318	0.920	2.118	0.984	0.006
Indole				
288	0.568	13.697	0.980	0.004
303	0.705	18.235	0.984	0.004
318	0.731	15.683	0.970	0.009
Redlich Peterson				
T(K)	K_R	a_r	β	R^2	SSE
Pyrrole					
288	3.298	4.549	0.737	0.990	0.004
303	2.966	3.939	0.784	0.994	0.002
318	3.039	4.109	0.780	0.993	0.002
Indole					
288	13.424	28.147	0.897	0.997	0.001
303	13.654	19.588	0.982	0.985	0.004
318	14.973	21.436	0.923	0.984	0.005

Table 4.3.4: Thermodynamic parameters for the adsorption of pyrrole and indole onto BFA (t=8 h, $C_{o,Py}$=1.49-14.91 mmol.l^{-1}, $C_{o,Ind}$=0.85-8.54 mmol.l^{-1}, m=15 g.l^{-1} for pyrrole and m=7 g.l^{-1} for indole).

Temp (K)	K x 10^3 (l.kg^{-1})	ΔG^0 (kJ.mol^{-1})	ΔH^0 (kJ.mol^{-1})	ΔS^0 (kJ.mol^{-1}K^{-1})
Pyrrole				
288	3.263	-19.38	2.05	74.36
303	3.402	-20.50		
318	3.538	-21.61		
Indole				
288	31.743	-24.83	32.22	198.88
303	86.034	-28.63		
318	111.580	-30.74		

4.3.2 Optimization of Parameters for Simultaneous Removal of Pyrrole and Indole by BFA using Taguch's Design of Experiments

4.3.2.1 Multi-component study using Taguchi's method

Again, Taguchi's L_{27} OA was used for studying the effects of parameters during simultaneous adsorption of pyrrole and indole onto BFA. The five process parameters and their levels are given in Table 4.3.5 and the conditions for each of the 27 experiments are given in Table 4.3.6. Two parameter interactions between initial concentrations of adsorbates ($C_{o,Py} \times C_{o,,Ind}$) was also studied. Values of the individual adsorption capacities of pyrrole and indole (q_{Py} and q_{Ind}) and the total adsorption capacity (q_{tot}) are also given in Table 4.3.6. It is seen that adsorption of both pyrrole and indole is highly dependent on the parametric conditions.

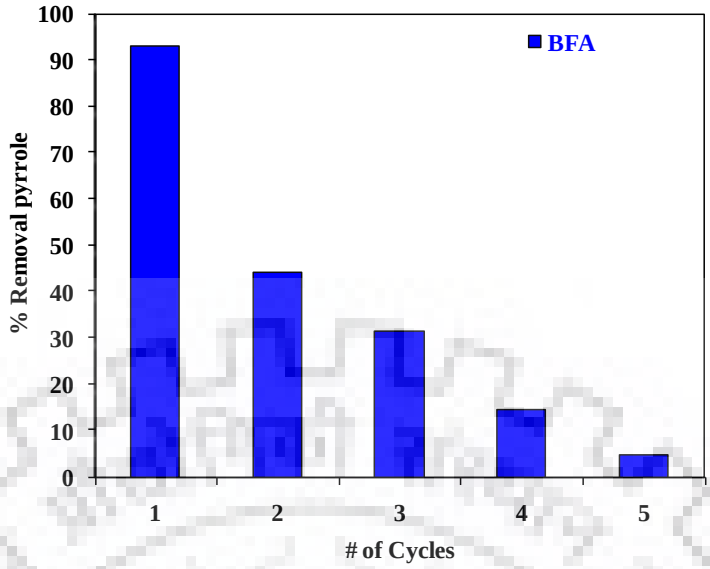

(a) Pyrrole desorption

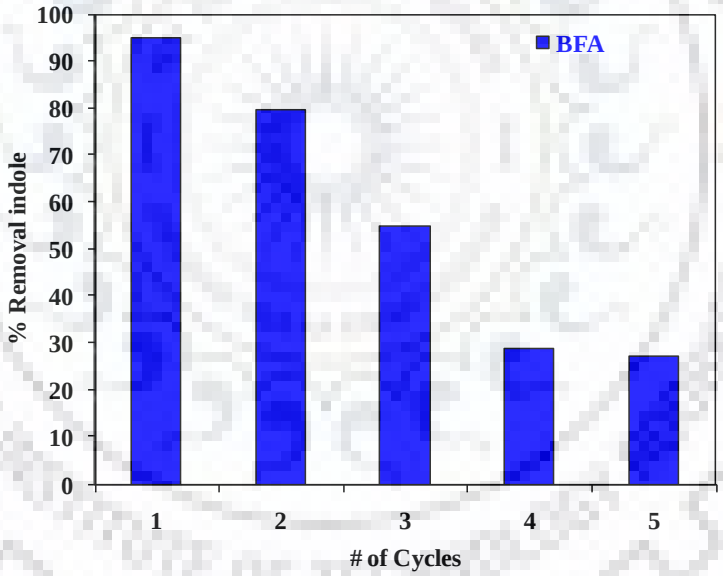

(b) Indole desorption

Figure 4.3.7: (a) Pyrrole and (b) indole removal efficiency of BFA after various thermal desorption-adsorption cycles.

Table 4.3.5: Multi-component adsorption study parameters for the adsorption of pyrrole and indole onto BFA using Taguchi's OA.

Parameters		Units		Levels		
				0	1	2
A:	Initial concentration of pyrrole	$\mathbf{C_{o,Py}}$	$mmol.l^{-1}$	0	3.73	7.45
B:	Initial concentration of indole	$\mathbf{C_{o,Ind}}$	$mmol.l^{-1}$	0	2.13	4.27
C:	Temperature	**T**	(°C)	15	30	45
D:	Adsorbent dose	**m**	($g\ L^{-1}$)	4	9	14
E:	Contact time	**t**	(min)	60	300	540

4.3.2.2 Process parameters effects

The effects of parameters (C_{oi} T, m and t) on q_{tot}, q_{Py} and q_{Ind} for adsorption of pyrrole and indole onto BFA are given in the Figure 4.3.8. Values of $q_{tot,}$ q_{Py} and q_{Ind} are found to be highly dependent on these parameters.

An increase in $C_{o,i,}$ and t from level 1 to 3 resulted in an increase in q_{tot} value. Temperature (T) is found to affect the q_{Py} and q_{Ind} values in different manner as was observed during the individual adsorption. An increase in T from 15°C to 45°C increases the q_{Py} slightly although marginal decrease in q_{Py} value is observed from 15°C to 30°C. However, q_{Ind} increases with an increase in T from 15°C to 45°C. Pyrrole and indole are found to have antagonistic affect on each other. When adsorption of pyrrole decreases, q_{Ind} increases and when adsorption of indole decreases, q_{Py} increases. This is because both pyrrole and indole compete for the same active sites of BFA during the simultaneous adsorption. But effective q_{tot} increases with increase in all other parameters except adsorbent dose. Results may vary from those that were obtained for individual adsorption as there was a lot of interaction between pyrrole and indole for same adsorption sites.

Table 4.3.6: Taguchi's L_{27} (3^{13}) orthogonal array for multi-component adsorption of pyrrole and indole system onto BFA.

Exp. No.	A	B	AxB	AxB	C	D	E	q_{Py}	q_{Ind}	q_{tot}
1	0	0	0	0	15	4	1	0.00	0.00	0.00
2	0	0	0	0	30	9	5	0.00	0.00	0.00
3	0	0	0	0	45	14	9	0.00	0.00	0.00
4	0	2.13	1	1	15	4	1	0.00	0.31	0.31
5	0	2.13	1	1	30	9	5	0.00	0.23	0.23
6	0	2.13	1	1	45	14	9	0.00	0.15	0.15
7	0	4.27	2	2	15	4	1	0.00	0.37	0.37
8	0	4.27	2	2	30	9	5	0.00	0.41	0.41
9	0	4.27	2	2	45	14	9	0.00	0.30	0.30
10	3.73	0	1	2	15	9	9	0.33	0.00	0.33
11	3.73	0	1	2	30	14	1	0.18	0.00	0.18
12	3.73	0	1	2	45	4	5	0.39	0.00	0.39
13	3.73	2.13	2	0	15	9	9	0.25	0.23	0.48
14	3.73	2.13	2	0	30	14	1	0.15	0.14	0.30
15	3.73	2.13	2	0	45	4	5	0.24	0.44	0.68
16	3.73	4.27	0	1	15	9	9	0.15	0.39	0.54
17	3.73	4.27	0	1	30	14	1	0.11	0.25	0.36
18	3.73	4.27	0	1	45	4	5	0.16	0.50	0.66
19	7.45	0	2	1	15	14	5	0.40	0.00	0.40
20	7.45	0	2	1	30	4	9	0.64	0.00	0.64
21	7.45	0	2	1	45	9	1	0.44	0.00	0.44
22	7.45	2.13	0	2	15	14	5	0.29	0.15	0.43
23	7.45	2.13	0	2	30	4	9	0.28	0.41	0.70
24	7.45	2.13	0	2	45	9	1	0.26	0.22	0.48
25	7.45	4.27	1	0	15	14	5	0.20	0.27	0.47
26	7.45	4.27	1	0	30	4	9	0.17	0.47	0.64
27	7.45	4.27	1	0	45	9	1	0.22	0.36	0.58
Total								4.9	5.60	10.50

It is observed that q_{tot} value increased with an increase in time from 1 h to 9 h. Adsorption of pyrrole and indole increased with an increase in contact time until equilibrium was achieved between the adsorbates and the BFA. As was the case with GAC, indole achieved equilibrium onto BFA earlier as compared to pyrrole. q_{tot} decreased with an increase in dose (m) from level 1 to 3 , however, percent removal (analyzed separately) increased with an increase in m due to presence of more sites at higher adsorbent dose for adsorption.

Analysis of Figure 4.3.8 shows that $C_{o,i}$ and time have strongest influence on q_{tot}. $C_{o,Py}$ and $C_{o,Ind}$ have highest effect at level 3 and m has the greatest effect at level 1 whereas T and t have highest influence at level 3. Highest difference between level 1 and level 2 for $C_{o,Py}$ indicates stronger influence on q_{Py} as compared to other parameters. Figure 4.3.9 shows the effect of concentration of one component with respect to other component. Existence of non-parallel lines indicates strong interaction between $C_{o,I}$ [Kim et al., 2003 and Singh et al., 2013]. ANOVA results for responses q_{tot}, q_{Py} and q_{Ind} during binary adsorption of pyrrole and indole onto BFA are given in Table 4.3.7.

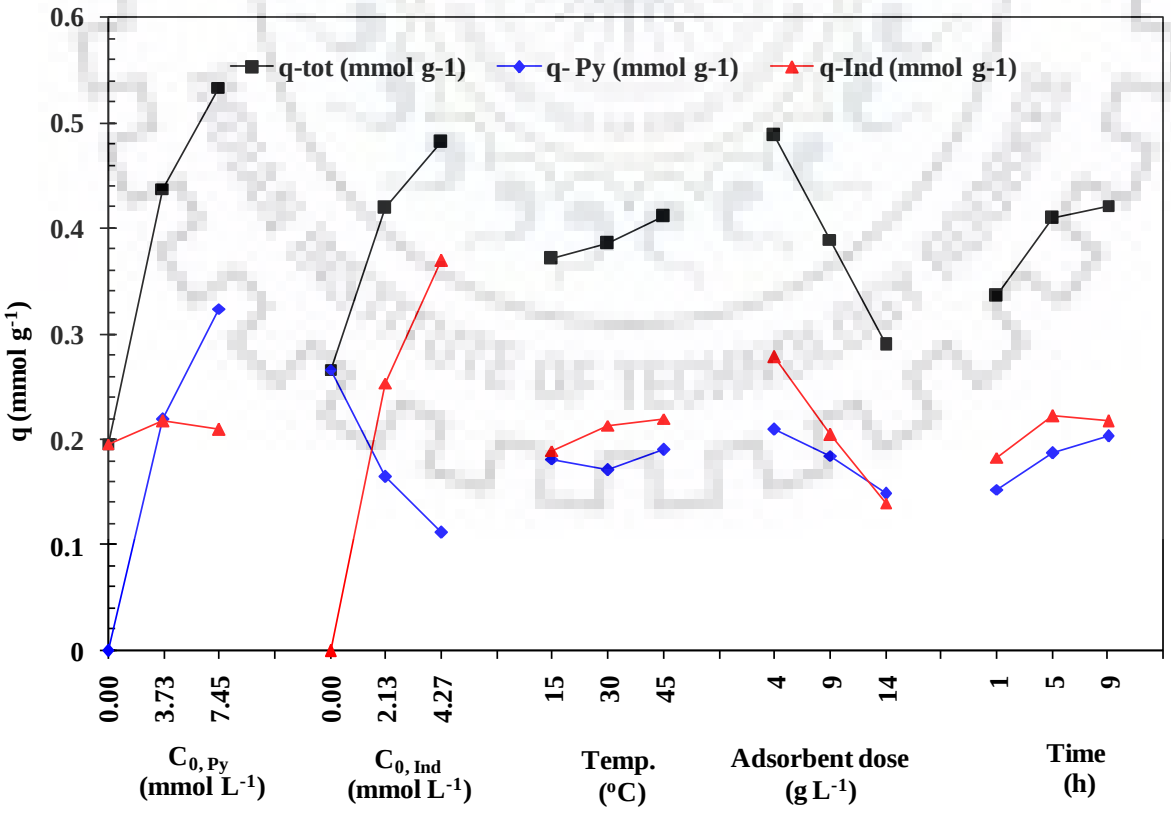

Figure 4.3.8: Effect of process parameters on q_{tot} for multicomponent adsorption of pyrrole and indole onto BFA.

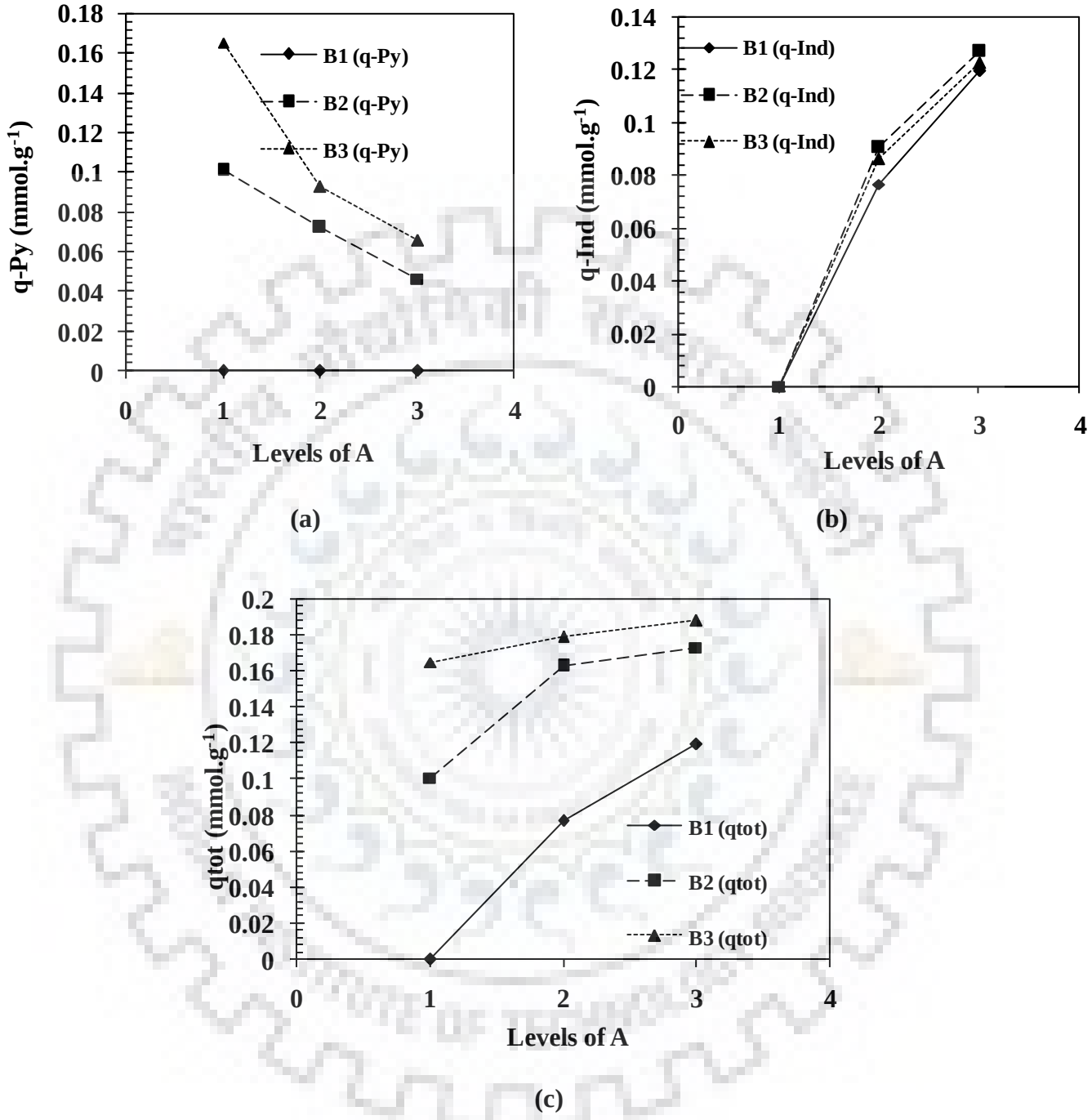

Figure 4.3.9: The effect of interaction between A and B at 3 levels on (a) q_{Py}, (b) q_{Ind} and (c) q_{tot} for multicomponent adsorption of pyrrole and indole onto BFA. B1, B2 and B3 are levels of B.

Table 4.3.7: ANOVA of q_{tot} for multicomponent adsorption of pyrrole and indole onto BFA.

	Sum of squares	DOF	Mean square	% contribution	F-value
			q_{tot}		
A	0.54	2	0.27	50.33	135.60
B	0.22	2	0.11	20.48	55.17
C	0.01	2	0.00	0.67	1.79
D	0.18	2	0.09	16.42	44.24
E	0.04	2	0.02	3.59	9.67
$A\times B$	0.07	4	0.02	6.29	8.47
Residual	0.02	12	0.00	2.23	
Model	1.05	14	0.51	97.77	254.94
Cor. total	1.08	26	0.51	100.00	
			q_{Ind}		
A	0.00	2	0.00	0.26	0.22
B	0.64	2	0.32	80.20	68.09
C	0.00	2	0.00	0.56	0.48
D	0.09	2	0.04	16.42	9.08
E	0.01	2	0.00	1.03	0.88
$A\times B$	0.00	4	0.00	0.18	0.07
Residual	0.06	12	0.00	7.07	
Model	0.74	14	0.37	92.93	78.82
Cor. total	0.80	26	0.38	100.00	
			q_{Py}		
A	0.49	2	0.25	66.48	86.38
B	0.11	2	0.06	14.93	19.40
C	0.00	2	0.00	0.23	0.30
D	0.02	2	0.01	2.24	2.91
E	0.01	2	0.01	1.65	2.14
$A\times B$	0.07	4	0.02	9.86	6.41
Residual	0.03	12	0.00	4.62	
Model	0.71	14	0.33	95.38	117.53
Cor. total	0.74	26	0.34	100.00	

4.3.2.3 Optimum level selection and optimum response characteristics estimation

Optimum levels of parameters for maximum adsorption were obtained by examining the q_{tot} values. First level parameter for D (m), and third levels parameter for A, B ($C_{o,i}$), C (temperature) and E (time) gave higher value of q_{tot}. Considering this, the optimal value of the response curve was calculated using the following relationship [Srivastava et al., 2007b, 2011]:

$$q_{tot,predicted} = \overline{T} + (\overline{A_3} - \overline{T}) + (\overline{B_3} - \overline{T}) + (\overline{C_3} - \overline{T}) + (\overline{D_1} - \overline{T}) + (\overline{E_3} - \overline{T}) \quad (4.3.1)$$

where, $\overline{C_3}$ and $\overline{D_1}$ is the average value of response at third level of parameter C and first level of parameter D, respectively. For parameters A and B, third level was chosen so as to check the adsorption efficiency for maximum concentration. The predicted maximum value of q_{tot}, q_{Py} and q_{Ind} for BFA were 0.78, 0.32 and 0.46 mmol.g^{-}1, respectively. The calculated value of q_{tot}, q_{Py} and q_{Ind} for three confirmation experiments were 0.78, 0.32 and 0.46 mmol.g^{-1}, respectively. These values are within 95% confidence interval.

4.3.3 Multi-Component Isotherm Study for Simultaneous Removal of Pyrrole and Indole by BFA

Binary isotherm study using BFA was done similar to that using GAC. From Table 4.3.8, it is observed that individual percent removal of indole decreased for the indole as pyrrole concentration increased. It is also seen that the equilibrium uptake of indole increased as its concentration increased (for fixed concentration of pyrrole). Similar trend was observed for pyrrole with increasing concentration of indole.

Binary isotherm study results show that for 4.27 mmol.l^{-1} (500 mg.l^{-1}) concentration of indole with presence of 7.45 mmol.l^{-1} (500 mg.l^{-1}) of pyrrole, q_{Ind} was 0.27 mmol.g^{-1}. Similarly for 6.402 mmol.l^{-1} (750 mg.l^{-1}) concentration of indole in presence of 11.17 mmol.l^{-1} (750 mg.l^{-1}) of pyrrole, q_{Ind} was 0.41 mmol.g^{-1}. Binary equilibrium adsorption data indicate that adsorption capacity of BFA is higher for indole than that of pyrrole.

Again, various multi-component isotherms like non-modified, modified and extended-Langmuir, R-P models, extended-Freundlich, etc. [Srivastava et al., 2008c] were used to fit the data obtained from simultaneous adsorption of pyrrole and indole onto BFA using SSE. Table 4.3.9 shows SSE values between calculated and experimental q_e values for pyrrole and indole data with various parameters of multi-component isotherms. Non-modified models show poor fit for adsorption data for binary system as SSE values are very large for these models. For non-modified Langmuir model, SSE value is found to be 1.73 which is much higher than extended-Langmuir and modified-Langmuir model. It is also found that extended-Langmuir with SSE value 0.23 has better fit as compared to modified-Langmuir with SSE value 0.35. In extended-Langmuir model, K_i value reflects the affinity between adsorbate and adsorbent in a binary mixture which is 5.48 for indole and 0.86 for pyrrole while overall adsorbate uptake q_{max} is 0.65 mmol.g^{-1}. Extended-Langmuir model and Extended-Freundlich model gives SSE value 0.23 and 0.16, respectively. The parity plots (Figure.4.3.10) presents comparison between actual and theoretical q_e values of pyrrole and indole.

Table 4.3.8: Comparison of individual and total adsorption uptakes and yields found at different pyrrole concentrations with increasing concentration of indole onto BFA.

$C_{e,Ind}$	$C_{e,Py}$	$q_{e,Ind}$	$q_{e,Py}$	Ad_{Ind}%	Ad_{Py}%	Ad_{tot}%
0.000	0.031	0.030	0.051	99.99	95.86	97.36
0.000	0.049	0.061	0.049	99.99	93.43	96.93
0.026	0.190	0.151	0.039	98.76	74.46	92.47
0.102	0.177	0.298	0.041	97.62	76.26	94.44
0.318	0.261	0.428	0.035	94.97	64.92	91.79
0.000	0.227	0.030	0.090	99.99	84.78	88.17
0.003	0.190	0.061	0.093	99.65	87.24	91.76
0.018	0.408	0.151	0.077	99.13	72.64	88.24
0.185	0.594	0.292	0.064	95.66	60.15	86.47
1.035	0.941	0.377	0.039	83.59	36.87	74.67
0.015	0.755	0.029	0.212	96.47	79.73	81.45
0.008	0.813	0.060	0.208	99.02	78.17	82.06
0.017	1.234	0.151	0.178	99.22	66.89	78.66
0.745	1.862	0.252	0.133	82.54	50.02	67.38
0.500	2.056	0.415	0.119	92.07	44.84	74.53
0.025	1.735	0.029	0.382	94.25	75.49	76.56
0.007	1.933	0.060	0.368	99.17	72.69	75.54
0.039	2.212	0.149	0.348	98.14	68.76	75.57
0.556	3.634	0.265	0.246	86.97	48.67	63.07
0.549	4.459	0.411	0.208	91.29	39.56	63.41
0.000	2.299	0.030	0.623	99.99	79.12	79.90
0.007	3.649	0.060	0.526	99.17	66.87	69.19
0.031	3.862	0.150	0.511	98.53	64.94	70.39
0.117	5.967	0.296	0.361	97.26	45.83	60.19
0.548	6.729	0.411	0.306	91.32	38.91	58.00

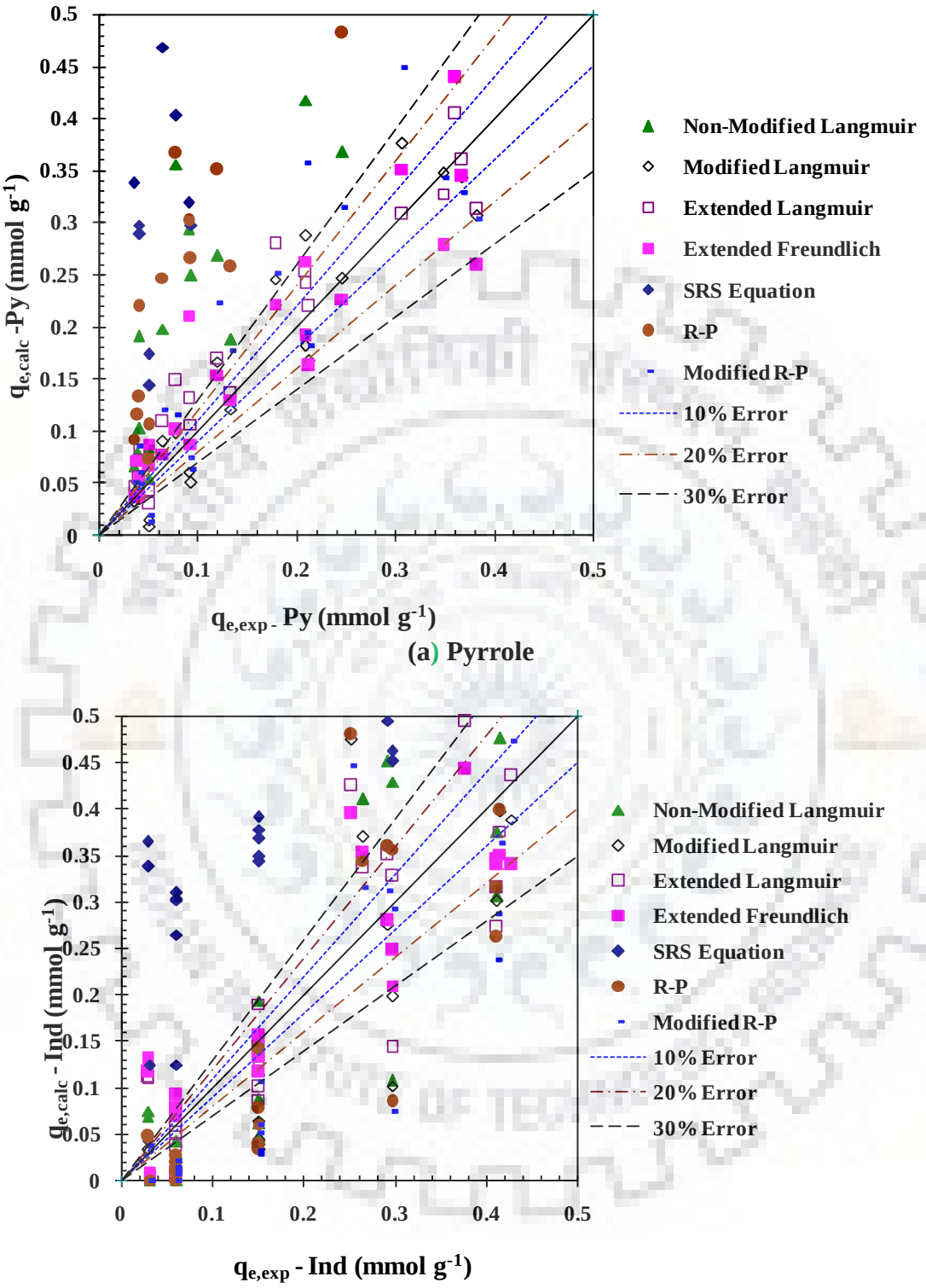

(a) Pyrrole

(b) Indole

Figure 4.3.10: Comparison of actual and theoretical equilibrium adsorption values of pyrrole (Py) and indole (Ind) in a binary mixture.

Table 4.3.9: Individual and multi-component isotherm parameter values for the pyrrole and indole adsorption onto BFA at 30°C.

Individual isotherm models [Ozacar and Sengil, 2005; Sengil et al., 2009]		**Parameter**	**Pyrrole**	**Indole**
Langmuir	$q_e = \frac{q_m k_L c_e}{1 + k_L c_e}$	q_m	0.93	0.705
		k_L	2.09	18.24
		SSE	0.005	0.004
Freundlich	$q_e = k_F c_e^{1/n}$	k_F	0.57	0.61
		$1/n$	0.42	0.16
		SSE	0.002	0.012
Redlich-Peterson	$q_e = \frac{k_R c_e}{1 + a_R c_e^{\beta}}$	k_R	2.97	13.65
		a_R	3.94	19.58
		β	0.78	0.98
		SSE	0.002	0.004
Multicomponent isotherm models				
Non-modified Langmuir model	$q_{e,i} = \frac{q_{m,i} K_{L,i} C_{e,i}}{1 + \sum_{j=1}^{N} K_{L,j} C_{e,j}}$	SSE	1.73	
Modified Langmuir model	$q_{e,i} = \frac{q_{m,i} K_{L,i} \left(\frac{C_{e,i}}{\eta_{L,i}}\right)}{1 + \sum_{j=1}^{N} K_{L,j} \left(\frac{C_{e,j}}{\eta_{L,j}}\right)}$	$\eta_{L,i}$	6.58	4.89
		SSE	0.35	
Extended Langmuir	$q_{e,i} = \frac{q_{\max} K_{EL,i} C_{e,i}}{1 + \sum_{j=1}^{N} K_{EL,j} C_{e,j}}$	K_i	0.86	5.48
		$q_{\max}$	0.65	
		SSE	0.23	
Extended Freundlich	$q_{e,1} = \frac{K_{F,1} C_{e,1}^{n_1 + x_1}}{C_{e,1}^{x_1} + y_1 C_{e,2}^{z_1}}$, $q_{e,2} = \frac{K_{F,2} C_{e,2}^{n_2 + x_2}}{C_{e,2}^{x_2} + y_2 C_{e,1}^{z_2}}$	X	0.41	0.35
		Y	6.60	0.46
		Z	0.29	0.12
		SSE	0.16	
Non-modified Redlich-Peterson	$q_{e,i} = \frac{K_{R,i} C_{e,i}}{1 + \sum_{j=1}^{N} a_{R,j} C_{e,j}^{\beta_j}}$	SSE	2.26	
Modified Redlich-Peterson	$q_{e,i} = \frac{K_{R,i} \left(\frac{C_{e,i}}{\eta_{R,i}}\right)}{1 + \sum_{j=1}^{N} a_{R,j} \left(\frac{C_{e,j}}{\eta_{R,j}}\right)^{\beta_j}}$	$\eta_{R,i}$	7.16	1.73
		SSE	0.43	

4.3.4 Economic Analysis of Adsorbents

The approximate economic evaluation of the adsorption process using GAC and BFA is presented in Table 4.3.10. Though the adsorbent dose of GAC was higher than that of BFA, the overall cost of treatment with GAC and BFA is comparable. This is because GAC could be used in five adsorption-desorption cycles whereas BFA can be used only once. Though BFA is available almost free of cost, however, for usage some transportation and handling charges are required. As the calorific value of both GAC and BFA are good, organic matter laden GAC and BFA could be used to make fire briquettes. Revenue generated from briquettes could compensate for transportation and handling charges of BFA.

Table 4.3.10: Economic evaluation of GAC and BFA.

Adsorbents	Adsorbate	Adsorbent dose ($kg.m^{-3}$)	Adsorbent cost ($ per kg)	Treatment cost ($ per m^3)
GAC	Pyrrole	$20/5^{\#}=4$	0.5	2
	Indole	$20/5^{\#}=4$	0.5	2
BFA	Pyrrole	15	0.08*	1.2
	Indole	7	0.08*	0.56

$^{\#}$Number of adsorption-desorption cycles in which GAC can be reused.

*Handling charges of adsorbents.

4.4 ELECTROCHEMICAL TREATMENT OF PYRROLE AND INDOLE BY PLATINUM COATED WITH TITANIUM (Pt/Ti) ELECTRODE

This section presents the results of the electrochemical treatment of pyrrole and indole present individually and simultaneously in aqueous solution with platinum coated titanium (Pt/Ti) electrode. First, optimization of parameters for individual mineralization of pyrrole and indole in aqueous solution using response surface methodology (RSM) is presented which includes studies on the effect of pH (pH_o), current density (j), conductivity (k) and time (t) on parameters like chemical oxygen demand (COD) removal (Y_1) and specific energy consumption (Y_2). Second, optimization of parameters for simultaneous electrochemical treatment of pyrrole and indole in aqueous solution by using Taguchi's methodology is presented. Studies related to mechanism of degradation of pyrrole and indole, filterability of the treated slurry, physico-chemical and thermal analysis of electrochemical residues are also presented in the last.

4.4.1 Individual Removal of Pyrrole and Indole by Electrochemical Treatment by using Response Surface Methodology

4.4.1.1 Statistical analysis and fitting of second-order polynomial equation

In the present study, 4-factor and 5-level full factorial central composite design (CCD) within RSM was used for experimental design to investigate the effect of various parameters [Zabeti et al., 2009; Mangwandi et al., 2013]. Individual treatment of pyrrole and indole in aqueous solution was studied using platinum coated titanium (Pt/Ti) electrode. 30 experiments were carried out as per matrix given in Tables 4.4.1 and 4.4.2. COD removal (Y_1, %) and specific energy consumption (Y_2, kWh per kg COD removed) were taken as response.

To obtain the best regression equations for representing the experimental data, models like linear, interactive, quadratic and cubic equations were fitted to the experimental data obtained. Adequacies of model were examined by sequential model sum of squares and model summary statistical tests. F-test for statistical significance check, coefficient of

determination (R^2) and adjusted R^2 were calculated and are shown in Tables 4.4.3 and 4.4.4, respectively, for pyrrole and indole removal. Both the tests suggested to use the quadratic second order polynomial equation for obtaining equations in terms of Y_1 and Y_2 for both pyrrole and indole removal.

Analysis of variance (ANOVA) results for quadratic model representling COD removal (Y_1) and specific energy consumption (Y_2) during electrochemical treatment of pyrrole are indole individually by Pt/Ti electrode are given in Tables 4.4.5 and 4.4.6. Values of "Prob > F" indicates that model terms are significant and highly significant for values less than 0.05 and 0.0001, respectively at 95% probability level.

Table 4.4.5 shows that model F-value during pyrrole mineralization for Y_1 and Y_2 are 24.12 and 10.57 implying quadratic model is significant. ANOVA analysis showed that for response Y_1 model terms j and t are highly significant whereas j^2, $pH_o \times j$, $pH_o \times k$, $j \times k$ and $j \times t$ are significant terms. The quadratic equation in terms of coded factors for COD removal (Y_1) during pyrrole mineralization is given as under:

$$Y_1 = 45.20 - 0.75X_1 + 11.37X_2 - 0.16X_3 + 10.06X_4 + 1.38X_1^2 - 2.10X_2^2 - 0.70X_3^2 - 1.36X_4^2 - 2.89X_1X_2 - 2.60X_1X_3 + 0.79X_1X_4 + 3.53X_2X_3 + 4.21X_2X_4 - 0.71X_3X_4 \quad (4.4.1)$$

For response Y_2 (specific energy consumption) during pyrrole mineralization, model terms j is highly significant whereas k, pH_o^2, and $j \times k$ are significant terms. The quadratic equations in terms of coded factors for specific energy consumption (Y_2) is given as under:

$$Y_2 = 243.75 - 7.37X_1 + 57.30X_2 - 23.16X_3 + 5.44X_4 - 16.52X_1^2 - 5.96X_2^2 - 4.25X_3^2 + 6.51X_4^2 + 15.24X_1X_2 + 3.95X_1X_3 - 4.61X_1X_4 - 29.43X_2X_3 - 8.19X_2X_4 + 1.67X_3X_4 \quad (4.4.2)$$

Intensity is indicated by the values present in the coded model terms and direction of influence by its algebraic sign (+/-) [Cruz-Gonzalez et al., 2010]. It is suggested that R^2 value should be at least 0.8 for good fit of model [Joglekar and May, 1987]. However, R^2 values of quadratic polynomial model for Y_1 and Y_2 during pyrrole mineralization were found to be 0.96 and 0.90 respectively.

Table 4.4.1: Actual and predicted results for the electrochemical treatment of pyrrole.

Std order	pH_o	Current density, j ($A.m^{-2}$)	Conductivity, k ($mS.cm^{-1}$)	Time, t (min)	% COD removal		Specific Energy Consumption (kWh per kg COD removed)	
					Actual	Predicted	Actual	Predicted
1	4.3	166.67	3.86	60	21.19	24.22	164.96	155.20
2	7.3	166.67	3.86	60	39.39	32.12	99.25	140.78
3	4.3	333.33	3.86	60	37.58	37.27	301.43	314.57
4	7.3	333.33	3.86	60	35.38	33.62	343.82	361.12
5	4.3	166.67	5.75	60	23.63	23.46	136.41	156.51
6	7.3	166.67	5.75	60	20.57	20.96	149.25	157.89
7	4.3	333.33	5.75	60	57.14	50.63	154.25	198.15
8	7.3	333.33	5.75	60	37.74	36.58	265.25	260.5
9	4.3	166.67	3.86	120	37.91	35.78	160.19	188.35
10	7.3	166.67	3.86	120	42.09	46.83	178.05	155.48
11	4.3	333.33	3.86	120	67.83	65.66	302.26	314.95
12	7.3	333.33	3.86	120	68.27	65.15	339.75	343.05
13	4.3	166.67	5.75	120	32.19	32.18	192.29	196.32
14	7.3	166.67	5.75	120	35.82	32.84	169	179.26
15	4.3	333.33	5.75	120	72.2	76.18	223.31	205.19
16	7.3	333.33	5.75	120	70.1	65.28	218	249.09
17	2.8	250	4.8	90	52.59	52.20	187.64	162.93
18	8.8	250	4.8	90	43.75	49.20	212.45	192.41
19	5.8	83.34	4.8	90	14.39	14.06	123.13	105.29
20	5.8	416.66	4.8	90	54.15	59.55	361.42	334.50
21	5.8	250	2.91	90	40.78	42.73	292.62	273.08
22	5.8	250	6.69	90	38.98	42.09	205.65	180.43
23	5.8	250	4.8	30	15.3	19.64	301.6	258.91
24	5.8	250	4.8	150	59.17	59.89	282.71	280.65
25	5.8	250	4.8	90	45.2	45.2	243.75	243.75
26	5.8	250	4.8	90	45.2	45.2	243.75	243.75
27	5.8	250	4.8	90	45.2	45.2	243.75	243.75
28	5.8	250	4.8	90	45.2	45.2	243.75	243.75
29	5.8	250	4.8	90	45.2	45.2	243.75	243.75
30	5.8	250	4.8	90	45.2	45.2	243.75	243.75

Table 4.4.2: Actual and predicted results for the electrochemical treatment of indole.

Std order	pH_0	Current density, j ($A.m^{-2}$)	Conductivity, k ($mS.cm^{-1}$)	Time, t (min)	% COD removal		Specific Energy Consumption (kWh per kg COD removed)	
					Actual	Predicted	Actual	Predicted
1	4.3	166.67	3.86	60	29.11	29.37	82.67	93.66
2	7.3	166.67	3.86	60	24.25	24.26	114.41	108.08
3	4.3	333.33	3.86	60	49.30	51.62	168.96	156.94
4	7.3	333.33	3.86	60	43.31	45.21	164.79	170.32
5	4.3	166.67	5.75	60	32.83	36.12	61.19	46.89
6	7.3	166.67	5.75	60	32.78	30.83	42.489	64.03
7	4.3	333.33	5.75	60	61.54	61.78	98.59	95.21
8	7.3	333.33	5.75	60	55.94	55.20	119.48	111.32
9	4.3	166.67	3.86	120	46.69	51.47	112.5	105.79
10	7.3	166.67	3.86	120	52.05	50.37	95.09	104.92
11	4.3	333.33	3.86	120	73.81	74.32	224.34	209.25
12	7.3	333.33	3.86	120	71.17	71.92	207.93	207.35
13	4.3	166.67	5.75	120	60.58	57.252	64.82	65.75
14	7.3	166.67	5.75	120	54.27	55.99	70.46	67.61
15	4.3	333.33	5.75	120	79.49	83.52	162.8	154.26
16	7.3	333.33	5.75	120	82.66	80.96	159.62	155.08
17	2.8	250	4.80	90	69.35	64.59	80.88	100.72
18	8.8	250	4.80	90	54.78	56.91	127.41	115.96
19	5.8	83.34	4.80	90	20.9	20.64	58.19	47.41
20	5.8	416.66	4.80	90	70.23	67.86	179	198.16
21	5.8	250	2.91	90	55.95	52.81	182.98	185.94
22	5.8	250	6.69	90	68.08	68.59	81.48	86.90
23	5.8	250	4.80	30	26.8	25.42	84.79	83.62
24	5.8	250	4.80	150	74.52	73.27	129.95	139.51
25	5.8	250	4.80	90	50.28	50.28	124.31	124.31
26	5.8	250	4.80	90	50.28	50.28	124.31	124.31
27	5.8	250	4.80	90	50.28	50.28	124.31	124.31
28	5.8	250	4.80	90	50.28	50.28	124.31	124.31
29	5.8	250	4.80	90	50.28	50.28	124.31	124.31
30	5.8	250	4.80	90	50.28	50.28	124.31	124.31

Table 4.4.3: Adequacy of the models tested for COD removal (Y_1) and specific energy consumption (Y_2) during electrochemical treatment of pyrrole.

	Sequential model sum of squares for pyrrole					
	Sum of Squares	**DOF**	**Mean Square**	**F Value**	**Prob. > F**	**Remark**
COD removal (Y_1)						
Mean	55413.25	1	55413.25			
Linear	5549.49	4	1387.37	27.01	<0.0001	
2FI	742.10	6	123.68	4.34	0.0064	Suggested
Quadratic	251.41	4	62.85	3.24	0.0418	Suggested
Cubic	211.28	8	26.41	2.33	0.1409	Aliased
Residual	79.33	7	11.33			
Total	62246.87	30	2074.90			
Specific energy consumption (Y_2)						
Mean	1.554×10^6	1	1.554×10^6			
Linear	93693.06	4	23423.27	13.85	<0.0001	Suggested
2FI	19287.43	6	3214.57	2.85	0.0483	
Quadratic	10494.34	4	2623.58	3.15	0.0459	Suggested
Cubic	6499.29	8	812.41	0.95	0.5358	Aliased
Residual	6011.31	7	858.76			
Total	1.690×10^6	30	56322.32			
	Model summary statistics					
	Std. Dev.	**R^2**	**Adjusted R^2**	**Predicted R^2**	**PRESS**	**Remarks**
COD removal (Y_1)						
Linear	7.17	0.8121	0.7820	0.7085	1991.85	
2FI	5.34	0.9207	0.8789	0.7730	1551.40	Suggested
Quadratic	4.40	0.9575	0.9178	0.7550	1673.90	Suggested
Cubic	3.37	0.9884	0.9519	-0.6716	11422.99	Aliased
Specific energy consumption (Y_2)						
Linear	41.13	0.6890	0.6392	0.5197	65308.75	Suggested
2FI	34.80	0.8308	0.7418	0.4690	72214.78	
Quadratic	28.88	0.9080	0.8221	0.4701	72061.05	Suggested
Cubic	29.30	0.9558	0.8169	-5.3656	8.656×10^5	Aliased

DOF: degree of freedom, PRESS: Predicted residual sum of square, 2FI: two factor interaction.

Table 4.4.4: Adequacy of the models tested for COD removal (Y_1) and specific energy consumption (Y_2) during electrochemical treatment of indole.

	Sequential model sum of squares					
	Sum of Squares	**DOF**	**Mean Square**	**F Value**	**Prob. > F**	**Remark**
COD removal (Y_1)						
Mean	84489.56	1	84489.56			
Linear	7240.78	4	1810.19	71.44	<0.0001	
2FI	30.86	6	5.14	0.16	0.9838	
Quadratic	472.25	4	118.06	13.59	<0.0001	Suggested
Cubic	79.78	8	9.97	1.38	0.3419	Aliased
Residual	50.57	7	7.22			
Total	92363.81	30	3078.79			
Specific energy consumption (Y_2)						
Mean	4.370×10^5	1	4.370×10^5			
Linear	53834.83	4	13458.71	57.15	<0.0001	Suggested
2FI	2126.12	6	354.35	1.79	0.1550	
Quadratic	1067.27	4	266.82	1.49	0.2560	
Cubic	2027.32	8	253.42	2.66	0.1074	Aliased
Residual	666.57	7	95.22			
Total	4.967×10^5	30	16556.64			
	Model summary statistics					
	Std. Dev.	**R^2**	**Adjusted R^2**	**Predicted R^2**	**PRESS**	**Remarks**
COD removal (Y_1)						
Linear	5.03	0.9196	0.9067	0.8772	966.81	
2FI	5.63	0.9235	0.8832	0.8444	1225.15	
Quadratic	2.95	0.9834	0.9680	0.9046	750.83	Suggested
Cubic	2.69	0.9936	0.9734	0.0752	7281.91	Aliased
Specific energy consumption (Y_2)						
Linear	15.35	0.9014	0.8856	0.8466	9160.16	Suggested
2FI	14.07	0.9370	0.9039	0.8020	11826.51	
Quadratic	13.40	0.9549	0.9128	0.7402	15516.82	
Cubic	9.76	0.9888	0.9538	-0.6072	95986.28	Aliased

DOF: degree of freedom, PRESS: Predicted residual sum of square, 2FI: two factor interaction.

Table 4.4.5: ANOVA for quadratic model representling COD removal (Y_1) and specific energy consumption (Y_2) during electrochemical treatment of pyrrole.

Source	Coefficient estimate	Sum of Squares	DOF	Mean Square	F Value	Prob. > F	Remark
COD removal (Y_1)							
Model		6543.006	14	467.36	24.12	<0.0001	HS
Intercept	45.20						
X_1	-0.75	13.49	1	13.49	0.69	0.4172	
X_2	11.37	3104.69	1	3104.69	160.25	< 0.0001	HS
X_3	-0.16	0.62	1	0.62	0.032	0.8607	
X_4	10.06	2430.69	1	2430.69	125.46	< 0.0001	HS
X_1^2	1.38	51.92	1	51.93	2.68	0.1224	
X_2^2	-2.10	120.85	1	120.85	6.24	0.0246	S
X_3^2	-0.70	13.31	1	13.31	0.69	0.4202	
X_4^2	-1.36	50.57	1	50.57	2.61	0.1270	
X_1X_2	-2.89	133.46	1	133.46	6.89	0.0191	S
X_1X_3	-2.60	107.90	1	107.90	5.57	0.0322	S
X_1X_4	0.79	9.94	1	9.94	0.51	0.4849	
X_2X_3	3.53	199.45	1	199.45	10.29	0.0059	S
X_2X_4	4.21	283.33	1	283.33	14.62	0.0017	S
X_3X_4	-0.71	8.02	1	8.02	0.41	0.5296	
Residual		290.61	15	19.37			
Lack of Fit		290.61	10	29.06			
Pure Error		0	5	0			
Cor Total		6833.613	29				
Specific energy consumption (Y_2)							
Model		123474.8	14	8819.63	10.57	< 0.0001	HS
Intercept	243.75						
X_1	7.37	1303.75	1	1303.75	1.56	0.2304	
X_2	57.30	78804.69	1	78804.69	94.48	< 0.0001	HS
X_3	-23.16	12875.57	1	12875.57	15.44	0.0013	S
X_4	5.44	709.05	1	709.05	0.85	0.3711	
X_1^2	-16.52	7485.25	1	7485.26	8.97	0.0091	S
X_2^2	-5.96	975.022	1	975.02	1.17	0.2967	
X_3^2	-4.25	494.77	1	494.77	0.59	0.4531	
X_4^2	6.51	1161.64	1	1161.65	1.39	0.2563	
X_1X_2	15.24	3717.036	1	3717.04	4.46	0.0520	
X_1X_3	3.95	249.71	1	249.72	0.30	0.5923	
X_1X_4	-4.61	340.13	1	340.13	0.41	0.5327	
X_2X_3	-29.43	13862.12	1	13862.12	16.62	0.0010	S
X_2X_4	-8.19	1074.04	1	1074.04	1.29	0.2743	
X_3X_4	-1.67	44.39	1	44.39	0.052	0.8207	
Residual		12510.6	15	834.04			
Lack of Fit		12510.6	10	1251.06			
Pure Error		0	5	0			
Cor Total		135985.4	29				

HS: Highly Significant, S: Significant.

Table 4.4.6: ANOVA for quadratic model representling COD removal (Y_1) and specific energy consumption (Y_2) during electrochemical treatment of indole.

Source	Coefficient estimate	Sum of Squares	DOF	Mean Square	F Value	Prob. > F	Remark
COD removal (Y_1)							
Model		7743.90	14	553.13	63.65	< 0.0001	HS
Intercept	50.28						
X_1	-1.92	88.39	1	88.39	10.17	0.0061	S
X_2	11.81	3344.59	1	3344.59	384.8	< 0.0001	HS
X_3	3.94	373.35	1	373.35	42.96	< 0.0001	HS
X_4	11.96	3434.43	1	3434.43	395.21	< 0.0001	HS
X_1^2	2.62	188.10	1	188.10	21.64	0.0003	S
X_2^2	-1.51	62.22	1	62.22	7.161	0.0173	S
X_3^2	2.61	186.31	1	186.31	21.43	0.0003	S
X_4^2	-0.23	1.48	1	1.48	0.170	0.6854	
X_1X_2	-0.32	1.69	1	1.69	0.194	0.6655	
X_1X_3	-0041	0.027	1	0.027	0.003	0.9561	
X_1X_4	1.01	16.16	1	16.16	1.85	0.1928	
X_2X_3	0.86	11.69	1	11.69	1.34	0.2641	
X_2X_4	0.15	0.36	1	0.36	0.042	0.8402	
X_3X_4	-0.24	0.92	1	0.92	0.106	0.7492	
Residual		130.35	15	8.69			
Lack of Fit		130.35	10	13.03			
Pure Error		0	5	0			
Cor Total		7874.2	29				
Specific energy consumption (Y_2)							
Model		57028.23	14	4073.44	22.68	< 0.0001	HS
Intercept	124.31						
X_1	3.81	348.53	1	348.53	1.94	0.1839	
X_2	37.69	34088.42	1	34088.42	189.8	< 0.0001	HS
X_3	-24.76	14713.43	1	14713.43	81.93	< 0.0001	HS
X_4	13.97	4684.45	1	4684.45	26.08	0.0001	S
X_1^2	-3.99	436.98	1	436.99	2.43	0.1396	
X_2^2	-0.38	3.93	1	3.93	0.022	0.8842	
X_3^2	3.03	251.78	1	251.78	1.40	0.2548	
X_4^2	-3.19	278.27	1	278.27	1.55	0.2323	
X_1X_2	-0.26	1.07	1	1.07	0.006	0.9395	
X_1X_3	0.68	7.42	1	7.42	0.041	0.8416	
X_1X_4	-3.82	233.47	1	233.47	1.3	0.2721	
X_2X_3	-3.74	223.64	1	223.64	1.24	0.2820	
X_2X_4	10.05	1615.21	1	1615.21	8.99	0.0090	S
X_3X_4	1.68	45.29	1	45.29	0.25	0.6228	
Residual		2693.89	15	179.59			
Lack of Fit		2693.89	10	269.39			
Pure Error		0	5	0			
Cor Total		59722.12	29				

HS: Highly Significant, S: Significant.

Table 4.4.6 shows that for indole mineralization, model F-values for Y_1 and Y_2 are 63.65 and 22.68, respectively, implying that the quadratic models used for representing the experimental data is significant. For COD removal (Y_1), model terms j, k and t are highly significant whereas pH_o, pH_o^2, j^2 and k^2 are significant terms. The quadratic equation in terms of coded factors for COD removal (Y_1) during indole mineralization is given as under:

$$Y_1 = 50.28 - 1.92X_1 + 11.81X_2 + 3.94X_3 + 11.96X_4 + 2.62X_1^2 - 1.51X_2^2 + 2.61X_3^2 - 0.23X_4^2 - 0.32X_1X_2 - 0.041X_1X_3 + 1.01X_1X_4 + 0.86X_2X_3 + 0.15X_2X_4 - 0.24X_3X_4 \quad (4.4.3)$$

For response Y_2 (specific energy consumption), model terms j and k are highly significant whereas t and j×t are significant terms. The quadratic equations in terms of coded factors for response Y_2 is given as under:

$$Y_2 = 124.31 + 3.81X_1 + 37.69X_2 - 24.76X_3 + 13.97X_4 - 3.99X_1^2 - 0.38X_2^2 + 3.03X_3^2 - 3.19X_4^2 - 0.26X_1X_2 + 0.68X_1X_3 - 3.82X_1X_4 - 3.74X_2X_3 + 10.05X_2X_4 + 1.68X_3X_4 \quad (4.4.4)$$

R^2 values of quadratic models representing Y_1 and Y_2 during indole mineralization were found to be 0.98 and 0.95, respectively, indicating satisfactory fit of the experimental data.

4.4.1.2 Effect of parameters on COD removal and specific energy consumption

(a) Pyrrole mineralization: Three-dimensional response surface graphs for the effect of operating parameters j, k, t and pH on COD removal (Y_1) and specific energy consumption (Y_2) during pyrrole mineralization are shown in Figures 4.4.1 and 4.4.2, respectively. It may be seen that Y_1 increases with an increase in j and t (Figure 4.4.1a). An increase in j increases the rate of production of electrons which increases the rate of oxidation of pyrrole. At high j, H_2O_2 produced from cathodic reduction of molecular oxygen helps in increasing the COD removal efficiency [Bhaskar-Raju et al., 2008; Maljaei et al., 2009]. For j >179 ($A.m^{-2}$) and t > 150 min, an increase in j and t didn't improve much the value of Y_1. Similarly, Figure 4.4.2a shows that an increase in j and t increases the value of Y_2 as electrical power consumption is directly proportional to current and time. This may also be due to the

conversion of pyrrole to stable intermediates that resist further oxidation after certain time of treatment increasing the value of specific energy consumption. Passivation of electrodes due to formation of impermeable film during electrolysis and oxygen gas evolution at anode can also increase specific energy consumption [Bhaskar Raju et al., 2009].

From Figure 4.4.1b, it observed that the effect of conductivity (k) and pH on COD removal (Y_1) is very marginal as compared to other parameters. Value of specific energy consumption (Y_2) also changes very marginally with an increase in k, though the Y_2 decreases with increase in pH (Figure 4.4.2b).

(b) **Indole mineralization:** Effects of various parameters on COD removal (Y_1) and specific energy consumption (Y_2) during indole mineralization by electrochemical treatment with Pt/Ti electrode are shown in Figures 4.4.3 and 4.4.4. Again, COD removal (Y_1) and specific energy consumption (Y_2) continuously increase with increase in current density (j) and time (t) (Figures 4.4.3a and 4.4.4a). For j > 161 ($A.m^{-2}$) and t > 150 min, an increase in j and t didn't improve the COD removal efficiency further. These results and reasons are same as for pyrrole mineralization. Similarly, Figures 4.4.3b and 4.4.4b show that the parameters pH and conductivity have marginal effect on COD removal (Y_1) and specific energy consumption (Y_2). This may be due to the overriding effect of j and t on Y_1 and Y_2.

4.4.1.3 Multi-response optimization

Since this study involves evaluation of two responses, multi-response optimization by desirability function approach was used so as to maximize COD removal (Y_1) and minimize specific energy consumption (Y_2). Using minimum and maximum acceptable response values, one sided desirability d_i for various responses and overall desirability (D) were calculated using equations 3.5.3 and 3.5.4, respectively. Constraints applied for optimization of various operational parameters during electrochemical treatment of pyrrole and indole is given in Table 4.4.7.

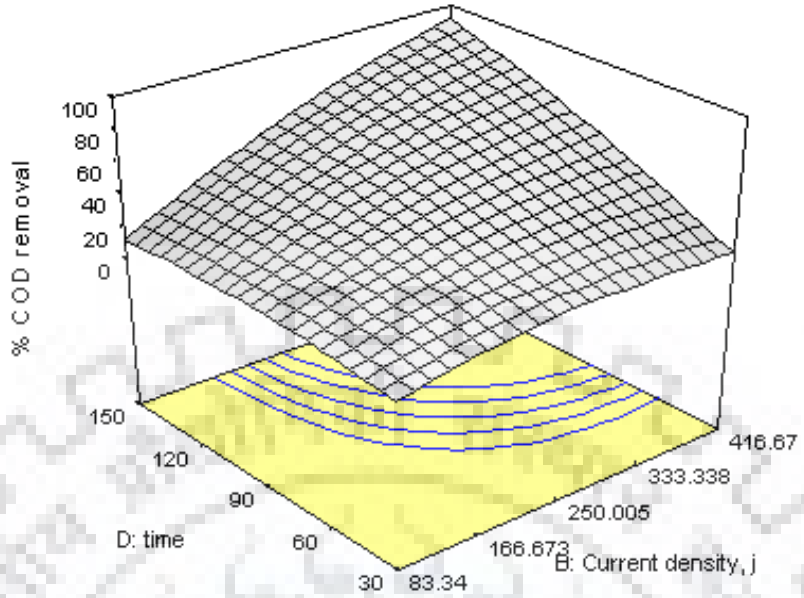

(a)

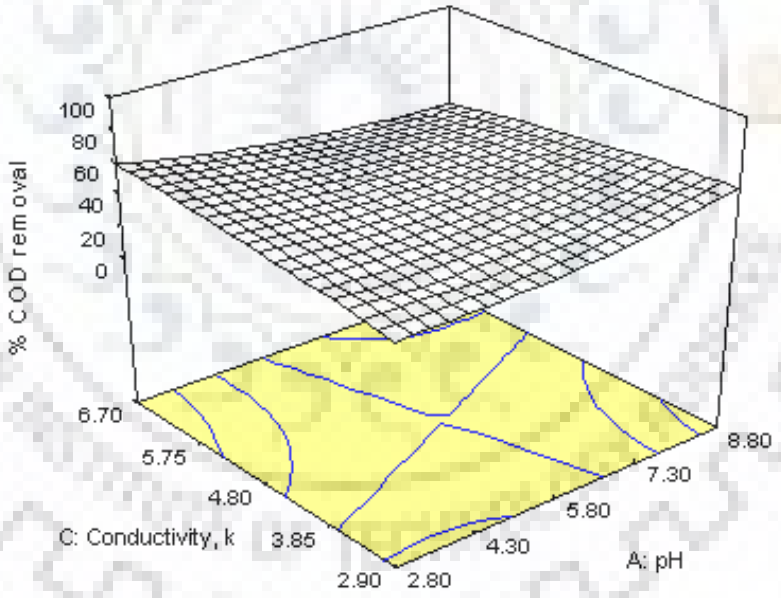

(b)

Figure 4.4.1: Effect of various parameters on COD removal during electrochemical treatment of pyrrole, (a) current density and time, (b) pH and conductivity.

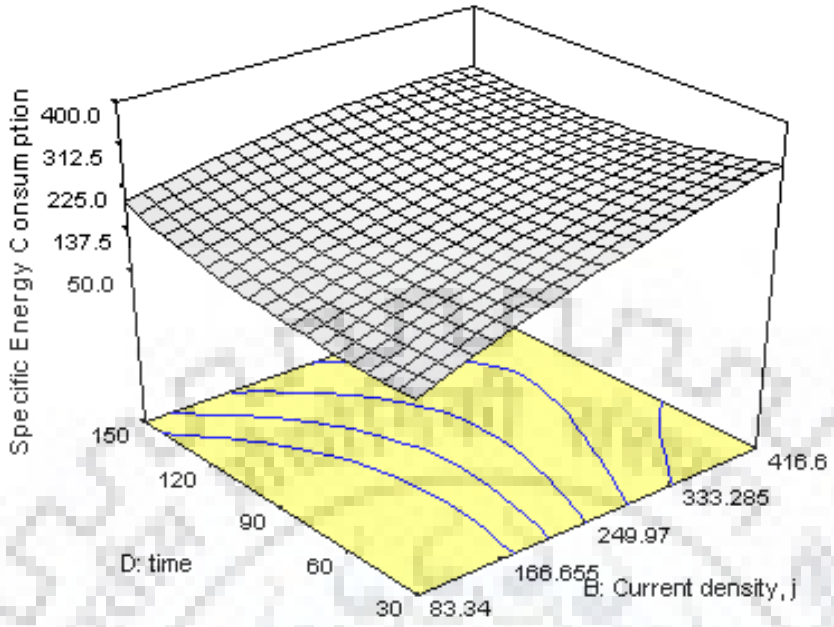

(a)

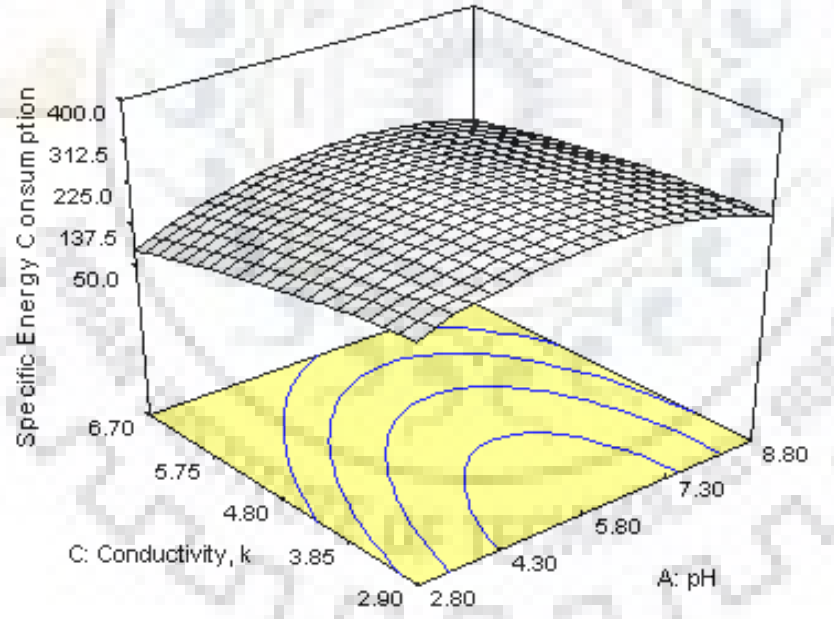

(b)

Figure 4.4.2: Effect of various parameters on specific energy consumption during electrochemical treatment of pyrrole, (a) current density and time, (b) pH and conductivity.

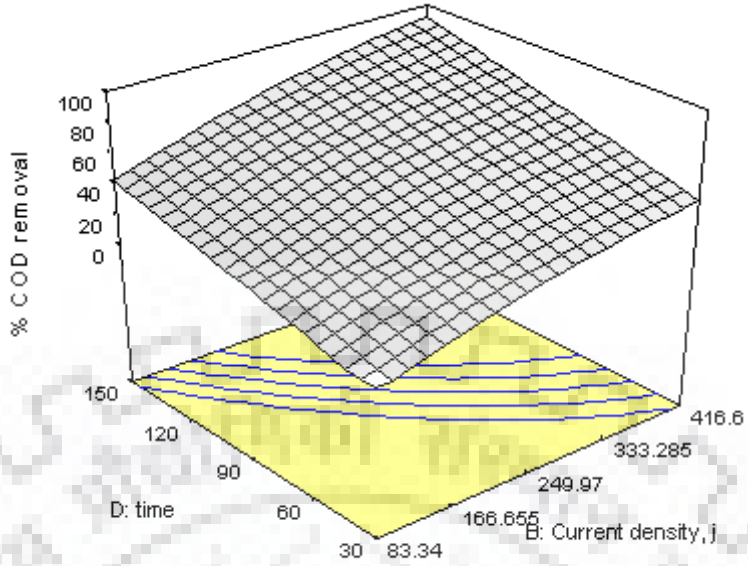

(a)

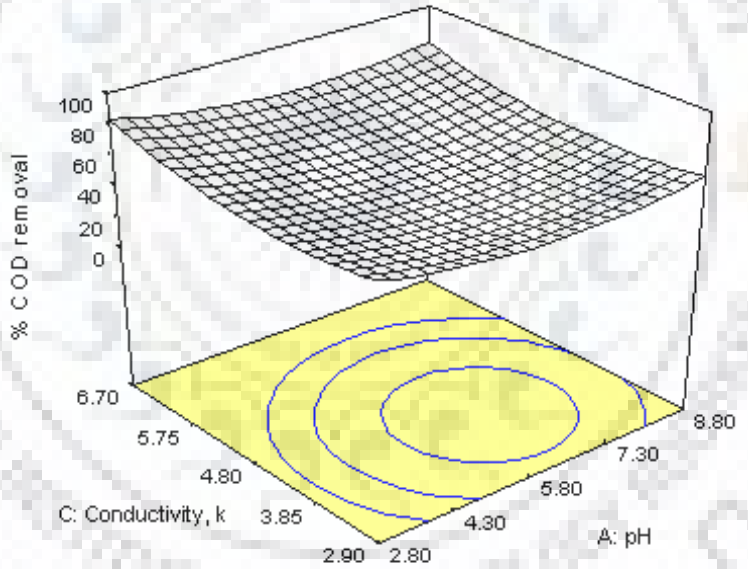

(b)

Figure 4.4.3: Effect of various parameters on COD removal during electrochemical treatment of indole, (a) current density and time, (b) pH and conductivity.

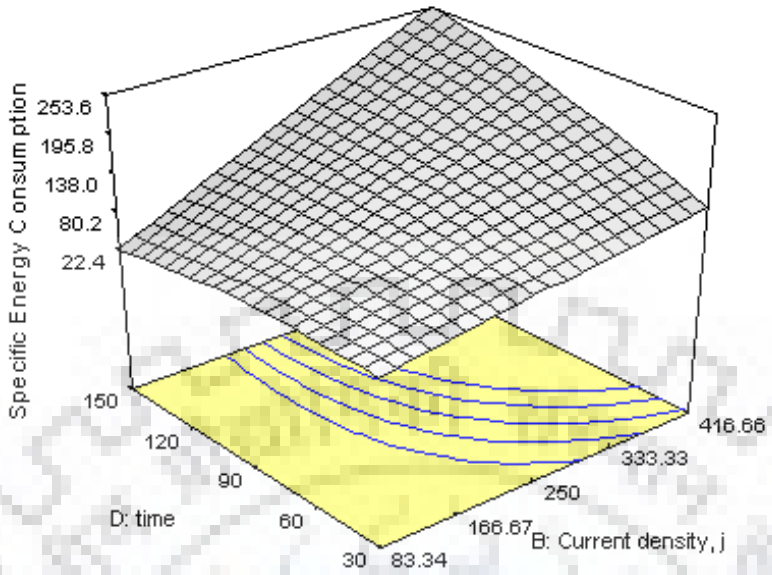

(a)

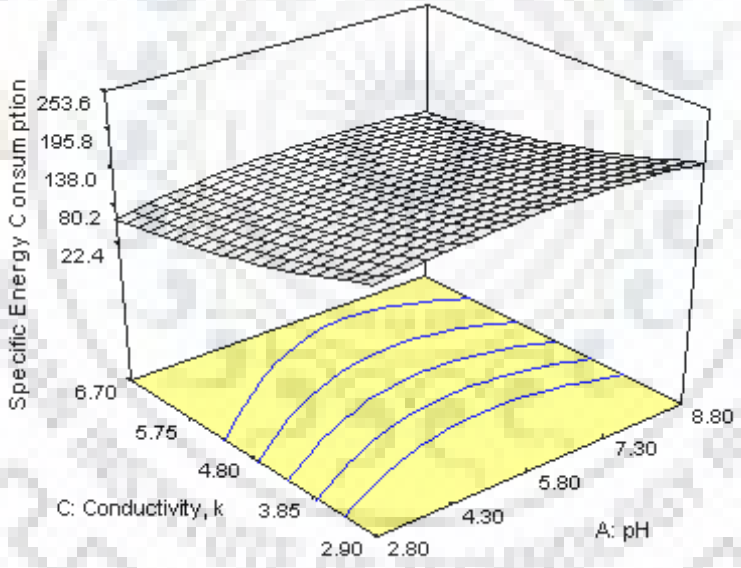

(b)

Figure 4.4.4: Effect of various parameters on specific energy consumption during electrochemical treatment of indole, (a) current density and time, (b) pH and conductivity.

(a) Pyrrole mineralization: In this work, the minimum and maximum acceptable values were obtained from experimental data for Y_1 and Y_2. For Y_1, minimum and maximum values were 14.39% and 72.2%, respectively. Similarly for Y_2, minimum and maximum values were 99.25 and 361.42 kWh per kg of COD removed, respectively. Thus, one sided desirability for Y_1 (d_1) was calculated using as follows:

$$d_1 = \begin{cases} 0 & if \quad Y_1 \le 14.39 \\ [\dfrac{Y_1 - 14.39}{72.2 - 14.39}] & If \ 14.39 < Y_1 < 72.2 \\ 1 & if \ Y_1 \ge 72.2 \end{cases} \qquad (4.4.5)$$

Similarly, one sided desirability for Y_2 (d_2) was calculated as:

$$d_2 = \begin{cases} 1 & if \quad Y_2 \le 99.25 \\ [\dfrac{361.42 - Y_2}{361.42 - 99.25}] & If \ 99.25 < Y_2 < 361.42 \\ 0 & if \ Y_2 \ge 361.42 \end{cases} \qquad (4.4.6)$$

Table 4.4.7: Constraints applied for the optimization of operational parameters during electrochemical treatment of pyrrole and indole.

Variables	Objective	Lower Limit	Upper Limit	Lower Weight	Upper Weight	Importance
pH	is in range	2.8	8.8	1	1	3
j ($A.m^{-2}$)	is in range	83.33	416.7	1	1	3
k ($mS.cm^{-1}$)	is in range	2.91	6.7	1	1	3
t (min)	is in range	30	150	1	1	3

Value of *r* was taken as 1 in both above equations, and thus overall desirability was calculated using equation 3.5.4. The optimum operational parameters during electrochemical treatment of pyrrole were found to be: pH=8.7, j=175 $A.m^{-2}$, k=2.9 $mS.cm^{-1}$, t=150 min. Under this optimized conditions, predicted values of percent COD removal and specific energy consumption were found to be 69.30% and 99.25 kWh per kg of COD removed,

respectively. The value of overall desirability (D) was found to be equal to 0.975. Three runs at predicted optimum conditions gave an average of 67.3% COD and 96.1 kWh per kg of COD removed.

(b) Indole mineralization: Minimum and maximum values for Y_1 during indole mineralization were found to be: 20.9% and 82.66%, respectively. Similarly for Y_2, minimum and maximum values were: 42.49 and 224.34 kWh per kg of COD removed, respectively. Thus, one sided desirability for Y_1 (d_1) was calculated as follows:

$$d_1 = \begin{cases} 0 & if \quad Y_1 \le 20.9 \\ [\dfrac{Y_1 - 20.9}{82.66 - 20.9}] & If \ 20.9 < Y_1 < 82.66 \\ 1 & if \ Y_1 \ge 82.66 \end{cases} \qquad (4.4.7)$$

Similarly, one sided desirability for Y_2 (d_2) was calculated as:

$$d_2 = \begin{cases} 1 & if \quad Y_2 \le 42.49 \\ [\dfrac{224.34 - Y_2}{224.34 - 42.49}] & If \ 42.49 < Y_2 < 224.34 \\ 0 & if \ Y_2 \ge 224.34 \end{cases} \qquad (4.4.8)$$

The optimum operational parameters during electrochemical treatment of indole were found to be: pH=8.6, j=161 $A.m^{-2}$, k=6.7 $mS.cm^{-1}$, t=150 min. Under this optimized conditions, predicted values of percent COD removal and specific energy consumption were found to be 82.9%, 37.75 kWh per kg of COD removed, respectively. The value of overall desirability (D) was found to be equal to one. In order to validate the optimization, three runs at these optimum conditions were conducted which gave an average of 83.8% COD and 36.3 kWh per kg of COD removed.

4.4.2 Simultaneous Removal of Pyrrole and Indole by Electrochemical Treatment using Taguchi's Design of Experiments

Much of the work on the electrochemical treatment of heterocyclic compounds by various types of electrodes has focused on the mineralization of single compound. Since industrial effluents contain several compounds, it is necessary to study the simultaneous electrochemical treatment if two or more compounds and also to quantify the interference of one on the removal of the other. Therefore, simultaneous mineralization of pyrrole and indole by electrochemical treatment using Pt/Ti electrode was studied.

4.4.2.1 Effect of process parameters

Parameters for electrochemical treatment of binary mixture of pyrrole and indole by platinum coated titanium (Pt/Ti) electrode were optimized by using Taguchi's design of experiments. The process parameters and their level are given in Table 3.5.4. The experimental results of pyrrole, indole and COD removal efficiencies, and specific energy consumption are given in Table 4.4.8. The effects of process parameters on pyrrole, indole and COD removal efficiencies, and specific energy consumption are shown in Figures 4.4.5 and 4.4.6.

Figure 4.4.5a shows that each parameter has significant effect on removal efficiency of pyrrole. At level 1, pyrrole and indole concentrations ($C_{o,Py}$, $C_{o,Ind}$) have highest influence whereas current density (j) and time (t) have greater influence at level 4. Conductivity (k) is found to have greater influence at level 3. Difference between two successive levels of each parameter indicates relative importance of parameter. Higher difference in values at two successive levels shows strong influence (Table 4.4.9). For pyrrole removal, parameter t shows largest difference (26.43) for change in parameter from level 1 to level 2. Similarly, for indole removal, at level 1, parameters $C_{o,Py}$ and $C_{o,Ind}$ have highest influence whereas j and t have greater influence at level 4. Parameter k is found to have greater influence at level 3. For indole removal, parameter t, shows largest difference (26.08) for change in parameter from level 1 to level 2. For COD removal, at level 1, parameter $C_{o,Py}$ has highest influence whereas parameters $C_{o,Ind,}$ j, k and t have greater influence at level 4. For COD removal, j

shows largest difference (16.67) for change in parameter from level 2 to level 3. For specific energy consumption, at level 1, parameters $C_{o,Py,}$ j and k have highest influence whereas parameters $C_{o,Ind,}$ and t have greater influence at levels 4 and 3, respectively.

It can be seen from Figures 4.4.5 and 4.4.6 that an increase in $C_{o,Py}$ from level 1 to 3 decreased percent removal of pyrrole, indole and COD. However, from level 3 to level 4, marginal increase in pyrrole and indole removal was observed whereas COD removal decreased further at level 4. Specific energy consumption increased continuously with an increase in $C_{o,Py}$ because of the decrease in COD removal.

An increase in $C_{o,Ind,}$ from level 1 to 4, decreased the percent removal of pyrrole and indole. However, COD removal first decreased from level 1 to level 2 and then increased from level 2 to level 4. Specific energy consumption decreased with an increase in $C_{o,Ind}$ from level 1 to 4.

An increase in parameters j and t from level 1 to 4, continuously increased the pyrrole, indole and COD removal efficiencies. However, specific energy consumption increased with an increase in j from level 1 to level 2 then decreased from level 2 to level 3 and again increased from level 3 to level 4. Decrease in specific energy consumption with an increase in j from level 2 to 3 is because of the high increase in COD removal between these levels. Similarly, specific energy consumption decreased with an increase in t from level 1 to 2, then showed marginal change from level 2 to 3 and increased from level 3 to 4.

Conductivity (k) had marginal effect on pyrrole and indole removal efficiencies as compared to other parameters, though these responses were found to be maximum at level 3. COD removal decreased with an increase in k from level 1 to 2, then showed marginal change from level 2 to 3 and increased from level 3 to 4. Specific energy consumption increased with an increase in k from level 1 to 3 and decreased from level 3 to 4.

It must be mentioned that since Taguchi' design methodology is based on statistical in nature and that change in a response because of one parameter is significantly influenced by changes in the other parameters.

Table 4.4.8. Results of pyrrole, indole and COD removal efficiencies, and specific energy consumption during simultaneous electrochemical treatment of pyrrole and indole by Pt/Ti electrode.

Exp. no.	Std. order	$C_{o,Py}$ ($mg.l^{-1}$)	$C_{o,Ind}$ ($mg.l^{-1}$)	j ($A.m^{-2}$)	k ($mS.cm^{-1}$)	t (min)	Removal efficiencies (%)			SEC
							Pyrrole	Indole	COD	
1	1	50	50	83.33	2.44	30	10.14	17.37	23.21	72.12
2	2	50	200	166.7	3.86	70	45.50	51.38	19.29	166.67
3	3	50	350	250	5.28	110	83.73	93.23	49.15	106.18
4	4	50	500	333.3	6.7	150	72.13	86.38	97.58	74.38
5	5	200	50	166.7	5.28	150	83.22	84.94	34.10	225.93
6	6	200	200	83.33	6.7	110	32.68	37.95	23.94	47.33
7	7	200	350	333.3	2.44	70	58.46	56.26	43.00	115.74
8	8	200	500	250	3.86	30	15.67	12.30	30.92	32.82
9	9	350	50	250	6.7	70	55.15	56.83	35.57	103.11
10	10	350	200	333.3	5.28	30	26.03	26.98	9.69	265.92
11	11	350	350	83.33	3.86	150	25.73	31.00	11.91	87.65
12	12	350	500	166.7	2.44	110	37.62	33.36	37.00	60.83
13	13	500	50	333.3	3.86	110	81.42	77.73	36.27	244.43
14	14	500	200	250	2.44	150	73.50	68.24	42.86	174.51
15	15	500	350	166.7	6.7	30	6.00	9.40	1.45	278.00
16	16	500	500	83.33	5.28	70	4.46	5.90	3.80	74.06

SEC: Specific energy consumption.

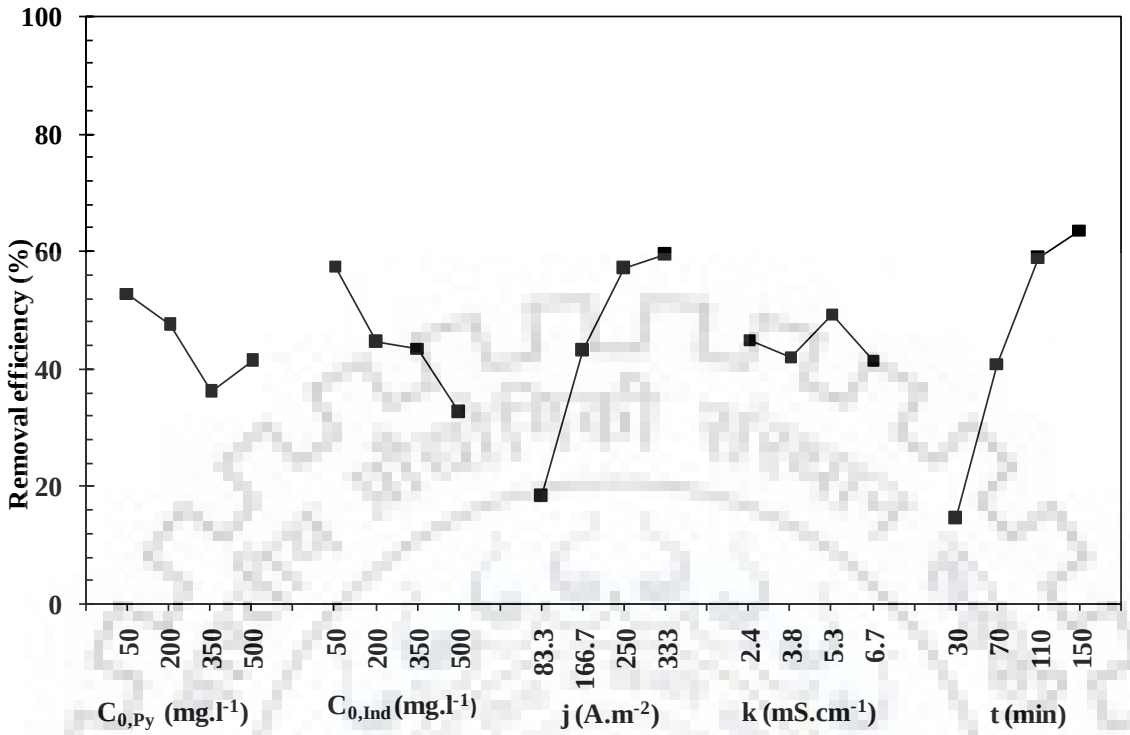

(a) Pyrrole removal efficiency

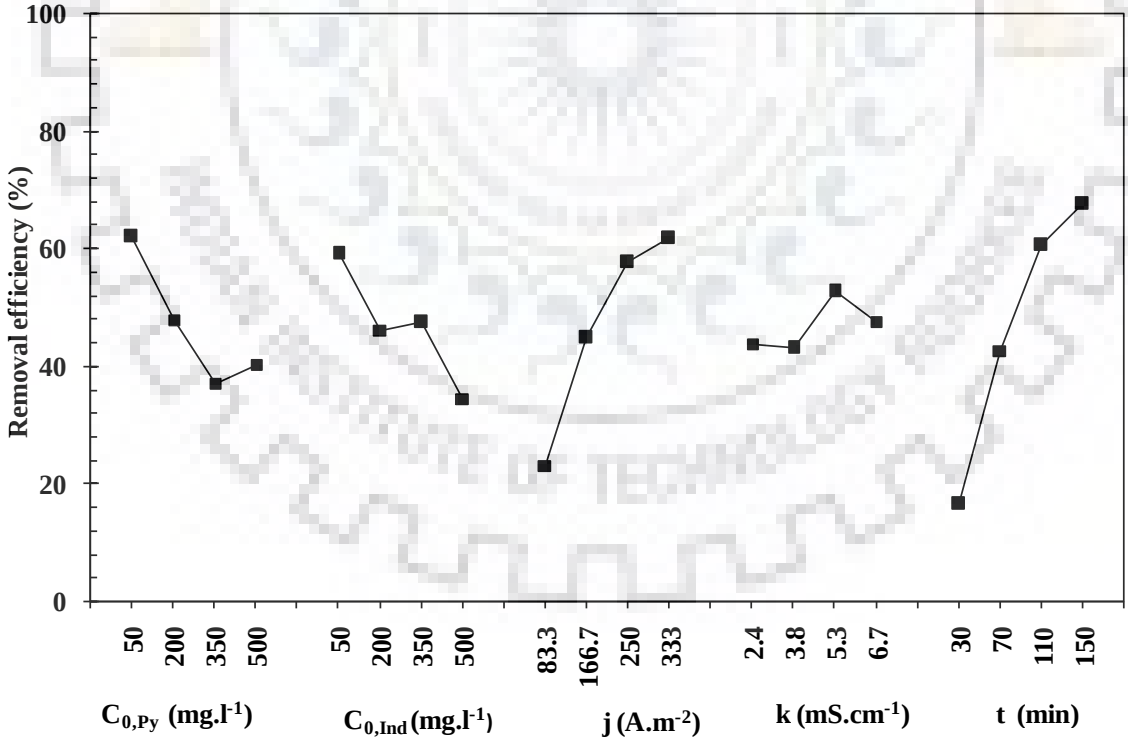

(b) Indole removal efficiency

Figure 4.4.5: Effect of process parameters on pyrrole and indole removal efficiencies during simultaneous mineralization of pyrrole and indole by electrochemical treatment using Pt/Ti electrode.

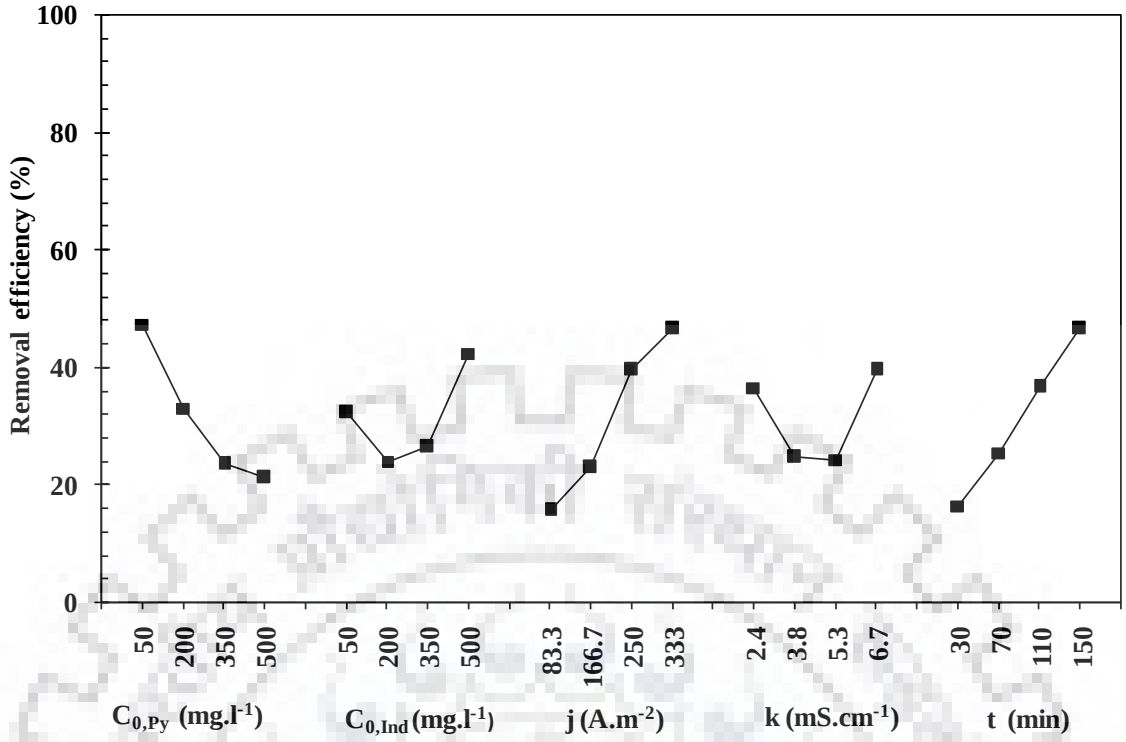

(a) COD removal efficiency

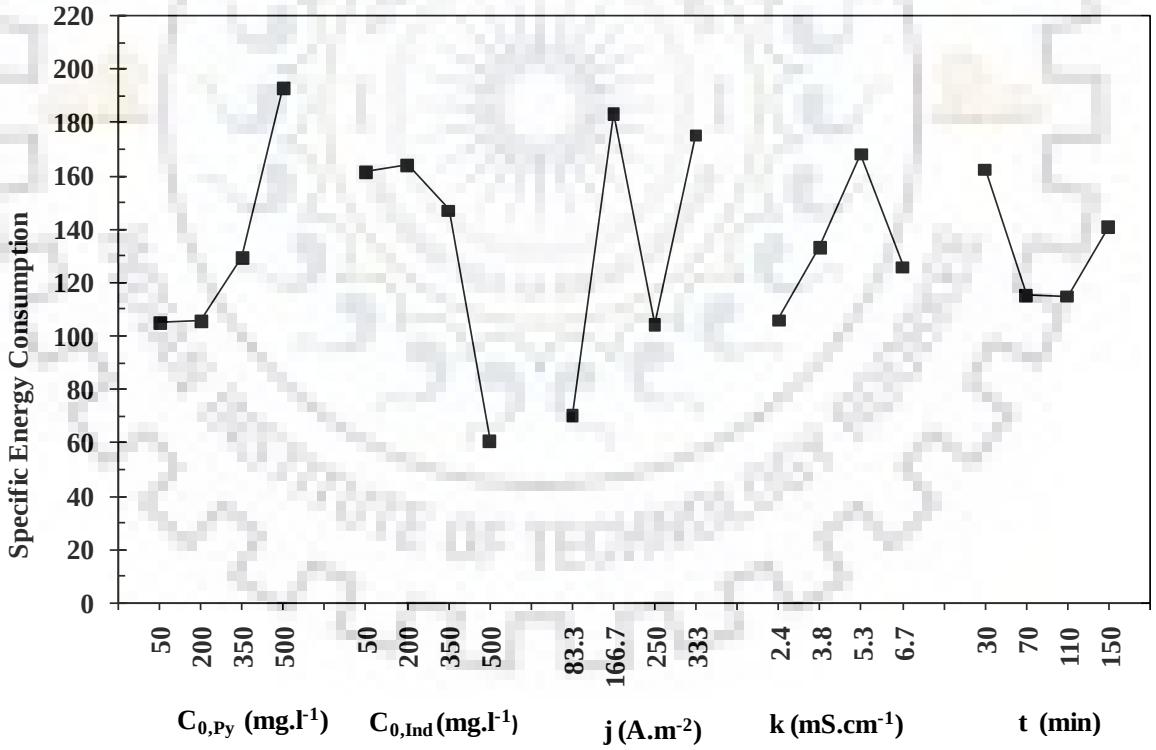

(d) Specific energy consumption

Figure 4.4.6: Effect of process parameters on COD removal and specific energy consumption during simultaneous mineralization of pyrrole and indole by electrochemical treatment using Pt/Ti electrode.

Table 4.4.9: Average and main effect for pyrrole, indole and COD removal efficiencies, and specific energy consumption.

Parame	Raw data, Average value				Main effect		
ter	L1	L2	L3	L4	L2-L1	L3-L2	L4-L3
Pyrrole removal (%)							
A	52.87	47.51	36.13	41.35	-5.37	-11.38	5.22
B	57.48	44.43	43.48	32.47	-13.05	-0.95	-11.01
C	18.25	43.08	57.01	59.51	24.83	13.93	2.50
D	44.93	42.08	49.36	41.49	-2.85	7.28	-7.87
E	14.46	40.89	58.86	63.64	26.43	17.97	4.78
Indole removal (%)							
A	62.09	47.86	37.04	40.32	-14.23	-10.82	3.28
B	59.22	46.14	47.47	34.48	-13.08	1.33	-12.99
C	23.05	44.77	57.65	61.84	21.71	12.88	4.19
D	43.81	43.10	52.76	47.64	-0.70	9.66	-5.13
E	16.51	42.59	60.57	67.64	26.08	17.98	7.07
COD removal (%)							
A	47.31	32.99	23.54	21.09	-14.32	-9.45	-2.45
B	32.29	23.94	26.38	42.32	-8.34	2.43	15.95
C	15.72	22.96	39.62	46.64	7.24	16.67	7.01
D	36.52	24.60	24.19	39.64	-11.92	-0.41	15.45
E	16.32	25.41	36.59	46.61	9.10	11.18	10.02
Specific energy consumption							
A	104.84	105.45	129.38	192.75	0.62	23.93	63.37
B	161.40	163.61	146.89	60.52	2.21	-16.72	-86.37
C	70.29	182.86	104.15	175.12	112.57	-78.70	70.96
D	105.80	132.89	168.02	125.71	27.09	35.13	-42.32
E	162.21	114.89	114.69	140.62	-47.32	-0.20	25.93

4.4.2.2 ANOVA results

ANOVA gives an idea about percent contribution of individual parameters on the pyrrole, indole and COD removal efficiencies and specific energy consumption during simultaneous mineralization of pyrrole and indole by electrochemical treatment with Pt/Ti electrode. ANOVA parameters such as degree of freedom **(**DOF), pure sum of square of error, variance, percent contribution, variance ratio (F-value) for Taguchi's method were calculated as per the methods reported in the literature [Srivastava et al., 2007b; Yousefich et al., 2012]. Results are shown in Table 4.4.10 for all the responses. It is seen that time (t) is the most influencing factor for pyrrole removal efficiency with highest contribution of 48.42% followed by j, $C_{o,Ind,}$ $C_{o,Py}$ and k having contribution of 34.91%, 10.23%, 5.18% and 1.26%, respectively. For indole removal efficiency also, t has highest contribution of 48.59% followed by j, $C_{o,Py,}$ $C_{o,Ind}$ and k. However, current density (j) is having highest contribution of 31.56% for COD removal efficiency followed by t, $C_{o,Py}$, $C_{o,Ind}$ and k having contribution 26.68%, 21.66%, 10.27% and 9.83%, respectively. Similarly, for specific energy consumption, j is having highest contribution of 36.18% followed by $C_{o,Ind,}$ $C_{o,Py,}$ k and t having contribution 28.82%, 20.59%, 8.10% and 6.31%, respectively.

Mean of the various responses are generally represented within a confidence interval (CI). Range of the response between a maximum and a minimum value at same stated level of confidence is termed as CI. It is defined for all the experimental runs termed as population (CI_{pop}), and for confirmation experiments under specified condition (CI_{CE}) [Roy, 1990; Oguz et al., 2006; Srivastava et al., 2007b]. Least significant parameter k was pooled so as to obtain value of error variance (V_e) which itself was required for calculating the value of CI_{POP} and $CI_{CE.}$ Table 4.4.11 shows the result of pooled ANOVA of pyrrole, indole and COD removal efficiencies and specific energy consumption.

4.4.2.3 Optimum level selection and optimum response characteristics estimation

Optimum levels of parameters for pyrrole, indole and COD removal efficiencies and specific energy consumption were decided by maximum average value at different level.

Table 4.4.10: ANOVA results for pyrrole, indole and COD removal efficiencies, and specific energy consumption.

Factors	Total Variance of Each Factor, S	DOF, f	Variance, V (S/f)	Pure sum of sq. (S`=S-f*V_{error})	Percent Contribution, P ($P_A=S_A*100/S_{T)}$
Pyrrole removal (%)					
A	636.78	3	212.26	636.78	5.18
B	1257.15	3	419.05	1257.15	10.23
C	4291.35	3	1430.45	4291.35	34.91
D	154.84	3	51.61	154.84	1.26
E	5952.82	3	1984.27	5952.82	48.42
Error	0.00	0		-2.91×10^{-11}	-2.37×10^{-13}
Model	12292.95	15	819.53	12292.95	100
Total	12292.95	15	819.53	15.00	100
Indole removal (%)					
A	1488.73	3	496.24	1488.73	11.60
B	1227.09	3	409.03	1227.09	9.56
C	3647.60	3	1215.87	3647.60	28.42
D	235.60	3	78.53	235.60	1.84
E	6236.30	3	2078.77	6236.30	48.59
Error	0.00	0		1.45×10^{-11}	1.13×10^{-13}
Model	12835.33	15	855.69	12835.33	100
Total	12835.33	15	855.69	15.00	100
COD removal (%)					
A	1693.70	3	564.57	1693.70	21.66
B	803.30	3	267.77	803.30	10.27
C	2467.55	3	822.52	2467.55	31.56
D	768.80	3	256.27	768.80	9.83
E	2086.10	3	695.37	2086.10	26.68
Error	0.00	0		0	0
Model	7819.45	15	521.30	7819.45	100
Total	7819.45	15	521.30	15.00	100
Specific energy consumption					
A	20541.31	3	6847.10	20541.31	20.59
B	28756.26	3	9585.42	28756.26	28.82
C	36096.39	3	12032.13	36096.39	36.18
D	8078.54	3	2692.85	8078.54	8.10
E	6297.39	3	2099.13	6297.39	6.31
Error	0.00	0		-3.49×10^{-10}	-3.5×10^{-13}
Model	99769.89	15	6651.33	99769.89	100
Total	99769.89	15	6651.33	15.00	100

Table 4.4.11: Pooled ANOVA results for pyrrole, indole and COD removal efficiencies, and specific energy consumption.

Factors	Total Variance of Each Factor, S	DOF, f	Variance, V (S/f)	Pure sum of sq. (S`=S-f*V_{error})	Percent Contribution, P ($P_A=S_A*100/S_{T)}$	Variance ratio (F-value)
Pyrrole removal (%)						
A	636.78	3	212.26	481.93	3.92	4.11
B	1257.15	3	419.05	1102.30	8.97	8.12
C	4291.35	3	1430.45	4136.51	33.65	27.71
D	Pooled	Pooled	Pooled	Pooled	Pooled	Pooled
E	5952.82	3	1984.27	5797.98	47.17	38.44
Error	154.84	3	51.61	774.22	6.30	
Model	12138.10	12	1011.51	11518.73	93.70	19.60
Total	12292.95	15	819.53	12292.95	100	
Indole removal (%)						
A	1488.73	3	496.24	1253.13	9.76	6.32
B	1227.09	3	409.03	991.49	7.72	5.21
C	3647.60	3	1215.87	3412.00	26.58	15.48
D	Pooled	Pooled	Pooled	Pooled	Pooled	Pooled
E	6236.30	3	2078.77	6000.70	46.75	26.47
Error	235.60	3	78.53	1178.02	9.18	
Model	12599.73	12	1049.98	11657.31	90.82	13.37
Total	12835.33	15	855.69	12835.33	100	
COD removal (%)						
A	1693.70	3	564.57	924.90	11.83	2.20
B	803.30	3	267.77	34.49	0.44	1.04
C	2467.55	3	822.52	1698.75	21.72	3.21
D	Pooled	Pooled	Pooled	Pooled	Pooled	Pooled
E	2086.10	3	695.37	1317.30	16.85	2.71
Error	768.80	3	256.27	3844.02	49.16	
Model	7050.65	12	587.55	3975.43	50.84	2.29
Total	7819.45	15	521.30	7819.45	100	
Specific energy consumption						
A	20541.31	3	6847.10	12462.77	12.49	2.54
B	28756.26	3	9585.42	20677.72	20.73	3.56
C	36096.39	3	12032.13	28017.85	28.08	4.47
D	Pooled	Pooled	Pooled	Pooled	Pooled	Pooled
E	6297.39	3	2099.13	-1781.15	-1.79	0.78
Error	8078.54	3	2692.85	40392.71	40.49	
Model	91691.35	12	7640.95	59377.19	59.51	2.84
Total	99769.89	15	6651.33	99769.89	100	

Since the aim of the study was to have the maximum mineralization of pyrrole and indole from the aqueous solutions with the highest possible concentrations of pyrrole and indole, therefore, the third level of parameters A and B ($C_{o,Py}$ and $C_{o,Ind}$) were taken for optimizing the COD removal efficiency. Parameters, j and t were selected at level 4 and parameter k was neglected as it was least significant. Thus, parameters which affected significantly are A_3, B_3, C_4 and E_4 having highest response values. The optimal values of the response curve were measured by following relationship:

$$Y_{opt} = \overline{T} + (\overline{A_4} - \overline{T}) + (\overline{B_4} - \overline{T}) + (\overline{C_4} - \overline{T}) + (\overline{E_4} - \overline{T}) \qquad (4.4.9)$$

Optimum values for removal efficiency of pyrrole, indole and COD were found to be 44.46%, 63.79% and 62.98%, respectively. Optimum value of specific energy consumption was found to be 169.71 kWh per kg COD removed. The confirmation experiments were done three times at estimated optimum conditions by electrochemical treatment and compared with the results obtained (Table 4.4.12). It was found that values of confirmation experimental results are within the predicted range within the confidence interval of 95%.

Table 4.4.12: Comparison of predicted optimal values and results of confirmation experiments simultaneous mineralization of pyrrole and indole during electrochemical treatment with Pt/Ti electrode.

System	Predicted optimal values	Average of Confirmation experiments
Pyrrole removal (%)	44.46	46.1
Indole removal (%)	63.79	62.4
COD removal (%)	62.98	61.4
Specific energy consumption	169.71	165.5

4.4.3 Physico-Chemical Analysis of Treated Slurry, Electrode and Residue

4.4.3.1 Mineralization mechanism

Electrochemical treatment of pyrrole and indole from aqueous solution were studied by using Pt/ Ti electrode. Pt/Ti is dimensionally stable anode (DSA) highly stable electrode with high mechanical and chemical resistance even under strong acid conditions. Moreover, it produces powerful oxidants such as hydroxyl and other radicals, chlorine and ozone which oxidize the organic pollutants. Mineralization of pyrrole and indole in aqueous solution during electrochemical treatment occurs both by direct and indirect oxidation. These mechanisms are discussed in this section. First, the electrode surface (denoted by M) produces hydroxyl radicals during electrochemical treatment [Kumar et al., 2015].

$$M + H_2O \rightarrow M(HO^{\bullet}) + H^+ + e^- \quad (4.4.10)$$

Reactivity of hydroxyl radicals depends upon interaction between electrode and electrolyte. Metal oxide conversion of metal is due to hydroxyl radicals generation and its reactivity with metal.

$$M(HO^{\bullet}) \rightarrow MO + H^+ + e^- \quad (4.4.11)$$

Oxidation of organic pollutant is possible only when redox couple (M/MO) is formed [Martínez-Huitle and Ferro, 2006; Panizza and Cerisola, 2006]. Meanwhile, evolution of oxygen also takes place due to chemical decomposition of higher oxides.

$$MO + R \rightarrow M + RO \quad (4.4.12)$$

$$MO \rightarrow M + 1/2O_2 \quad (4.4.13)$$

$$M(HO^{\bullet}) \rightarrow M + H^+ + e^- + 1/2O_2 \quad (4.4.14)$$

Complete mineralization of organic pollutant in presence of hydroxyl radicals results in the evolution of carbon dioxide [Martínez-Huitle and Ferro, 2006; Kumar et al., 2015].

$$M(HO^{\bullet}) + R \rightarrow M + H^+ + e^- + mCO_2 + nH_2O \quad (4.4.15)$$

Indirect oxidation occurs because of generation of various oxidative species within the solution during electrochemical treatment. Comninellis and Nerini [1995] observed that long life-time species (chlorine, hypochlorous acid, or hypochlorite), short life time species

(chloro and oxychloro radicals) are responsible for oxidation of pollutant in presence of chlorine. Mineralization of pollutant occurs due to incineration with hydroxyl radical discharged at anode:

$$MO_x + H_2O \rightarrow MO_x(HO^{\bullet}) + H^+ + e^- \quad (4.4.16)$$

Interaction between oxygen and hydroxyl radicals results in conversion into higher oxide.

$$MO_x(HO^{\bullet}) \rightarrow MO_{x+1} + H^+ + e^- \quad (4.4.17)$$

$MO_x(HO^{\bullet})$ interact with Cl^- obtained from NaCl supporting electrolyte according to following reaction:

$$MO_x(HO^{\bullet}) + Cl^- \rightarrow MO_x(O^{\bullet}Cl) + H^+ + 2e^- \quad (4.4.18)$$

Further absorption of hypochloride radicals interact with Cl^- ion resulted following reaction

$$MO_x(O^{\bullet}Cl) + Cl^- \rightarrow MO_{x+1} + Cl_2 + e^- \quad (4.4.19)$$

$$MO_x(O^{\bullet}Cl) + Cl^- \rightarrow MO_x + (1/2)\,O_2 + (1/2)\,Cl_2 + e^- \quad (4.4.20)$$

Complete mineralization of pollutant depends on the physio-sorption and chemisorption of the active species on the electrode surface. During electrochemical treatment, evolved gases take the original organic pollutants and the oxidized species to the top of solution and form scum. Thus, electro-floatation also helps in the removal of pyrrole and indole from aqueous solution.

4.4.3.2 UV-visible, UPLC, FTIR and cyclic voltammetric analysis

Degradation mechanism of pyrrole and indole during electrochemical treatment was studied at various time intervals by using UV-visible, UPLC, FTIR and cyclic voltammetric (CV) analysis. Results for UV-visible analysis are shown in Figure 4.4.7. Peak of initial concentration of pyrrole was observed at 205 nm and that of indole was observed at 270 nm. During electrochemical treatment of pyrrole and indole, it was observed that these peaks faded with treatment time with continuous decrease in intensity showing continuous decrease in the concentration of pyrrole and indole in the solution.

Results for UPLC analysis are shown in Figure 4.4.8. It shows over-layed chromatograms at various time intervals analyzed using Empower chromatographic software of UPLC. Peak separation was accomplished after 0.9 min for pyrrole solution and 2.15 min for indole solution. From the chromatograms, it is observed that initial concentration of pyrrole and indole decreased with increase in time of electrochemical treatment from 0 to 150 min. It may be observed that other peaks appear at shorter retention time during the treatment for both pyrrole and indole confirming mineralization of pyrrole and indole into smaller species.

Degradation mechanisms of pyrrole and indole were also studied by analyzing FTIR spectra of pyrrole and indole solutions during the treatment (Figure 4.4.9). FTIR spectrums show broad band with peak at ≈3400 cm^{-1} indicating free and hydrogen-bonded OH groups. Peak at ≈1634 cm^{-1} indicating C=C stretch. The band at 1375 cm^{-1} is ascribed to be C-H bending in plane. The sharp band at 3464.82 cm^{-1} is attributed to N-H stretching [Chen-Yang et al., 2004]. Band at 1590 cm^{-1} shows stretching and deformation of N-H bond and vibration modes of C_2 and C_3 aromatic bonds in pyrrole (Figure 4.4.9a). Very intense band at 1035 cm^{-1} assigned to the N-H in plane vibration deformation due to pyrrole ring vibration [Zaid et al., 1994]. Also band at 1354 cm^{-1} is related to modes involving the C8-N-C2-C3 group of indole (Figure 4.4.9b). During initial phases of treatment ($t \leq 60$ min), a large number of peaks observed between 3100 and 3600 cm^{-1} are due to the presence of a number of hydroxyl groups that get generated during the initial phases of electrochemical treatment (shown in equation 11). Alteration in transmittance after treatment of various peaks suggests the breaking of bonds at particular wave number. After 120 min of treatment, the transmittance intensity for most of the peaks increases indicating oxidation and conversion of aromatic ring structure. This results in decrease in pyrrole and indole concentration from aqueous medium by electrochemical treatment with increase in time.

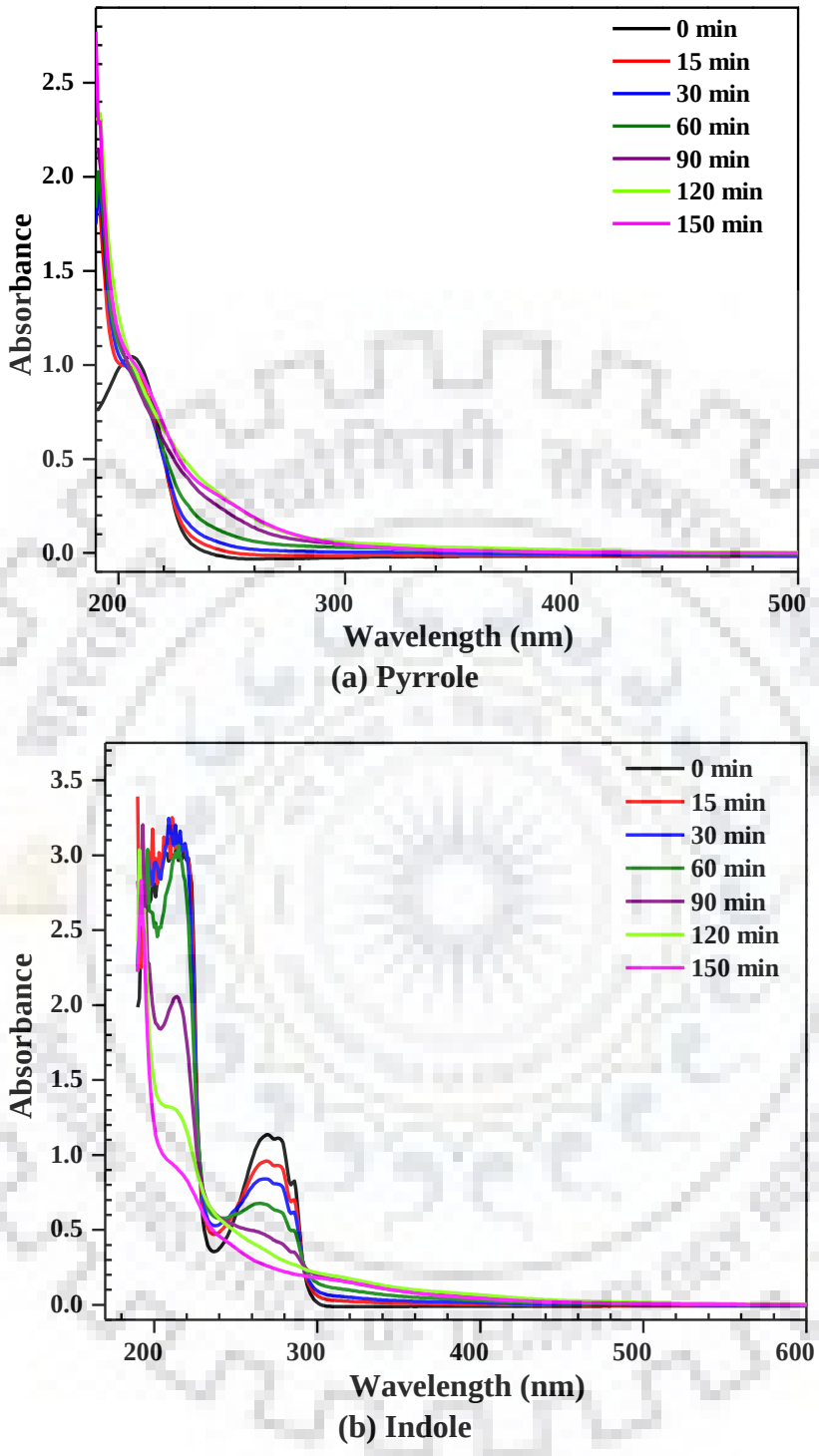

Figure 4.4.7: UV-visible spectra of pyrrole and indole at different time intervals during the electrochemical treatment.

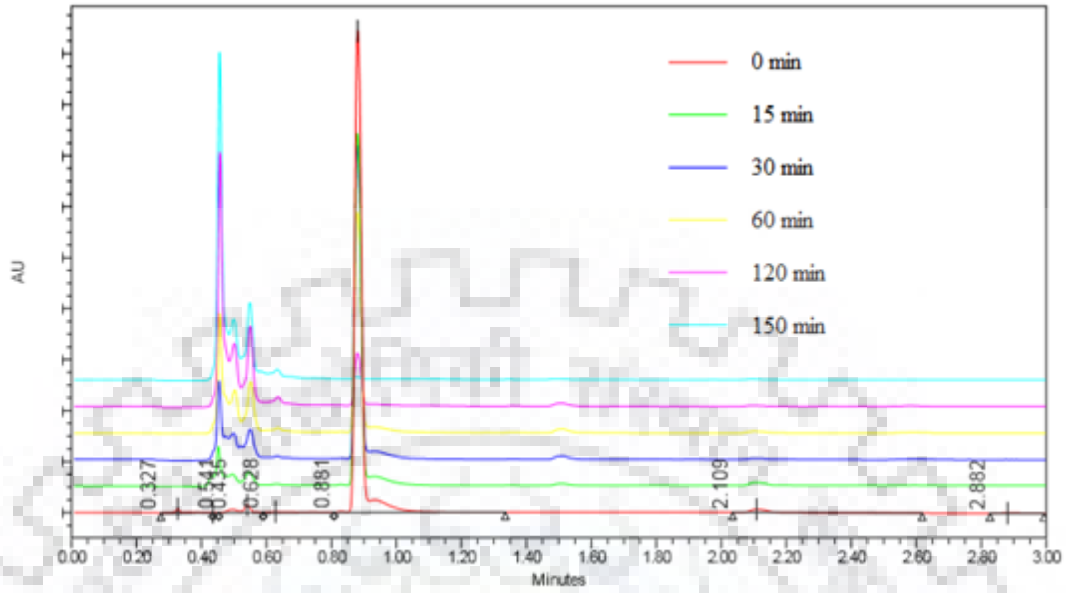

(a) Pyrrole

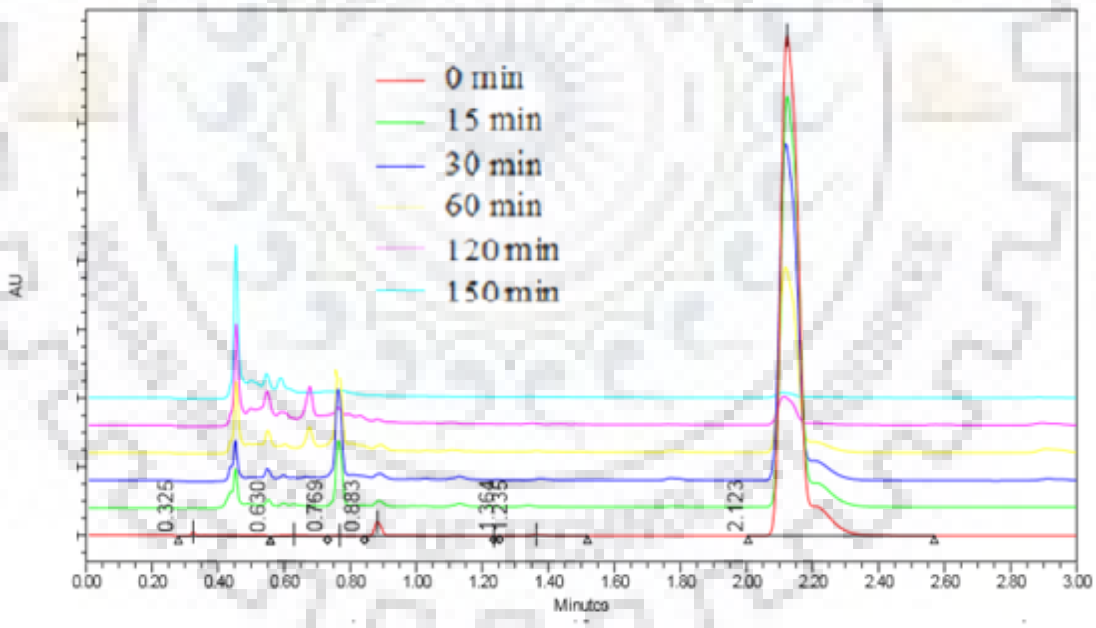

(b) Indole

Figure 4.4.8: Overlay chromatogram of pyrrole at different time intervals during the electrochemical treatment analyzed by UPLC.

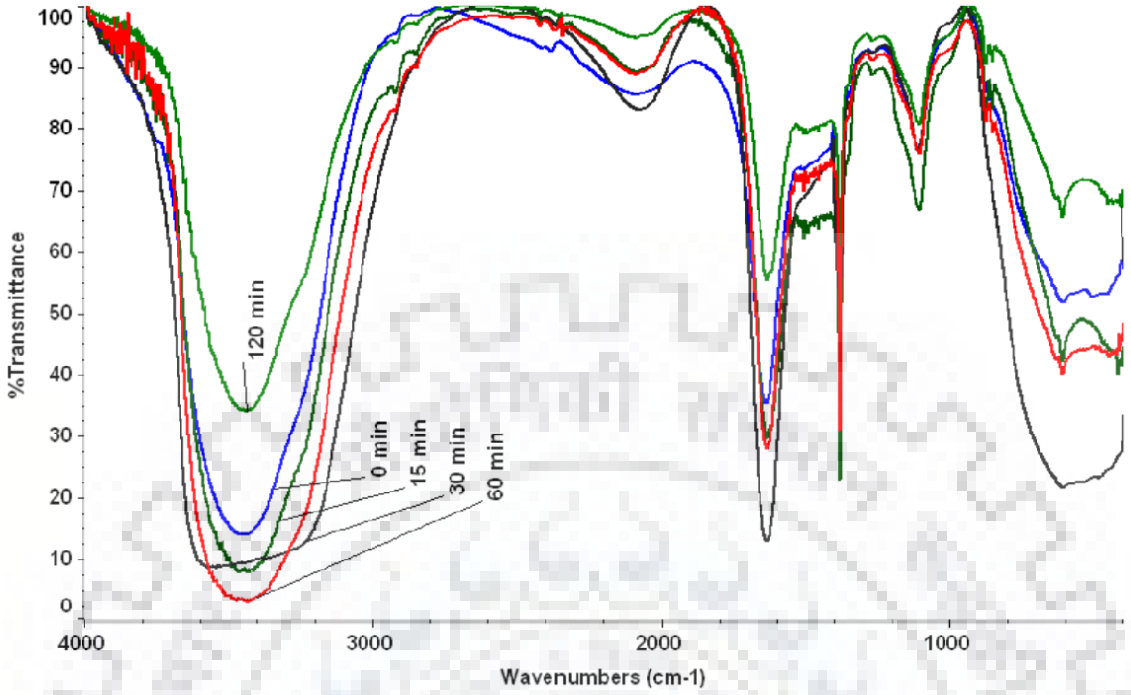

(a) Pyrrole

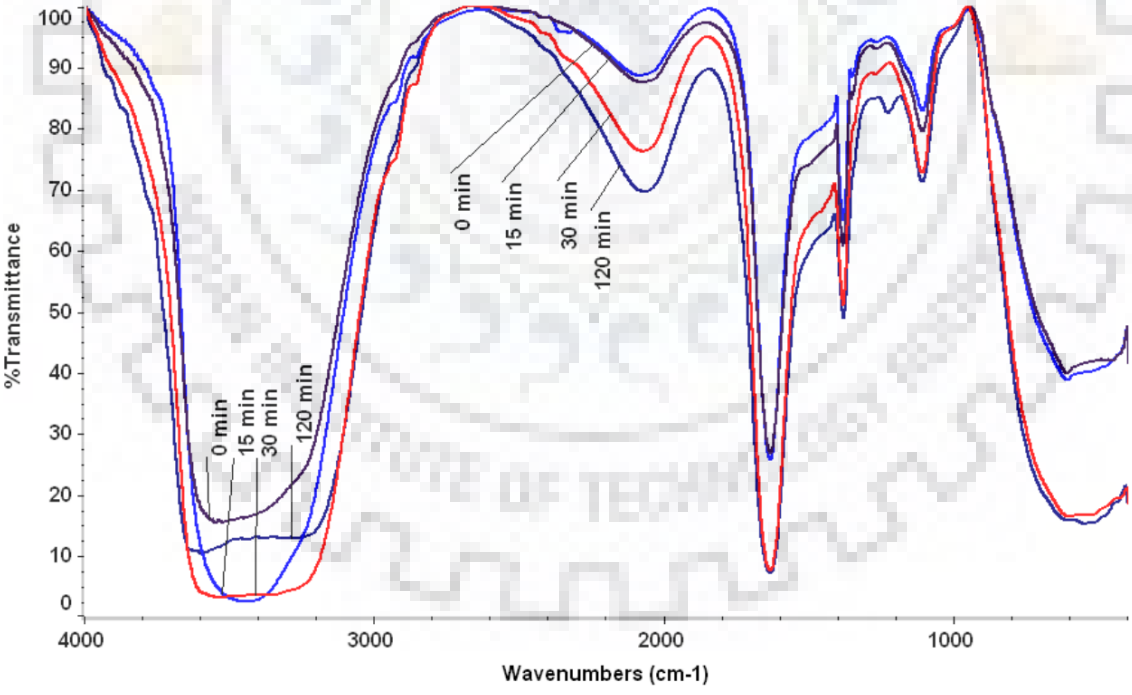

(b) Indole

Figure 4.4.9: FTIR spectra of pyrrole at different time intervals during electrochemical treatment.

CV studies of pyrrole and indole were done to determine the presence of oxidizable and reducible species in the aqueous solution which are helpful in electrochemical treatment (Figure 4.4.10 and Figure 4.4.11). Experiments were performed using pyrolytic graphite as working electrode. CV of these solutions before electrochemical treatment exhibited some chemically irreversible oxidation peaks which correspond to the direct oxidation of pyrrole or indole present in the solution. After electrochemical treatment with Pt/Ti electrode, earlier peaks in the voltammogram disappeared indicating the oxidation of pyrrole or indole [Linares-Hernandez et al., 2010]. In pyrrole solution, after addition of sodium chloride, peak was observed at potential -0.05 V which after treatment shifted to -1.2 V. Similarly for indole solution after addition of sodium chloride, peak was observed at potential -0.9 V which treatment shifted to -1.2 V. This variation in peaks before and after treatment suggest that there is reduction in concentration of pyrrole and indole solution during electrochemical treatment.

4.4.3.3 Filterability

In the present study, most of the residue was obtained as scum and negligible amount of sludge was obtained during pyrrole and indole mineralization by electrochemical treatment with Pt/Ti electrode. Mahesh et al. [2006b] showed that gravity filtration can be used for generating data for filtration of the slurry obtained after electrochemical treatment. Filter media used is the filter paper on Buechner funnel. Force balance against this gravity filtration can be written as:

$$\frac{\Delta t}{\Delta V} = \frac{\mu}{A\Delta P}\left(\frac{\alpha C V}{A} + R_m\right) \qquad (4.4.21)$$

Rearranging,

$$\frac{\Delta t}{\Delta V} = \frac{\mu \alpha C}{A^2\ \Delta P} V + \frac{\mu}{A\Delta P} R_m \qquad (4.4.22)$$

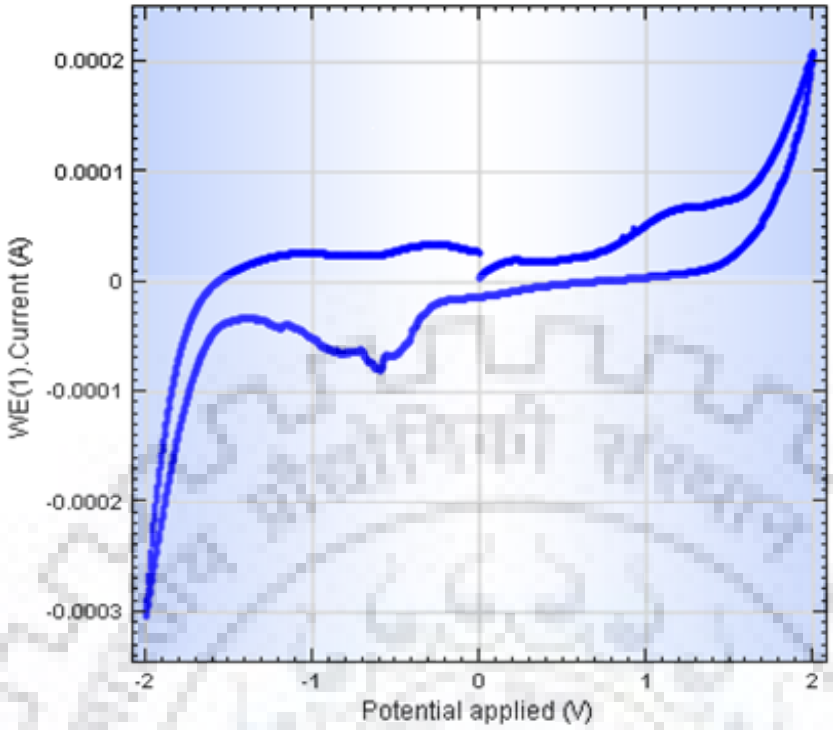

(a) Pyrrole before treatment

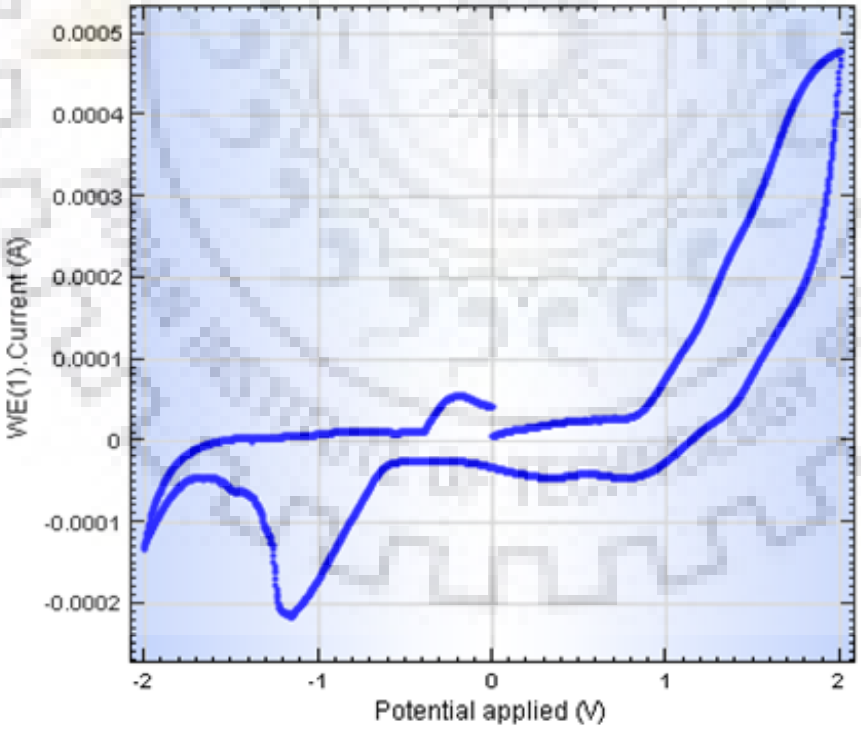

(b) Pyrrole after treatment

Figure 4.4.10: Cyclic voltammetric (CV) of pyrrole (a) before and (b) after treatment.

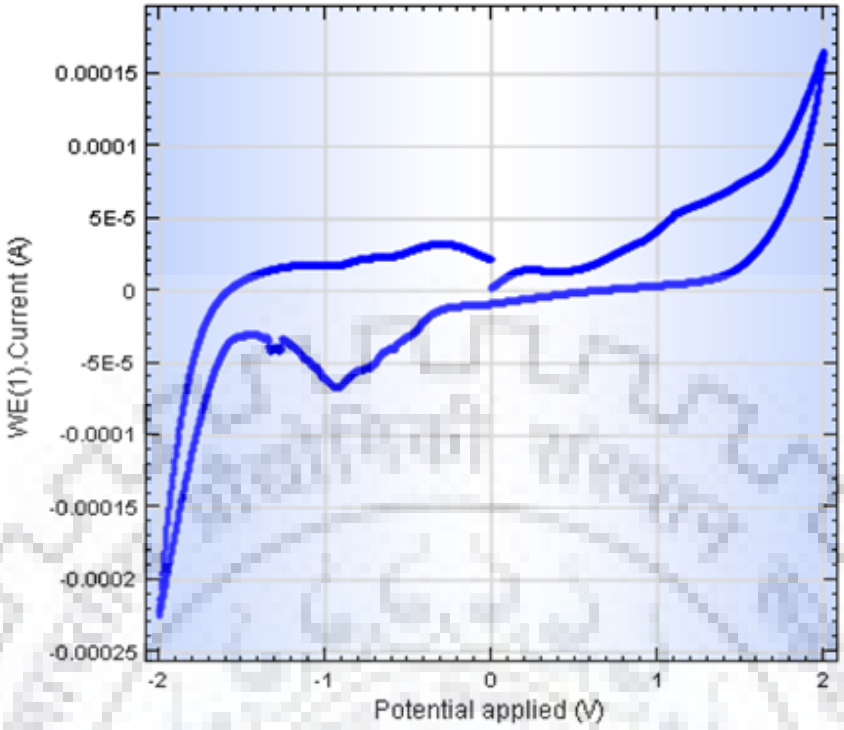

(a) Indole before treatment

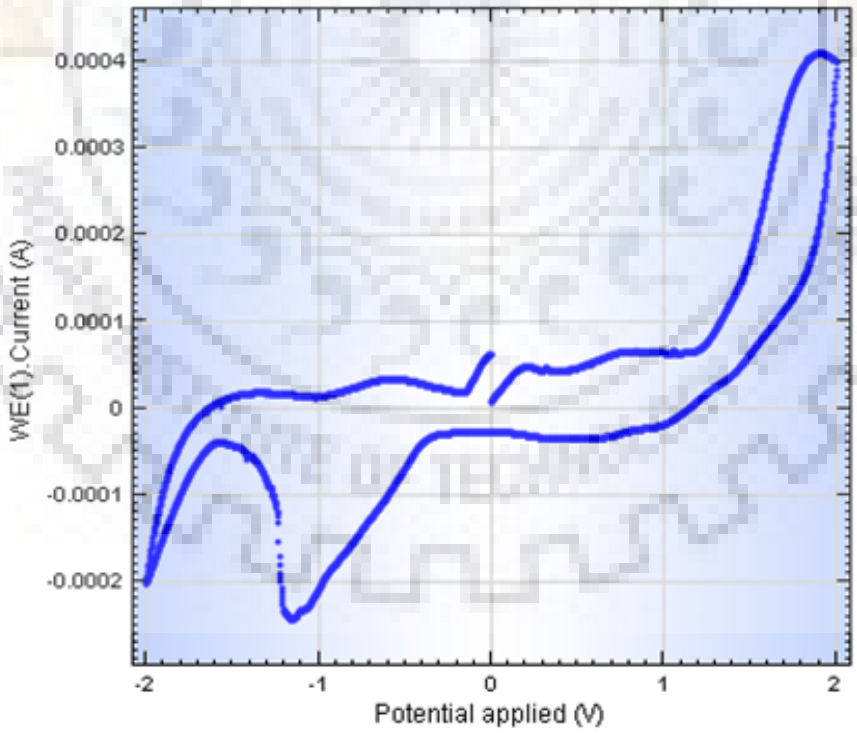

(b) Indole after treatment

Figure 4.4.11: Cyclic voltammetric (CV) of indole (a) before and (b) after treatment.

where, Δt is the interval of filtration (s), ΔV is the filtrate volume (m^3), C is the solid concentration in slurry ($kg.m^{-3}$), μ is the viscosity of liquid filtrate in (Pa.s), A is the filtration area (m^2). R_m is the resistance of filter medium in (m^{-1}) and α is specific cake resistance to filtration. After recording the volume of filtrate with time, the straight line plots of $\Delta t/\Delta V$ verses V were obtained (Figure 4.4.12). The values of R_m and α were calculated from the slope and intercept of straight line obtained. Values of R_m and α for treated-pyrrole slurry were 3.43×10^5 $m.kg^{-1}$ and 1.84×10^6 m^{-1}, respectively. Respective values for treated-indole slurry were 5.95×10^5 $m.kg^{-1}$ and 3.44×10^6 m^{-1}. Thus, treated-pyrrole slurry had better filtration characteristic.

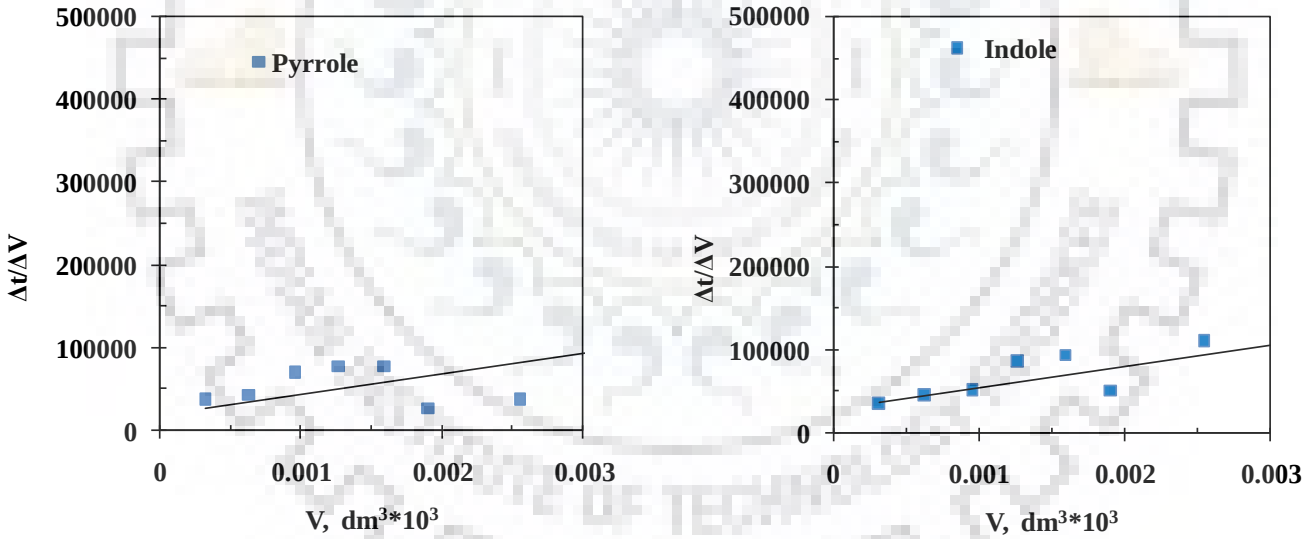

(a) Pyrrole slurry filtration **(b) Indole slurry filtration**

Figure 4.4.12: $\Delta t/\Delta V$ as function of filtrate volume for (a) pyrrole and (b) indole generated slurry after electrochemical treatment with electrode.

4.4.3.4 Morphology of electrode before and after treatment

SEM analysis of electrodes was done so as to investigate the changes on anode surface area before and after pyrrole and indole mineralization during electrochemical treatment of pyrrole and indole by. Scanning electron micrographs were used to detect the changes on the anodic area of electrode. It is seen that SEM images of fresh Pt/Ti electrode shows rough surface whereas dents are found around the nucleus of active sites after several experiments **(**Figure 4.4.13**)**. This is due to dissolution take place on anodic area producing ions during electrochemical treatment of pyrrole and indole. Distribution of elements on the virgin electrode was as follows: C (7.86%), O (8.43%), Al (3.27%), Ti (1.37%), Pt (79.08%). Elements present on the electrode after treatment of pyrrole were: C (15.11%), O (7.34%), Al (0.07%), Ti (0.52%), Pt (76.96%). Similarly elements present in the scum of pyrrole were: C (50.21%), O (15.09%), Na (7.56%) and Cl (27.14%). Similar investigation was carried out for indole electrochemical treatment where elements present on electrode after treatment were: C (43.76%), O (9.77%), Al (0.95%), Ti (1.12%), Pt (44.40%). Similarly elements present in the scum of indole were: C (76.20%), O (12.63%), Na (2.93%) and Cl (8.23%). Thus, most of the carbon, oxygen, sodium salt goes into the scum. It seems that some deposition of mineralized species also takes place on the electrodes. Therefore, electrochemical treatment of pyrrole and indole occurred by a combination of electro-oxidation and electro-floatation process. Electro-oxidation process generally dominates the treatment process with minor contribution of electro-floatation process. This is supported by the fact that only very small amount of scum ($\leq$ 20 mg/l) was collected at the end of each run.

4.4.3.5 Disposal of scum

Thermogravimetric analysis (TGA) was performed to understand the degradation kinetics of scum in presence of air. TGA and DTA analysis of scum obtained from electrochemical treatment of pyrrole and indole were done at 10 K min^{-1} heating rate in presence of air (Figure 4.4.14). For pyrrole scum, weight loss of 5.18% due to loss of moisture occurred up to 100°C. From 100°C to 800°C, scum showed 14.28% weight loss. Maximum weight loss of 69.77% occurred between 800-1003°C with maximum rate of degradation 0.75 $mg.min^{-1}$ as observed in differential thermal (DTG) plot. This study shows pyrrole scum is highly stable up to 800°C. Similarly, indole-scum showed weight loss of 11.36% up to 400°C due to loss of moisture and light volatiles. There is no endothermic transition indicating no phase changes during the heating process up to this temperature. From 400 to 534°C, scum showed 27.04% weight loss with degradation rate of 0.38 $mg.min^{-1}$

(Figure 4.4.14). Indole scum showed 57.07% weight loss in the range of 534-1002°C with maximum rate of degradation of 0.51 $mg.min^{-1}$ in the last zone. Overall pyrrole scum showed ≈90% degradation whereas indole scum showed ≈96% degradation. Inorganic content in both the sludge is due to the presence of minor amount of electrode material which gets deteriorated during each run. Higher organic content in indole sludge is due to the presence of intermediates that get formed during degradation of indole (which itself contains both benzene and pyrrole ring). This study shows that both pyrrole and indole scum can be dried and used utilized in making fuel-briquettes which could be fired in the boilers/incinerators to recover its energy value.

4.4.4 Operating Cost Analysis

Operating cost of electrochemical system mainly consists of cost of electrode and electrical energy consumed at optimum conditions was selected for treating 1 m^3 of wastewater containing pyrrole and indole. Electrical energy consumption for individual pyrrole and indole mineralization were found to be ~62 and 30 $kWh.m^{-3}$. In India, price of electrical energy is $0.07 per kWh, therefore, cost of energy for pyrrole treatment was found to be $ 4.3 per m^3. Similarly, cost of energy for indole treatment was calculated as: $ 2.1 per m^3. Now, it was observed that consumption of electrode took place in 50 runs treating one litre of aqueous solution in each run. Since cost of each electrode was ~$11, therefore, total cost of electrode was $220 per m^3 for both pyrrole and indole. Total combined electrochemical treatment cost (C_{energy} and $C_{electrode}$ cost) for pyrrole degradation was: $224.3 per m^3 and that of indole degradation was: $222.1 per m^3. It may be mentioned that operating cost obtained during electrochemical treatment of pyrrole and indole is approximate analysis only.

Operating cost for treatment of butyric acid by conductive diamond electrochemical oxidation (CDEO), ozonation and Fenton oxidation were found to be 12 $ per m^3, 270 $ per m^3 and 46 $ per m^3, respectively [Canizares et al., 2009]. For treatment of pyridine bearing wastewater by wet peroxidation, cost of treatment was 248 $ per m^3 [Subbaramaiah et al., 2013]. Kumar et al. [2015] estimated the cost of electrochemical treatment of nitorphenol bearing aqueous solution by ruthenium oxide coated titanium electrode to be 226.7 $ per m^3. It may be concluded that operating cost depend upon method of treatment, type of compound and its initial concentration. Operating cost decreases exponentially with increase in scale of operation under continuous treatment.

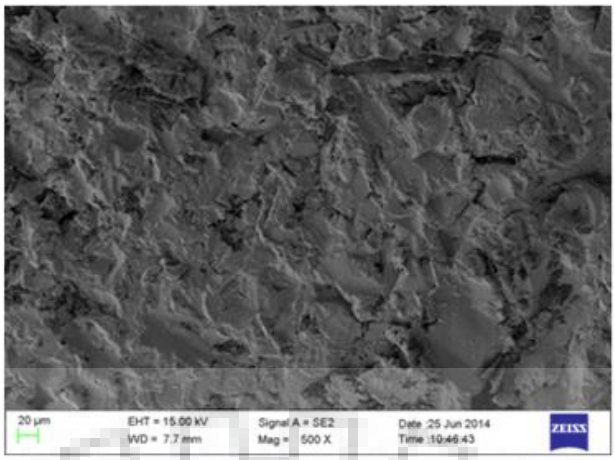

(a) Virgin electrode

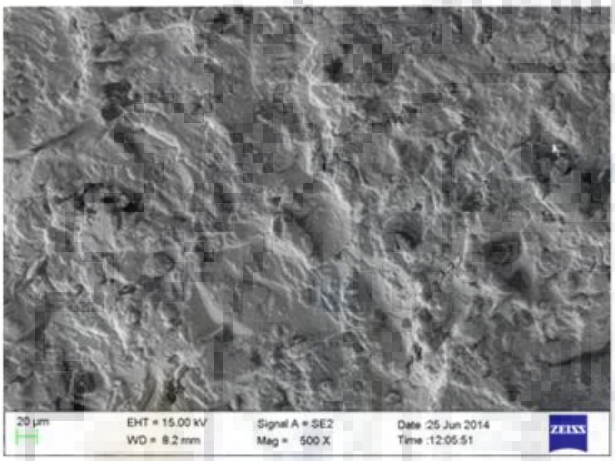

(b) Used electrode for pyrrole

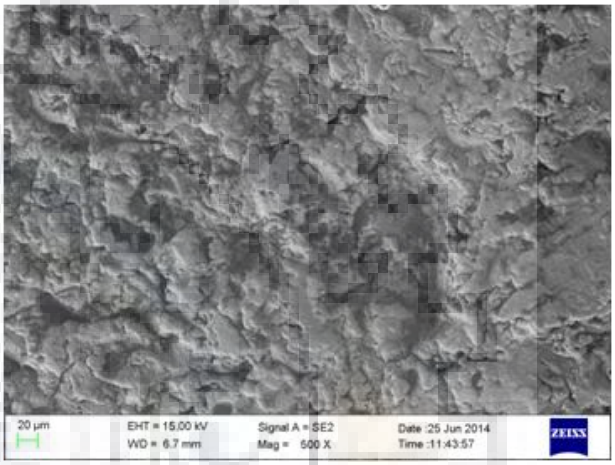

(c) Used electrode for indole

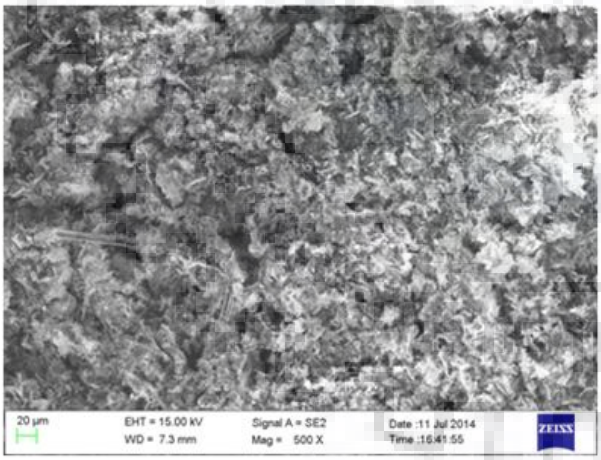

(d) Scum of Pyrrole

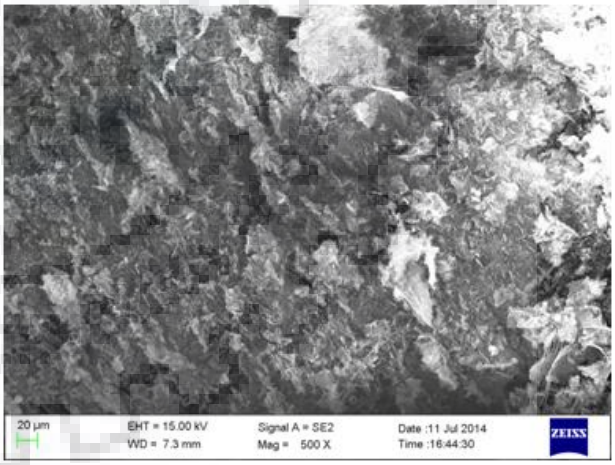

(e) Scum of indole

Figure 4.4.13: SEM images of fresh and used Pt/Ti electrode and scum generated during electrochemical treatment of pyrrole and indole.

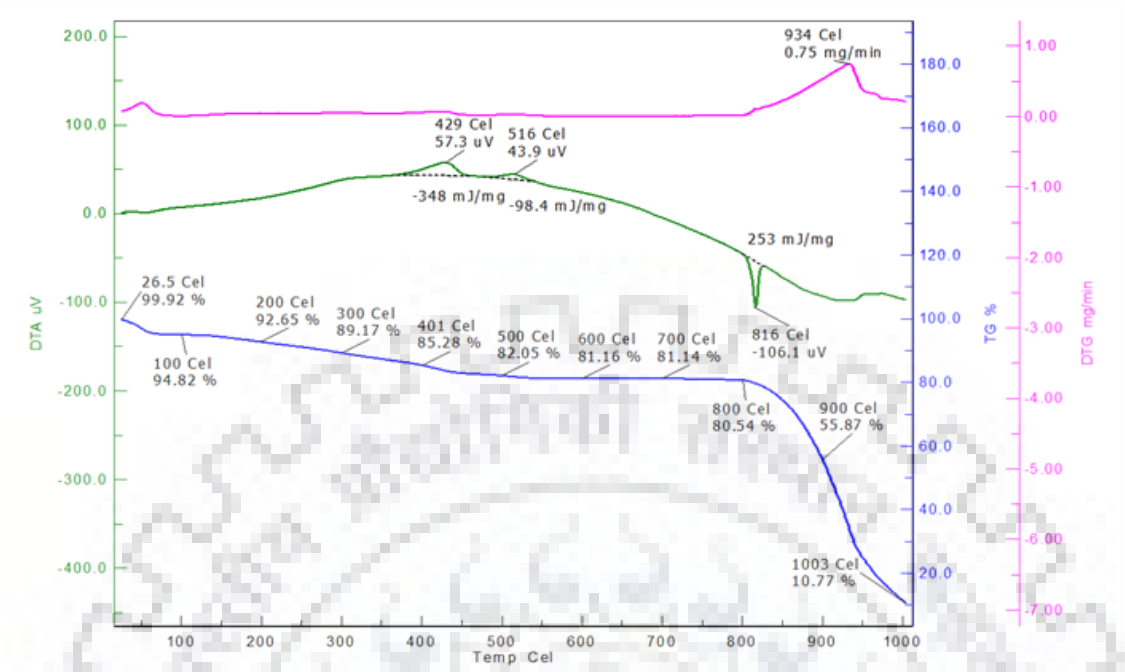

(a) Pyrrole scum

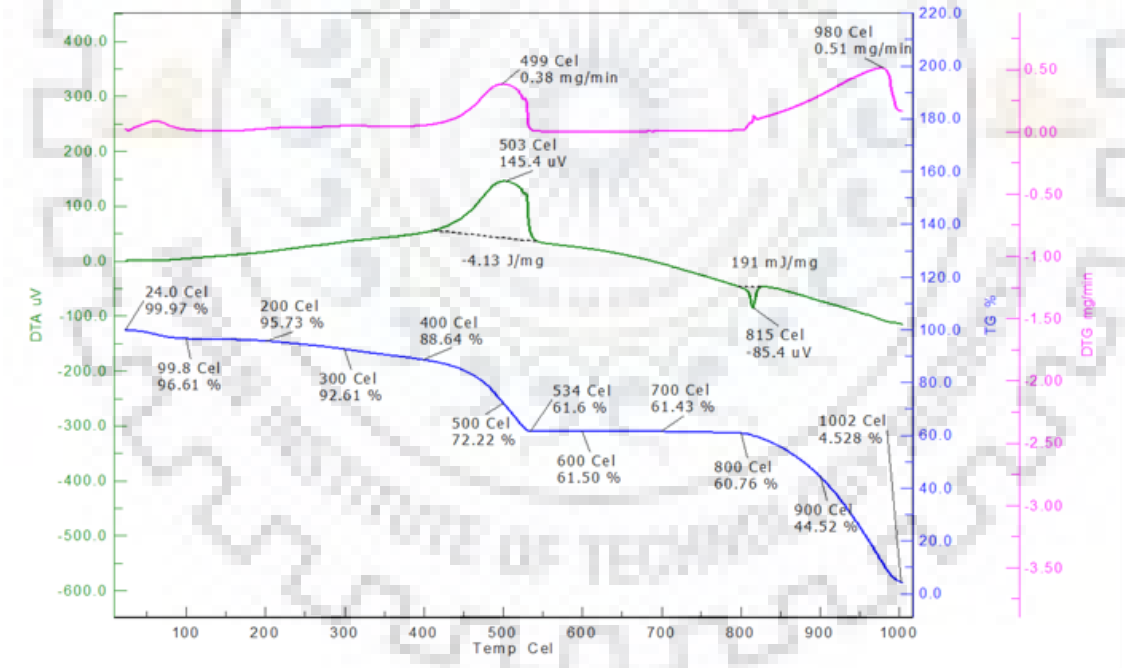

(b) Indole scum

Figure 4.4.14: Thermogravimetric analysis of scum obtained after electrochemical treatment of pyrrole and indole in aqueous solution.

Chapter –5

CONCLUSIONS & RECOMMENDATIONS

5.1 CONCLUSIONS

In the present study, work was carried out as per the aims and objectives given in section 1.6 which themselves were decided on the basis of the literature survey presented in Chapter 2 and the research gaps identified in section 2.7. First, individual and simultaneous removal of pyrrole and indole from aqueous solution was studied using adsorption onto granular activated carbon (GAC) and bagasse fly ash (BFA). Thereafter, individual and simultaneous mineralization of pyrrole and indole was studied using platinum coated titanium (Pt/Ti) electrode. On the basis of the results and discussion presented heretofore, following major conclusions can be drawn from the present study.

5.1.1 Adsorptive removal of pyrrole and indole by GAC and BFA

- Proximate and energy-dispersive X-ray (EDX) spectroscopy analysis showed that the GAC contained more amount of carbon as compared to BFA.
- Pore size distribution analysis indicated mesoporous nature of both GAC and BFA. GAC (355 $m^2.g^{-1}$) was found to have greater Brunauer-Emmett-Teller (BET) surface area as compared to BFA (201 $m^2.g^{-1}$).
- FTIR spectra indicated the presence of various types of functional groups e.g. free and hydrogen bonded OH group, the silanol groups (Si-OH) and CO group stretching on the surface of both GAC and BFA.
- The natural solution pH was found to be optimum for the individual removal of pyrrole and indole from aqueous solution by both GAC and BFA.
- Adsorption of pyrrole and indole was found to predominantly occur on the mesopores of the adsorbents.
- Kinetic study revealed that pyrrole and indole adsorption onto GAC and BFA followed pseudo-second-order kinetic model.
- Equilibrium isotherm experimental data of pyrrole and indole adsorption onto GAC and BFA were well-represented by the Redlich-Peterson isotherm at all temperatures.
- Indole adsorption onto both GAC and BFA was endothermic in nature, however, pyrrole adsorption onto GAC was slightly exothermic that onto BFA was endothermic.
- For initial concentration (C_o) of 500 $mg.l^{-1}$ and GAC dose (m)=20 $g.l^{-1}$, removal efficiency of pyrrole and indole by GAC was found to be 84% and 95%, respectively. Similarly using BFA, for C_o=500 $mg.l^{-1}$, removal efficiency of pyrrole was found to be 93% at m=15 $g.l^{-1}$ and that for indole was 95% at m=7 $g.l^{-1}$. Thus, BFA exhibited

higher adsorption capacity than GAC in the single stage adsorption for adsorptive removal of pyrrole and indole.

- Thermal desorption-adsorption cycle showed that the GAC can be used for more than five cycles whereas it is better to use fresh BFA during the adsorption process as its adsorption capacity decreased sharply during repeated desorption-adsorption cycles.
- Taguchi's method was found to be very useful and economical for optimizing the operating parameters for simultaneous adsorptive removal of pyrrole and indole from binary solution onto GAC.
- Adsorbent dose and interaction between $C_{0,i}$'s were found to be the most significant factors for simultaneous adsorption.
- In the binary system, adsorption was found to be antagonistic in nature, and the adsorption capacity for indole was found to be higher than that of pyrrole for both GAC and BFA.
- Overall extended-Freundlich isotherm and extended-Langmuir model best represented the binary adsorption data for the adsorptive removal of pyrrole and indole from binary aqueous solution using GAC and BFA.
- Thermo-gravimetric analysis (TGA) of the GAC and BFA showed that the spent adsorbents can be used as a fuel. The organics bearing bottom ash obtained after the combustion of the spent adsorbents can be blended with cementitious mixture for making building blocks or fire bricks.

5.1.2 Mineralization of Pyrrole and Indole using Platinum coated Titanium (Pt/Ti) Electrode

- Full factorial central composite (CCD) design was used to study the effect of four key process parameters such as pH, current density (j), conductivity (k) and electrolysis time (t) on the chemical oxygen demand (COD) removal and specific energy consumption during individual mineralization of pyrrole and indole by Pt/Ti electrode. Desirability approach was found to be simultaneously maximizing COD removal and minimizing specific energy consumption.
- Optimum operational parameters during electrochemical treatment of pyrrole were found to be: pH=8.7, j=175 $A.m^{-2}$, k=2.94 $mS.cm^{-1}$ and t=150 min. Under these optimized conditions, percent COD removal and specific energy consumption were found to be 68.8%, 99.25 kWh/kg of COD removed, respectively.
- Similarly, optimum operational parameters during electrochemical treatment of indole were found to be: pH=8.6, j=161 $A.m^{-2}$, k=6.69 $mS.cm^{-1}$ and t=150 min. Under these

optimized conditions, percent COD removal and specific energy consumption were found to be: 82.92% and 37.75 kWh/kg of COD removed, respectively.

- Optimization of parameters for simultaneous mineralization of pyrrole and indole in binary solution was done using Taguchi's design of experiments (L_{16} orthogonal array). Optimum values for pyrrole, indole and COD removal efficiencies were found to be 46.1%, 62.4% and 61.4%, respectively.
- UV-visible and ultra performance liquid chromatograph (UPLC) study showed that different bonds were broken and most of the aromatic rings were mineralized during electrochemical treatment with Pt/Ti electrode.
- FTIR study showed that transmittance of various peaks increased after treatment suggesting that the quantity of various functional groups initially present in the pyrrole or indole bearing aqueous solution decreased after electrochemical treatment.
- Electrochemical treatment of pyrrole and indole was found to occurr by a combination of electro-oxidation and electro-floatation process.
- TGA study showed that the scum generated during electrochemical treatment can be used as a fuel in boilers/incinerators, or can be used for the production of fuel-briquettes.

Finally, optimum conditions for the individual and simultaneous removal of pyrrole and indole from aqueous solution by various treatment methods studied in the present work and their treatment efficiencies are as follows:

Treatment Method	**Pollutant**	**Initial Concentration ($mg.l^{-1}$)**	**Optimum Conditions**	**Removal efficiencies**
Adsorption by GAC	Pyrrole	500	m=20 $g.l^{-1}$, t=8 h, pH_o=5.7, T=303 K	84%
	Indole	500	m=20 $g.l^{-1}$, t=8 h, pH_o=5.7, T=303 K	95%
	Pyrrole-Indole	500 each	m=20 $g.l^{-1}$, t=11 h, pH_o=5.7, T=303 K	Pyrrole=26%, Indole=82%
Adsorption by BFA	Pyrrole	500	m=15 $g.l^{-1}$, t=8 h, pH_o=5.7, T=303 K	93%
	Indole	500	m=7 $g.l^{-1}$, t=8 h, pH_o=5.7, T=303 K	95%
	Pyrrole-Indole	500 each	m=14 $g.l^{-1}$, t=11 h, pH_o=5.7, T=318 K	Pyrrole=48%, Indole=87%
Electrochemical treatment by Pt/Ti electrode	Pyrrole	250	pH=8.7, j=175.19$A.m^{-2}$, k=2.94 $mS.cm^{-1}$, t=150 min	COD=68.80%
	Indole	250	pH=8.6, j=161.02 $A.m^{-2}$, k=6.69 mS/cm, t=150 min	COD=82.92%
	Pyrrole-Indole	500 each	j=333 $A.m^{-2}$, k=5.3 mS/cm, t=150 min	Pyrrole=46.1%, Indole=62.4%, COD=61.4%

Overall, adsorptive removal of pyrrole and indole by BFA was economical among the treatment methods studied. Though, considering the mineralization of pyrrole and indole, electrochemical treatment by Pt/Ti is a good option of treatment.

5.2 RECOMMENDATIONS

Based on the experiences gained during the present work, the following recommendations are being made for future research:

- Column and scale-up studies should be conducted to evaluate the suitability of GAC and BFA as adsorbent for the removal of pyrrole and indole from wastewater.
- Other electrodes in series and bipolar arrangements need to be studied in both batch and continuous electrochemical reactors and compared for their adoption in electrochemical treatment of nitrogenous heterocyclic compounds from aqueous solutions.
- Since the electrochemical treatment is not able to remove completely remove the COD, therefore, it may further be treated by other methods like adsorption to meet the stipulated regulatory discharge standards.
- Studies may be carried out for reutilizing and reusing the GAC, BFA and electrochemical treatment generated scum for wastewater treatment either as an adsorbent or by making nano-particles through thermal route.

REFERENCES

Abdallah, W. A.; Nelson, A. E. Pyrrole adsorption and reaction on Mo(110) and C/N-Mo(110). Surface Science, 585, 113-122, (2005).

Aeiyach, S.; Zaid, B.; Lacaze, P. C. A one-step electrosynthesis of PPy films on zinc substrates by anodic polymerization of pyrrole in aqueous solution. Electrochimica Acta, 44, 2889-2898, (1999).

Agrahari, G. K.; Shukla, S. K.; Verma, N.; Bhattacharya, P. K. Model prediction and experimental studies on the removal of dissolved NH_3 from water applying hollow fiber membrane contactor. Journal of Membrane Science, 390-391, 164-174, (2012).

Ahmed, I.; Khan, N. A.; Hasan, Z.; Jhung, S. H. Adsorptive denitrogenation of model fuels with porous metal-organic framework (MOF) MIL-101 impregnated with phosphotungstic acid: Effect of acid site Inclusion. Journal of Hazardous Materials, 250-251, 37-44, (2013a).

Ahmed, I.; Hasan, Z.; Khan, N. A.; Jhung, S. H. Adsorptive denitrogenation of model fuels with porous metal-organic frameworks (MOFs): Effect of acidity and basicity of MOFs. Applied Catalysis B: Environmental, 129, 123-129, (2013b).

Ahmed, I.; Khan, N. A.; Jhung, S. H. Graphite oxide/metal−organic framework (MIL-101): remarkable performance in the adsorptive denitrogenation of model fuels. Inorganic Chemistry, 52, 14155−14161, (2013c).

Almarri, M.; Ma, X.; Song, C. Role of surface oxygen-containing functional groups in liquid-phase adsorption of nitrogen compounds on carbon-based adsorbents. Energy & Fuels, 23, 3940-3947, (2009).

An, H.; Seki, M.; Sato, K.; Kadoi, K.; Yosomiya, R. Electrochemical polymerization of methyl substituted quinoline. Polymer, 30, 1076-1078, (1989).

Andrieux, C. P.; Hapiot, P.; Audebert, P.; Guyard, L.; Nguyen Dinh An M.; Groenendaal, L.; Meijer, E. W. Substituent effects on the electrochemical properties of pyrroles and small oligopyrroles. Chemistry of Materials, 9(3), 723-729, (1997).

Aravindhan, R.; Rao, J. R.; Nair, B. U. Removal of basic yellow dye from aqueous solution by adsorption on green algae: *Caulerpa scalpelliformis*. Journal of Hazardous Materials, 142, 68-76, (2007).

Aroua, M. K.; Daud, W. M. A. W.; Yin, C. Y.; Adinata, D. Adsorption capacities of carbon dioxide, oxygen, nitrogen and methane on carbon molecular basket derived from polyethyleneimine impregnation on microporous palm shell activated carbon. Separation and Purification Technology, 62, 609-613, (2008).

Azadi, P.; Carrasquillo-Flores, R.; Pagán-Torres, Y. J.; Gurbuz, E. I.; Farnood, R.; Dumesic, J. A. Catalytic conversion of biomass using solvents derived from lignin. Green Chemistry, 14, 1573, (2012).

Azadi, P.; Afif, E.; Foroughi, H.; Dai, T.; Azadi, F.; Farnood, R. Catalytic reforming of activated sludge model compounds in supercritical water using nickel and ruthenium catalysts. Applied Catalysis B: Environmental, 134-135, 265-273, (2013).

Audebert, P.; Guyard, L.; An, M. N. D.; Hapiot, P.; Chahma, M.; Combelas, C.; Thiebault, A. Electrochemical studies of the oxidation of sterically hindered pyrroles and thiophenes. Journal of Electroanalytical Chemistry, 407, 169-173, (1996).

Bai, Y.; Sun, Q.; Zhao, C.; Wen, D.; Tang, X. Microbial degradation and metabolic pathway of pyridine by a Paracoccus sp. strain BW001. Biodegradation, 19, 915-926, (2008).

Bai, Y.; Sun, Q.; Xing, R.; Wen, D.; Tang, X. Removal of pyridine and quinoline by biozeolite composed of mixed degrading bacteria and modified zeolites. Journal of Hazardous Materials, 181, 916-922, (2010a).

Bai, Y.; Sun, Q.; Zhao, C.; Wen, D.; Tang, X. Bioaugmentation treatment for coking wastewater containing pyridine and quinoline in a sequencing batch reactor. Applied Microbiology and Biotechnology, 87, 1943-1951, (2010b).

Bai, Y.; Sun, Q.; Sun, R.; Wen, D.; Tang, X. Bioaugmentation and adsorption treatment of coking wastewater containing pyridine and quinoline using zeolite-biological aerated filters. Environmental Science & Technology, 45, 1940-1948, (2011).

Bai, Y.; Sun, Q.; Sun, R.; Wen, D.; Tang, X. Comparison of denitrifier communities in the biofilms of bioaugmented and non-augmented zeolite-biological aerated filters. Environmental Technology, 33, 1993-1998, (2012).

Becerik, I.; Kadirgan, F. An investigation on the adsorption characteristics and orientations model of pyrrole on smooth platinum electrode. Electrochimica Acta, 42, 283-289, (1997).

Bellot, J. C.; Condoret, J. S. Modelling of liquid chromatography equilibrium. Process Biochemistry, 28, 365-376, (1993).

Bethea, R. M.; Narayan, R. S. Identification of beef cattle feedlot odors. Transactions American Society of Agriculture and Engineers, 15, 1135-1137, (1972).

Bhaskar Raju, G.; Thalamadai Karuppiah, M.; Latha, S. S.; Latha Priya, D.; Parvathy, S.; Prabhakar, S. Treatment of wastewater from synthetic textile industry by electrocoagulation-electrooxidation. Chemical Engineering Journal, 144, 51-58, (2008).

Bhaskar Raju, G.; Thalamadai Karuppiah, M.; Latha, S. S.; Latha Priya, D.; Parvathy, S.; Prabhakar S. Electrochemical pretreatment of textile effluents and effect of electrode materials on the removal of organics. Desalination, 249, 167-174, (2009).

Broholm, M. M.; Broholm, K.; Arvin, E. Sorption of heterocyclic compounds on natural clayey till. Journal of Contaminant Hydrology, 39, 183-200, (1999).

Burgos, W. D.; Pisutpaisal, N.; Mazzarese, M. C.; Chorover, J. Adsorption of quinoline to kaolinite and montmorillonite. Environmental Engineering Science, 19(2), 59-68, (2002).

Canizares, P.; Martinez, F.; Rodrigo M. A.; Jimenez C.; Saez, C.; Lobato, J. Modeling of wastewater electro coagulation processes: Part I. General description and application to kaolin-polluted wastewaters. Separation and Purification Technology, 60, 155-161, (2008a).

Canizares, P.; Martinez, F.; Rodrigo, M. A.; Jimenez, C.; Saez, C.; Lobato, J. Modelling of wastewater electro coagulation processes Part II: Application to dye-polluted wastewaters and oil-in-water emulsions. Separation and Purification Technology, 60, 147-154, (2008b).

Canizares, P.; Paz, R.; Saez, C.; Rodrigo, M. A. Costs of the electrochemical oxidation of wastewaters: A comparison with ozonation and Fenton oxidation processes. Journal of Environmental Management, 90, 410-420, (2009).

Chandra, R.; Bharagava, R. N.; Kapley, A.; Purohit, H. J. Isolation and characterization of potential aerobic bacteria capable for pyridine degradation in presence of picoline, phenol and formaldehyde as co-pollutants. World Journal of Microbiology Biotechnology, 25, 2113-2119, (2009).

Chen, J. P.; Wang, L. Characterization of metal adsorption kinetic properties in batch and fixed bed reactors. Chemosphere, 54, 397-404, (2004).

Chen, W. S.; Huang, C. P. Mineralization of aniline in aqueous solution by electrochemical activation of persulfate. Chemosphere, 125, 175-181, (2015).

Chen-Yang, Y. W.; Li, J. L.; Wu, T. L.; Wang, W. S.; Hon, T. F. Electropolymerization and electrochemical properties of (N-hydroxyalkyl) pyrrole/pyrrole copolymers. Electrochiimica Acta, 49, 2031-2040, (2004).

Chiang, K. T. Optimization of the design parameters of parallel-plain fin heat sink module cooling phenomenon based on the Taguchi method. International Communications in Heat and Mass Transfer, 32, 1193-1201, (2005).

Choy, K. K. H.; Allen, S. J.; Mckay, G. Multicomponent equilibrium studies for the adsorption of basic dyes from solution on lignite. Adsorption, 11, 255-259, (2005).

Collin, G.; Hoke, H. Indole. In: Elvers, B.; Hawkins, S.; Ravenscroft, M.; Schulz, G. (Eds.), Ullmann's encyclopedia of industrial chemistry, VCH, Weinheim, A14, 167-170, (1989).

Collin, G.; Hoke, H. Quinoline and isoquinoline. In: Elvers, B.; Hawkins, S.; Russey, W.; Schulz, G. (Eds.), Ullmann's Encyclopedia of Industrial Chemistry, VCH, Weinheim, A22, 465-469, (1993).

Collin, G.; Hoke, H. Tar and pitch In: Elvers, B.; Hawkins, S.; Russey, W. (Eds.), Ullmann's Encyclopedia of Industrial Chemistry, VCH, Weinheim, A26, 91-127, (1995).

Comninellis, C.; Vercesi, G. P. Characterization of DSA-type oxygen evolving electrodes: choice of a coating. Journal of Applied Electrochemistry, 21 335-345, (1991).

Comninellis C.; Nerini, A. Anodic oxidation of phenol in the presence of NaCl for waste water treatment. Journal of Applied Electrochemistry, 25, 23-28, (1995).

Cruz-Gonzalez, K.; Tores-Lopez, O.; Garcia-Leon, A.; Guzman-Mar, J. L.; Reyes, L. H.; Hernandez-Ramirez, A.; Peralta-Herandez, J. M. Determination of optimum parameter for acid yellow 36 decolorization by electron-Fenton process using BDD cathode. Chemical Engineering Journal, 160, 199-206, (2010).

De, S.; Bhattacharya, P. K. Modeling of ultrafiltration process for a two-component aqueous solution of low and high (gel-forming) molecular weight solutes. Journal of Membrane Science, 136, 57-69, (1997).

Deng, X.; Wei, C.; Ren, Y.; Chai, X. Isolation and identification of *Achromobacter sp.* DN-06 and valuation of its pyridine degradation kinetics. Water Air and Soil Pollution, 221, 365-375, (2011).

Desai, K. R.; Murthy, Z. V. P. Removal of Ag(I) and Cr(VI) by complexation-ultrafiltration and characterization of the membrane by CFSK model. Separation Science and Technology, 49, 2620-2629, (2014).

Devillers, C. H.; Dime, A. K. D.; Cattey, H.; Lucas, D. Crystallographic, spectroscopic and electrochemical characterization of pyridine adducts of magnesium(II) and zinc(II) porphine complexes. Comptes Rendus Chimie, 16, 540-549, (2013).

Diez, P. R.; Amalvy J. I. A density functional study of the adsorption of pyridine, 2-vinylpyridine, and 4-vinylpyridine onto a silica surface. Journal of Molecular Structure-THEOCHEM, 634, 187-193, (2003).

Dobson, K. R.; Stephenson, M.; Greenfield, P. F.; Bell, P. R. F. Identification and treatability of organics in oil shale retort water. Water Research, 19, 849, (1985).

DuBois, M. R.; Vasquez, L. D.; Ciancanelli, R. F.; Noll, B. C. Electrophilic substitution of nitrogen heterocycles by molybdenum sulfide complexes. Organometallics, 19, 3507, (2000).

Ellis, J.; Korth, J. Removal of nitrogen compounds from hydrotreated shale oil by adsorption on zeolite. Fuel, 73 (10), 1569-1573, (1994).

Enache, T. A.; Brett, A. M. O. Pathways of electrochemical oxidation of indolic compounds. Electroanalysis, 23(6), 1337-1344, (2011).

Erciyes, N.; Gürten, A.; Abdullah, M.; Ahmed, A. Adsorption of indole and 2-methylindole on ligand-exchange matrix. Journal of Colloid and Interface Science, 278, 91-95, (2004).

Ferreira, M.; Pinto, M. F.; Neves, I. C.; Fonseca, A. M.; Soares, O. S. G. P.; Órfao, J. J. M.; Pereira, M. F. R.; Figueiredo, J. L.; Parpot, P. Electrochemical oxidation of aniline at mono and bimetallic electrocatalysts supported on carbon nanotubes. Chemical Engineering Journal 260, 309-315, (2015).

Faruk, O.; Sain, M.; Farnood, R.; Pan, Y.; Xiao, H. Development of lignin and nanocellulose enhanced bio PU foams for automotive parts. Journalof Polymers and the Environment, 22, 279-288, (2014).

Fetzner, S. Bacterial degradation of pyridine, indole, quinoline, and their derivatives under different redox conditions. Applied Microbiology and Biotechnology, 49, 237-250, (1998).

Freundlich, H. M. F. Over the adsorption in solution. Journal of Physical Chemistry, 57, 385-471, (1906).

Friedrich, M.; Seidel, A.; Gelbin, D. Kinetics of adsorption of phenol and indole from aqueous solutions on activated carbons. Chemical Engineering and Processing: Process Intensification, 24(1), 33-38 (1988).

Fritz, W.; Schluender, E. U. Simultaneous adsorption equilibria of organic solutes in dilute aqueous solutions on activated carbon. Chemical Engineering Science, 29, 1279-1282, (1974).

Fukuoka, K.; Tanaka, K.; Ozeki, Y.; Kanaly, R. A. Biotransformation of indole by *Cupriavidus sp.* strain KK10 proceeds through N-heterocyclic-and carbocyclic-aromatic ring cleavage and production of indigoids. International Biodeterioration & Biodegradation, 97, 13-24, (2015).

Gao, Y.; Wang, M.; Yang, X.; Sun, Q.; Zhao, J. Rapid detection of quinoline yellow in soft drinks using polypyrrole/single-walled carbon nanotubes composites modified glass carbon electrode. Journal of Electroanalytical Chemistry, 735, 84-89, (2014).

Gale, R. S. The filtration theory with special reference to sewage sludges. Water Pollution Control, 6, 222, (1967).

Gercel, O.; Ozcan, A.; Ozcan, A. S.; Gercel, H. F. Preparation of activated carbon from a renewable bio plant of *Euphorbia rigida* by H_2SO_4 activation and its adsorption behavior in aqueous solutions. Applied Surface Science, 253, 4843-4852, (2007).

Glocheux, Y.; Pasarin, M. M.; Albadarin, A. B.; Allen, S. J.; Walker, G. M. Removal of arsenic from groundwater by adsorption onto an acidified laterite by-product. Chemical Engineering Journal, 228, 565-574, (2013).

Gundlach, E. R.; Boehm, P. D.; Marchand, M.; Atlas, R. M.; Ward, D. M.; Wolfe, D. A. The fate of amoco cadiz oil. Science, 221, 122-129, (1983).

Gupta, V. K.; Mittal, A.; Gajbe, V. Adsorption and desorption studies of a water soluble dye, quinoline yellow, using waste materials. Journal of Colloid and Interface Science, 284, 89-98(2005).

Han, X.; Lin, H.; Zheng, Y. Regeneration methods to restore carbon adsorptive capacity of dibenzothiophene and neutral nitrogen heteroaromatic compounds. Chemical Engineering Journal, 243, 315-325, (2014).

Hongwei, Y.; Zhanpeng, J.; Shaoqi, S. Biodegradability of nitrogenous compounds under anaerobic conditions and its estimation. Ecotoxicology and Environmental Safety, 63, 299-305, (2006).

Hasan, D. B.; Aziz, A. B. A.; Daud, W. M. A. W. Oxidative mineralisation of petroleum refinery effluent using Fenton-like process. Chemical Engineering Research and Design, 90, 298-307, (2012).

Higasio, Y. S.; Shoji, T. Heterocyclic compounds such as pyrroles, pyridines, pyrollidins, piperdines, indoles, imidazol and pyrazins. Applied Catalysis A: General, 221, 197-207, (2001).

Hiwarkar, A. D.; Srivastava, V. C.; Mall, I. D. Comparative studies on adsorptive removal of indole by granular activated carbon and bagasse fly ash. Environmental Progress & Sustainable Energy, 34(2), 492-503, (2015).

Hiwarkar, A. D.; Srivastava, V. C.; Mall, I. D. Simultaneous adsorption of nitrogenous heterocyclic compounds by granular activated carbon: parameter optimization and multicomponent isotherm modeling. RSC Advances, 4, 39732-39742, (2014).

Ho, Y. S.; McKay, G. Sorption of dye from aqueous solution by peat. Chemical Engineering Journal, 70, 115-124, (1998).

Ho, Y. S; Mckay, G. Pseudo-second order model for sorption processes. Process Biochemistry, 34, 451-465, (1999).

Hongwei, Y.; Zhanpeng, J.; Shaoqi. S. Biodegradability of nitrogenous compounds under anaerobic conditions and its estimation. Ecotoxicology and Environmental Safety, 63, 299-305. (2006).

Hosseini, M. G.; Sajjadi, S. A. S.; Momeni, M. M. Electrodeposition of platinum metal on titanium and anodised titanium from P salt: application to electrooxidation of glycerol. Surface Engineering, 23, 419-424, (2007).

Hu, C. C.; Lee, C. H.; Wen, T. C. Oxygen evolution and hypochlorite production on Ru-Pt binary oxides. Journal of Applied Electrochemistry, 26, 72-82, (1996).

Hu, L.; Yang, X.; Dang, S. An easily recyclable Co/SBA-15 catalyst: Heterogeneous activation of peroxymonosulfate for the degradation of phenol in water. Applied Catalysis B: Environmental, 102, 19-26, (2011).

Hu, R.; Wang, X.; Dai, S. Shao, D.; Hayat, T.; Alsaedi, A. Application of graphitic carbon nitride for the removal of Pb(II) and aniline from aqueous solutions. Chemical Engineering Journal, 260, 469-477, (2015).

Huang, X.; Wang, X. M. Toxicity change patterns and its mechanism during the degradation of nitrogen heterocyclic compounds by O_3/UV. Chemosphere, 69, 747-754, (2007).

Jadhav, A. J.; Srivastava, V. C. Adsorbed solution theory based modeling of binary adsorption of nitrobenzene, aniline and phenol onto granulated activated carbon. Chemical Engineering Journal, 229, 450-459, (2013).

Jena, B. K.; Raj, C. R. Electrocatalytic applications of nanosized Pt particles self assembled on sol gel-derived three-dimensional silicate network. Journal of Physical Chemistry C, 112, 3496-3502, (2008).

Jensen, K. B.; Arvin, E.; Gundersen, T. Biodegradation of nitrogen-and oxygen-containing aromatic compounds in groundwater from an oil-contaminated aquifer. Journal of Contaminant Hydrology, 3, 65-75, (1988).

Jianlong, W.; Liping, H.; Hanchang, S.; Yi, Q. Biodegradation of quinoline by gel immobilized *Burkholderia sp.* Chemosphere, 44, 1041-1046, (2001).

Jones, R. A.; Bean, G. P. The Chemistry of pyrroles. Academic Press, New York, (1977).

Jorgebsen, W. L.; Salem, L. The organic chemists book of orbitals. Academic Press, New York, (1973).

Joglekar, A. M.; May, A. T. Product excellence through design of experiments. Cereal Foods World, 32, 857-868, (1987).

Kaiser, J. P.; Feng, Y.; Bollag, J. M. Microbial metabolism of pyridine, quinoline, acridine and their derivatives under aerobic and anaerobic conditions. Microbiology Review, 60, 483-498, (1996).

Kamachi Mudali, U.; Dayal, R. K.; Gnanamoorthy, J. B. Mixed $RuO_2/TiO_2/PtO_2$-coated titanium anodes for the electrolytic dissolution of nuclear fuels. Nuclear Technology, 100, 395, (1992).

Kamachi Mudali, U.; Raju, V. R.; Dayal, R. K. Preparation and characterization of platinum and platinum iridium coated titanium electrodes. Journal of Nuclear Materials, 277, 49-56, (2000).

Kamath, A. V.; Vaidyanathan, C. S. Biodegradation of indoles. Journal of the Indian Institute of Science, 71, 1-24, (1991).

Katapodis, P.; Moukouli, M.; Christakopoulos, P. Biodegradation of indole at high concentration by persolvent fermentation with the thermophilic fungus *Sporotrichum thermophile*. International Biodeterioration & Biodegradation, 60, 267-272, (2007).

Kavitha, D.; Namasivayam, C. Experimental and kinetic studies on methylene blue adsorption by coir pith carbon. Bioresource Technology, 98, 14-21, (2007).

Khandegar, V.; Saroha, A. K. Electrochemical treatment of distillery spent wash using aluminum and iron electrodes. Chinese Journal of Chemical Engineering, 20, 439-443, (2012).

Khandegar, V.; Saroha, A. K. Electrochemical treatment of effluent from small-scale dyeing unit. Indian Chemical Engineer, 55, 111-120, (2013).

Khandegar, V.; Saroha, A. K. Electrochemical treatment of textile effluent containing acid red 131 dye. Journal of Hazardous, Toxic and Radioactive Waste, 18, 38-44, (2014).

Kim, J. J.; Shin, G. S. Surface enhanced Raman scattering of pyridine and benzene in non-aqueous electrochemical systems of alcoholic solvents. Chemical Physics Letters, 118, 493-497, (1985).

Kim, K.; Han, J.; Kang, T.; Ihm, K.; Jeon, C.; Moon, S.; Hwang, C.; Hwang, H.; Kim, B. Adsorption configuration of pyrrole (C_4H_4NH) on Si(100)-2×1 by using PES and angle resolved NEXAFS. Journal of Electron Spectroscopy and Related Phenomena, 144-147, 429-431, (2005).

Kim, J. H.; Ma, X.; Zhou, A.; Song, C. Ultra-deep desulfurization and denitrogenation of diesel fuel by selective adsorption over three different adsorbents: A study on adsorptive selectivity and mechanism. Catalysis Today, 111, 74-83, (2006).

Kim, S.; Park, C.; Kim, T.; Lee, J.; Kim, S. COD reduction and decolorization of textile effluent using a combined process. Journal of Bioscience and Bioengineering, 95(1), 102-105, (2003).

Kirk, R. E.; Othmer, D. F. Pyridine and pyridine derivatives. In Encyclopedia of Chemical Technology 4th ed., John Wiley Science, New York, 20, 641-679, (1996).

Kuhn, E. P.; Suflita, J. M. Microbial degradation of nitrogen, oxygen and sulphur heterocyclic compounds under anaerobic conditions: Studies with aquifer samples. Environmental Toxicology and Chemistry, 8, 1149-1158, (1989).

Kumar, S.; Singh, S.; Srivastava, V. C. Electro-oxidation of nitrophenol by ruthenium oxide coated titanium electrode: Parametric, kinetic and mechanistic study. Chemical Engineering Journal, 263, 135-143, (2015).

Kumar, R.; Mishra, I. M.; Mall, I. D. Treatment of pyridine bearing wastewater using activated carbon. Research and Industry, 40, 33-37, (1995).

Kushwaha, J. P.; Srivastava, V. C.; Mall, I. D. Organics removal from dairy wastewater by electrochemical treatment and residue disposal. Separation and Purification Technology, 76, 198-205, (2010).

Kushwaha, J. P.; Srivastava, V. C.; Mall, I. D. Studies on electrochemical treatment of dairy wastewater using aluminum electrode. AIChE Journal, 57/9, 2589-2598, (2011).

Lagergren, S. About the theory of so-called adsorption of soluble substance, Kungliga Sevenska Vetenskapasakademiens, Handlingar, 24, 1−39, (1898).

Langmuir, I. The adsorption of gases on plane surfaces of glass, mica and platinum. Journal of American Chemical Society, 40, 1361-1403, (1918).

Lataye, D. H.; Mishra, I. M.; Mall, I. D. Removal of pyridine from aqueous solution by adsorption on bagasse fly ash. Industrial & Engineering Chemistry Research, 45, 3934-3943, (2006).

Lataye, D. H.; Mishra, I. M.; Mall, I. D. Pyridine sorption from aqueous solution by rice husk ash (RHA) and granular activated carbon (GAC): Parametric, kinetic, equilibrium and thermodynamic aspects. Journal of Hazardous Materials, 154, 858-870, (2008a).

Lataye, D. H.; Mishra, I. M.; Mall, I. D. Multicomponent sorptive removal of toxics pyridine, 2-picoline, and 4-picoline from aqueous solution by bagasse fly ash:optimization of process parameters. Industrial & Engineering Chemistry Research, 47, 5629-5635, (2008b).

Larrubia, M. A.; Alejandre, A. G.; Ramirez, J.; Busca, G. A FT-IR study of the adsorption of indole, carbazole, benzothiophene, dibenzothiophene and 4, 6-dibenzothiophene over solid adsorbents and catalysts. Applied Catalysis A: General, 224, 167-178, (2002).

Li, Y. M.; Gu, G. W.; Zhao, J. F.; Yu, H. Q.; Qiu, Y. L.; Peng, Y. Z. Treatment of coke-plant wastewater by biofilm systems for removal of organic compounds and nitrogen. Chemosphere, 52, 997-1005, (2003).

Li, Y.; Yan, L.; Xiang, C.; Hong, L. J. Treatment of oily wastewater by organic inorganic composite tubular ultrafiltration (UF) membranes. Desalination, 196, 76-83, (2006a).

Li, G. T.; Qu, J. H.; Zhang, X. W.; Ge, J. T. Electrochemically assisted photo catalytic degradation of acid orange 7 with β-PbO_2 electrodes modified by TiO_2. Water Research, 40, 213-224, (2006b).

Li, Y.; Wang, L.; Liao, L.; Sun, L.; Zheng, G.; Luan, J; Gu, G. Nitrate-dependent biodegradation of quinoline, isoquinoline and 2-methylquinoline by acclimated activated sludge. Journal of Hazardous Materials, 173, 151-158, (2010).

Lide, D. R. (Ed.) CRC Handbook of Chemistry and Physics, 73rd edition, CRC Press, New York, USA, (1992).

Lin, S.; Carlson, R. M. Susceptibility of environmentally important heterocycles to chemical disinfection: reactions with aqueous chlorine, chlorine dioxide and chloramine. Environment Science & Technology, 18, 743, (1984).

Lin, Q.; Jianlong, W. Biodegradation characteristics of quinoline by Pseudomonas putida. Bioresource Technology, 101, 7683-7686, (2010).

Linares-Hernandez, I.; Barrera-Diaz, C. ; Roa-Morales, G. ; Bilyeu, B. ; Urena-Nunez, F. Influence of the anodic material on electrocoagulation performance. Chemical Engineering Journal, 148, 97-105, (2009).

Linares-Hernandez, I.; Barrera-Diaz, C.; Bilyeu, B.; Juarez-GarciaRojas, P.; Campos-Medina E. A combined electrocoagulation-electroxidation treatment of industrial wastewater. Journal of Hazardous Materials, 175, 688-694, (2010).

Liu, D.; Gui, J.; Sun, Z. Adsorption structures of heterocyclic nitrogen compounds over Cu(I)Y zeolite: A first principle study on mechanism of the denitrogenation and the effect of nitrogen compounds on adsorptive desulfurization. Journal of Molecular Catalysis A: Chemical, 291, 17-21, (2008).

Liu, Y.; Liu, H.; Ma, J.; Li, J. Preparation and electrochemical properties of Ce-Ru-SnO_2 ternary oxide anode and electrochemical oxidation of nitrophenols. Journal of Hazardous Materials, 213-214, 222-229, (2012).

Madaeni, S. S.; Koocheki, S. Application of Taguchi method in the optimization of wastewater treatment using spiral-wound reverse osmosis element. Chemical Engineering Journal, 119, 37-44, (2006).

Mahesh, S.; Prasad, B.; Mall, I. D.; Mishra, I. M. Electrochemical degradation of pulp and paper mill wastewater. Part 1. COD and color removal. Industrial & Engineering Chemistry Research, 45, 2830-2839, (2006a).

Mahesh, S.; Prasad, B.; Mall, I. D.; Mishra, I. M. Electrochemical degradation of pulp and paper mill wastewater. Part 2. Characterization and analysis of sludge. Industrial & Engineering Chemistry Research, 45, 5766-5774, (2006b).

Mall, I. D. Petrochemical Process Technology. Macmillan India Ltd, India, (2007).

Maljaei, A.; Arami, M.; Mahmoodi, N. M. Decolorization and aromatic ring degradation of colored textile wastewater using indirect electrochemical oxidation method. Desalination, 249, 1074-1078, (2009).

Mallika, C.; Keerthika, B.; Kamachi Mudali, U. Platinum-modified titanium anodes for the electrolytic destruction of nitric acid. Electrochimica Acta, 52, 6656-6664, (2007).

Mangwandi, C.; Albadarin, A. B.; Al-Muhtaseb, A. H.; Allen, S. J.; Walker, G. M. Optimization of high shear granulation of multi-component fertilizer using response surface methodology. Powder Technology, 238, 142-150, (2013).

Mane, V.; Mall, I. D.; Srivastava, V. C. Use of bagasse fly ash as an adsorbent for the removal of brilliant green dye from aqueous solution. Dyes and Pigments, 73, 269-278, (2007).

Marquardt, D.W. An algorithm for least-squares estimation of nonlinear parameters, Journal of the Society for Industrial and Applied Mathematics, 11, 431-441, (1963).

Marandi, M.; Kallip, S.; Sammelselg, V.; Tamm, J. AFM study of the adsorption of pyrrole and formation of the polypyrrole film on gold surface. Electrochemistry Communications, 12, 854-858. (2010).

Martínez-Huitle, C. A.; Ferro, S. Electrochemical oxidation of organic pollutants for the wastewater treatment: direct and indirect processes. Chemical Society Reviews, 35, 1324-1340, (2006).

Maya, J. A. Pyridines in foods. Journal of Agricultural and Food Chemistry, 25, 895, (1981).

Meyer, S.; Cartellieri, S.; Steinhart, H. Simultaneous determination of PAHs, hetero-PAHs (N. S. O) and their degradation products in creosote-contaminated soils. Method development, validation, and application to hazardous waste sites. Analytical Chemistry, 71, 4023-4029, (1999).

Mensah, K.; Forster, C. An examination of the effects of detergents on anaerobic digestion. Bioresource Technology, 90, 133-138, (2003).

Mirzaei, A.; Ebadi, A.; Khajavi, P. Kinetic and equilibrium modeling of single and binary adsorptionof methyl tert-butyl ether (MTBE) and tert-butyl alcohol (TBA) onto nano-perfluorooctyl alumina. Chemical Engineering Journal, 231, 550-560, (2013).

Mohammadi, T.; Moheb, A.; Sadrzadeh, M; Razmi, A. Separation of copper ions by electrodialysis using Taguchi experimental design. Desalination, 169, 21-31, (2004).

Mohan, S. V.; Karthikeyan, J. Removal of lignin and tannin colour from aqueous solution by adsorption onto activated charcoal. Environmental Pollution, 97(1-2), 183-187, (1997).

Mohan, S. V.; Rao, N. C.; Karthikeyan, J. Adsorptive removal of direct azo dye from aqueous phase onto coal based sorbents: A kinetic and mechanistic study. Journal of Hazardous Materials, 90, 189-204, (2002).

Mohan, S. V.; Ramanaiah, S. V.; Sarma, P. N. Biosorption of direct azo dye from aqueous phase onto *Spirogyra sp.* I02: Evaluation of kinetics and mechanistic aspects. Biochemical Engineering Journal, 38, 61-69, (2008).

Mohan, S. V.; Sistla, S.; Guru, R. K.; Prasad, K. K.; Kumar, C. S.; Ramakrishna, S. V.; Sarma, P. N. Microbial degradation of pyridine using *Pseudomonas sp.* and isolation of plasmid responsible for degradation. Waste Management, 23, 167-171, (2003).

Mohan, D.; Singh, K. P.; Sinha, S.; Gosh, D. Removal of pyridine derivatives from aqueous solution by activated carbon developed from agricultural waste materials. Carbon, 43, 1680-1693, (2005).

Mohan, D.; Pittman, C. U.; Steele, P. H. Single, binary and multi-component adsorption of copper and cadmium from aqueous solutions on Kraft lignin-a biosorbent. Journal of Colloid and Interface Science, 297, 489-504, (2006).

Moon, J.; Dons, K. K.; Won, K. L. Adsorption equillibria for m-cresol, quinoline, and1-naphthol onto silica gel. Korean Journal of Chemical Engineering, 6 (3), 172-178, (1989).

Molina, J.; del Río, A. I.; Bonastre, J.; Cases, F. Chemical and electrochemical polymerisation of pyrrole on polyester textiles in presence of phosphotungstic acid. European Polymer Journal, 44, 2087-2098, (2008).

Mudliar, S. N.; Padoley, K. V.; Bhatt, P.; Sureshkumar, M.; Lokhande, S. K.; Pandey, R. A.; Vaidya, A. N. Pyridine biodegradation in a novel rotating rope bioreactor. Bioresource Technology, 99, 1044-1051, (2008).

Nemmani, G. R.; Suggala, S. V.; Bhattacharya, P. K. NSGA-II for multiobjective optimization of pervaporation process: removal of volatile organics from water. Industrial & Engineering Chemistry Research, 48, 1543-1550, (2009).

Ng, J. C. Y.; Cheung, W. H.; McKay, G. Equilibrium studies of the sorption of Cu(II) ions onto chitosan. Journal of Colloid and Interface Science, 255, 64-74 (2002).

Niu, J.; Conway, B. E. Development of techniques for purification of waste waters: removal of pyridine from aqueous solution by adsorption at high-area C-cloth electrodes using in situ optical spectrometry. Journal of Electroanalytical Chemistry, 52, 16-28, (2002).

Novotny, M.; Starand, J. W.; Smith, S. L.; Wiesler, D.; Schwende, F. J. Compositional studies of coal tar by capillary gas chromatography/mass spectrometry. Fuel, 60, 213, (1981).

Nuzhdin, L.; Kovalenko, K. A.; Dybtsev, D. N.; Bukhtiyarova, G. A. Removal of nitrogen compounds from liquid hydrocarbon streams by selective sorption on metal-organic framework MIL-101. Mendeleev Communications, 20, 57-58, (2010).

Ochiai, M.; Wakabayash, K.; Sugimura, T.; Nagao, M. Mutagenicities of indole and 30 derivatives after nitrite treatment. Mutation Research, 172-189, (1986).

Ozacar, M.; Sengil, I. A. Adsorption of metal complex dyes from aqueous solutions by pine sawdust. Bioresource Technology, 96, 791-795, (2005).

Padoley, K V.; Rajvaidya, A. S.; Subbarao, T. V.; Pandey, R. A. Biodegradation of pyridine in a completely mixed activated sludge process. Bioresource Technology, 97, 1225-1236, (2006).

Padoley, K. V.; Mudliar, S. N.; Pandey, R. A. Heterocyclic nitrogenous pollutants in the environment and their treatment options-An overview. Bioresource Technology, 99, 4029-4043, (2008).

Padoley, K. V.; Mudliar, S. N.; Pandey, R. A. Microbial degradation of pyridine and picoline using a strain of the genera *Pseudomonas* and *Nocardia sp.* Bioprocess and Biosystems Engineering, 32, 501-510, (2009).

Padoley, K. V.; Mudliar, S. N.; Banerjee, S. K.; Deshmukh, S. C.; Pandey, R. A. Fenton oxidation: A pretreatment option for improved biological treatment of pyridine and 3-cyanopyridine plant wastewater. Chemical Engineering Journal, 166, 1-9, (2011).

Pandey, R. A.; Padoley, K. V.; Mukherji, S. S.; Mudliar, S. N.; Vaidya, A. N.; Rajvaidya, A. S.; Subbarao, T. V. Biotreatment of waste gas containing pyridine in a biofilter. Bioresource Technology, 98, 2258-2267, (2007).

Pahari, P. K.; Sharma, M. M. Recovery of heterocyclic amines from dilute aqueous waste streams. Industrial & Engineering Chemistry Research, 30, 8, (1991).

Pan, F. M.; Stair, P. C. Chemisorption of pyridine and pyrrole on iron oxide surfaces studied by XPS. Surface Science, 177, 1-13, (1986).

Panizza, M.; Cerisola, G. Electrochemical oxidation of aromatic sulphonated acids on a boron-doped diamond electrode. International Journal of Environment and Pollution, 27, 64-74, (2006).

Panizza, M.; Cerisola, G. Direct and mediated anodic oxidation of organic pollutants. Chemical Review, 109, 6541-6569, (2009).

Paudler, W. W.; Cheplen, M. Nitrogen bases in solvent-refined coal. Fuel, 58, 775, (1979).

Pearlman, R. S.; Yalkowski, S. H.; Banerjee, S. Water solubilities of polynuclear aromatic and heteroaromatic compounds. Journal of Physical Chemistry Reference Data, 13, 555-562, (1984).

Pereira, W. E.; Rosad, C. E.; Garbarino, J. R.; Hult, M. F. Groundwater contamination by organic bases derived from coal-tar wastes. Environmental Toxicology and Chemistry, 2(3), 283-294, (1983).

Plessis, B. J. D.; Villiers, G. H. D. The application of the Taguchi method in the evaluation of mechanical flotation in waste activated sludge thickening. Resources, Conservation and Recycling, 50(2), 202-210, (2007).

Prissanaroon, W.; Brack, N.; Pigram, P. J.; Liesegang, J. Electropolymerisation of pyrrole on copper in aqueous media. Synthetic Metals, 142, 25-34, (2004).

Qiao, M. H.; Tao, F.; Cao, Y.; Xu, G. Adsorption and thermal dissociation of pyrrole on Si(100)-2 x1. Surface Science, 544, 285-294, (2003).

Rameshraja, D.; Srivastava, V. C.; Kushwaha, J. P.; Mall, I. D. Quinoline adsorption onto granular activated carbon and bagasse fly ash. Chemical Engineering Journal, 181-182, 343-351, (2012).

Rauthula, M. S.; Srivastava, V. C. Studies on adsorption/desorption of nitrobenzene and humic acid onto/from activated carbon. Chemical Engineering Journal, 168, 35-43, (2011).

Redlich, O.; Peterson, D. L. A useful adsorption isotherm. Journal of Physical Chemistry, 63, 1024-1026, (1959).

Ren, J.; Wang, J.; Huo, C. F.; Wen, X.; Cao, Z.; Yuan, S.; Li, W.; Jiao, H. Adsorption of NO, NO_2, pyridine and pyrrole on the α-Mo_2C(0001): A DFT study. Surface Science, 601, 1599-1607, (2007).

Reschke, G.; Radeke, K. H.; Gelbin, D. Breakthrough curves for single solutes in Beds of activated carbon with a broad pore-size distribution-ii: Measuring and calculating Breakthrough curves of phenol and indole from aqueous solutions on activated carbons. Chemical Engineering Science, 41(3), 549-554, (1986).

Rogers, J. E.; Riley, R. G.; Li, S. W.; O'malley, M. L.; Thomas, B. L. Microbial transformation of alkyl pyridines in groundwater. Water Air and Soil Pollution, 24, 443-454, (1985).

Samah, M.; Merabet, S.; Bouguerra, M.; Bouhelassa, M.; Ouhenia, S.; Bouzaza, A. Photo oxidation process of indole in aqueous solution with ZnO catalyst: Study and optimization. Kinetics and Catalysis, 52, 34-39, (2011).

Sakalis, A.; Mpoulmpasakos, K.; Nickel, U.; Fytianos, K.; Voulgaropoulos, A. Evaluation of a novel electrochemical pilot plant process for azo dyes removal from textile wastewater. Chemical Engineering Journal, 111, 63-70, (2005).

Sarac¸ A. S.; Sonmez, G.; Ustamehmetoglu, B. Electrochemical polymerization of pyrrole in acrylamide solution. Synthetic Metals, 98, 177-182, (1999).

Sartori, P.; Velayutham, D.; Ignatev, N.; Noel, M. Investigations on the product distribution pattern during the electrochemical fluorination of 2-fluoropyridine and pyridine. Journal of Fluorine Chemistry, 87, 3l-36, (1998).

Scienza, L. C.; Thompson, G. E. Preparation and surface analysis of PPY/SDBS films on aluminum substrates. Ciênciae Tecnologia, 11, 3, 142-148, (2001).

Sengil, I. A.; Ozacar, M.; Turkmenler, H. Kinetic and isotherm studies of Cu(II) biosorption onto valonia tannin resin. Journal of Hazardous Materials, 162, 1046-1052, (2009).

Sengil, I. A.; Ozdemir, A. Simultaneous decolorization of binary mixture of blue disperse and yellow basic dyes by electrocoagulation. Desalination and Water Treatment, 46, 215-226, (2012).

Sexton, B. A. A vibrational and TDS study of the adsorption of pyrrole, furan and thiophene on Cu(100): Evidence for bonded and inclined species. Surface Science, 163, 99-113, (1985).

Sharma, Y. C.; Uma; Singh, S. N.; Paras; Gode, F. Fly ash for the removal of Mn(II) from aqueous solutions and wastewaters. Chemical Engineering Journal, 132, 319-323, (2007).

Sharma, Y. C.; Uma; Upadhyay, S. N.; Weng, C. H. Studies on an economically viable remediation of chromium rich waters and wastewaters by PTPS fly ash. Colloids and Surfaces A: Physicochemical Engineering Aspects, 317, 222-228, (2008).

Sharma, S.; Mukhopadhyay, M.; Murthy, Z. V. P. Degradation of 4-chlorophenol in wastewater by organic oxidants. Industrial & Engineering Chemistry Research, 49, 3094-3098, (2010a).

Sharma, Y. C.; Uma; Sinha, A. S. K.; Upadhyay, S. N. Characterization and adsorption studies of *Cocos nucifera* l. activated carbon for the removal of methylene blue from aqueous solutions. Journal of Chemical and Engineering Data, 55, 2662-2667, (2010b).

Sharma, S.; Mukhopadhyay, M.; Murthy, Z. V. P. Treatment of chlorophenols from wastewaters by advanced oxidation processes. Separation and Purification Reviews, 42, 263-295, (2013).

Sharma P.; Das M. Removal of a cationic dye from aqueous solution using graphene oxide nanosheets: Investigation of adsorption parameters. Journal of Chemical and Engineering Data, 58, 151−158, (2013).

Sheindorf, C.; Rebhum, M.; Sheintuch, M. A. Freundlich-type multicomponent isotherm. Journal of Colloid and Interface Science, 79, 136-142, (1981).

Shiu; K. K; Zhang, Y.; Wong, K. Y. AC voltammetric and impedance studies of the electrochemical oxidation of pyrrole in aqueous medium. Journal of Electroanalytical Chemistry, 389, 105-114, (1995).

Sims, G. K.; Loughlin, E. J. O. Degradation of pyridines in the environment. Critical Reviews in Environmental Control, 19, 309-340, (1989).

Singh, S.; Srivastava, V. C.; Mall, I. D. Multi-step optimization and residue disposal study for electrochemical treatment of textile wastewater using aluminium electrode. International Journal of Chemical Reactor Engineering, 11(1), 31-46, (2013).

Srivastava, V. C.; Mall, I. D.; Mishra, I. M. Treatment of pulp and paper mill wastewaters with poly aluminium chloride and bagasse fly ash. Colloids and Surfaces A: Physicochemical and Engineering Aspects, 260, 17-28, (2005).

Srivastava, V. C.; Prasad, B.; Mall, I. D.; Mahadevswamy, M.; Mishra, I. M. Adsorptive removal of phenol by bagasse fly ash and activated carbon: equilibrium, kinetics and thermodynamics. Colloids Surfaces A: Physicochemical Engineering Aspects, 272, 89-104, (2006).

Srivastava, V. C.; Mall, I. D.; Mishra, I. M. Adsorption thermodynamics and isosteric heat of adsorption of toxic metal ions onto bagasse fly ash (BFA) and rice husk ash (RHA). Chemical Engineering Journal, 132(1-3), 267-278, (2007a).

Srivastava, V. C.; Mall, I. D.; Mishra, I. M. Multi-component adsorption study of metal ions onto bagasse fly ash using Taguchi's design of experimental methodology. Industrial & Engineering Chemistry Research, 46, 5697-5706, (2007b).

Srivastava, V. C.; Prasad, B.; Mishra, I. M.; Mall, I. D.; Mahadevswamy, M. Prediction of breakthrough curves for sorptive removal of phenol by bagasse fly ash packed bed. Industrial & Engineering Chemistry Research, 47, 1603-1613, (2008a).

Srivastava, V. C.; Mall, I. D.; Mishra, I. M. Adsorption of toxic metal ions onto activated carbon study of sorption behaviour through characterization and kinetics. Chemical Engineering and Processing, 47, 1275-1286, (2008b).

Srivastava, V. C.; Mall, I. D.; Mishra, I. M. Antagonistic competitive equilibrium modeling for the adsorption of ternary metal ions mixtures onto bagasse fly ash. Industrial & Engineering Chemistry Research, 47(9), 3129-3137, (2008c).

Srivastava, V. C.; Patil, D.; Srivastava, K. K. Parametric optimization of dye removal by electrocoagulation using Taguchi methodology. International Journal of Chemical Reactor Engineering, 9, A8, (2011).

Subbaramaiah, V.; Srivastava, V. C; Mall, I. D. Catalytic wet peroxidation of pyridine bearing wastewater by cerium supported SBA-15. Journal of Hazardous Materials, 248-249, 355-363, (2013).

Sun, M.; Nelson, A. E.; Adjaya, J. Adsorption and hydrogenation of pyridine and pyrrole on NiMoS :An ab initio density-functional theory study. Journal of Catalysis, 231, 223-231, (2005).

Sun, Q.; Bai, Y.; Zhao, C.; Xiao, Y.; Wen, D.; Tang, X. Aerobic biodegradation characteristics and metabolic products of quinoline by a *Pseudomonas* strain. Bioresource Technology, 100, 5030-5036, (2009).

Suresh, S.; Srivastava, V. C.; Mishra, I. M. Adsorptive removal of phenol from binary aqueous solution with aniline and 4-nitrophenol by granular activated carbon. Chemical Engineering Journal, 171, 997-1003, (2011a).

Suresh, S.; Srivastava, V. C.; Mishra, I. M. Study of catechol and resorcinol adsorption mechanism through granular activated carbon characterization, pH and kinetic study. Separation Science and Technology, 46(11), 1750-1766, (2011b).

Suresh, S.; Srivastava, V. C.; Mishra, I. M. Isotherm, thermodynamics, desorption and disposal study for the adsorption of catechol and resorcinol onto granular activated carbon. Journal of Chemical and Engineering Data, 56(4), 811-818, (2011c).

Temkin, M. J.; Pyzhev V. Kinetics of ammonia synthesis on promoted iron catalysts. Acta Physiochimica URSS, 12, 217-222, (1940).

Thakur, C.; Srivastava, V. C.; Mall, I. D. Electrochemical treatment of a distillery wastewater: Parametric and residue disposal study. Chemical Engineering Journal, 148, 496-505, (2009).

Thomsen, B.; Kilen, H. H. Supercritical water oxidation of quinoline in a continuous plug flow reactor-part 1: effect of key operating parameters. Water Research, 32, 3353-3361, (1998).

Tourillon, G.; Raaen, S. A near edge x-ray absorption fine structure study of the adsorption of pyrrole and n-methylpyrrole on Pt (l l l): Orientation and dissociation of the adsorbed molecules. Surface Science, 184, 345-354, (1987).

Tuo, B.; Yan, J.; Fan, B.; Yang, Z.; Liu, J. Biodegradation characteristics and bioaugmentation potential of a novel quinoline-degrading strain of Bacillus sp.

Isolated from petroleum-contaminated soil. Bioresource Technology, 107, 55-60, (2012).

Uma, B.; Sandhya, S. Pyridine degradation and heterocyclic nitrification by Bacillus coagulance. Canadian Journal of Microbiology, 43, 595-598, (1997).

Vaghela S. S.; Jethva, A. D.; Mehta, B. B.; Dave, S. P.; Adimurthy, S.; Ramachandraiah, G. Laboratory studies of electrochemical treatment of industrial azo dye effluent. Environmental Science & Technology, 39, 2848-2855, (2005).

Voorde, B. V.; Boulhout, M.; Vermoortele, F.; Horcajada, P.; Cunha, D.; Lee, J. S.; Chang, J. S.; Gibson, E.; Daturi, M.; Lavalley, J. C.; Vimont, A.; Beurroies, I.; De Vos, D. E. N/S-Heterocyclic contaminant removal from fuels by the mesoporous metal-organic framework MIL-100: The role of the metal ion. Journal of American Chemical Society, 135, 9849−9856, (2013).

Wang, H. L.; Jiang, W. F. Adsorption of dinitro-butyl phenol (DNBP) from aqueous solutions by fly ash. Industrial & Engineering Chemistry Research, 46, 5405-5411, (2007).

Wang, C. T.; Chou, W. L.; Kuo, Y. M. Removal of COD from laundry wastewater by electrocoagulation/electroflotation. Journal of Hazardous Materials, 164, 81-86, (2009).

Wen, J.; Hanb, X.; Lin, H.; Zheng, Y.; Chu, W. A critical study on the adsorption of heterocyclic sulfur and nitrogen compounds by activated carbon: Equilibrium, kinetics and thermodynamics. Chemical Engineering Journal, 164, 29-36, (2010).

Weber, W. J.; Morris, J. C. Kinetics of adsorption on carbon from solution. Journal of Sanitary Engineering Division, ASCE, 89, 31-59, (1963).

Wiener, J.; Ramadan, M. A.; Gomaa, R.; Abbassi, R.; Hebeish, A. Preparation and characterization of conductive cellulosic fabric by polymerization of pyrrole. Materials Sciences and Applications, 4, 649-655, (2013).

Wong, C. W.; Barford, J. P.; Chen, G.; McKay, G. Kinetics and equilibrium studies for the removal of cadmium ions by ion exchange resin. Journal of Environmental Chemical Engineering, 2, 698-707, (2014).

Wu, M.; We, Z.; Jin, J.; Cui, Y. Effects of combinatorial $AlCl_3$ and pyrrole on the SEI formation and electrochemical performance of Li electrode. Electrochimica Acta, 103, 199-205, (2013).

Yamamoto, K.; Park, Y. S.; Takeoka S.; Tsuchida, E. J. Electropolymerization of pyrrole on a tantalum electrode. Journal of Electroanalytical Chemistry and Interfacial Electrochemistry, 318, 171-181, (1991).

Yaneva, Z. L.; Koumanova, B. K.; Allen, S. J. Applicability comparison of different kinetic/diffusion models for 4-nitrophenol sorption on *Rhizopus oryzae* dead biomass. Bulgarian Chemical Communications 45, 161-168, (2013).

Yang, R. T. Gas Separation by adsorption processes. Boston, MA: Butterworths, (1987).

Yao, H.; Ren, Y.; Deng, X.; Wei, C. Dual substrates biodegradation kinetics of m-cresol and pyridine by *Lysinibacillus cresolivorans*. Journal of Hazardous Materials, 186, 1136-1140, (2011).

Yin, B.; Gu, J. D.; Wan, N. Degradation of indole by enrichment culture and *Pseudomonas aeruginosa* Gs isolated from mangrove sediment. International Biodeterioration & Biodegradation, 56, 243-248, (2005).

Yousefich, M.; Shamanian, M.; Saatchi, A. Optimization of experimental conditions of the pulsed current GTAW parameters for mechanical properties of SDSS UNS S32760 welds based on the Taguchi design method. Journal of Materials Engineering and Performance, 21(9), 1978-1988, (2012).

Zabeti, M.; Daud, W. M. A. W.; Aroua, M. K. Optimization of the activity of CaO/Al2O3 catalyst for biodiesel production using response surface methodology. Applied Catalysis A: General, 366, 154-159, (2009).

Zaggout, F. R.; Ghalwa, N. A. Removal of o-nitrophenol from water by electrochemical degradation using a lead oxide/titanium modified electrode. Journal of Environmental Management, 86, 291-296, (2008).

Zaid, B.; Aeiyach, S.; Lacaze, P. C. Electropolymerization of pyrrole in propylene carbonate on zinc electrodes modified by heteropolyanions. Synthetic Metals, 65, 27-34, (1994).

Zaid, B.; Aeiyach, S.; Lacaze, P. C.; Takenouti, H. A two-step electropolymerization of pyrrole on Zn in aqueous media. Electrochimica Acta, 43 (16-17), 2331-2339, (1998).

Zhang, C.; Li, M.; Liu, G.; Luo, H.; Zhang, R. Pyridine degradation in the microbial fuel cells. Journal of Hazardous Materials, 172, 465-471, (2009).

Zhang, H.; Song, H. Study of adsorptive denitrogenation of diesel fuel over mesoporous molecular sieves based on breakthrough curves. Industrial & Engineering Chemistry Research, 51, 16059−16065, (2012).

Zhang, H.; Li, G.; Jia, Y.; Liu, H. Adsorptive removal of nitrogen-containing compounds from fuel. Journal of Chemical and Engineering Data, 55, 173-177, (2010).

Zhao, J.; Zhang, Y.; Wu, K.; Chen, J.; Zhou, Y. Electrochemical sensor for hazardous food colourant quinoline yellow based on carbon nanotube-modified electrode. Food Chemistry 128, 569-572, (2011).

Zhao, G.; Chen, S.; Ren, Y.; Wei, C. Interaction and biodegradation evaluate of m-cresol and quinoline in co-exist system. International Biodeterioration & Biodegradation, 86, 252-257, (2014).

Zhuang, H.; Han, H.; Xu, P.; Hou, B.; Jia, S.; Wang, D.; Li, K. Biodegradation of quinoline by *Streptomyces sp.* N01 immobilized on bamboo carbon supported Fe3O4 nanoparticles. Biochemical Engineering Journal, 99, 44-47, (2015).

Zingler, E. Significance and limits of the Buechner funnel filtration test. Water Pollution Research: International Conference Proceeding, 5, II-31, (1969).

Zolfaghari, G.; Sari A. E.; Anbia M.; Younesi H.; Amirmahmoodi S.; Nazari A. G. Taguchi optimization approach for Pb(II) and Hg(II) removal from aqueous solutions using

modified mesoporous carbon. Journal of Hazardous Materials, 192, 1046-1055, (2011).

Zogorski, J. S.; Faust, S. M.; Hass, J. M. The kinetics adsorption of phenols by granular activated carbon. Journal of Colloid and Interface Science, 55(2), 329-341, (1976).

Zhu, S.; Bell P. R. F.; Greenfield P. F. Quinoline adsorption onto combusted rundle shale in dilute aqueous solution at the natural pH 8. Water Research, 29, 5, 1393-1400, (1995).

Zhu, S.; Liu, D.; Fan, L.; Ni, J. Degradation of quinoline by *Rhodococcus sp*. QL2 isolated from activated sludge. Journal of Hazardous Materials, 160, 289-294, (2008).

Zhu, Y.; Tang, W.; Chen, W.; Li, B.; Zhao, G. Observing electrochemiluminescence behavior of quinoline in acetonitrile at a glassy carbon electrode. Journal of Luminescence, 131, 1982-1985, (2011).

PUBLICATIONS FROM THESIS

Papers Published in SCI (International) Journals

1. Hiwarkar, A.D.; Srivastava, V.C.; Mall, I.D. Simultaneous adsorption of nitrogenous heterocyclic compounds by granular activated carbon: parameter optimization and multicomponent isotherm modeling. **RSC Advances,** 4**,** 39732-39742, (2014).

2. Hiwarkar, A.D.; Srivastava, V.C.; Mall, I.D. Comparative studies on adsorptive removal of indole by granular activated carbon and bagasse fly ash. **Environmental Progress & Sustainable Energy**, 34(2), 492–503, (2015).

3. Hiwarkar, A.D.; Srivastava, V.C.; Mall, I.D. Studies on mineralization of pyrrole and indole by electrochemical treatment. (*To be communicated*)

4. Hiwarkar, A.D.; Srivastava, V.C.; Mall, I.D. Simultaneous mineralization of pyrrole and indole by platinum coated titanium electrode. (*To be communicated*)

5. Hiwarkar, A.D.; Srivastava, V.C.; Mall, I.D. Simultaneous adsorption of pyrrole and indole by bagasse fly ash. (*To be communicated*)